Meteorological Impacts on Streamflow: Analyzing Anthropogenic Climate Change's Effect on Runoff and Streamflow Magnitudes in Virginia's Chesapeake Bay Watershed

Daniel S. Hildebrand

Thesis submitted to the Faculty of the

Virginia Polytechnic Institute and State University

in partial fulfillment of the requirements for the degree of

Master of Science

in

Biological Systems Engineering

Durelle T. Scott, Chair

Julie E. Shortridge

Robert W. Burgholzer

July 8, 2020

Blacksburg, Virginia

Keywords: Hydrologic modeling, water supply, climate modeling, land use runoff, streamflow

Meteorological Impacts on Streamflow: Analyzing Anthropogenic Climate Change's Effect on Runoff and Streamflow Magnitudes in Virginia's Chesapeake Bay Watershed

Daniel S. Hildebrand

(ABSTRACT)

Anthropogenic climate change will impact Virginia's hydrologic processes in unforeseen ways in the coming decades. This research describes variability in meteorology (temperature and precipitation) and associated hydrologic processes (evapotranspiration) throughout an ensemble of 31 general circulation models (GCMs) used by the Chesapeake Bay Program (CBP). Trends are compared with surface runoff generation patterns for a variety of land uses to investigate climate's effect on runoff generation. Scenarios representing pairings of the tenth, fiftieth, and ninetieth percentiles of precipitation and temperature in the CBP 31-model ensemble were run through VADEQ's VA Hydro hydrologic model to investigate streamflow's response to climate. Temperature changes across the study area were minimized in the tenth percentile scenario (+1.02 to +1.24°C) and maximized in the ninetieth (+2.20 to +3.02°C), with evapotranspiration change following this trend (tenth: +2.84 to +3.81%; ninetieth: +6.53 to +10.2%). Precipitation change ranged from -10.9 to -7.30% in the tenth to +22.1 to +28.0% in the ninetieth. Runoff per unit area was largely dependent on land use, with the most extreme changes in runoff often seen in forested and natural land uses (-24% in tenth; +53% in ninetieth) and the least extreme seen in impervious and feeding space land (tenth: -11%; ninetieth: +30%). Both overall runoff per unit area and streamflow changed drastically from the base in the tenth (-20.4% to -25.9% change in median runoff; -19.8% to -27.1% change in median streamflow) and ninetieth (+30.4% to +53.7% change in median runoff; +33.0% to +77.8% change in median streamflow) percentile scenarios.

Meteorological Impacts on Streamflow: Analyzing Anthropogenic Climate Change's Effect on Runoff and Streamflow Magnitudes in Virginia's Chesapeake Bay Watershed

Daniel S. Hildebrand

(GENERAL AUDIENCE ABSTRACT)

Human-caused climate change will impact Virginia's hydrologic processes in unforeseen ways in the coming decades. This research describes variability in meteorology (temperature and precipitation) and associated hydrologic processes (evapotranspiration) throughout an ensemble of 31 general circulation models (GCMs) used by the Chesapeake Bay Program (CBP). Trends are compared with surface runoff generation patterns for a variety of land uses to investigate climate's effect on runoff generation. Scenarios representing pairings of the tenth, fiftieth, and ninetieth percentiles of precipitation and temperature in the CBP 31-model ensemble were run through VADEQ's VA Hydro hydrologic model to investigate streamflow's response to climate. Temperature changes across the study area were minimized in the tenth percentile scenario (+1.02 to +1.24°C) and maximized in the ninetieth (+2.20 to +3.02°C), with evapotranspiration change following this trend (tenth: +2.84 to +3.81%; ninetieth: +6.53 to +10.2%). Precipitation change ranged from -10.9 to -7.30% in the tenth to +22.1 to +28.0% in the ninetieth. Runoff per unit area was largely dependent on land use, with the most extreme changes in runoff often seen in forested and natural land uses (-24% in tenth; +53% in ninetieth) and the least extreme seen in impervious and feeding space land (tenth: -11%; ninetieth: +30%). Both overall runoff per unit area and streamflow changed drastically from the base in the tenth (-20.4% to -25.9% change in median runoff; -19.8% to -27.1% change in median streamflow) and ninetieth (+30.4% to +53.7% change in median runoff; +33.0% to +77.8% change in median streamflow) percentile scenarios.

Acknowledgments

First and foremost, I would like to thank Dr. Durelle Scott for accepting me into the Scott Lab's Hydrologic Analysis Research Program (HARP) group and stimulating my interest in hydrologic data processing and analysis. I'd also like to thank the other graduate students in the Scott Group, Alyssa Ford and Katie Wardinski, for always being available to answer questions and provide feedback on my work throughout this past year. During my time in HARP, Rob Burgholzer and Joey Kleiner have both always been available to help me with the numerous issues and questions I've run into during my first real deep dive into a hydrologic model – thank you both for that, as well as for being infectiously passionate and curious about the numerous water resource issues we've looked into in the past few years. Similarly, thanks to my HARP co-researchers Kelsey Reitz, Hailey Alspaugh, Kevin D'Andrea, and Emma Aguero – I appreciate all the help resolving problems that I've struggled with throughout the years, and similarly, for allowing me to deepen my own understanding of our research by helping work to answer your own questions and problems. I'd like to thank Dr. Julie Shortridge for sharing with me her extensive knowledge on climate change and her advice on methods to analyze and visualize different types of data – your suggestions were always a massive help. Also, thanks to Lal Sangha for helping with a number of R scripts to analyze flow data and communicate with the VA Hydro system – it was always a pleasure to have somebody to bounce ideas off of when I ran into issues. I'd also like to thank all my family and friends. Thanks to my parents and sister for always welcoming me back into your home when I needed a change of scenery, and for always being willing to grab a beer and unwind after a long day of research. Thank you to Sophie, Casey, Jason, Liam, Eric, Alex, Jeremy and all my other friends, new and old, for always being ready for a hike or a swim or a happy hour when I was burnt out from running models and digging through data. Lastly, I'd like to thank all the members of the Scuba Club at Virginia Tech for always being willing to go on impromptu trips to the New River, Gray Quarry, or even the springs of Florida – your constant willingness to drop everything to spend a day or two diving kept me intimately connected to the water bodies that I've always been so fascinated by, rekindling my passion in times where my head was so jammed up with numbers and programming issues that it was starting to slip away from me.

Contents

List of Figures

List of Tables

List of Abbreviations

ALF August Low Flow

BMP Best Management Practice

CBP Chesapeake Bay Program

cfs cubic feet per second

CSS Combined Sewer System

EPA Environmental Protection Agency

GCM General Circulation Model

ivld interval of the data

l30 30-Day Minimum Flow

l90 90-Day Minimum Flow

MS4 Municipal Separate Storm Sewer System

OMF Overall Mean Flow

PET Potential Evapotranspiration

RCP Representative Concentration Pathway

S10% September 10% Flow

USGS United States Geological Survey

VADEQ Virginia Department of Environmental Quality

Chapter 1

Introduction

1.1 Climate Change

Anthropogenic climate change is a process whose existence is accepted by the vast majority of climate scientists. The severity of this change in climate, as well as its impacts on the world's meteorologic and hydrologic processes, will largely depend on the success of human efforts to reduce greenhouse gas (GHG) emissions in the present and the near future. A number of different possibilities of how socioeconomic factors (population, energy use), emissions factors (anthropogenic GHG emissions, aerosol emissions), and GHG concentration factors (terrestrial and oceanic cycling of carbon) may change over the upcoming decades exist (Moss et al., 2010). These possibilities are quantified by their associated change in radiative forcing (difference between energy absorbed from sunlight and energy radiated back to space, measured in Watts per square meter) since the pre-industrial year 1750 CE, and are known as representative concentration pathways (RCPs) (Moss et al., 2010).

Commonly discussed RCPs are associated with radiative forcing increases of 2.6, 4.5, 6.0, and 8.5 W/m^2. The moderate RCP 4.5 and RCP 6.0 emissions scenarios experience increases in GHG concentration (and thus, in radiative forcing) for all of the 21st century before stabilizing by the year 2150 CE (Meinshausen et al., 2011, Moss et al., 2010). The least extreme RCP 2.6 scenario experiences a peak GHG concentration (and peak radiative forcing of about 3 W/m^2) in about 2050 CE before gradually decreasing, while the most extreme

RCP 8.5 scenario experiences increases in radiative forcing throughout the entire century, with GHG concentration continuing to climb past the year 2150 CE (Meinshausen et al., 2011, Moss et al., 2010). The concentrations of GHGs in the atmosphere for each of these RCP scenarios over the time period 2000-2150 CE is shown in Fig. 1.1 (Clarke et al., 2007, Fujino et al., 2006, Hijioka et al., 2008, Riahi et al., 2007, Smith and Wigley, 2006, van Vuuren et al., 2007, Wise et al., 2009). However, these commonly analyzed RCP emissions scenarios should not be mistakenly considered ”best” or ”worst” case scenarios – the true impacts of climate change could be more severe than, less severe than, or anywhere between these representative scenarios. Similarly, when fed inputs meant to represent one RCP, different general circulation models (GCMs) output different predicted changes in temperature and precipitation which can vary widely from each other. These vast differences in predicted temperature and precipitation, even within a single RCP, contribute further uncertainty to how water supply and hydrologic processes will be affected in the coming decades.

1.2 The Chesapeake Bay Watershed

The Chesapeake Bay Watershed is an approximately 167,000 km^2 watershed containing land within Virginia, West Virginia, Maryland, Delaware, Pennsylvania, New York, and the District of Columbia (Rice et al., 2017). This land drains to the Chesapeake Bay, the largest estuary in the United States, via a number of rivers: the Susquehanna, which drains the northernmost reaches of the watershed in New York and Pennsylvania; the Patuxent and Choptank, which drain Maryland and part of Delaware from opposite directions; the Potomac, which gains water from tributaries through parts of northern Virginia, West Virginia, Pennsylvania, and Maryland; and the York, Rappahannock, and James, which flow to the Bay through northern and central Virginia (Rice et al., 2017). Additionally, areas

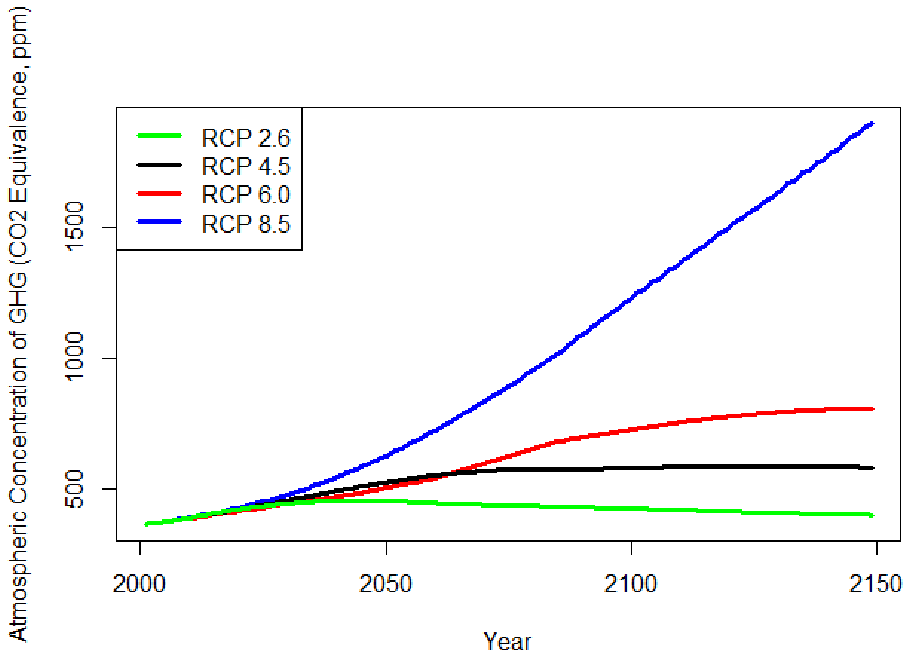

Figure 1.1: Greenhouse Gas Concentrations in Emissions Scenarios RCP 2.6, RCP 4.5, RCP 6.0, and RCP 8.5 (Clarke et al., 2007, Fujino et al., 2006, Hijioka et al., 2008, Riahi et al., 2007, Smith and Wigley, 2006, van Vuuren et al., 2007, Wise et al., 2009)

of Maryland along the Chesapeake's western shore, as well as parts of Delaware, Maryland, and Virginia along the Chesapeake's eastern shore, drain to the Chesapeake Bay without first joining a major contributing river. These major river basins within the Chesapeake Bay Watershed are shown in Fig. 1.2, with the basins further subdivided into their minor basins with white borders.

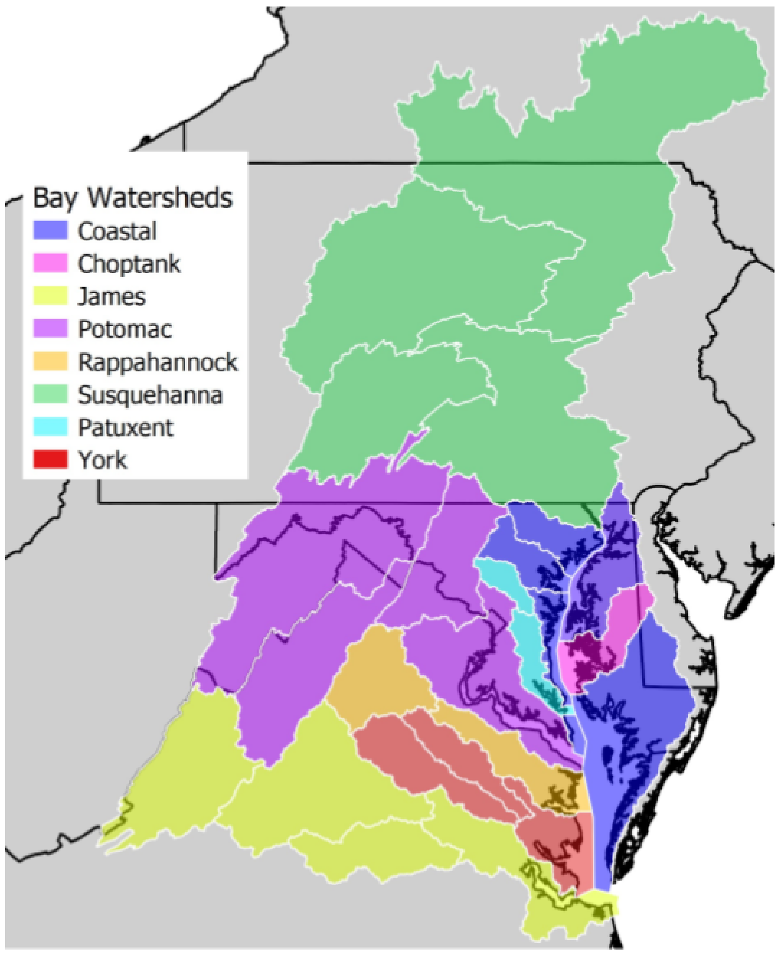

Figure 1.2: River Basins in the Chesapeake Bay Watershed (Krstolic et al., 2005)

As a result of high nutrient and sediment inputs to the Chesapeake Bay, the Bay experiences the formation of hypoxic dead zones (Zhang et al., 2013). High nutrient levels accelerate the growth of phytoplankton, which can block sunlight from reaching submerged aquatic vegetation (SAV) and reduce dissolved oxygen concentration in the water when decomposing

(Zhang et al., 2013). Suspended sediment compounds this issue by increasing the turbidity of the water, further reducing the penetration of sunlight and inhibiting the growth of SAV (Zhang et al., 2013). Heavy freshwater flows to the Chesapeake Bay via rivers also contribute to these water quality issues, as they strengthen the stratification of the water column and prevent the replenishment of oxygen to these submerged hypoxic regions (Zhang et al., 2013).

As a result, Total Maximum Daily Loads (TMDLs) restricting nutrient inputs have been applied to the Bay and its contributing rivers since 1992 in an effort to reduce the hypoxic conditions (Linker et al., 2013). Additionally, TMDLs for sediment were implemented in 2010 in an attempt to reduce the Bay's turbidity with the end goal of reducing the extent of hypoxic zones and replenishing the Bay's living resources (Linker et al., 2013). The Bay's water quality issues persist to this day, necessitating the existence of the Chesapeake Bay Program, which monitors the restoration of the Bay and creates a number of models of the Bay's current and future hydrologic and quality characteristics.

1.3 Streamflow in Virginia

Although much of Virginia drains to the Chesapeake Bay, many of the southernmost reaches do not. Northern and central Virginia drain to the Chesapeake Bay via the Shenandoah, Potomac, Rappahannock, York, and James Rivers. The Eastern Shore of Virginia, composed of Virginia's land on the Delmarva peninsula, drains either to the Chesapeake Bay or to the Atlantic Ocean via surface runoff and small streams. Much of southeast and south-central Virginia drains to the Albermarle Sound via the Roanoke River or via rivers such as the Meherrin, Nottoway, and Blackwater Rivers in the Chowan River basin. A minute section of Virginia, consisting of small portions of Grayson, Carroll, and Patrick Counties, is in the Upper Yadkin watershed, gradually flowing into the Pee Dee River and entering the Atlantic

Ocean near Georgetown, South Carolina. The remainder of southwest Virginia drains to the Ohio River via the Big Sandy, Tennessee, and New Rivers. All of these Virginian river basins are shown in Fig. 1.3 (Esri, 2014, Krstolic et al., 2005).

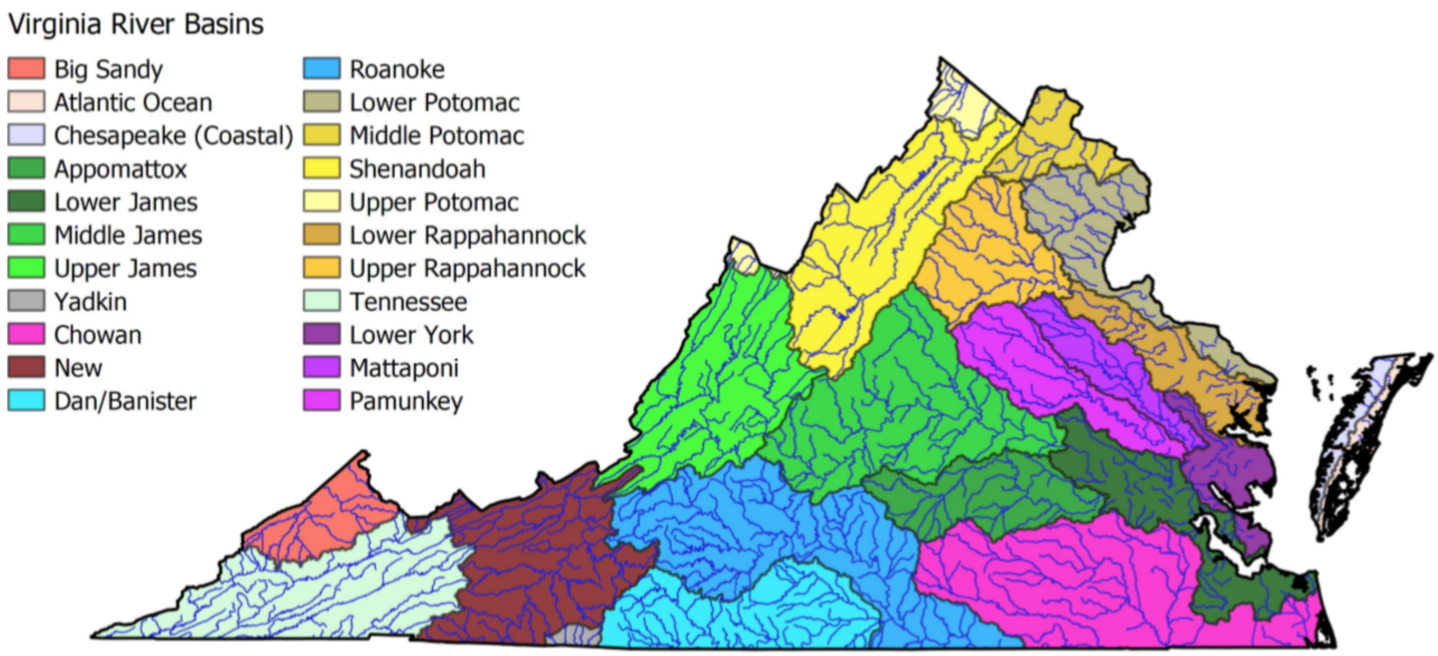

Figure 1.3: River Basins in the Commonwealth of Virginia (Esri, 2014, Krstolic et al., 2005)

The magnitude of streamflow in Virginian rivers and those rivers' response to storms and other weather conditions varies widely across Virginia as a result of differing climate, topography, land cover and use, withdrawals, and impoundments. For example, highly sloped land near mountains may accelerate runoff transport, reducing infiltration into the ground and increasing streamflow in flashy mountain streams. In highly urbanized areas, streamflow may be unable to infiltrate through impermeable surfaces such as roadways, parking lots, and buildings, similarly resulting in the quick conveyance of rainfall through storm sewers to streams and rivers throughout the area. Water that is withdrawn from rivers for consumptive uses (such as agricultural irrigation, in which most of the water is evapotranspired or transported out of the watershed within the crop) will reduce the streamflow downstream of the withdrawal point (VADEQ, 2018). Similarly, water trapped within man-made impoundments will alter the magnitude of downstream flows depending on the schedule of dam releases, often reducing downstream peak flows and smoothing the naturally dynamic nature of the flow regime which is critical to biodiversity and ecosystem function (Poff et al., 1997).

1.4 Purpose and Scope

The goal of this study is to identify the extent of possible responses in precipitation, temperature, and evapotranspiration to the RCP 4.5 climate change emissions scenario and to identify how these meteorological changes may affect runoff from different land uses and resulting streamflow in Virginia rivers draining to the Chesapeake Bay. To do this, meteorological and runoff changes for a variety of land uses will be spatially analyzed and hotspots of especially low or high change will have their hydrologic responses analyzed. Streamflow will be analyzed both on an individual watershed and overall basin scale to identify how flow might respond to climate change at different spatial resolutions.

Chapter 2

Review of Literature

2.1 Meteorological Alterations from Climate Change

The intensity and frequency of large storm events are expected to increase as a result of climate change, with more precipitation falling as rain due to increasing temperatures (Mukundan et al., 2020). In a study conducted by Rice, Moyer, and Mills, precipitation amount, frequency, and intensity were found to have increased in the eastern U.S. between 1910 and 1996, with this trend expected to continue into the future (2017). However, the extent of precipitation and temperature change in the coming decades is uncertain. Predicted precipitation and temperature from different GCMs can vary widely, resulting in claims that the greatest source of uncertainty in modeling streamflow's response to climate change comes from the meteorological conditions predicted by the GCMs themselves (Teng et al., 2011). For example, in a study by Teng et al., variability in mean annual streamflow within one rainfall-runoff model when fed meteorological data from fifteen different GCMs had an approximately 30% difference between the minimum and maximum results (2011). However, variability in mean annual streamflow between five different rainfall-runoff models when fed meteorological data from the same GCM was less than 7% between the minimum and maximum results (Teng et al., 2011).

One way to mitigate uncertainty arising from such large variability between conditions predicted by different GCMs is to assemble a large ensemble of GCMs and to create different precipitation and temperature scenarios based on some of the largest, smallest, and most average GCM precipitation and temperature outputs. In a study by Mukundan et al. which used twenty GCMs applied to a south-central New York watershed to estimate meteorological changes from the RCP 8.5 emissions scenario, mean air temperature was projected to increase by +1.4 to +4.7°C while average precipitation was projected to change between -2.0 to +17.8% (2020). The use of a large ensemble of GCMs had the benefit of showing a wide range of possible future climates to more accurately account for uncertainty in future climatic change (Mukundan et al., 2020).

Issues also arise during the creation of a meteorological time series meant to represent future temperature and precipitation. Specifically, shortcomings exist in the Change Factor Method (CFM) often used to create meteorological time series to describe climate change scenarios. In the CFM, multiplicative or additive factors are applied to an observed meteorological time series, changing the magnitude of observed storms (Mukundan et al., 2019). However, the timing, frequency, duration, and relative frequency of large- and small-magnitude storms are unaltered – all of which will in reality be changed by uncertain climatic futures and can greatly affect antecedent conditions of soil moisture, in turn affecting hydrologic processes such as infiltration, surface runoff, and streamflow (Mukundan et al., 2019). These issues can partially be remedied by the use of a stochastic weather generator (SWG), which can model plausible storm events which were not observed during the duration of the historical meteorological time series through statistical methods (Mukundan et al., 2019). In one study by Mukundan et al., streamflow modeled using synthetic time series of precipitation and temperature from a stochastic weather generator was found to capture the seasonal timing and magnitude of observed extreme hydrologic events (Mukundan et al., 2020).

2.2 Flow Regime Alterations Resulting from Changes in Land Use/Land Cover

As population increases in certain areas and land is converted from natural land and cropland to the paved surfaces associated with urban cities and their surrounding suburbs, hydrologic processes including infiltration, surface runoff creation, and streamflow are affected. Hydrologic response varies widely across any given region as a result of varying land use and land cover. Impervious surfaces, such as roads and buildings, are linked with increased runoff and flashier responses. Natural surfaces, such as forests, have comparatively more water infiltrated into the ground and taken up by plants as a result of the surface's increased permeability. In a study conducted on a large (54,972 km^2) river basin in south-central India, hydrologic changes were found to be minimized on the whole-basin spatial scale as a result of opposing trends in land use/land cover change which induced runoff reduction in 1087 km^2 of the basin but induced runoff increases in 1150 km^2 (Garg et al., 2017). On smaller spatial scales, runoff and PET changes resulting from land use and land cover change do not balance out, resulting in decreased runoff generation and increased PET in some areas (such as where cropland is converted into a water body through the creation of impoundments) and increased runoff generation and decreased PET in other areas (such as where cropland is converted to built-up land as a result of urbanization) (Garg et al., 2017).

Hydrologic response to land use changes tends to be quite similar throughout the globe, with urbanization resulting in decreased infiltration and increased runoff but afforestation and conversion to grasslands and other natural cover resulting in increased uptake and infiltration and decreased surface runoff. In many cases, the reduced permeability of surfaces resulting in rapid transport of precipitation to streams and rivers in the form of runoff results in flashy behavior and reduced baseflow in the stream (Dow, 2007). Deforestation is found to affect different magnitude flows in unique ways. In East Africa, peak flows, mean annual discharge, and surface runoff were all found to increase as a result of deforestation, while the lowest flows were found to decrease (Guzha et al., 2018). A similar effect of deforestation on the flow regime was seen in two watersheds in India, where the decrease in low flows was found to be a result of reduced percolation resulting in reduced baseflow, exhibiting the increased flashiness of the hydrologic response when less infiltration and plant uptake occurs (Sajikumar and Remya, 2015). Within the eastern Piedmont region of the U.S., in watersheds with an urban land coverage of above 10-15%, the runoff pattern was found to be dominantly controlled by that urban land (Julian and Gardner, 2012). These urban-dominated watersheds tended to have flashier responses to storms and tended to have shorter hydrologic system memory than land in its pre-urbanized forest state (Julian and Gardner, 2012). A study on historical streamflow change in the whole of the Chesapeake Bay over the years 1927-2014 noted the significant change in land use resulting from urbanization during the study period, implying that the streamflow of the studied Chesapeake Bay watershed will also be significantly impacted as a result of land use change (Rice et al., 2017).

Urbanization and deforestation are both found to reduce the infiltration of water, in turn resulting in an increase in runoff and overall streamflow but a decrease in baseflow (Rodrigues et al., 2019). In a study in southeast Brazil by Rodrigues et al., the transformation of forested to agricultural land predicts a mean flow increase of 52% between 2017 and 2030, although the implementation of a variety of BMPs such as bioretention cells, rain gardens, infiltration trenches, and permeable pavements was found to reduce the predicted 2030 flow by 44% (Rodrigues et al., 2019). In another Brazilian study, extreme land use change resulting from conversion of forest land to agricultural land was found to result in significantly increased surface runoff – however, due to heavy withdrawals for irrigation in newly created croplands, changes in river flows were found to be minimal (Calijuri et al., 2015). Additionally, runoff generation from lands within the watershed that had been converted to agricultural land depended highly on the planted crop – perennial plants, such as coffee, had a far lesser impact on runoff when compared to annual plants, such as a number of vegetables (Calijuri et al., 2015). A study in the tropical Upper Brantas watershed of Indonesia showed a similar response: loss in forest cover, with increases in agricultural and urbanized land, were linked with increased runoff and increased water yield reaching rivers (Astuti et al., 2019). These land use changes from existing natural land to urban land and cropland are seen in a number of developing areas, such as in Pune, India, where urban area has increased from 5.1% to 10.1% and cropland has increased from 9.7% to 13.5% of the catchment area between 1990 and 2010 (Wagner et al., 2013).

In the watershed of the Rhine in western Europe, two competing trends in land use change with opposite impacts on runoff generation exist: urbanization and the conversion of cropland to grassland, forest, and other natural areas (Hurkmans et al., 2008). Although these two land use changes may cancel each other out (or at least reduce the impact of each other) on smaller scales, urbanization is expected to lead to dramatically increased flows in some areas of the basin while afforestation and conversion to grasslands are expected to lead to reduced flows in other areas of the basin (Hurkmans et al., 2008, Wagner et al., 2013). Warming of the Rhine basin is also expected to accelerate, shifting the system from a snowmelt-driven regime to a less predictable rainfall-driven regime with higher peak flows and decreased low flows (Hurkmans et al., 2008).

Although increases in urban land and cropland often have opposite impacts on PET and runoff which can offset each other to some degree, they can also significantly impact the timing of flows (Wagner et al., 2013). Urbanization leads to increased runoff during precipitation events, increasing streamflow during the already high-flow rainy season and worsening floods, while increased cropland leads to increased demand for water and increased withdrawals during the already high-demand and low-streamflow growing season, worsening growing-season droughts (Wagner et al., 2013). In northeast China, conversion of land from forest to farmland resulting from China's land reform policy pushing towards increased agricultural production resulted in slightly reduced runoff reaching streams and rivers – this reduction was concluded to be a result of vastly increased agricultural withdrawals in the region (Zhang et al., 2012). This trend was not evident in many of the other river basins of China, where increasing trends in water yield and runoff were seen in the vast majority of Chinese river basins between 1900 and 2000 (Liu et al., 2008). Evapotranspiration in China was found to be drastically increased in areas of deforestation, largely due to that land's conversion to rice paddies and irrigated croplands post-deforestation (Liu et al., 2008).

Increases in runoff resulting from land use change are also found to be linked with increases in certain types of non-point source (NPS) pollution. In Indiana, an 18% increase in urban areas was linked with a 80% increase in runoff volume and an associated 50% increase in loads of lead, copper and zinc (Bhaduri et al., 2000). However, a decrease of 15% in nitrogen and phosphorus loads was also estimated, thought to be a result of the loss of heavily fertilized agricultural land in the watershed (Bhaduri et al., 2000).

2.3 Flow Regime Alterations Resulting from Climate Change

Increased precipitation and hotter temperatures resulting from climate change will have drastic impacts on the flow regime of rivers, although the impact of a changing climate is often intertwined with the previously discussed changes in land use and land cover. Correlations simply between precipitation and streamflow alone are relatively weak, resulting from the large number of other factors (lag times between precipitation occurrence and resulting peak flows, uneven travel times throughout a watershed for precipitated water to reach any given point, differing land uses and land covers, changes in temperature and evapotranspiration throughout the year, and antecedent moisture conditions affecting infiltration and surface runoff) that can drastically impact the timing and magnitude of quickflow (Rice et al., 2017). In the U.S.'s Mississippi River basin, streamflow has been steadily increasing since the 1940's, partially as a result of increased precipitation linked with a changing climate (Zhang and Schilling, 2006). This increased streamflow is also linked with changing land use, including the conversion of wildlands covered by perennial vegetation to agricultural lands planted with seasonal row crops, which has led to reduced PET and surface runoff, increased groundwater recharge, and increased baseflow and streamflow within the basin (Zhang and Schilling, 2006). This increase in the magnitude of flows across the flow regime can be beneficial (increased low flows result in increased water supply during droughts) but can also be harmful (increased high flows resulting in the increased severity of floods and a reduction in aquatic organisms as they become entrained in the flow and washed away).

A similar study conducted in the Missouri River system noted a positive relationship between precipitation change and baseflow but a negative relationship between conversion to agricultural land use and baseflow (Ahiablame et al., 2017). The severity of precipitation change's impact on baseflow (1.5% increase in baseflow per 1% increase in precipitation) was found to be greater than the severity of agricultural land use change's impact (0.2% decrease in baseflow per 1% increase in agricultural land), suggesting that climate change might have a more severe impact on baseflow than land use change (Ahiablame et al., 2017). However, in some other studies, the opposite was found to be true, suggesting that the relative importance of precipitation changes and land use changes are largely region-specific. In the wetland-rich upper Mississippi River basins in Minnesota, less than half of the increase in river flows was found to result from changes in precipitation and crop evapotranspiration, with the rest found to result from artificial drainage systems associated with agriculture and from the loss of depressed wetland areas which previously stored significant quantities of water (Schottler et al., 2013). In some systems where groundwater withdrawals are the primary source of water supply, such as in Hanoi, Vietnam, urbanization is linked with the draining and conversion of local surface-water bodies (Kuroda et al., 2017). In Hanoi's case, these local surface-water bodies were found to be primarily responsible for the recharge of the unconfined aquifers from which water was commonly withdrawn, with vertical rainwater infiltration playing a much smaller role – thus, the elimination of surface-water bodies is linked with significantly reduced groundwater recharge, leading to water supply issues if these drainings were to continue (Kuroda et al., 2017).

How the flow regime changes as a result of climate change is largely region-dependent, although streamflow has generally been found to decrease when associated with increased temperatures or decreased precipitation. In small, seasonally dry river basins in the Mediterranean, climate change was found to substantially reduce the magnitude and increase the seasonality of streamflow through the intensification of winter floods and prolonging of summer droughts (Pumo et al., 2015). For each of the case study watersheds in Pumo et al.'s study, the RCP 8.5 emissions pathway was found to have more drastic reductions in streamflow than the moderate RCP 4.5 emissions pathway (2015). Additionally, streamflow based on predicted climate conditions for the year 2090 was found to be more dramatically reduced than streamflow based on predicted climate conditions for the year 2055 (Pumo et al., 2015). In a similar study conducted in the Athabasca oil sands of Canada, the frequency of low flows was found to increase as a result of warmer temperatures resulting from climate change (Leong and Donner, 2014). Other processes are occasionally found to have a more drastic impact on streamflow than either land use or climate change. In some rapidly developing areas, including Lagos, Nigeria, mechanisms including drastically increased demand resulting from rapid population growth and distribution losses resulting from an inadequate water distribution system were found to have a greater impact on water supply than either climate change or land use change (Kandissounon et al., 2018).

2.4 Impacts of Changing Flow Regime on Biota

As a result of altered streamflow resulting from both climate and land use change, the riparian ecosystem in which much aquatic biota resides is altered. The increased frequency and severity of both extreme high and low flows can lead to increased entrainment and washout of aquatic organisms or insufficient dilution of pollution, respectively. Anthropogenic land uses (such as agriculture) in close proximity to streams were found to lead to geomorphological changes such as channel incision, which in turn led to deeper channels, increased sediment loads, and a reduction in the density and diversity of fish (Burcher et al., 2007). Channel widening is another source of sediment resulting from the increased river flows often seen as a result of increased precipitation and urbanization (Schottler et al., 2013). On the other hand, urban land cover was linked with a reduction of the in-stream suspended sediment concentration, creating a more hospitable ecosystem for many fish (Burcher et al., 2007). However, urban land cover is linked with increased concentrations of a variety of other pollutants which can contribute to stream water quality impairment.

Chapter 3

Research Questions

The relationship between a variety of climatic changes (including those relating to temperature, evapotranspiration and precipitation) and a number of hydrologic responses (surface runoff and streamflow) are important to quantify for effective water supply planning for a future with uncertain conditions. The primary questions involving these changes are:

- How might temperature, evapotranspiration, and precipitation change in the study region as a result of climate change?
- How will the aforementioned changes in temperature, evapotranspiration, and precipitation affect the magnitude of surface runoff generated from a variety of different land uses?
- How will the streamflow regime change throughout the study area between scenarios representing meteorological conditions predicted by the tenth percentile, fiftieth percentile, and ninetieth percentile of global circulation models in the Chesapeake Bay Program's model ensemble?

To investigate these questions, meteorological data and simulated hydrologic responses to different land uses from the Chesapeake Bay Program's suite of modeling tools will be coupled with the VADEQ VA Hydro hydrologic model, which features improved modeling of consumptive water use and impoundments within the Commonwealth of Virginia.

Chapter 4

Methods

4.1 Spatial Scope

As a result of the Virginia Department of Environmental Quality's (VADEQ) primary interest in the waterways of Virginia, research was confined to the borders of the Commonwealth of Virginia. Furthermore, as a result of limited available GCM data, the area of study was pared down to solely the areas of Virginia contained within the Chesapeake Bay Watershed. The Chesapeake Bay's health has been jeopardized by pollution and invasive species, resulting in both governmental and non-legislative attempts to restore the health of the Bay. Due to urbanization, population growth, and changing land use in the Chesapeake Bay watershed, the benefits of a number of Bay restoration attempts have been offset (Goetz et al., 2004). Due to the rapidly changing nature of this area, the Chesapeake Bay watershed was selected as ideal to determine how changing land use and population may result in changes to the magnitude of surface runoff and river flows. To remove the confounding impacts of tidal forces present in the easternmost regions of Virginia, streamflow was primarily investigated in areas lying outside of Virginia's Coastal Plain physiographic province. As a result, streamflow analysis is focused in the Shenandoah prior to its confluence with the Potomac; in the James above the Fall Line; in the Appomattox upstream of the George F. Brasfield Dam; in the Mattaponi and Pamunkey above the Fall Line (and prior to their confluence with the York); and in the Rappahannock above the Fall Line. The watersheds contained within this study area are shown in Fig. 4.1.

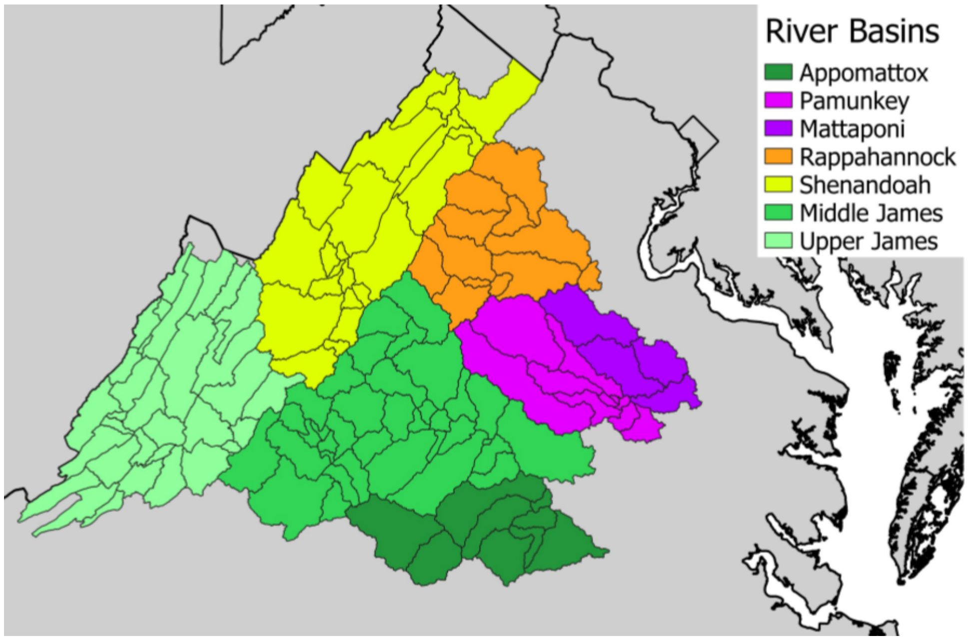

Figure 4.1: River Segments in the Study Area (Non-Coastal Virginia Watersheds in Major Basins Draining to the Chesapeake Bay)

4.2 Chesapeake Bay Model

The Chesapeake Bay Program, a multi-state partnership responsible for restoring and protecting the Chesapeake Bay, has created a suite of models to predict the effects of watershed management, population growth, climate change, and other systematic alterations on the quality and quantity of water within the Bay and its contributing waters. The Chesapeake Bay suite of modeling tools is composed of an airshed model, a land change model, a scenario builder, a watershed model, and an estuary model (Paolisso et al., 2015). The airshed model, an application of the U.S. EPA's Community Multi-scale Air Quality (CMAQ) modeling system on a 12x12 km grid scale over the Chesapeake Bay watershed, assesses the transport, transformation, and deposition of pollutants using meteorological and emissions inputs (Paolisso et al., 2015). The land use change model quantifies changes in nitrogen, phosphorus, and sediment loads in the Bay based on changing land use (from satellite imagery), population projections, and sewer/septic system usage (Paolisso et al., 2015). The scenario builder generates inputs for the watershed model based on airshed model and land use change model outputs in addition to data on the presence and performance of best management practices (BMPs), on plant growth and uptake, and on other processes (Paolisso et al., 2015, Shenk and Linker, 2013). The watershed model uses hourly values for rainfall, snowfall, temperature, potential evapotranspiration, wind, solar radiation, dewpoint, and cloud cover, as well as scenario builder inputs and data used in previous models such as the annual area of each land use (obtained from land cover data at a one-meter by one-meter resolution), to simulate streamflow and loadings of nitrogen, phosphorus, and sediment (CBP, 2017a,b, Paolisso et al., 2015, Shenk and Linker, 2013, Shenk et al., 2012). The watershed model is an application of Hydrological Simulation Program-Fortran (HSPF), through which hydrologic, sediment, and pollutant transport properties are simulated for land surfaces of varying perviousness, within the soil profile, within streams and rivers, and within well-mixed impoundments (Donigian et al., 1984, Paolisso et al., 2015, Shenk et al., 2012). HSPF is a continuous, conceptual, lumped-element model – meaning that the Chesapeake Bay application is a time-varying representation of the rivers of the Chesapeake Bay, split up into land segments treated as meteorologically and hydrologically homogeneous entities (Shenk et al., 2012). The Chesapeake Bay watershed model differs from most HSPF models in that its land and river simulations are separated, allowing flows from one land segment to enter many different river segments (Martucci et al., 2005, Shenk et al., 2012). The streamflow outputs of this watershed model, as well as the precipitation, potential evapotranspiration, and unit runoff by land use values used as inputs to this model, will be the primary focus of this report. The estuary model is used to create water quality standards based on dissolved oxygen concentration, chlorophyll concentration, and water clarity outputs (Paolisso et al., 2015). It is a coupled model, describing hydrodynamics, biogeochemical processes, sediment transport, and living resources (Paolisso et al., 2015).

The spatial extent of the Chesapeake Bay watershed is divided into river segments, land segments, and land-river segments for the purpose of calculating different population-linked and hydrologic properties. Land segments are largely county- or city-scale areas of land, representing the smallest scale that much of the pertinent information about crop types, nutrient application rates, and other inputs is commonly available at (USEPA, 2010). Land segments are sometimes further divided based on physiographic or topographical differences to improve the simulation of meteorological variables, especially near the Appalachian Mountains where orographic effects may significantly impact variance in in-county precipitation (Andrews, 2008, USEPA, 2010). Each land segment in the Bay watershed has a separate simulation of runoff for each of the Chesapeake Bay model's land use types (Shenk et al., 2012). River segments are the spatial extents of watersheds draining to each river reach (section of river that is simulated as a single unit in the model) (USEPA, 2010). Only river reaches with discharges of 100 cubic feet per second (cfs) or larger had their watersheds delineated and defined as river segments, unless streamflow monitoring data (such as from a USGS discharge gage) in a reach with discharges of at least 50 cfs was available (Shenk et al., 2012, USEPA, 2010). The numeric connection scheme between river segments, with the last four numerals in a river segment name defining the immediately downstream segment, is shown in Fig. 4.2. Land-river segments were then defined as the intersection between the politically- and meteorologically-bounded land segments and the hydrologically-bounded river segments. Land-river segments have the purpose of routing flows and nutrient loads from the land simulation to the river simulation based on the proportions of common area between a land segment and its overlapping river segments (Martucci et al., 2005).

Within the phase 6 CBP watershed model, land can be classified into over forty land uses

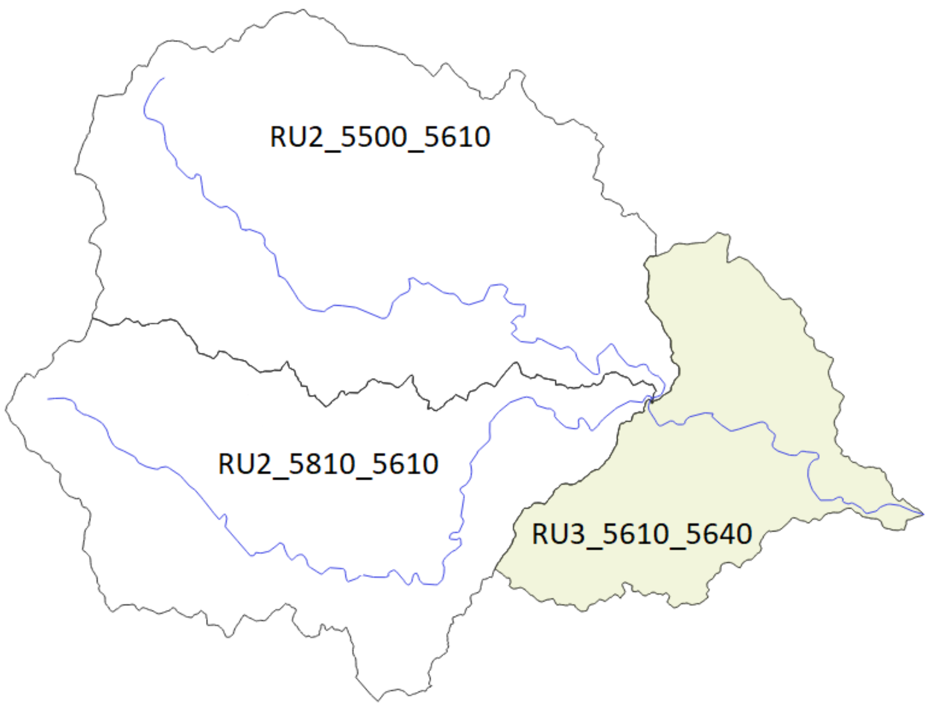

Figure 4.2: Depiction of Upstream River Segments (RU2_5500_5610 and RU2_5810_5610) Flowing into a Downstream River Segment (RU3_5610_5640)

within three categories: natural, agricultural, and developed (CBP, 2017a). Land use, representing how land is used by humans (such as for agricultural or residential purposes), is different than land cover, representing land surface characteristics that are observable (such as tree canopy cover) (CBP, 2017a). Both land cover and land use can impact loadings of nutrients and quantities of flows, so the CBP's land use classification schema is meant to take both into consideration (CBP, 2017a). Due to the limited temporal availability of land use data, land use areas were often estimated through linear interpolation for the many years without existing data (CBP, 2017a). Accurate prediction of land use conversion, primarily from agricultural, wetland, or forest to residential, industrial, or commercial uses, is essential in the modeling of stream ecosystems, especially due to the reduced infiltration, reduced base flows, and reduced lag time between storm events and peak discharge seen in watersheds with large proportions of impervious area (Goetz et al., 2004).

Natural land uses include true forest (”for”), harvested forest (”hfr”), non-tidal floodplain wetlands (”wfp”), and water (”wat”) (CBP, 2016, 2017a). The developed category of land uses is further split into combined sewer system (CSS), municipal separate storm sewer system (MS4), and non-regulated developed area subcategories (CBP, 2016, 2017a). Each of these subcategories has its own land use for turf grass (”ctg”/”mtg”/”ntg”), tree canopy over turfgrass (”cch”/”mch”/”nch”), tree canopy over impervious (”cci”/”mci”/”nci”), roads (”cir”/”mir”/”nir”), and buildings/other (”cnr”/”mnr”/”nnr”) (CBP, 2016, 2017a). The CSS and MS4 subcategories additionally have a land use for construction (”ccn”/”mcn”), while the CSS subcategory has further land uses for true forest (”cfr”) and mixed open (”cmo”) (CBP, 2016, 2017a).

Similarly, the agricultural category is further split into four subcategories: commodity crops, hay and forage, specialty crops, and other (CBP, 2016). The commodity crops agricultural subcategory includes land uses such as full season soybeans (”soy”), grain with/without manure ("gwm"/"gom"), silage with/without manure ("swm"/"som"), and other agronomic crops ("oac") (CBP, 2016). The hay and forage agricultural subcategory consists of pasture ("pas"), legume hay ("lhy"), and other hay ("ohy"). Low-density ("scl") and high-density ("sch") specialty crops compose the specialty crops agricultural land use (CBP, 2016). Other agricultural land uses include agricultural open space ("aop") and permitted/non-permitted feeding space ("fsp"/"fnp") (CBP, 2016).

Nutrient loadings and runoff flows are quantified on the land-river segment scale. The nutrient load per unit area or surface runoff per unit area value for each land use is multiplied by the number of acres of each land use within the land-river segment (USEPA, 2010). These land-river segment loadings and flows are subsequently delivered to their corresponding river reach for the simulation of transport (USEPA, 2010).

However, the CBP modeling suite has a number of shortcomings. There is no quantification of uncertainty involved in the models, leading some of the stakeholders in the Bay's plans for water quality improvement to question their effectiveness at creating limits for TMDL requirements (Paolisso et al., 2015). Withdrawals are not explicitly considered in the CBP model, leading to inabilities in determining how withdrawals will affect river flow during droughts and regular conditions. Additionally, shortcomings with how the CBP watershed model handles impoundments, with all but the largest impoundments assumed to have a negligible effect on flow, have necessitated the development of VADEQ's VA Hydro hydrologic modeling system.

4.3 VA Hydro Hydrologic Model

VADEQ has created a hydrologic modeling system with the goal of improving the modeling of impoundments and withdrawals throughout the Commonwealth of Virginia. Each river segment in the Chesapeake Bay watershed model has a corresponding feature in the VA Hydro system, which is linked with that watershed's local wells, withdrawal facilities, and other surface water intakes. These features are also linked with the water model nodes which serve as containers for the data used and generated by the VA Hydro hydrologic model. Linked parameters include river channel characteristics (channel slope and length, Manning's roughness coefficients, the channel's local drainage area, etc.), withdrawals and discharges calculated based on linked facility data, time series tables of land use areas and runoff for each land use for each land-river segment within the watershed, and precipitation and evaporation time series. From this water model node page, the model can be run for scenarios with options to alter the start and end dates, the model timestep, the run mode to alter withdrawals (with options to switch between historical conditions, current conditions, maximum permitted withdrawals, 2020 demand conditions, 2040 demand conditions, and more), and the flow mode to alter the runoff dataset (including the CB model phase 6 base dataset and each of the climate change scenario datasets, among others).

VA Hydro adapts the unit runoff values for each land use to an overall quantity of unit runoff generated by each land-river segment by multiplying each land use unit runoff value with its associated area, summing the surface runoff, interflow, and groundwater outflow values within the land-river segment, and dividing by the land-river segment's area. This land-river segment unit flow represents how much surface runoff will enter the river segment's channel per unit area within the land-river segment. Numerous land-river segments are often associated with one river segment, with the total runoff entering the channel equivalent to the summed products of each land-river segment's unit flow and area. After this runoff reaches the channel, it is routed via the Muskingum method of flow routing (Brogan, 2018). At the outlet of the river segment, the flow can optionally be routed through an impoundment with a user-defined stage-storage-discharge relationship, with flow routing in this impoundment conducted via the Modified Puls method (Brogan, 2018). Flow is then routed into the immediately downstream basin. A visual example of how flow routing and hydrologic processes such as precipitation, potential evapotranspiration, and runoff work in the VA Hydro modeling context are shown in Fig. 4.3

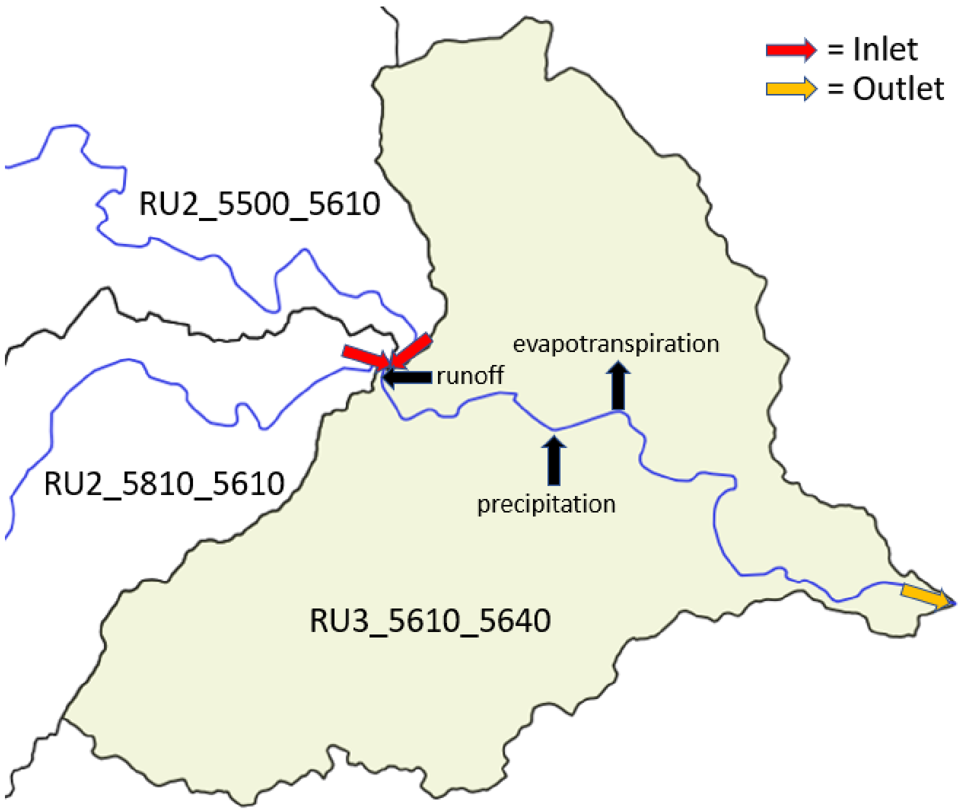

Figure 4.3: Depiction of Flow Routing between Upstream River Segments (RU2_5500_5610 and RU2_5810_5610) and a Downstream River Segment (RU3_5610_5640), with Modeled Hydrologic Processes

4.4 CBP 31 Member Climate Model Ensemble

As a result of the inherent variability involved with climate modeling, an ensemble of 31 general circulation models (GCMs) was created by the CBP. This ensemble was created with the intention of capturing the range of possible future climate conditions in the RCP

4.5 emissions pathway during the 2040-2070 timespan. The temperature and precipitation conditions seen in these GCMs are then statistically downscaled to the city- and county-scale using the bias corrected spatial disaggregation (BCSD) method (G. Bhatt, personal communication, December 20, 2019). A full list of the GCMs used in this climate ensemble, along with their average temperature and precipitation changes in the Chesapeake Bay watershed, is shown in Table 4.1.

Table 4.1: Models in CBP's 31-Member Model Ensemble and their Associated Temperature (°C) and Precipitation (%) Change over the 1940-1970 Time Period for the RCP 4.5 Emission Scenario

GCM ID	GCM Name (Country)	Changes in Air Temperature (°C)	Changes in Precipitation (%)
GCM1	ACCESS1-0.1 (Australia)	2.3	7.1
GCM2	BCC-CSM1-1.1 (China)	2.2	-1.3
GCM3	BCC-CSM1-1-1.1 (China)	1.9	3.2
GCM4	CanESM2.1 (Canada)	2.5	2.8
GCM5	CCSM4.1 (USA)	2.1	10.6
GCM6	CESM1-BGC.1 (USA)	2.2	9.5
GCM7	CESM1-CAM5.1 (USA)	2.3	18.3
GCM8	CMCC-CM.1 (Italy)	2.1	9
GCM9	CNRM-CM5.1 (France)	1.7	7.8
GCM10	CSIRO-Mk3-6-0.1 (Australia)	2.2	20.1
GCM11	EC-Earth.8 (Europe)	1.3	6.5
GCM12	FGOALS-g2.1 (China)	2.1	-1.3
GCM13	FIO-ESM.1 (China)	1	7
GCM14	GFDL-CM3.1 (USA)	3.2	16.8
GCM15	GFDL-ESM2G.1 (USA)	1.4	5.7
GCM16	GFDL-ESM2M.1 (USA)	1.3	8.6
GCM17	GISS-E2-R.1 (USA)	1.7	8.6
GCM18	HadGEM2-AO.1 (United Kingdom)	2.8	4.2
GCM19	HadGEM2-CC.1 (United Kingdom)	3	7.8
GCM20	HadGEM2-ES.1 (United Kingdom)	3.2	8.6
GCM21	INMCM4.1 (Russia)	0.9	2.3
GCM22	IPSL-CM5A-LR.1 (France)	1.9	3.5
GCM23	IPSL-CM5A-MR.1 (France)	2	0.7
GCM24	IPSL-CM5B-LR.1 (France)	2.2	1.3
GCM25	MIROC5.1 (Japan)	2.6	11.6
GCM26	MIROC-ESM.1 (Japan)	2.4	4.4
GCM27	MIROC-ESM-CHEM.1 (Japan)	2.9	9.3
GCM28	MPI-ESM-LR.1 (Germany)	1.2	8.7
GCM29	MPI-ESM-MR.1 (Germany)	1.7	7.6
GCM30	MRI-CGCM3.1 (Japan)	1.2	2.8
GCM31	NorESM1-M.1 (Norway)	2	7.9

The range of temperature and precipitation change resulting from the RCP 4.5 emissions scenario seen within this 31-member ensemble of GCMs is shown in Fig. 4.4. Although no outliers exist for temperature, a wide range of temperature increases ranging from +0.9°C in model INMCM4.1 (developed at the Russian Institute of Numerical Mathematics) to a high of +3.2°C seen in the GFDL-CM3.1 (developed at the American Geophysical Fluid Dynamics Laboratory) and HadGEM2-ES.1 (developed at the Met Office Hadley Centre in the United Kingdom) models. Two outlying models predicted extraordinarily large precipitation changes (+20.1% in the CSIRO-Mk3-6-0.1, developed by the Australian Commonwealth Scientific and Industrial Research Organization, and +18.3 in the CESM1-CAM5.1 GCM developed by the National Center of Atmospheric Research and the University Corporation for Atmospheric Research). Slight reductions in average precipitation of -1.3% were seen in the BCC-CSM1-1.1 and FGOALS-g2.1 models, which were both developed in China at the Beijing Climate Center and Institute of Atmospheric Physics, respectively. Mean changes of +2.0°C and +7.1% in the model ensemble were seen in temperature and precipitation.

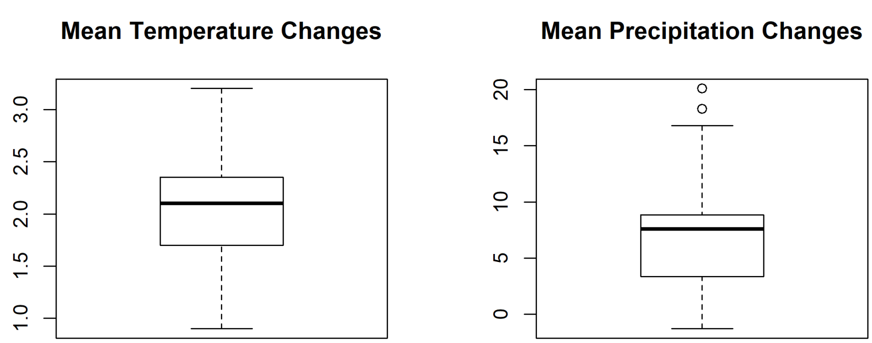

Figure 4.4: Temperature (°C) and Precipitation (%) Change seen in Models of the RCP 4.5 Emissions Scenario

4.5 Climate Change Scenarios

Four scenarios of the CBP's phase 6 Chesapeake Bay Model were provided. One of these scenarios (”base”), representing current precipitation and temperature conditions, was used as the baseline for comparison. The other three scenarios, representing the tenth percentile of precipitation and temperature (”ccP10T10”), fiftieth percentile of precipitation and temperature (”ccP50T50”), and ninetieth percentile of precipitation and temperature (”ccP90T90”) of the 31-member climate model ensemble reflecting the 30-year period centered on the year 2055, were respectively meant to represent lower, medium, and higher bounds in likely changes in climate conditions resulting from the RCP 4.5 pathway of anthropogenic climate change. The models representing the tenth, fiftieth, and ninetieth percentile of precipitation and temperature were selected individually for every city/county. Although this ensured that severe changes were seen throughout the entire state in the ccP10T10 and ccP90T90 scenarios, this piecemeal approach to selecting models had the unfortunate side effect of masking more pronounced spatial trends exhibited by the individual GCMs. The locality-scale definition of 10th, 50th, and 90th percentile climate models also resulted in the blurring of the physical definition of the scenarios – rather than serving as scenarios reflecting the conditions exhibited by any one GCM, they are qualitative scenarios, representing combinations of minor warming and wetting, moderate warming and wetting, and major warming and wetting, respectively. Each scenario also incorporated 2055 projections of land use, which took into account changes in population and septic loads. The effects of elevated ambient carbon dioxide level on transpiration was also included. These scenarios were then run through VADEQ's VA Hydro hydrologic model for a ten-year representative time period to model the effects of each of these possible climatic changes on future streamflow.

Precipitation and evaporation time series data for each of the river segments in the study area were obtained from the Chesapeake Bay Program for each of the climate change scenarios. Temperature data reflecting the tenth, fiftieth, and ninetieth percentiles of temperature predicted by the GCMs of the 31-member ensemble was also obtained from the CBP. Similarly, tables of annual land use change, as well as time series of surface runoff per acre from each of the land uses for each of the climate change scenarios were obtained and linked into the VA Hydro model.

4.6 Precipitation, Temperature, and Evapotranspiration Analysis

Monthly temperature changes (°C) in each city and county in Virginia were obtained from the Chesapeake Bay program and spatially mapped in R. When trends in latitude became visually apparent in the temperature maps, scatterplots of monthly and overall temperature against latitude and longitude were created for each climate change scenario. Further investigation was also conducted into the GCMs commonly linked with the extreme P10 and P90 temperature change predictions as well as into the temporal variability of temperature change.

Precipitation and potential evapotranspiration magnitudes (inches/ivld, where ”ivld” stands for ”interval of the data”) for each scenario were also provided on an hourly timescale for each city and county in Virginia as inputs to the Chesapeake Bay model. These values were aggregated to a daily interval, and then the mean of these daily values were taken to represent the average precipitation and potential evapotranspiration values over the period of study. Percent changes in precipitation and evaporation between the base and climate change scenarios were then calculated through the equation 4.1.

$$\% \text{ Change} = 100 * \frac{\text{Climate Change Value - Base Value}}{\text{Base Value}} \tag{4.1}$$

Just like with temperature, maps were created of precipitation and potential evapotranspiration change and spatial patterns correlated with longitude and latitude were investigated.

4.7 Land Use Unit Runoff Analysis

The values of unit runoff for each land use in each Virginian land segment were stripped from the model and investigated. Since the magnitude of unit runoff for each land use in the CBP model is primarily a function of permeability, a number of the land uses with similar or identical permeabilities were found to have identical unit runoff values. These land uses are distinguished within the CB modeling framework as they can exhibit wildly different nutrient concentrations in runoff which can have drastic impacts on water quality. True forest draining to a combined sewer system ("cfr") exhibited unique runoff generation, while natural true forest ("for"), non-tidal floodplain wetlands ("wfp"), and headwater/isolated wetlands ("wto") generated identical magnitudes of runoff per unit area. Similarly, mixed open area draining to a combined sewer system ("cmo") exhibited runoff generation behavior distinct from any other land use, as did natural mixed open area ("osp"). Meanwhile, land uses associated with hay and forage, including pasture ("pas"), legume hay ("lhy") and other hay ("ohy") all exhibited the same runoff generation potential. Another group of land uses exhibiting identical runoff generation behavior were land uses associated with commodity crop growth, including full season soybeans ("soy"), grain with or without manure ("gom"/"gwm"), silage with or without manure ("som"/"swm"), small grains ("sgg"), specialty crops ("scl"/"sch"), double-cropped land ("dbl") and other agronomic crops ("oac"). The developed land uses associated with turf grass or tree canopy over turf grass ("cch",

”ctg”, ”mch”, ”mtg”, ”nch”, and ”ntg”), regardless of whether they are in non-regulated developed areas or areas serviced by CSSs or MS4s, also generated identical runoff. The last major group of land uses which exhibited identical surface runoff generation is the group of land uses associated with impervious surfaces – that is, roads, tree canopy over impervious, and buildings/other in non-regulated developed areas and in areas serviced by CSSs or MS4s. All of these groups of land uses exhibiting identical runoff generation traits are shown in Tab. 4.2, and these land use runoff groups will be treated as uniform and not be further distinguished for the remainder of this paper.

The average percent changes in each land use group’s unit runoff was calculated and shown on radar plots (Figs. 5.25, 5.26, and 5.27). Five land use groups with especially distinct runoff responses were selected (Natural Pervious, Hay and Forage, Commodity Crops, Turf Grass, and Impervious) for further spatial investigation. Certain land segments in each scenario which exhibited the lowest or highest percent change in runoff generation for most or all of the land uses were identified. These land segments were: Amherst (low) and Harrisonburg (high) for the ccP10T10 scenario; Giles (low) and Culpeper (high) for the ccP50T50 scenario, and Highland (low) and Nottoway (high) for the ccP90T90 scenario. For each of these land segments, percent exceedance plots were created and analyzed to determine how unit runoff changed throughout the runoff regime in the climate change scenarios. Multiple linear regression was also conducted to determine how reliant runoff change for each land use was on precipitation and potential evapotranspiration.

4.8 Overall Unit Runoff Analysis

Next, each of the river basins in the study area were run through the VA Hydro model for a representative ten year period using withdrawals representing 2020 demand. In the

Table 4.2: Land Use Runoff Groups

Group	Land Use Abbreviation	Land Use Name
CSS True Forest	cfr	CSS True Forest
Natural Pervious	for	Natural True Forest
	wfp	Non-tidal Floodplain Wetland
	wto	Headwater/Isolated Wetland
CSS Mixed Open	cmo	CSS Mixed Open
Natural Mixed Open	osp	Natural Mixed Open
Hay and Forage	pas	Pasture
	lhy	Legume Hay
	ohy	Other Hay
Ag Open Space	aop	Ag Open Space
Commodity Crops	soy	Full Season Soybeans
	dbl	Double Cropped Land
	gom	Grain without Manure
	gwm	Grain with Manure
	som	Silage without Manure
	swm	Silage with Manure
	sgg	Small Grains and Grains
	scl	Specialty Crop Low
	sch	Specialty Crop High
	oac	Other Agronomic Crops
Harvested Forest	hfr	Harvested Forest
Turf Grass	cch	CSS Tree Canopy over Turf Grass
	ctg	CSS Turf Grass
	mch	MS4 Tree Canopy over Turf Grass
	mtg	MS4 Turf Grass
	nch	Non-Regulated Tree Canopy over Turf Grass
	ntg	Non-Regulated Turf Grass
Construction	ccn	CSS Construction
	mcn	MS4 Construction
Feeding Space	fnp	Non-Permitted Feeding Space
	fsp	Permitted Feeding Space
Impervious	cci	CSS Tree Canopy over Impervious
	cir	CSS Roads
	cnr	CSS Buildings and Other
	mci	MS4 Tree Canopy over Impervious
	mir	MS4 Roads
	mnr	MS4 Buildings and Other
	nci	Non-regulated Tree Canopy over Impervious
	nir	Non-regulated Roads
	nnr	Non-regulated Buildings and Other

process of calculating the streamflow in any given reach of a river, the VA Hydro hydrologic model first calculates the runoff which is entering the channel in any given reach and all of the upstream reaches. Each reach's runoff value, calculated using each of the land uses' unique unit runoff values and the amount of area of each land use within the river segment, is stored within the VA Hydro system, attached to each river segment's model property for each scenario. As a result, this overall runoff value per unit area is a simple way to evaluate the runoff production capacity of a reach in any given scenario and to compare it with the runoff production capacity of other segments throughout the state, as it serves as a representation of the capacity of all land uses present within the segment to generate runoff. In addition, this overall runoff value can be compared across the different climate change scenarios for an individual river segment in order to evaluate how runoff generation may change as a culmination of both land use unit runoff and land use area changes.

4.9 Streamflow Comparison to Historical Gage Data

To assure the quality of the coupled CBP/VA Hydro model, daily streamflow values of the base scenario were compared with historical data from USGS streamflow gages for 63 river segment-gage pairings within the study area (De Cicco et al., 2018). Two statistics were used to test how well the modeled data fit the observed historical data. The Nash-Sutcliffe Efficiency (NSE), which compares the relative magnitude of the variance in model residuals and in the observed data was calculated using equation 4.2 (Mauricio Zambrano-Bigiarini, 2020, Nash and Sutcliffe, 1970).

$$\mathrm{NSE} = 1 - \frac{\sum_{i=1}^{N}(S_i - O_i)^2}{\sum_{i=1}^{N}(O_i - \overline{O})^2} \tag{4.2}$$

Similarly, the coefficient of determination (R^2) shows how well observed outcomes are exhibited by the modeled data based on the proportion of variance explained by the model. For USGS gages with incomplete historical streamflow records, these statistics were calculated after streamflow data had been trimmed to the dates of available data. Due to slight differences between the USGS gage drainage areas and the river segment areas stored on VA Hydro, modeled streamflow values were area-weighted using Equation 4.3 prior to the calculation of these metrics (De Cicco et al., 2018).

$$\text{Area-Weighted Daily Streamflow} = \text{Unweighted Daily Streamflow} * \frac{\text{USGS Gage Drainage Area}}{\text{VA Hydro River Segment Area}} \tag{4.3}$$

These 63 river segment-gage pairings, the start and end dates for available historical gage data, and each pairing's NSE and R^2 values are shown in Tab. 4.3. Overall, the model performed moderately well, with a mean NSE of 0.41 throughout the entire study area. Some river basins performed far better than others, with the Appomattox (mean NSE = 0.67, mean R^2 = 0.67), Upper James (mean NSE = 0.53, mean R^2 = 0.64), and Pamunkey (mean NSE = 0.53, mean R^2 = 0.57) performing especially well and the Shenandoah (mean NSE = 0.23, mean R^2 = 0.27) and Rappahannock (mean NSE = 0.09, mean R^2 = 0.18) performing especially badly.

To determine if the base scenario systematically over- or under-modeled streamflow quantities throughout the flow regime, the OMF and a number of low-flow metrics (l30, l90, ALF, S10%) were calculated for both the USGS gage and modeled data. Tables showing all of these calculated metrics, as well as the percent difference between them, are shown in Appendix B. The model was found to systematically underestimate the magnitudes of both mean flows (OMF median: -5.9% difference between gage and modeled flow) and, more severely, low

Table 4.3: Model Performance Assessment between Historical Streamflow and VA Hydro Base Scenario

River Segment	USGS Gage	Gage Start Date	Gage End Date	NSE	R^2
PS5_4380_4370	01636500	1991-01-01	2000-12-31	0.25	0.26
PS1_4790_4830	01634500	1991-01-01	2000-12-31	0.16	0.19
PS5_5240_5200	01631000	1991-01-01	2000-12-31	0.21	0.21
PS4_5840_5240	01629500	1991-01-01	2000-12-31	0.24	0.24
PS4_6360_5840	01628500	1991-01-01	2000-12-31	0.11	0.18
PS2_6490_6420	01627500	1991-01-01	2000-12-31	0.28	0.29
PS2_6660_6490	01626850	1991-01-01	1996-12-10	0.18	0.20
PS2_6730_6660	01626000	1991-01-01	2000-12-31	0.43	0.44
PS3_5100_5080	01634000	1991-01-01	2000-12-31	0.01	0.12
PS2_5560_5100	01633000	1991-01-01	2000-12-31	0.20	0.26
PS2_5550_5560	01632000	1991-01-01	2000-12-31	0.51	0.57
PS3_6161_6280	01622000	1991-01-01	2000-12-31	0.11	0.18
PS3_6460_6230	01625000	1991-01-01	2000-12-31	0.29	0.34
YM1_6370_6620	01674500	1991-01-01	2000-12-31	-0.03	0.55
YM2_6120_6430	01674000	1991-01-01	2000-12-31	0.86	0.86
YP4_6720_6750	01673000	1991-01-01	2000-12-31	0.72	0.74
YP1_6570_6680	01671100	1991-01-01	2000-12-31	0.73	0.74
YP3_6470_6690	01672500	1991-01-01	1997-09-29	0.71	0.71
YP3_6330_6700	01671020	1991-01-01	2000-12-31	0.31	0.37
YP2_6390_6330	01670400	1991-01-01	1995-09-30	0.20	0.31
RU5_6030_0001	01668000	1991-01-01	2000-12-31	0.17	0.23
RU2_5220_5640	01664000	1991-01-01	2000-12-31	0.17	0.35
RU3_6170_6040	01667500	1991-01-01	2000-12-31	-0.05	0.08
RU2_5940_6200	01666500	1991-01-01	2000-12-31	0.13	0.19
RU2_6090_6220	01665500	1991-01-01	2000-12-31	0.04	0.05
JA5_7480_0001	02041650	1991-01-01	2000-12-31	0.82	0.82
JA1_7600_7570	02041000	1991-01-01	2000-12-31	0.66	0.66
JA4_7280_7340	02040000	1991-01-01	2000-12-31	0.76	0.76
JA2_7550_7280	02039500	1991-01-01	2000-12-31	0.42	0.43
JU5_7500_7420	02019500	1991-01-01	2000-12-31	0.67	0.68
JU1_7750_7560	02018500	1991-01-01	2000-12-31	0.49	0.49
JU3_7490_7400	02018000	1991-01-01	2000-12-31	0.56	0.56
JU1_7630_7490	02017500	1991-01-01	2000-12-31	0.60	0.61
JU3_6650_7300	02016500	1991-01-01	2000-12-31	0.21	0.74
JU1_6300_6650	02015700	1991-01-01	2000-12-31	0.64	0.64
JU4_7000_7300	02016000	1991-01-01	2000-12-31	0.07	0.62
JU2_7450_7360	02014000	1991-01-01	2000-12-31	0.68	0.68
JU2_7140_7330	02013000	1991-01-01	2000-12-31	0.64	0.65
JU3_6950_7330	02013100	1991-01-01	2000-12-31	0.57	0.67
JU3_6900_6950	02011800	1991-01-01	2000-12-31	0.44	0.48
JU2_6600_6810	02011500	1991-01-01	2000-12-31	0.69	0.71
JU1_6590_6600	02011470	1991-01-01	2000-12-31	0.66	0.70
JU1_6290_6590	02011460	1991-01-01	2000-12-31	0.68	0.68
JU3_6380_6900	02011400	1991-01-01	2000-12-31	0.68	0.70
JU1_6880_7260	02024000	1991-01-01	2000-12-31	0.07	0.78
JU3_6640_6790	02021500	1991-01-01	2000-12-31	0.66	0.70
JU2_6410_6640	02020500	1991-01-01	2000-12-31	0.44	0.49
JL7_7070_0001	02037500	1991-01-01	2000-12-31	0.60	0.60
JL7_6800_7070	02037000	1991-01-01	2000-12-31	-0.47	0.00
JL7_7100_7030	02035000	1991-01-01	2000-12-31	0.67	0.67
JL4_6520_6710	02034000	1991-01-01	2000-12-31	0.07	0.16
JL2_6240_6520	02032680	1991-01-01	1992-10-05	0.08	0.17
JL2_7110_7120	02030500	1991-01-01	1995-10-15	0.71	0.72
JL2_6441_6520	02032515	1991-01-01	1997-10-22	-0.10	0.05
JL1_6560_6440	02031000	1991-01-01	2000-12-31	-0.09	0.09
JL1_6760_6910	02030000	1991-01-01	2000-12-31	0.66	0.66
JL6_6890_6990	02029000	1991-01-01	2000-12-31	0.64	0.64
JL1_6770_6850	02028500	1991-01-01	2000-12-31	0.67	0.68
JL1_7080_7190	02027500	1991-01-01	2000-12-31	0.49	0.57
JL6_7430_7320	02026000	1991-01-01	2000-12-31	0.65	0.65
JL2_7240_7350	02027800	1991-01-01	1995-09-30	0.72	0.74
JL1_6940_7200	02027000	1991-01-01	2000-12-31	0.63	0.64
JL6_7160_7440	02025500	1991-01-01	2000-12-31	0.71	0.71

flows (l30 median: -38.8%, l90 median: -17.4%, ALF median: -4.6%, S10% median: -36.9% difference between gage and modeled flow). Although this systematic underestimation of low flows is something that can be remedied during the creation of future scenarios, this study was buoyed by this systematic underestimation due to its focus on investigating low flows to ensure adequate future water supply. This large percent underestimation of low-flows, which often was only an underestimate of a few cfs, served as a margin of safety from a water supply perspective. Preparing for more severely reduced conditions and being happily surprised by future flows being slightly higher than predicted is safer than the opposite: preparing for moderately reduced conditions and running out of water due to flows being lower than expected.

4.10 Streamflow Analysis

Once routed through the VA Hydro hydrologic model, major differences in streamflow between the base and climate change scenarios throughout the flow regime became evident. Both flow exceedance plots and tables of important streamflow metrics were used to exhibit the extent of these changes and to illustrate the impacts that they might have on both water supply and riverine ecosystems throughout the state.

Streamflow metrics calculated for each river segment include the Overall Mean Flow (OMF), 30-Day Low Flow (l30), 90-Day Low Flow (l90), August Low Flow (ALF), and September 10% Flow (S10%). The Overall Mean Flow is a simple metric showing the average streamflow in the reach over the entire timescale. The 30-Day Low Flow is a slightly more complex statistic. First, the minimum of rolling 30-day mean flows are calculated for each water year (Oct. 1 - Sep. 30) within the study period (Richter et al., 1996). The 30-Day Low Flow is considered to be the minimum of these annual minima. The 90-Day Low Flow is calculated in the same way, but from rolling 90-day mean flows. Both the 30-Day Low Flow and 90-Day Low Flow metrics are calculated using the IHA (Indicators of Hydrologic Alteration) package in R (Law, 2013, R Core Team, 2019). The August Low Flow is also calculated using the IHA R package (Law, 2013, R Core Team, 2019). First, the minimum of daily flows in the month of August for each year in the study period is calculated. Then, the median of these annual minimum flows is calculated – this is the August Low Flow. The September 10% flow is simply the tenth percentile of all flows in the study period occurring within the month of September. The ALF and S10% flow can be used in conjunction with each other to identify shifts in drought timing, as droughts occurring earlier in the year will result in decreased ALFs but constant or increased S10%s while droughts occurring later in the year will result in constant or increased ALFs and decreased S10%s (Brogan, 2018). The 7Q10 metric, which quantifies the 7-day low flow which has a recurrence interval of ten years, was ignored in this analysis due to the inability to calculate a valid 7Q10 from the limited ten-year representative time period for the climate change scenarios.

Daily streamflow in each river segment contained within the basin was divided by its contributing drainage area, and all of these area-weighted flow values were then averaged to determine the basin's daily streamflow per unit area. The mean and low-flow metrics were then calculated on a full-basin scale from these daily streamflow per unit area values. Although much of the spatial resolution in streamflow is lost through this process, the resulting metrics exhibit basin-wide impacts which might result from these climate change scenarios. The actual modeled streamflow values and their percent changes from the base scenario for each river segment in the study area are shown in Appendices E and F, respectively.

Chapter 5

Results

5.1 Temperature Trends

Latitude-linked trends in temperature change exist in each of the climate change scenarios, with the largest changes seen in one scenario being of a similar magnitude to the smallest changes seen in the next, hotter scenario. Temperature changes throughout the land segments in the Commonwealth which drain to the Chesapeake Bay are shown in Fig. 5.1, although these latitude-associated trends are barely visible due to the uniform scaling across the scenarios. In the tenth percentile temperature scenario, temperature increases of about 1 to 1.25°C are seen, while increases of about 1.7 to 2.2°C are predicted for the fiftieth percentile temperature scenario. The ninetieth percentile temperature scenario experiences increases of 2.2 to 3.2°C.

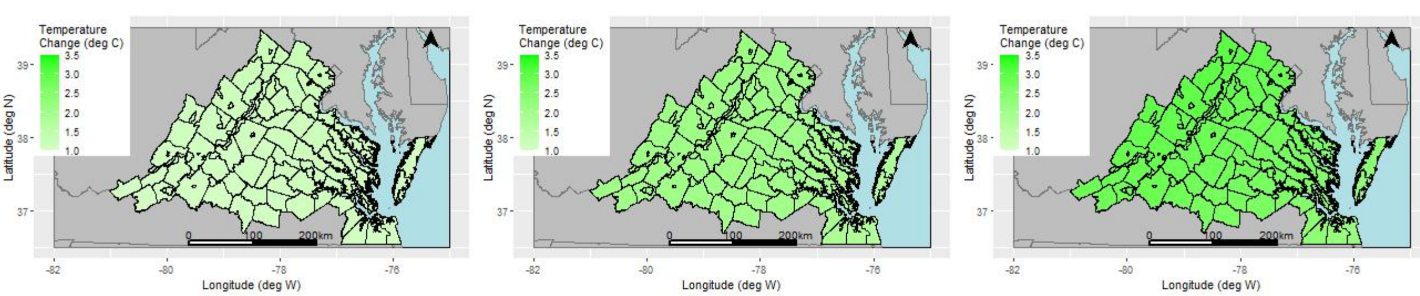

Figure 5.1: 10th, 50th, and 90th Percentile Temperature Changes in Virginia's Chesapeake Bay Watershed Land Segments

These trends of increasing temperature with increasing latitude are better seen in Figs. 5.2, 5.3, and 5.4, which have scales restricted to the minimum and maximum changes seen in each individual scenario. The tenth percentile scenario, shown in Fig. 5.2, sees the lowest temperature increases in the southern segments of Virginia's land segments in the Chesapeake Bay watershed, especially in the southwestern (Giles and Montgomery) and south-central (Charlotte and Campbell) counties. The highest temperature increases are seen in the northernmost Virginia counties (Frederick, Clarke, Loudon, and Fairfax). The fiftieth and ninetieth percentile temperature change scenarios see very similar trends, although with the lowest temperature increases seen in the southeast localities of Virginia such as Virginia Beach, Chesapeake, and Suffolk (Figs. 5.3 and 5.4) and an increasing trend visible when moving northeast towards Frederick, Shenandoah, and Rockingham counties. In these fiftieth and ninetieth percentile temperature scenarios, Northampton and Accomack counties (comprising Virginia's Eastern Shore on the Delmarva peninsula) are on the low end of temperature increase, similar in percent to that of Virginia Beach, as opposed to the more mid-level change seen in the tenth percentile temperature scenario.

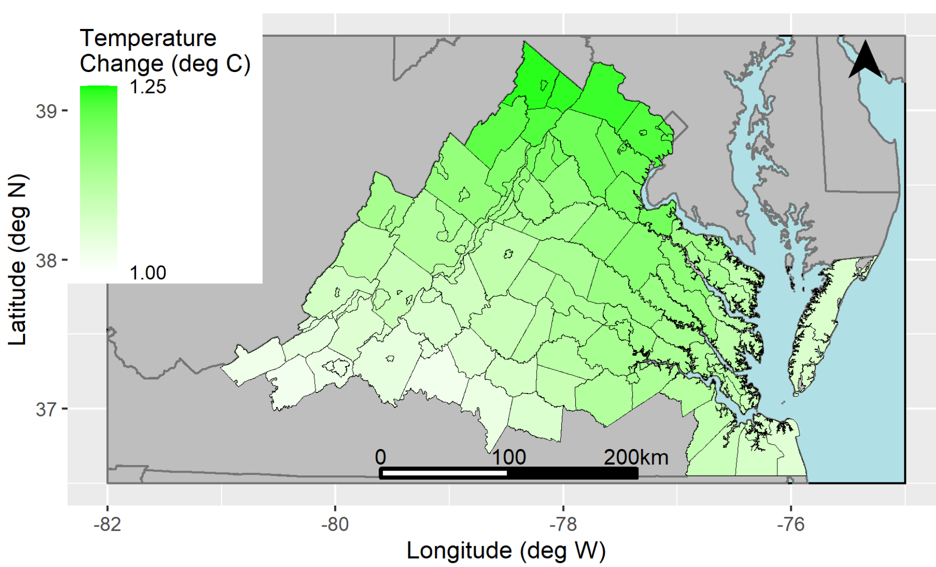

Figure 5.2: 10th Percentile Temperature Changes in Virginia's Chesapeake Bay Watershed Land Segments

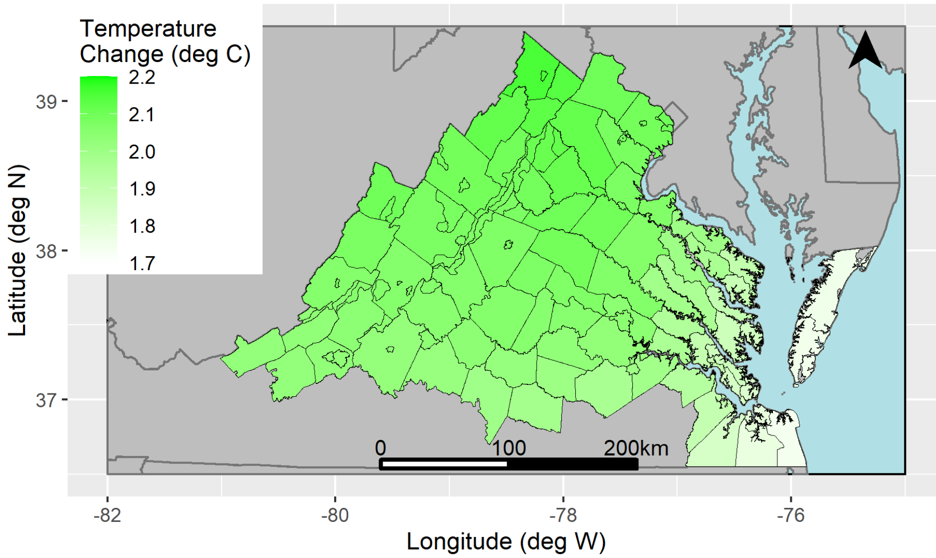

Figure 5.3: 50th Percentile Temperature Changes in Virginia's Chesapeake Bay Watershed Land Segments

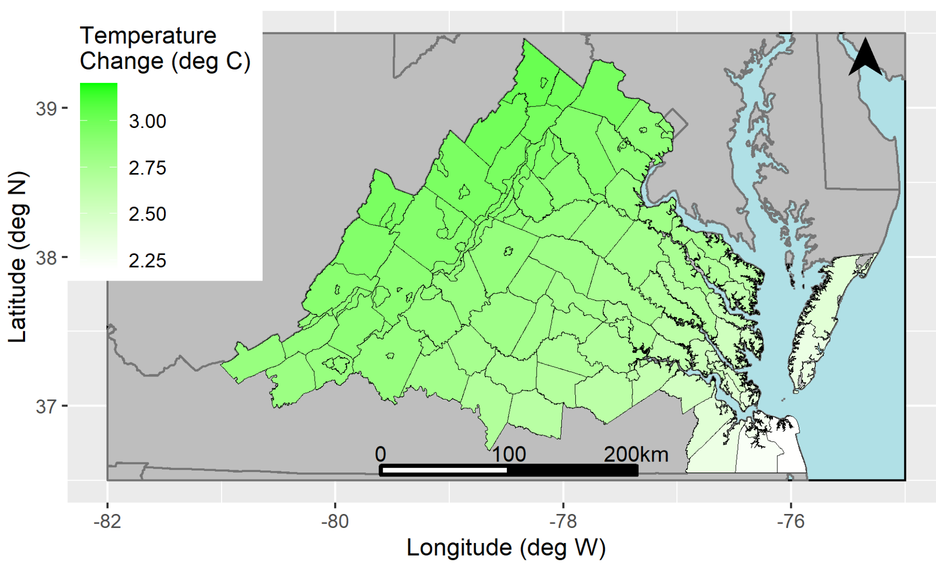

Figure 5.4: 90th Percentile Temperature Changes in Virginia's Chesapeake Bay Watershed Land Segments

As previously mentioned, temperature was moderately highly correlated with latitude, even though each temperature scenario was composed of a number of different GCMs. The tenth, fiftieth, and ninetieth percentile GCMs were determined on a land segment by land segment basis, with far fewer GCMs (four and three, respectively) composing the tenth and ninetieth percentile temperature scenarios than composed the fiftieth percentile temperature scenario (nine). These relationships between latitude and temperature change are shown in Figs. 5.5, 5.6, and 5.7. R-squared values, measuring the proportion of the variation in temperature change explained by the change in latitude, range from a low of 0.526 in the fiftieth percentile temperature scenario (about 53% of the variation in temperature explained by latitude) to a high of 0.662 (about 66% of the variation in temperature explained by latitude).

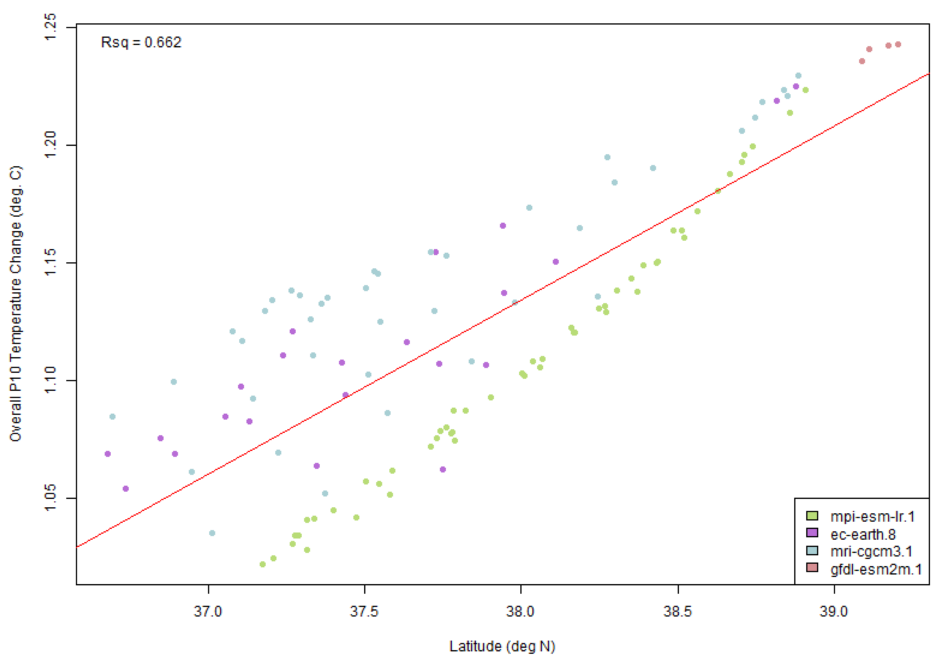

Figure 5.5: 10th Percentile Temperature Changes by Latitude

Some cursory investigation into the spatial trends of the assignment of GCMs to the climate change scenarios was also conducted. For each of these scenarios, large swaths of neighboring

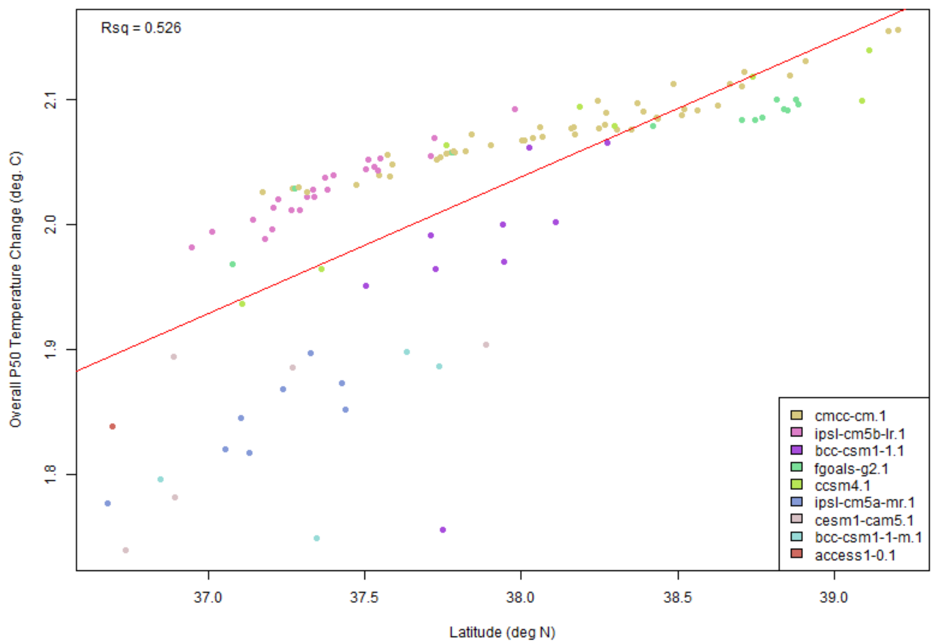

Figure 5.6: 50th Percentile Temperature Changes by Latitude

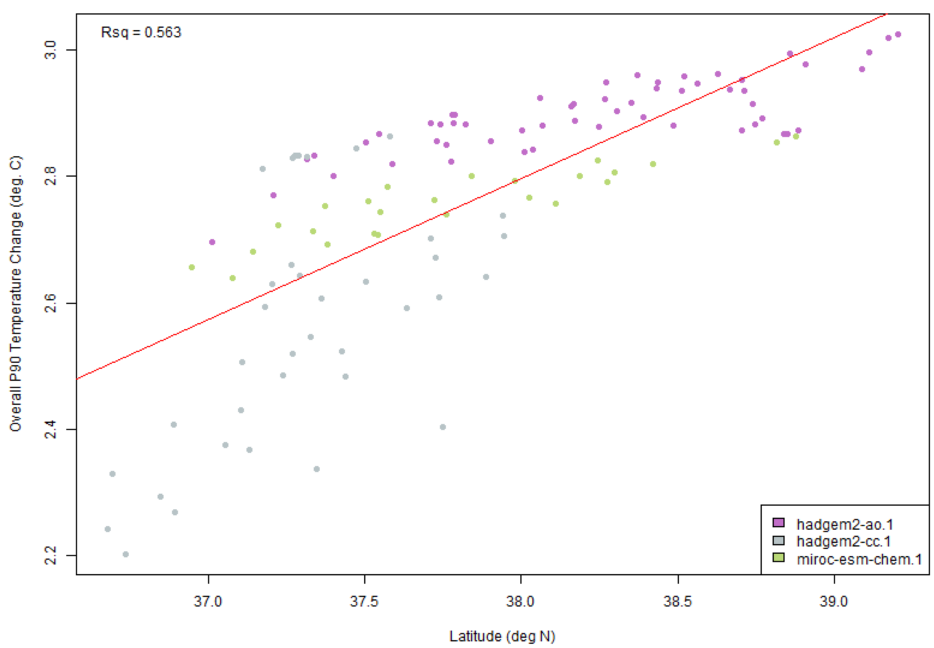

Figure 5.7: 90th Percentile Temperature Changes by Latitude

land segments were found to have been linked with the same GCMs. Maps of the GCMs associated with the tenth, fiftieth, and ninetieth percentile scenarios are shown in Figs. 5.8, 5.9, and 5.10.

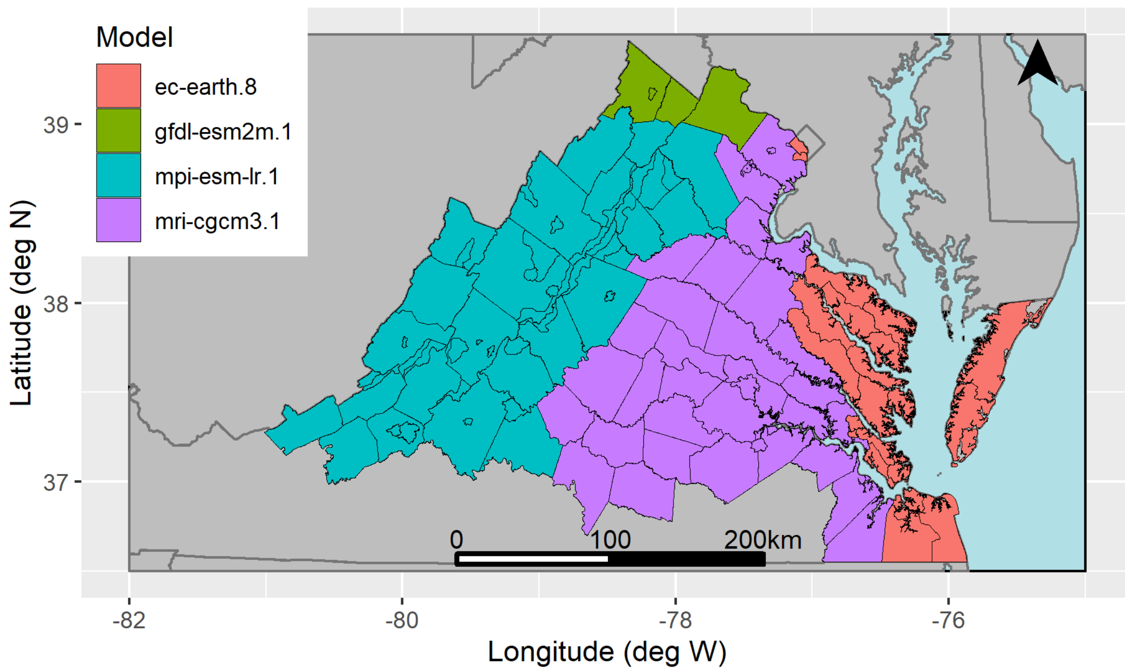

Figure 5.8: GCMs Used in the 10th Percentile Temperature Scenario

5.2 Potential Evapotranspiration Trends

Similar spatial trends exist in potential evapotranspiration (PET) percent change as existed in the temperature change data. This is likely due to the heavy dependence of both temperature and evapotranspiration on energy from solar radiation, as well as PET's partial dependence on temperature itself in many potential evapotranspiration calculation methods such as the Thornthwaite and Hargreaves-Samani equations (Lu et al., 2005). PET increased by between about 2.8% and 4.0% between the base and ccP10T10 scenario, between about 4.5% and 7.0% between the base and ccP50T50 scenario, and between about 6% to 11%

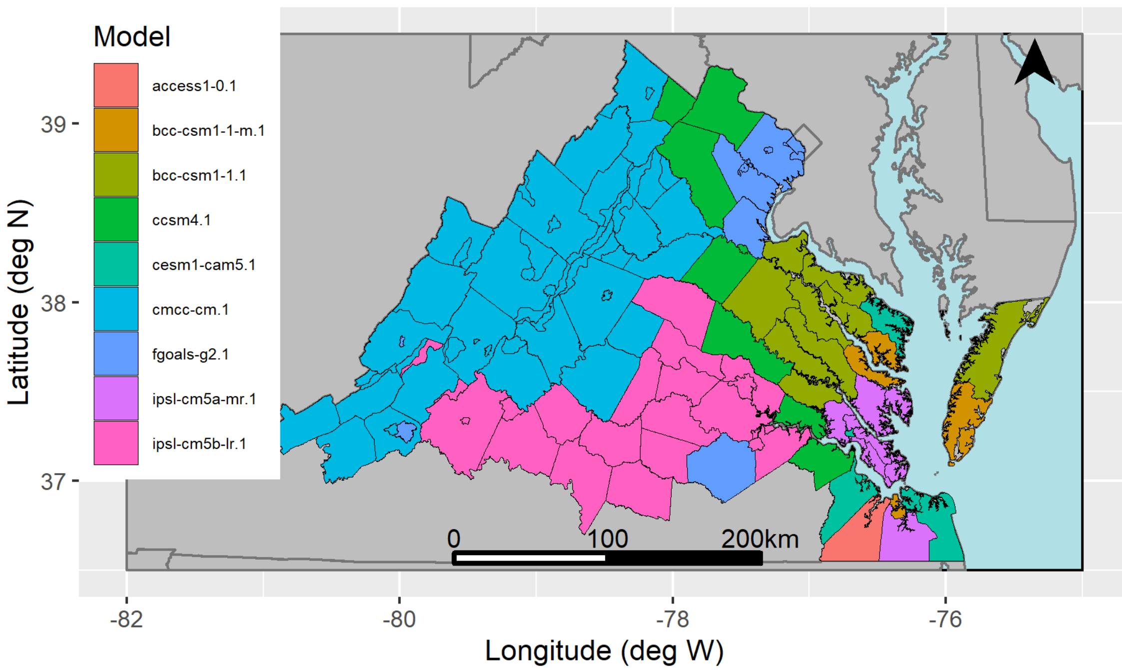

Figure 5.9: GCMs Used in the 50th Percentile Temperature Scenario

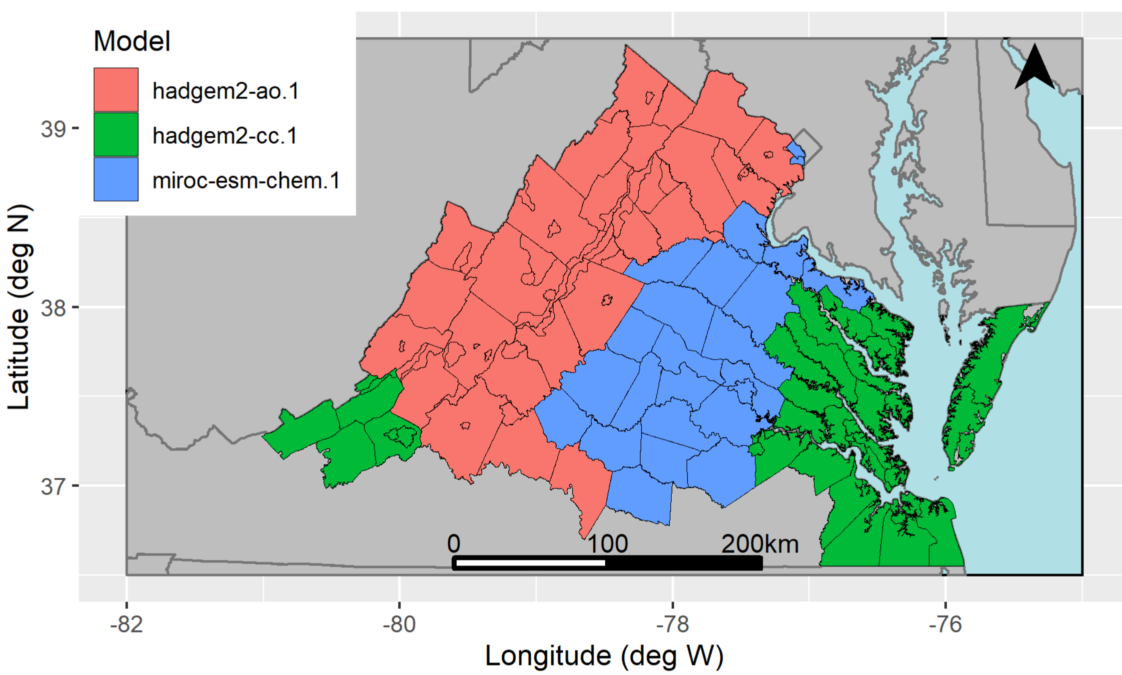

Figure 5.10: GCMs Used in the 90th Percentile Temperature Scenario

between the base and ccP90T90 scenario. These changes are shown in Fig. 5.11.

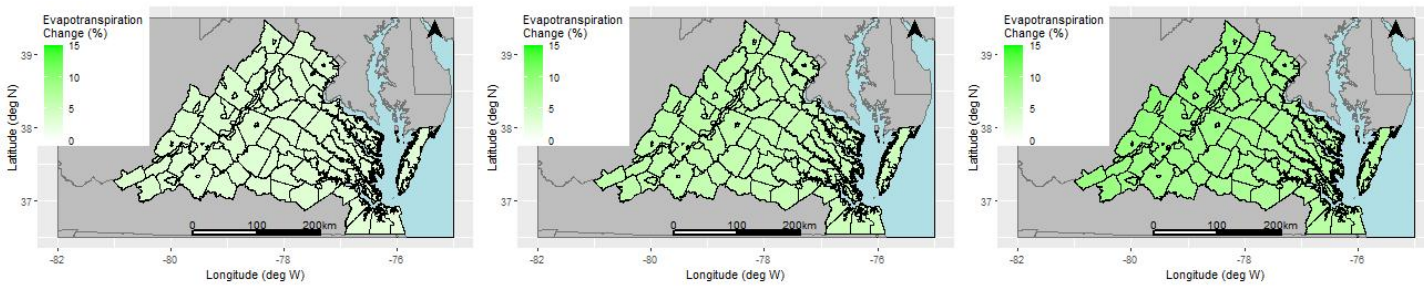

Figure 5.11: ccP10T10, ccP50T50, and ccP90T90 Potential Evapotranspiration Changes in Virginia's Chesapeake Bay Watershed Land Segments

The spatial trends in PET change shown within each climate change scenario mimic the trends seen in the temperature scenarios, although the intensity of the increasing southeast to northwest trend in each scenario led to high R-squared values being seen in PET change's relation to both latitude and longitude. These spatial changes are better shown in Figs. 5.12, 5.13, and 5.14. In the ccP10T10 scenario, PET change increases across the state with the lowest percent increases occurring in jurisdictions in southeast Virginia (Virginia Beach, Chesapeake, Suffolk, Northampton, and Accomack) and the highest percent increases occurring in the mid- to north-west of the study area (Highland County and its immediate surroundings). The same trend was visible in both the ccP50T50 and ccP90T90 scenarios, but with a higher percent change in PET in these higher-temperature scenarios. R-squared values between latitude and percent change in PET ranged from a low of 0.47 in scenarios ccP50T50 and ccP90T90 to a high of 0.63 in scenario ccP10T10, while R-squared values between longitude and percent change in PET ranged from a low of 0.44 in scenario ccP10T10 to a high of 0.66 in scenario ccP90T90. This moderate similarity in spatial trends between temperature and PET is reflected by moderate coefficients of determination between these two variables in scenarios ccP50T50 ($R^2 = 0.34$) and ccP90T90 ($R^2 = 0.50$).

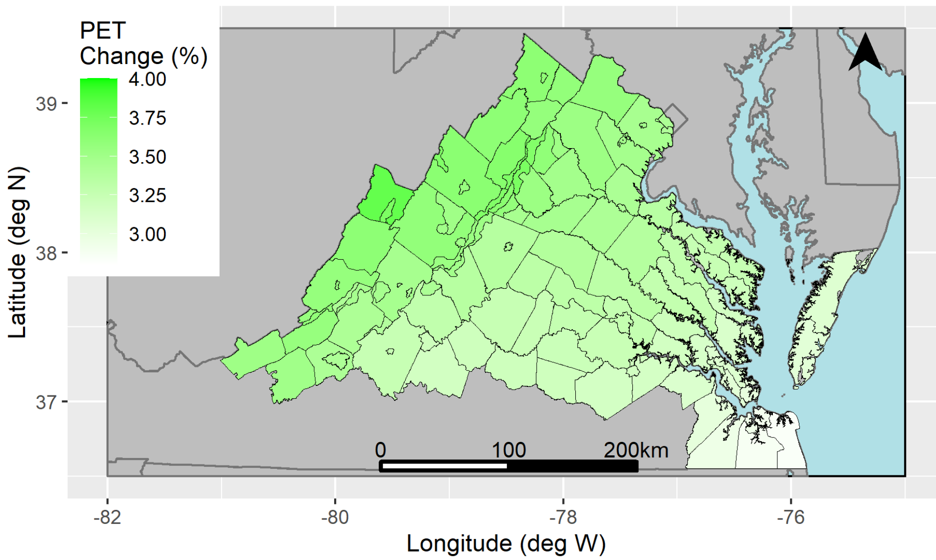

Figure 5.12: ccP10T10 PET Changes in Virginia's Chesapeake Bay Watershed Land Segments

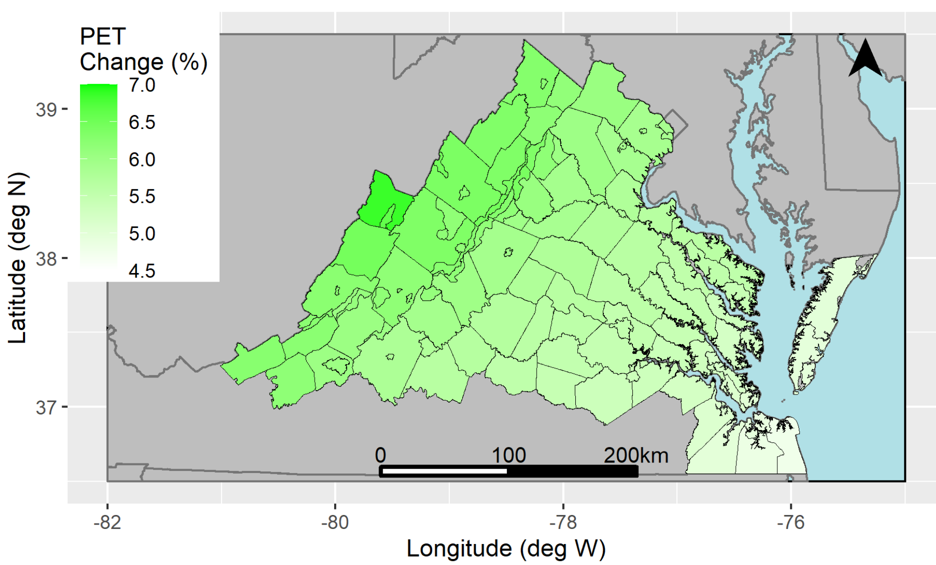

Figure 5.13: ccP50T50 PET Changes in Virginia's Chesapeake Bay Watershed Land Segments

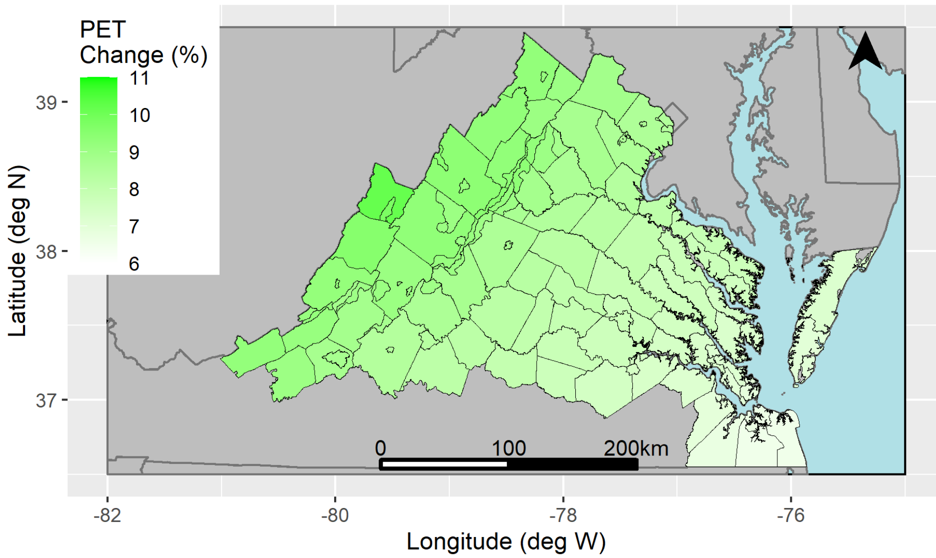

Figure 5.14: ccP90T90 PET Changes in Virginia's Chesapeake Bay Watershed Land Segments

5.3 Precipitation Trends

Distinct spatial trends exist for the percent change in precipitation seen between the base scenario and each climate change scenario, but the magnitude of these percent changes differs far more between the scenarios than within any scenario. These changes are shown in Fig. 5.15, in which scenario ccP10T10 experiences precipitation changes of about -11 to -7% from the base scenario, while ccP50T50 exhibits increases of about 3 to 8% and ccP90T90 exhibits increases of approximately 22 to 29%.

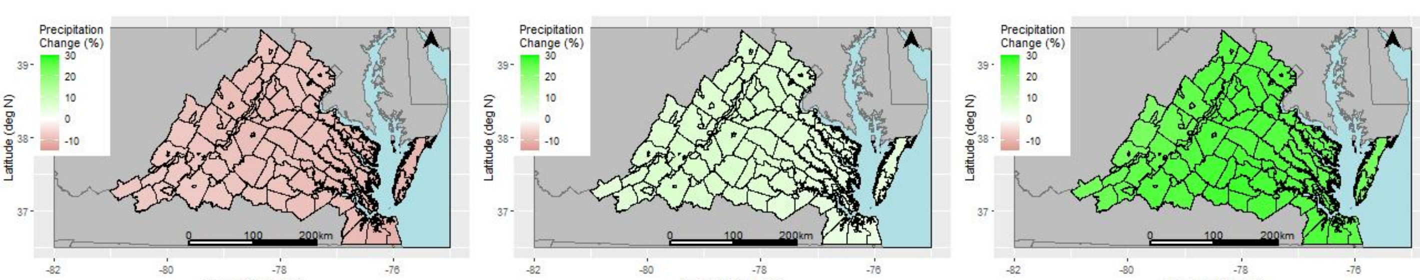

Figure 5.15: ccP10T10, ccP50T50, and ccP90T90 Precipitation Changes in Virginia's Chesapeake Bay Watershed Land Segments

The ccP10T10 scenario precipitation change is largely linked with longitude, with the most drastic decreases in precipitation occurring in the state's eastern areas (the Eastern Shore, Virginia Beach, Chesapeake) and the least drastic decreases seen in some of the western counties within the area of study (Bedford, Roanoke, Alleghany) (Fig. 5.16). All land segments within the Chesapeake Bay watershed in Virginia experienced decreases in precipitation between the base and this tenth percentile scenario. The strength of this relationship between longitude and precipitation in the ccP10T10 scenario is shown in Fig. 5.17 (R-squared = 0.57).

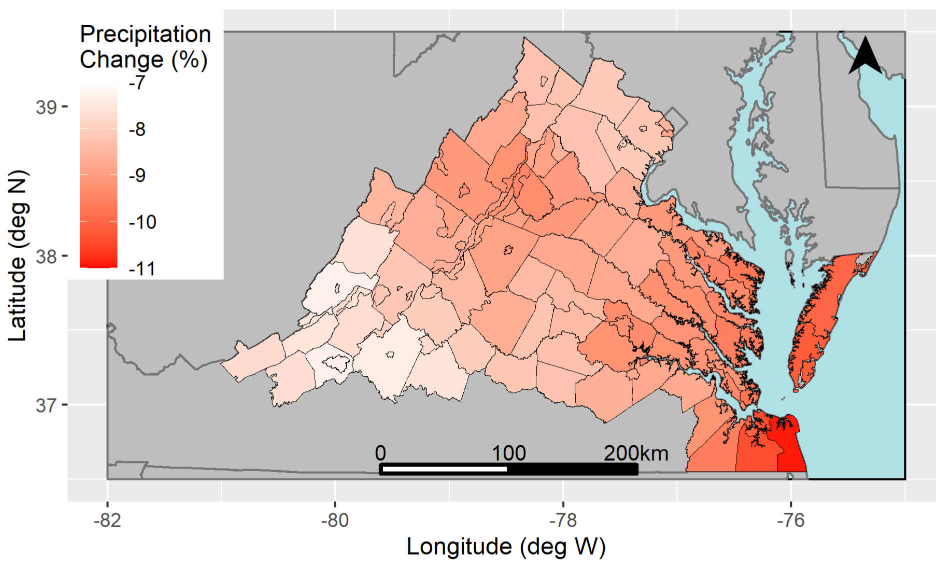

Figure 5.16: ccP10T10 Prcp. Changes in Virginia's Chesapeake Bay Watershed Land Segments

A more complex trend existed in precipitation change within the ccP50T50 scenario. Precipitation change increased in a northwest fashion from a low of about 3% in southeast Virginia, near Virginia Beach, to a high of about 8% in many of the central Virginian counties (Amherst, Nelson, Albermarle, Madison) just east of the Appalachian Mountains (Fig. 5.18. Immediately west of the Appalachian Mountains, the percent increase in precipitation began to drop, back down to about 5 to 6% in the westernmost counties including

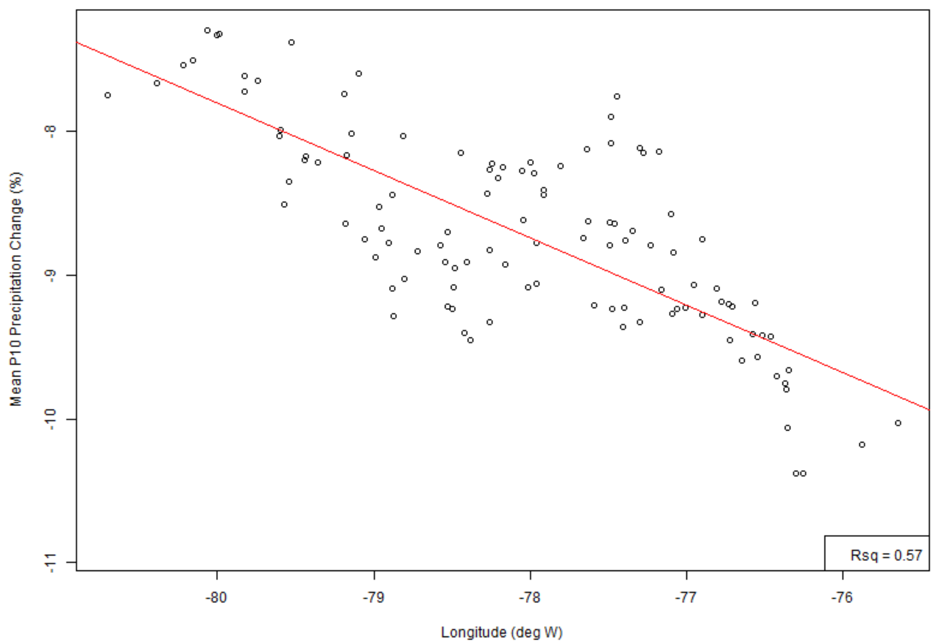

Figure 5.17: ccP10T10 Precipitation Changes by Longitude

Giles, Craig, and Bath. This decrease in the percent change in precipitation west of the Appalachian Mountains is likely a result of the rain shadow effect, whereby precipitation falls on the windward side of a mountain range as a result of water vapor condensing, forming clouds, and falling as rain as the air increases in elevation to rise over the mountain.

The ccP90T90 scenario exhibited a unique spatial trend. Two high-percent change hotspots existed in the Powhatan/Amelia/Cumberland area and in the Culpeper/Rappahonnock region. In these areas, shown in Fig. 5.19, precipitation change increased by amounts ranging up to about 29%. Precipitation change decreased to a low of about 22% when moving away from these hotspots, to the lowest areas on the fringes of the state, including the Eastern Shore and Highland/Bath counties.

One shortcoming in how modeled precipitation was handled during the creation of these climate change scenarios is that only the magnitudes of precipitation were changed from

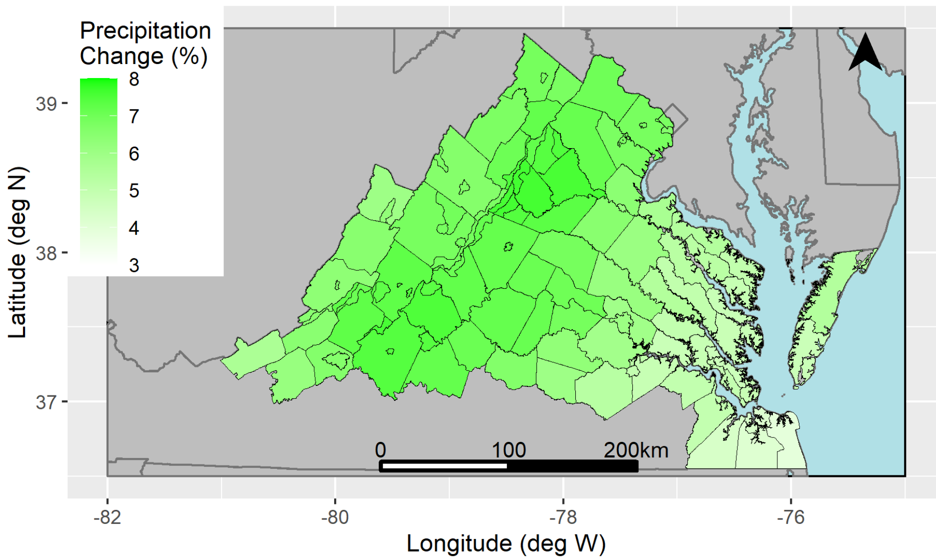

Figure 5.18: ccP50T50 Prcp. Changes in Virginia's Chesapeake Bay Watershed Land Segments

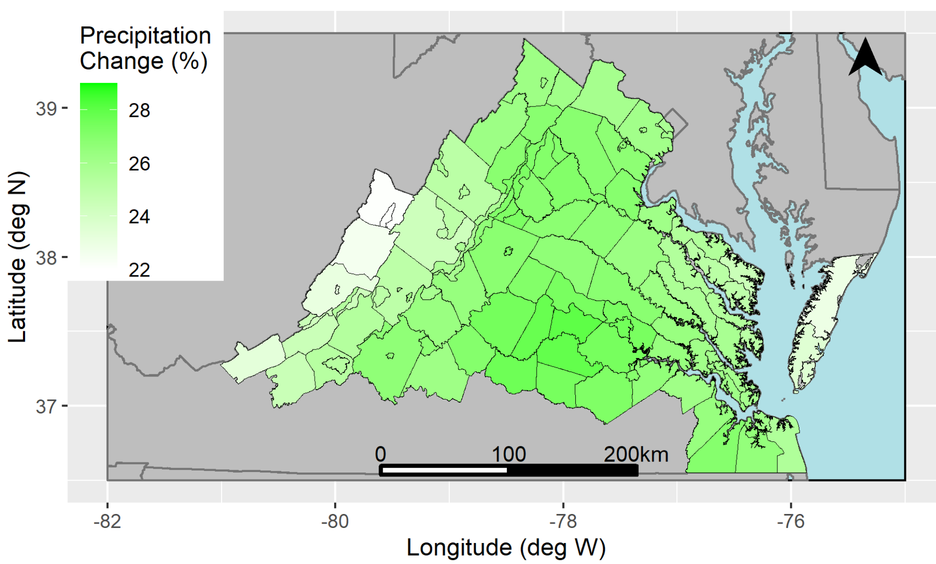

Figure 5.19: ccP90T90 Prcp. Changes in Virginia's Chesapeake Bay Watershed Land Segments

the base scenario. This change in the magnitudes of precipitation between the baseline and climate change scenarios is shown in Fig. 5.20. As a result of climate change, a number of other characteristics of precipitation, including the number of storms, their duration, their severity, and their relative magnitude to each other, may also be impacted. However, these changes are not taken into account by simple scaling of the magnitude of an existing precipitation time series.

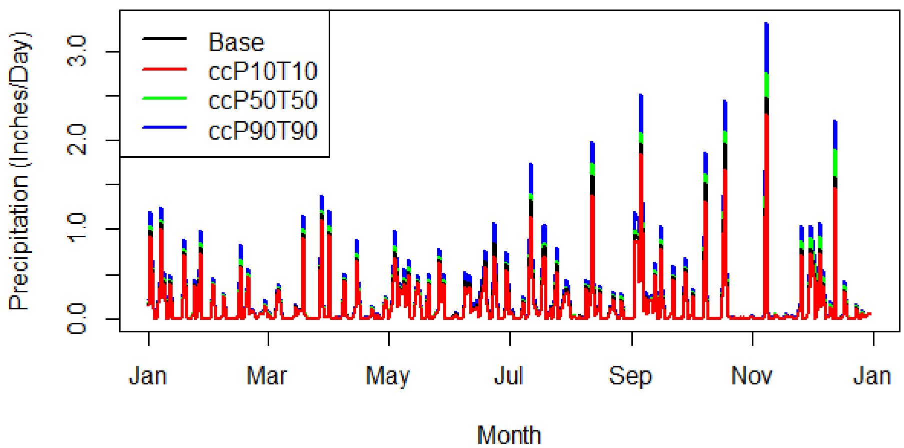

Figure 5.20: Precipitation in One Representative Model Year for Base and Climate Change Scenarios

Some cursory investigation into the spatial trends of the assignment of GCMs to the climate change scenarios was also conducted for the process of precipitation. For the tenth and ninetieth percentile scenarios, large swaths of neighboring land segments were found to have been linked with the same GCMs. The fiftieth percentile scenario was found to be a more piecemeal assortment of GCMs. Maps of the GCMs associated with the tenth, fiftieth, and ninetieth percentile scenarios are shown in Figs. 5.21, 5.22, and 5.23.

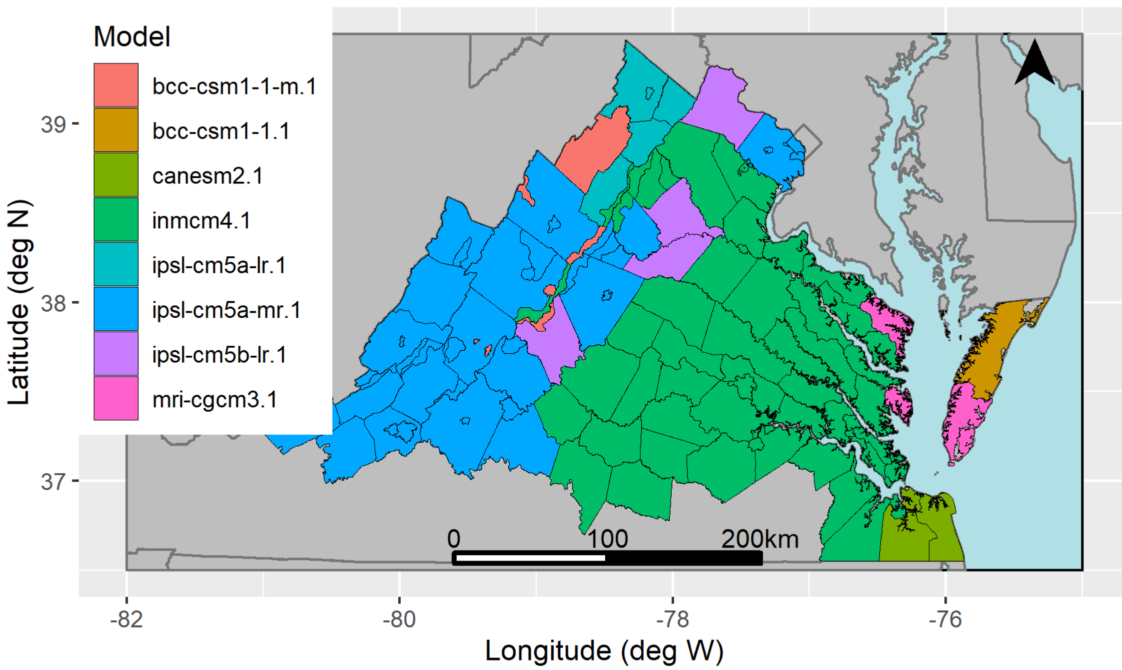

Figure 5.21: GCMs Used in the 10th Percentile Precipitation Scenario

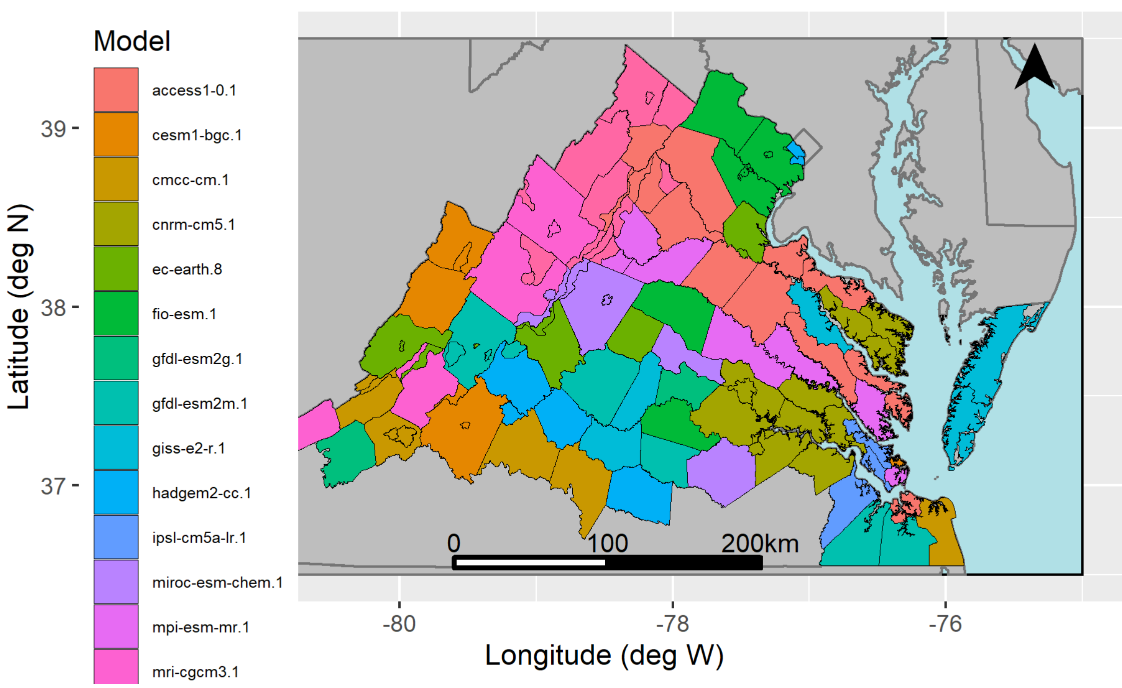

Figure 5.22: GCMs Used in the 50th Percentile Precipitation Scenario

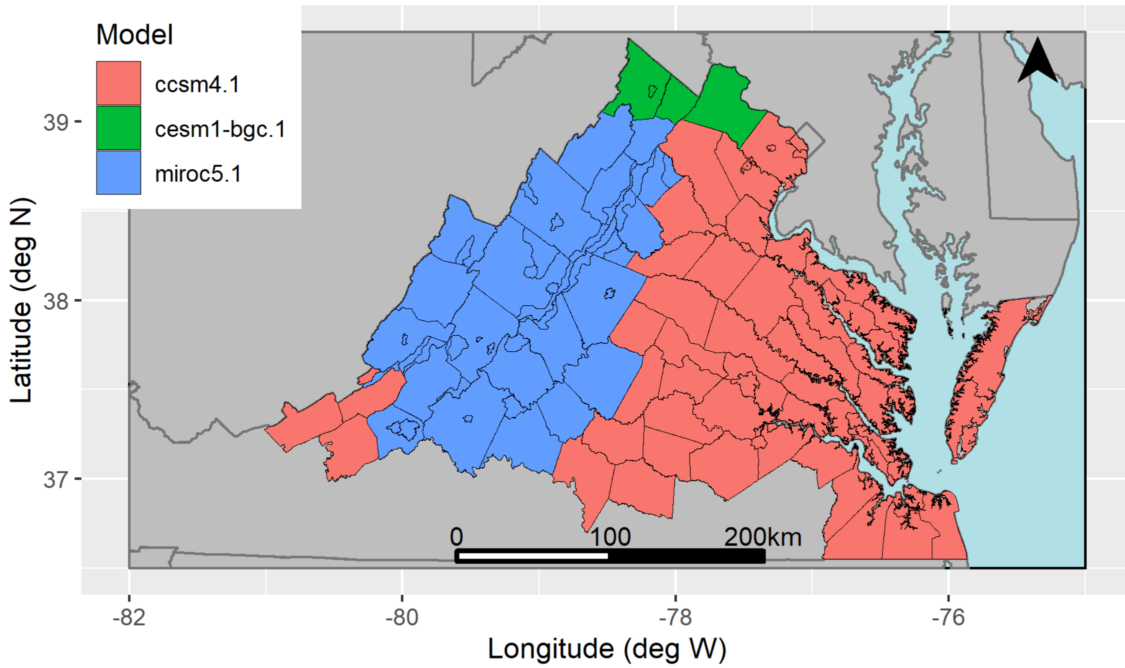

Figure 5.23: GCMs Used in the 90th Percentile Precipitation Scenario

5.4 Changes in Unit Runoff by Land Use

Scenario ccP10T10 is linked with decreases in the runoff per unit area which is generated from every land use group (ranging from an average percent decrease of -24.6% to -11.4% from the base scenario), while ccP50T50 is associated with a slight increase (mean percent change of +6.6% to +9.2%) and ccP90T90 conditions cause a large increase (mean percent increase of 30.5% to 57.2%). The mean percent change for each land use group in each scenario is shown in Fig. 5.24, which also shows that the ”CSS True Forest” and ”Natural Pervious” land use groups are linked with the most extreme percent decreases in the ccP10T10 scenario and the most extreme percent increases in the ccP90T90 scenario. On the other hand, the ”Impervious” and ”Feeding Space” land use groups exhibit the least extreme percent decrease in the ccP10T10 scenario and the least extreme percent increase in the ccP90T90 scenario. Therefore, the percent change in runoff generated from forested and natural land uses will be most significantly impacted by climate change. This is a result of reduced precipitation leading to drier antecedent moisture conditions, in turn allowing for an increased percent infiltration of precipitation, reducing runoff by a higher percent than precipitation is reduced. Conversely, increased precipitation leads to wetter antecedent moisture conditions, causing quickened exceedance of the land's infiltration capacity and increased runoff at a higher percent increase than precipitation. The impervious surfaces convert all precipitation that falls on them to surface runoff, so their runoff decrease/increase resulting from climate change is more directly related to the proportion of decrease/increase in precipitation associated with climate change.

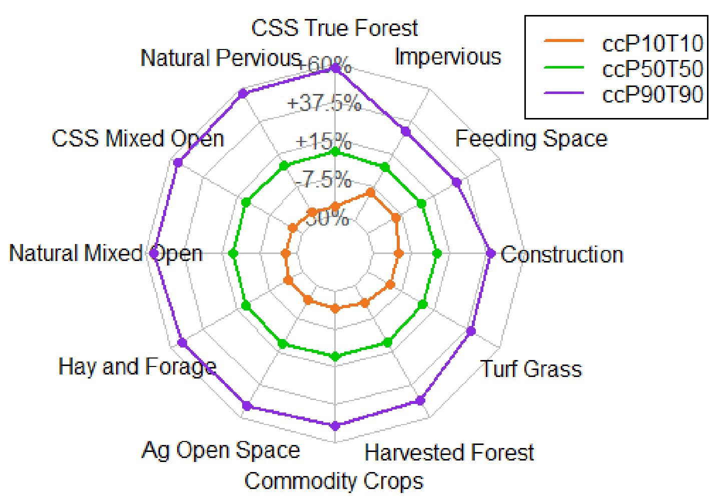

Figure 5.24: Mean Percent Changes in Runoff per Unit Area between the Base Scenario and Scenarios ccP10T10, ccP50T50, and ccP90T90

However, significant differences exist in how the generation of surface runoff in river segments across Virginia react to the same land use groups. The range of percent changes in surface runoff from impervious land is the smallest, signifying a relatively uniform hydrologic response throughout the Commonwealth. Conversely, the range of percent changes in surface runoff from forested and natural land is the largest, signifying a wide range of hydrologic responses to these land uses. The minimum, mean, and maximum percent change for each of the land use groups between the base and ccP10T10 scenario are shown in Fig. 5.25. The maximum percent change seen across each of the land use groups for the ccP10T10 scenario is quite constant, ranging from the most extreme change of -16.3% in the "Natural Pervious" land use group to the least extreme of -9.6% in the "Impervious" land use group. The mean percent change seen in the ccP10T10 scenario is a bit more variable, ranging from a maximum decrease of -24.6% in the "Natural Pervious" land use group to a minimum of -11.4% in the "Impervious" and "Feeding Space" land use groups, while the minimum percent change is still more diverse, ranging from a maximum of -36.1% in the "Natural Mixed Open" land use group to a minimum of -14.1% in the "Impervious" and "Feeding Space" land use groups.

Due to the reduced range of surface runoff percent changes seen in the ccP50T50 scenario, some of the minor differences in minimum (low of +3.4% in "Natural Pervious" land use group; high of +5.5% in "Construction" land use group) and maximum (low of +8.1% in "Impervious" and "Feeding Space" land use groups; high of 13.5% in "Hay and Forage" and "Ag Open Space" land use groups) percent change across the land use groups appear pronounced in Fig. 5.26. However, this accentuated visual change on the radar plot is largely due to the reduced range of axis scales compared with the visualization of the ccP10T10 and ccP90T90 scenarios. The fact that the mean percent change across the land use groups remains approximately constant (low of +6.6% in "Impervious" and "Feeding Space" land use groups; high of +9.2% in "Hay and Forage" and "Ag Open Space" land use group) is a testament to the uniformity of land use runoff responses within this ccP50T50 scenario.

The ccP90T90 scenario exhibits the most variable response of surface runoff percent change

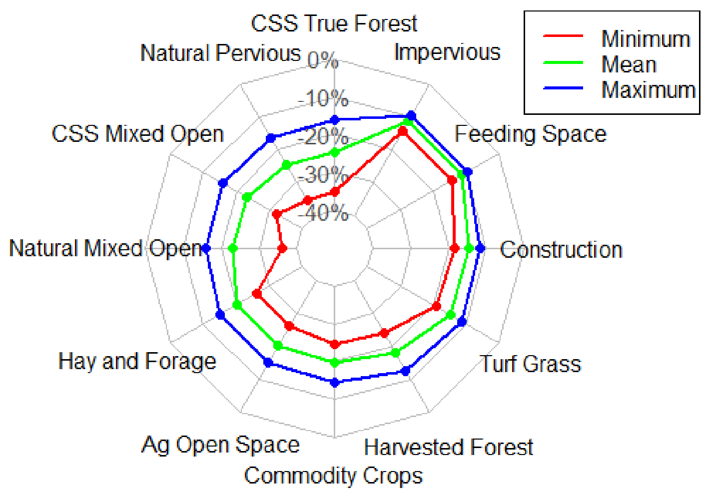

Figure 5.25: Minimum, Mean, and Maximum Percent Changes in Runoff per Unit Area between the Base Scenario and Scenario ccP10T10

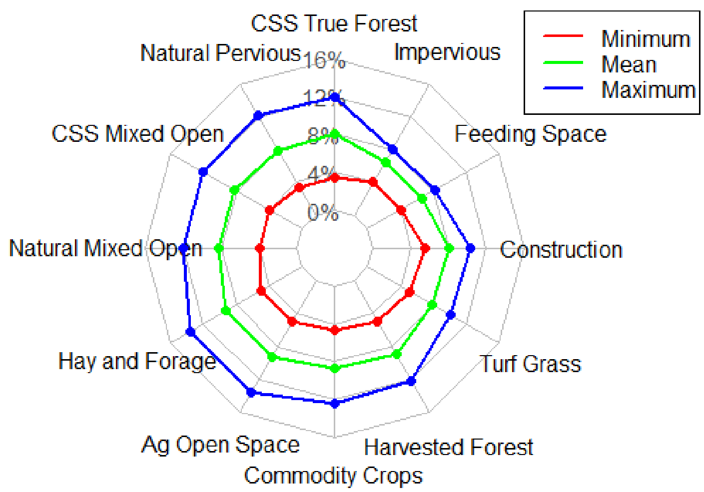

Figure 5.26: Minimum, Mean, and Maximum Percent Changes in Runoff per Unit Area between the Base Scenario and Scenario ccP50T50

amongst different land use groups of any of the climate change scenarios. The massive range in percent changes is especially pronounced in the means (low of +30.5% for "Feeding Space" and "Impervious" land use groups; high of +57.1% for "CSS True Forest" land use group) and maximums (low of 33.5% for "Feeding Space" and "Impervious" land use groups; high of +76.5% in "Natural Mixed Open" land use group) of the land use groups, as shown in Fig. 5.27. The minimum, on the other hand, is more consistent – it ranges from a low of +24.6% in the "Feeding Space" and "Impervious" land use groups to a high of 32.0% in the "CSS True Forest" land use group. Due to the uniqueness of land use group surface runoff responses across this and the other two scenarios, five land use groups were chosen for further investigation. These land use groups (Natural Pervious, Hay and Forage, Commodity Crops, Turf Grass, and Impervious) were spatially analyzed to determine if they exhibit different spatial trends in runoff percent change across the area of the Commonwealth within the Chesapeake Bay watershed. To investigate how each of the selected land use groups' runoff response varies throughout the runoff regime, runoff exceedance curves were created for the spatial regions commonly identified to exhibit some of the highest and lowest percent differences.

Similar radar plots showing the minimum, mean, and maximum percent changes in runoff per unit area between the base and climate change scenarios, calculated using the l30 and l90 metrics instead of the mean, are shown in Appendix G. The l30 tended to have near-zero magnitudes – this resulted in extraordinarily large percent changes from even small changes in magnitude. As a result, the percent changes for l30 oftentimes far exceeded +100 or -100%, as shown in Fig. G.1. The l90 tended to have larger magnitudes, resulting in more meaningful percent changes. The l90 tended to increase slightly in the ccP50T50 scenario, increased between about +50 to +100% for the ccP90T90 scenario, and decreased by less than 50% in the ccP10T10 scenario, as shown in Fig. G.5.

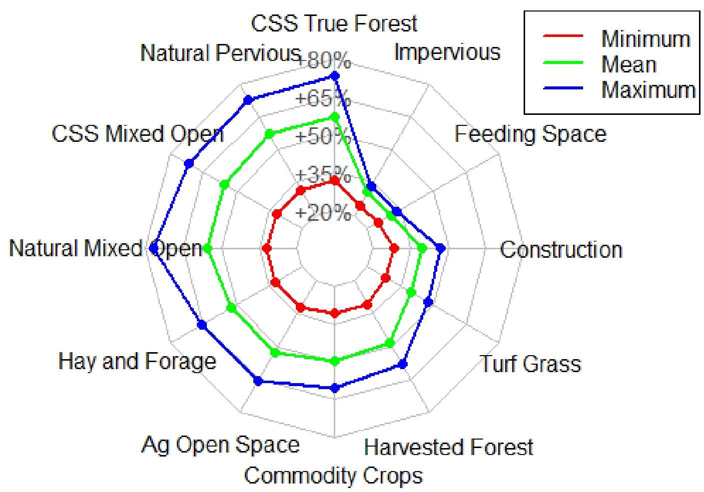

Figure 5.27: Minimum, Mean, and Maximum Percent Changes in Runoff per Unit Area between the Base Scenario and Scenario ccP90T90

5.4.1 Natural Pervious Runoff Change

The Natural Pervious land use group, as well as the very similar ”CSS True Forest” land use group, had the widest range of runoff percent changes in all three of the scenarios. In ccP10T10, runoff change ranged from a low of -35.3% in Harrisonburg to a high of -16.3% in the northern region of Amherst County. As shown in Fig. 5.28, Harrisonburg's enclaving Rockingham County and neighboring Page are also associated with dramatic runoff reductions from Natural Pervious land, as is the region in southeast Virginia near Virginia Beach and Chesapeake. Meanwhile, Nelson County (and neighboring Amherst) and parts of Madison and Greene Counties near the Appalachian Mountains have less dramatic changes in this scenario. In the ccP50T50 scenario, runoff change in the Natural Pervious land use group ranged from a low of +3.4% in Giles County to a high of +12.1% in Charlottesville. High-change hotspots near Culpeper/Orange, Fluvanna, and Campbell/Bedford were seen, with percent changes in runoff tending to decrease when moving away from these regions. Runoff change ranged from a low of +31.7 in the lowest part of Highland County to a high of +73.0% in Nottoway County for the ccP90T90 scenario. Most of southeast Virginia, from Virginia Beach to about Goochland, were linked with the highest percent changes in runoff in this scenario, while the western counties in the study area, ranging from Giles to Craig, as well as Nelson and some of the regions along the Appalachian Mountains in Rappahannock, Madison, and Greene experienced less dramatic (but still over 30%) increases in this ninetieth percentile scenario.

Next, runoff exceedance curves were created for some of the regions of highest and lowest change for each of the scenarios. The cities and counties showing some of least drastic changes between the base scenario and each respective climate change scenario are shown in the top row, while cities and counties exhibiting some of the highest percent changes from the base scenario are shown in the bottom row. As a result of the logarithmically decreasing

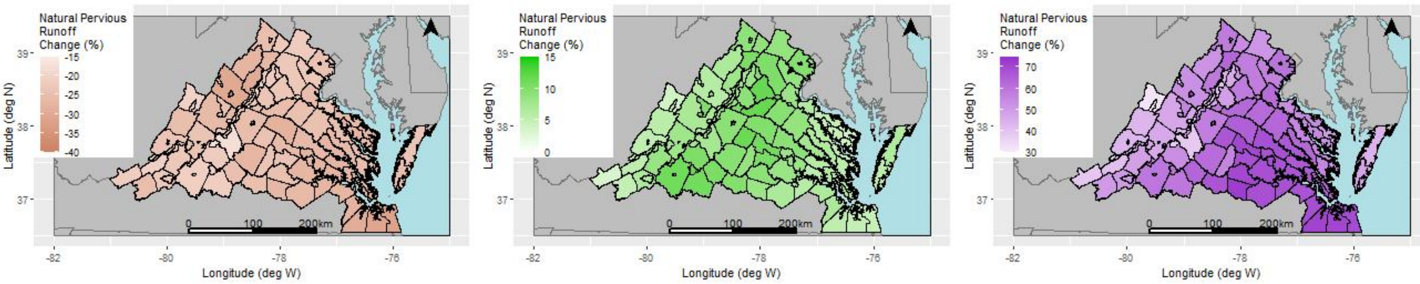

Figure 5.28: Percent Changes in Surface Runoff per Unit Area of Natural Pervious Land between the Base Scenario and Scenarios ccP10T10, ccP50T50, and ccP90T90

nature of these percent exceedance curves, they are plotted on a logarithmic y-axis to better exhibit differences throughout the entire runoff regime. The x-axis is trimmed to only show the flows between about 0 and 30% exceedance to trim out the lowest flows, which become infinitesimal in value as they approach zero.

For the natural pervious land use group, the percent difference between the base scenario and the low-precipitation ccP10T10 scenario remained approximately constant throughout the regime for many of the counties with the least drastic changes (such as in Amherst County, shown in the top left of Fig. 5.29) while the largest percent differences were seen in the lower magnitude runoff values in the jurisdiction with the largest percent change (Harrisonburg, shown in the bottom left). Although runoffs throughout the regime in both regions systematically show a decrease between the base and ccP10T10 scenario, Amherst's runoff exhibits similar behaviors between the two scenarios, while Harrisonburg experiences a widening of differences in the lower-magnitude runoffs. This decreased runoff may be a result of the decreased precipitation in this scenario (of which Harrisonburg experienced one of the larger percent decreases, as shown in Fig. 5.16) combined with the increased potential evapotranspiration (of which northeast Virginia experienced some of the heaviest increases, as shown in Fig. 5.12). The ccP50T50 scenario, shown in Giles and Culpeper in Fig. 5.29, experience small increases in unit runoff throughout the regime, reflecting the small average percent difference in unit runoff between the base and ccP50T50 scenarios. The ccP90T90 scenario, shown in Highland and Nottoway, exhibit visually similar differences across the regime. However, to delve into where these jurisdictions' regimes truly differ, the values within the regime must be investigated. At the 20th percent of exceedance, Highland exhibits a unit runoff value of 0.0675 in/day/acre in the base scenario and 0.0855 in/day/acre in the ccP90T90 scenario – a percent difference of 26.6%. However, Nottoway exhibited a unit runoff value of 0.0363 in/day/acre in the base scenario and 0.0551 in/day/acre in the ccP90T90 scenario – a percent difference of 52.0%. Thus, although unit runoff differs by approximately 0.02 in/day/acre for both Nottoway and Highland, the percent difference in Nottoway is far higher as a result of the lower magnitudes of the values seen there. Nottoway was associated with some of the most dramatic percent increases in precipitation for the P10 scenario (Fig. 5.19) while Highland was associated with the most dramatic percent increases in potential evapotranspiration (Fig. 5.14). These conflicting forces result in less dramatically increased percents of runoff in Highland, and more dramatically increased percents of runoff in Nottoway.

5.4.2 Hay and Forage Runoff Change

The Hay and Forage land use group had similar percent runoff changes to the ”CSS Mixed Open”, ”Natural Mixed Open”, and ”Ag Open Space” land use groups in each of the climate change scenarios. For the scenario ccP10T10, runoff change for Hay and Forage ranged from a low of -26.3% in Virginia Beach to a high of -15.0% in the highest parts of Amherst County. As in the ”Natural Pervious” land use group, additional areas of drastic decrease were concentrated in southeast Virginia and in Harrisonburg/Rockingham, while areas of minor decrease were clustered near Nelson and along the ridge of the Appalachians (Fig. 5.30. In scenario ccP50T50, the smallest change of +4.9% was seen in Giles County, while

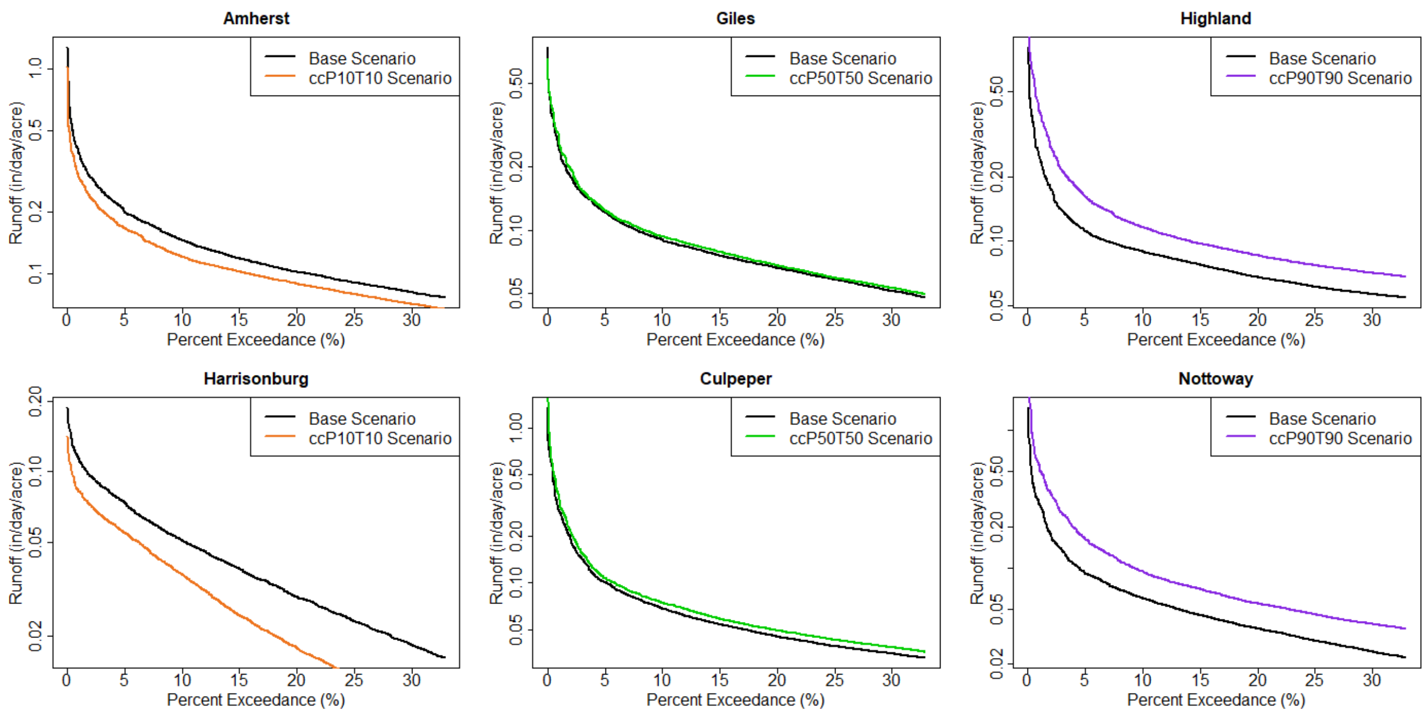

Figure 5.29: Percent Exceedance of Runoff per Unit Area of Natural Pervious Land in Low- and High-Change Jurisdictions of Virginia

the highest change of +13.5% was seen in Harrisonburg. Once again, this followed the trend seen in the ”Natural Pervious” land use group for this scenario, where hotspots were clustered near Campbell and Orange Counties, with percent increase generally decreasing in magnitude away from these areas. In the ccP90T90 scenario, surface runoff change was bounded by a low of +32.0% in the southern parts of Highland County and a high of +65.7% in Nottoway County. These minimum and maximum percent changes in runoff are quite spatially consistent with the ”Natural Pervious” land use group – in two of the three scenarios, the minimum percent change occurs in the identical land segment as the minimum percent change of the ”Natural Pervious” land use group, and the same is true for the maximum percent change. This land use group also followed the spatial trend seen in the ”Natural Pervious” land use group for the ninetieth percentile scenario, with the highest percent changes seen in south-central and southeast Virginia and the lowest percent changes seen in the the westernmost counties such as Alleghany and Bath. It is worth noting that in the Hay and Forage land use group, Harrisonburg had one of the highest percent changes in each of the scenarios, especially when compared with nearby counties such as Augusta and Highland.

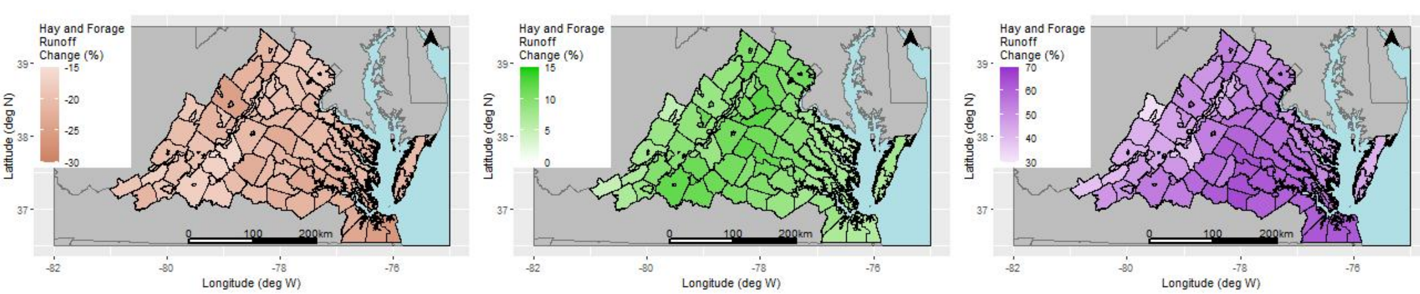

Figure 5.30: Percent Changes in Surface Runoff per Unit Area of Hay and Forage Land between the Base Scenario and Scenarios ccP10T10, ccP50T50, and ccP90T90

Trends seen in the percent exceedance plots of unit runoff in the ”Hay and Forage” land use group similarly echoed those seen in the ”Natural Pervious” group, as shown in Fig. 5.31. In the ccP10T10 scenario, the high-decrease (Harrisonburg) city exhibited larger percent decreases in lower magnitude unit runoff values. This may partially be a result of the incredibly low magnitudes of runoff existing throughout the entire regime in this city, with the largest values capping out at just over 0.15 in/day/acre compared with the far larger 1.0 or so seen in Amherst. The ccP50T50 scenario closely followed the base scenario in both the smallest-difference and largest-difference regions, while the ccP90T90 scenario followed the trend of the base scenario in both jurisdictions, with Nottoway's larger percent increase a result of the smaller magnitudes of flows seen when compared with Highland.

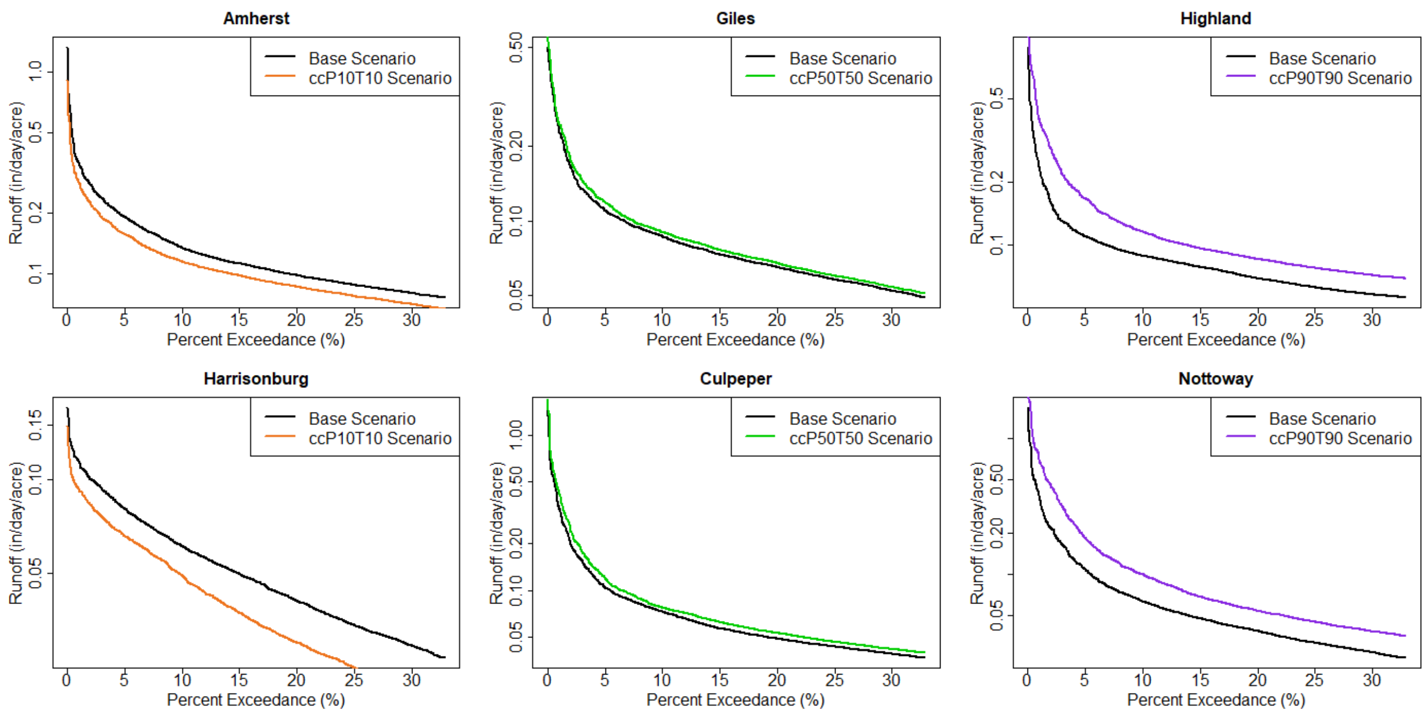

Figure 5.31: Percent Exceedance of Runoff per Unit Area of Hay and Forage Land in Low- and High-Change Jurisdictions of Virginia

5.4.3 Commodity Crops Runoff Change

The Commodity Crops land use group was chosen for further investigation due to its distinguished response from both the "Ag Open Space" and the "Turf Grass" land use groups.

It had quite similar percent changes as the "Harvested Forest" land use group, as shown in Fig. 5.32. In the ccP10T10 scenario, a low of -24.5% in Virginia Beach and a high of -14.7% in the northern reaches of Amherst County were seen. In ccP50T50, percent changes ranged from a low of +4.7% in Giles County to a high of +12.5% in Harrisonburg. The scenario ccP90T90 experienced changes between +31.0% in southern Highland County and +60.7% in Nottoway County. All of these minimum and maximum percent changes occurred in the same land segments as in the "Hay and Forage" land use group. For all three of the climate change scenarios, very similar spatial trends existed between the "Commodity Crops" and "Natural Pervious" land groups,

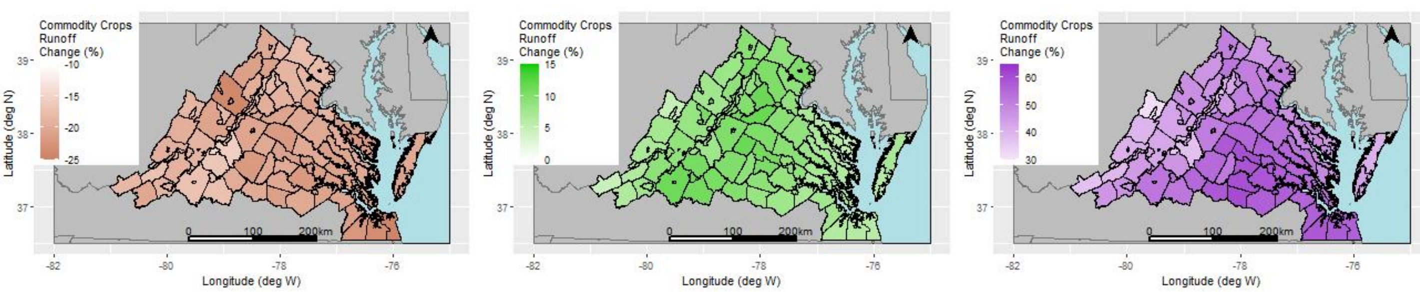

Figure 5.32: Percent Changes in Surface Runoff per Unit Area of Commodity Cropland between the Base Scenario and Scenarios ccP10T10, ccP50T50, and ccP90T90

Once again, similar trends in how the unit runoff produced by commodity cropland changed throughout the flow regime existed as those seen in the "Natural Pervious" and "Hay and Forage" land use groups. However, the slightly decreased mean percent difference between the base and climate change scenarios exhibited by the "Commodity Crop" land use in both ccP10T10 (shown in 5.25, where unit runoff drops by about 20%, compared with the "Natural Pervious" land use group's 25%) and ccP90T90 (shown in 5.27, where unit runoff increases by about 50%, compared with the "Natural Pervious" land use group's 60%) can visually be seen in Fig. 5.33. In many of the jurisdictions which exhibited high differences between the base and climate change scenarios (such as Harrisonburg, Highland, and Nottoway), this decreased change can be shown through the smaller differences (and tighter fit) in the range of about 10% to 30% exceedance seen in these jurisdictions in Fig. 5.33 compared with Fig. 5.29.

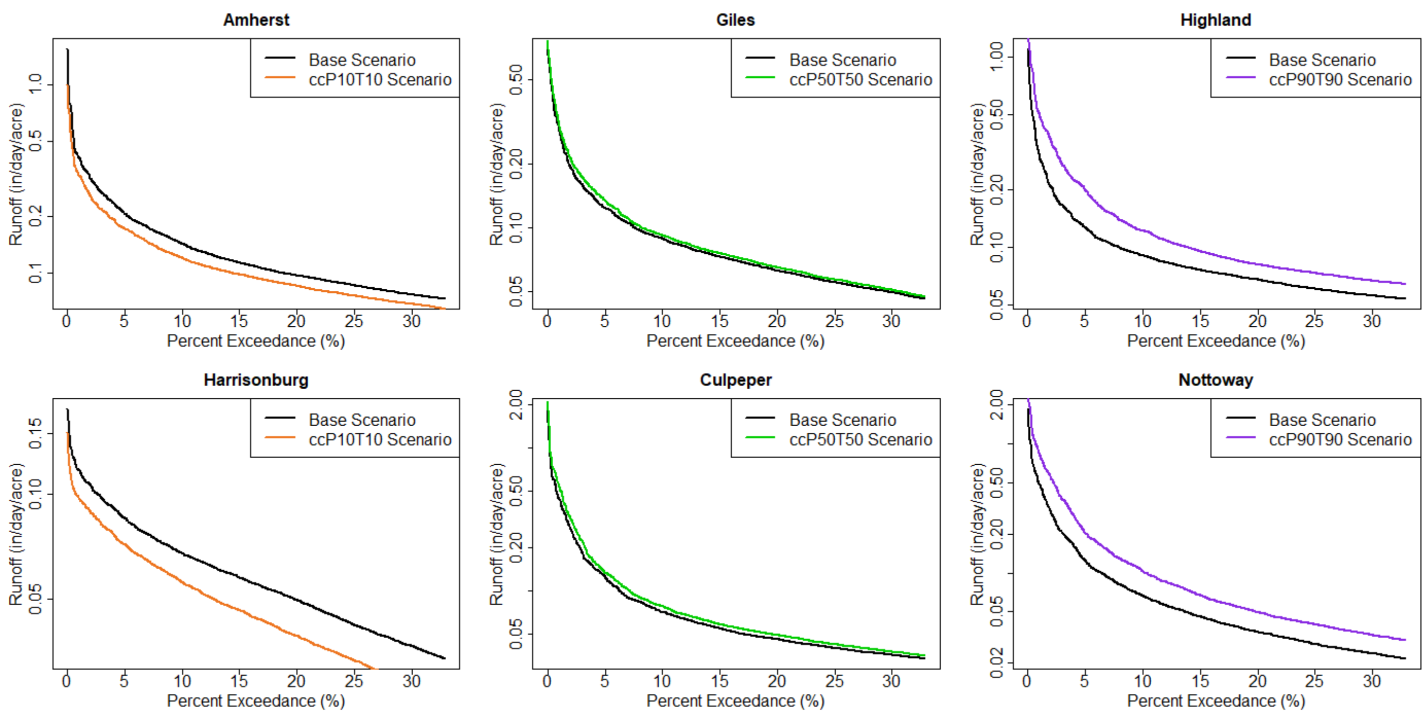

Figure 5.33: Percent Exceedance of Runoff per Unit Area of Commodity Cropland in Low- and High-Change Jurisdictions of Virginia

5.4.4 Turf Grass Runoff Change

The Turf Grass land use group exhibited similar percent changes as the Construction land use group. In the ccP10T10 scenario, changes were bounded on the end of largest decrease at -19.2% in Virginia Beach and on the end of smallest decrease at -11.12% in Falls Church. Bedford, Campbell, and Amherst also stand out as counties with a small change in percent runoff, as seen in Fig. 5.34. In ccP50T50, runoff percent changes ranged from +5.2% in Giles County to +10.0 in Culpeper County. The hotspots seen in previous land use groups in the ccP50T50 scenario are not as prominent in the turf grass land use group, with the entire strip from Bedford and Charlotte to Clarke and Fairfax standing out as the area of highest change as opposed to any individual counties. A low of +28.4% in the south of Highland County and a high of +47.8% in Chesterfield County were exhibited in the ccP90T90 scenario. Most of the highest percent changes in runoff were seen in the southeast of Virginia.

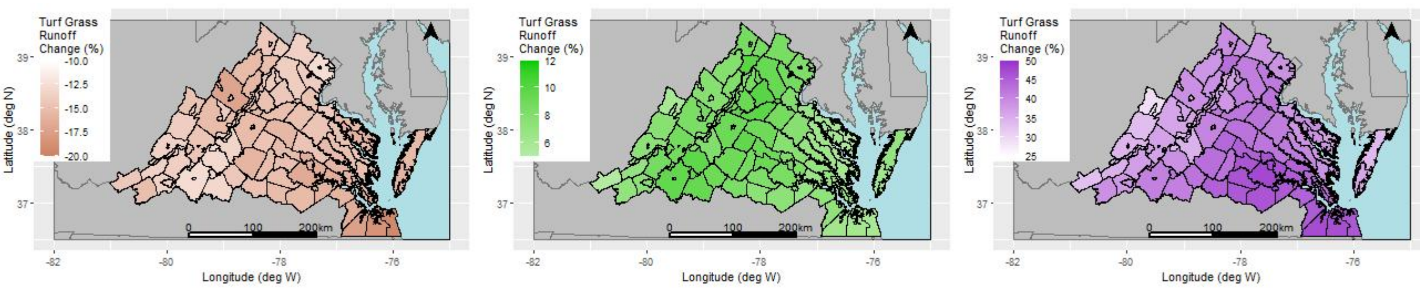

Figure 5.34: Percent Changes in Surface Runoff per Unit Area of Turf Grassland between the Base Scenario and Scenarios ccP10T10, ccP50T50, and ccP90T90

The changes in unit runoff resulting from the turf grass land use group were far more uniform than for previously discussed land use groups. In Harrisonburg, rather than diverging from the base scenario in the low unit runoff values, the ccP10T10 scenario differences remained relatively constant throughout, as seen in Fig. 5.35. Just as in previous land use groups, Amherst in ccP10T10 and Giles and Culpeper in ccP50T50 exhibited very similar unit runoff generation as the base scenario. In the ccP90T90, instead of diverging at low unit runoff scenarios as previous land use groups had done, the responses grew closer to each other symbolizing a more uniform response throughout the regime. Instead, the largest differences were seen in the moderately high flows (about 5 to 15% exceedance) in both Highland and Nottoway.

5.4.5 Impervious Runoff Change

The Impervious land use group had near-identical responses to the "Feeding Space" land use group in the vast majority of Virginian land segments. Runoff response to climate change

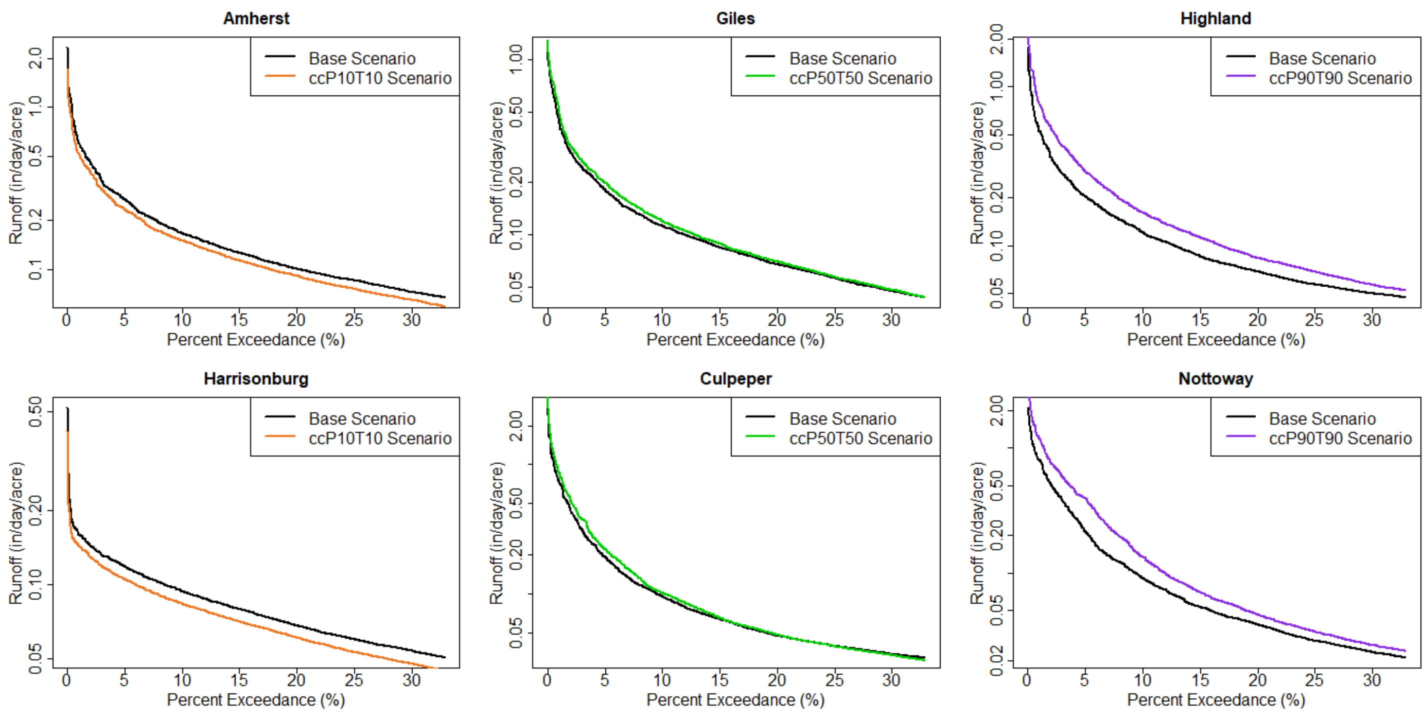

Figure 5.35: Percent Exceedance of Runoff per Unit Area of Turf Grassland in Low- and High-Change Jurisdictions of Virginia

ranged from -14.1% in Virginia Beach to -9.6% in Roanoke County in scenario ccP10T10, while it ranged from +4.0% in Virginia Beach to +8.1% in Culpeper County in the fiftieth percentile scenario and +24.6% in the southern part of Highland County to +33.5% in Powhatan County in the ninetieth. Spatial trends were less visible and more uniform in each scenario in the Impervious land use group, as shown in Fig. 5.36. In scenario ccP50T50, the smallest changes were seen in the easternmost (from Westmoreland to Virginia Beach) and westernmost (Highland to Giles) areas, while the smallest changes were just seen in the westernmost areas and the Eastern Shore in the ccP90T90 scenario.

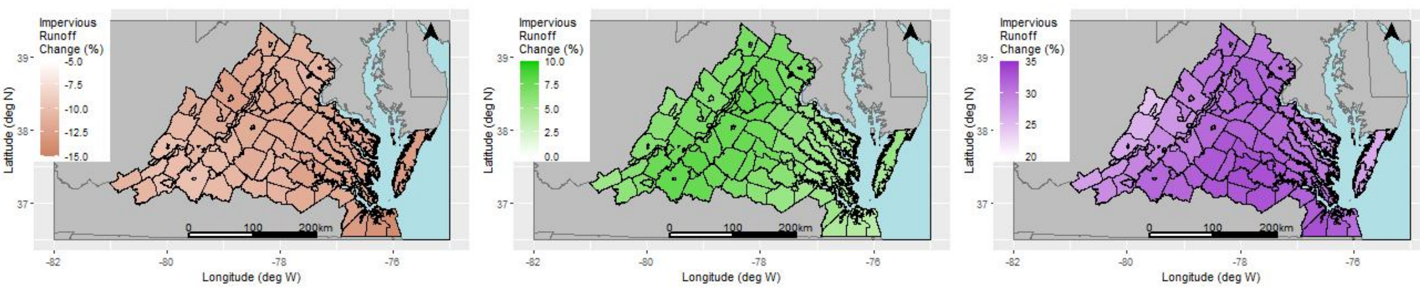

Figure 5.36: Percent Changes in Surface Runoff per Unit Area of Impervious Land between the Base Scenario and Scenarios ccP10T10, ccP50T50, and ccP90T90

The shape of the impervious land use group's runoff exceedance curve drastically differed from that of any previous land use group, with inflection points visible on each jurisdiction's curve between about 10% and 15% exceedance on Fig. 5.37. This inflection point, between the low percent exceedance's upwardly concave and downwardly concave decreases, is indicative of the sharp drop-off in daily unit runoff volumes resulting from impervious surfaces' rapid runoff response. When precipitation occurs on these surfaces, it is rapidly conveyed to nearby drainage systems or streams as surface runoff. In times when precipitation is not occurring, no runoff at all is generated, since impervious surfaces do not store water. In addition to this altered curve shape, the runoff generated by the climate change scenarios more closely follows the trend of the base scenario. This similarity in response throughout the regime is also a result of impervious surfaces' uncomplicated response to precipitation – in climate change scenarios with increased precipitation, more runoff is immediately generated, while in climate change scenarios with decreased precipitation, less runoff is immediately generated. This simple response leads to a rather uniform upward/downward shift in the ccP90T90 and ccP10T10 scenarios, respectively.

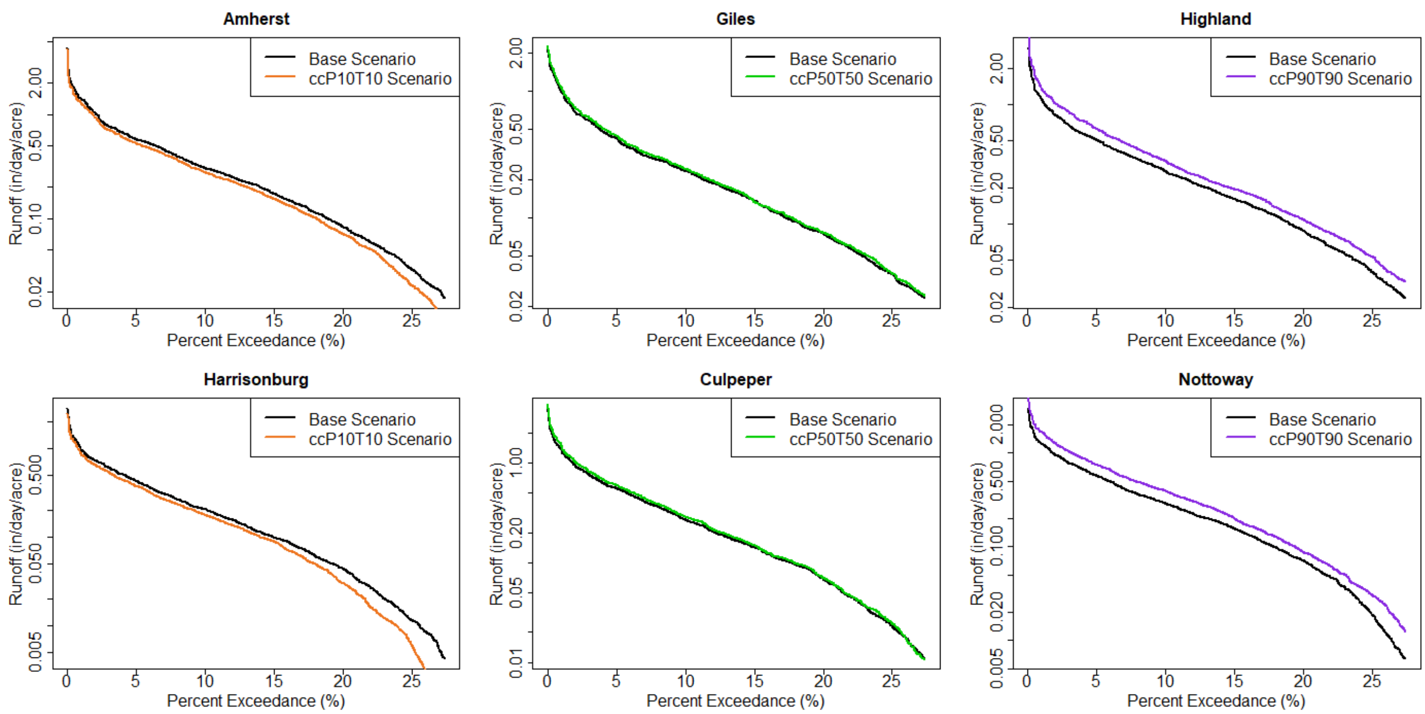

Figure 5.37: Percent Exceedance of Runoff per Unit Area of Impervious Land in Low- and High-Change Jurisdictions of Virginia

5.4.6 Land Use Runoff Change Summary

Overall, the spatial trends in percent change in runoff were not heavily dependent upon the land use group, with similar trends being seen across the vast majority of land use groups within the same climate change scenario. In general, the most drastic decreases in the ccP10T10 scenario were concentrated around the Harrisonburg/Rockingham and Virginia Beach/Chesapeake areas. In the ccP50T50 scenario, the highest increases tended to occur in central Virginia, concentrated around hotspots near Culpeper, Fluvanna, and Bedford. On the other hand, the ccP90T90 scenario, the highest percent changes were concentrated in the region near Nottoway, Amelia, Chesterfield, and Dinwiddie.

Throughout the ”Natural Pervious”, ”Hay and Forage” and ”Commodity Crop” land use groups, similar changes in the runoff regime were observed. In the ccP10T10 scenario, Amherst followed the base scenario while Harrisonburg had far smaller runoff generation at percent exceedances ranging from about 15% to above 30%. Scenario ccP50T50 exhibited very similar runoff generation to the base scenario almost uniformly throughout the state. Scenario ccP90T90 exhibited far higher runoff magnitudes than the base scenario, in both locations with high precipitation (Nottoway) and with high potential evapotranspiration (Highland). The ”Turf Grass” land use group exhibited similar trends to the other three, although the climate change scenario runoff responses were more similar to the base scenario's. The ”Impervious” land use group had a completely unique response – although the climate change scenarios most closely followed the base scenario for this land use group, runoff generation was largely all-or-nothing, as either precipitation would occur and runoff would immediately be generated, or no precipitation would occur and no runoff would occur.

Multiple linear regression was also conducted for each of these major land use groups to determine the extent that change in runoff from each land use depended on potential evapotranspiration and precipitation. Impervious land was found to be highly dependent on potential evapotranspiration and precipitation, with between 88.1% (ccP10T10) and 97.1% (ccP50T50) of variation in runoff explained by the two predictors. This relationship between precipitation, potential evapotranspiration, and runoff from impervious surfaces is shown in Figs. 5.38 (ccP10T10), 5.39 (ccP50T50), and 5.40 (ccP90T90) with the correlation between precipitation and impervious runoff especially strong due to the rapid conversion of precipitation to runoff on impermeable surfaces which do not allow for significant infiltration.

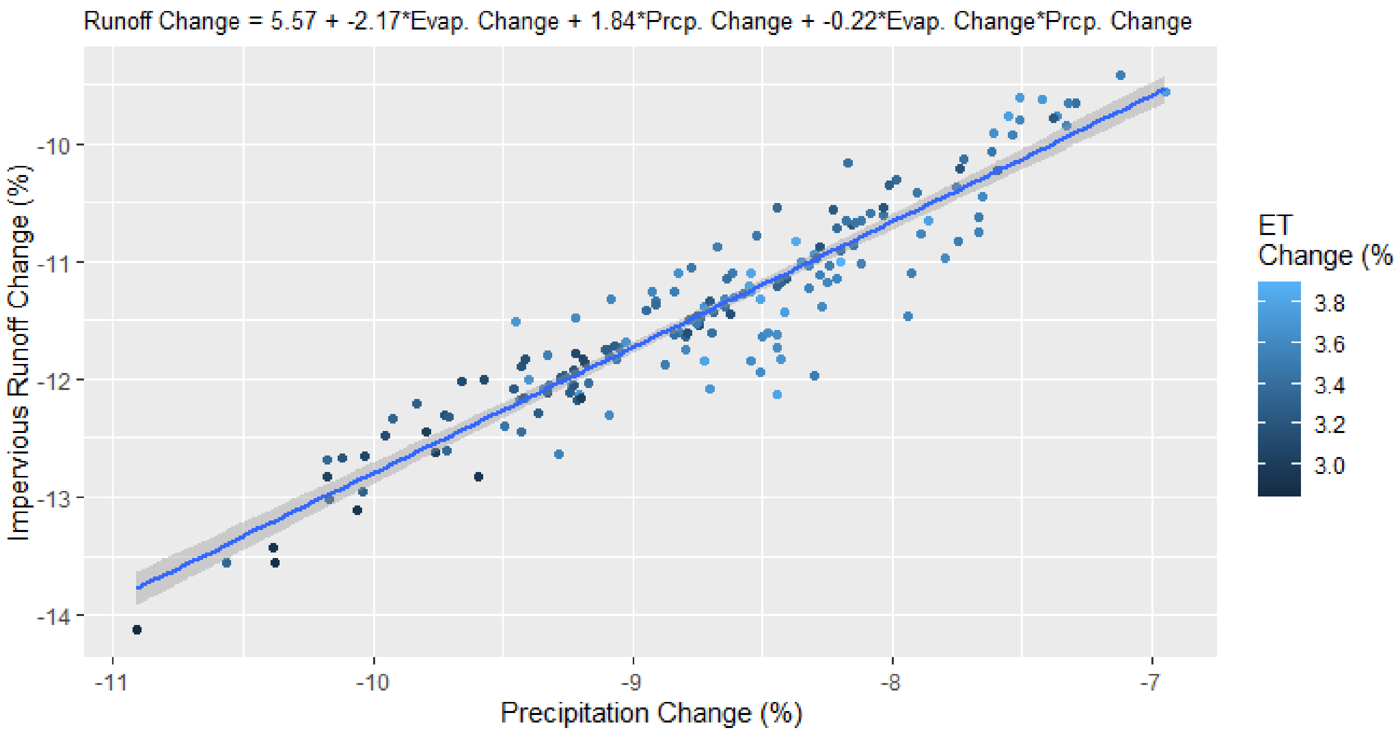

Figure 5.38: Relationship between Evapotranspiration, Precipitation, and Runoff from Impervious Surfaces in the ccP10T10 Scenario (R^2 = 0.881)

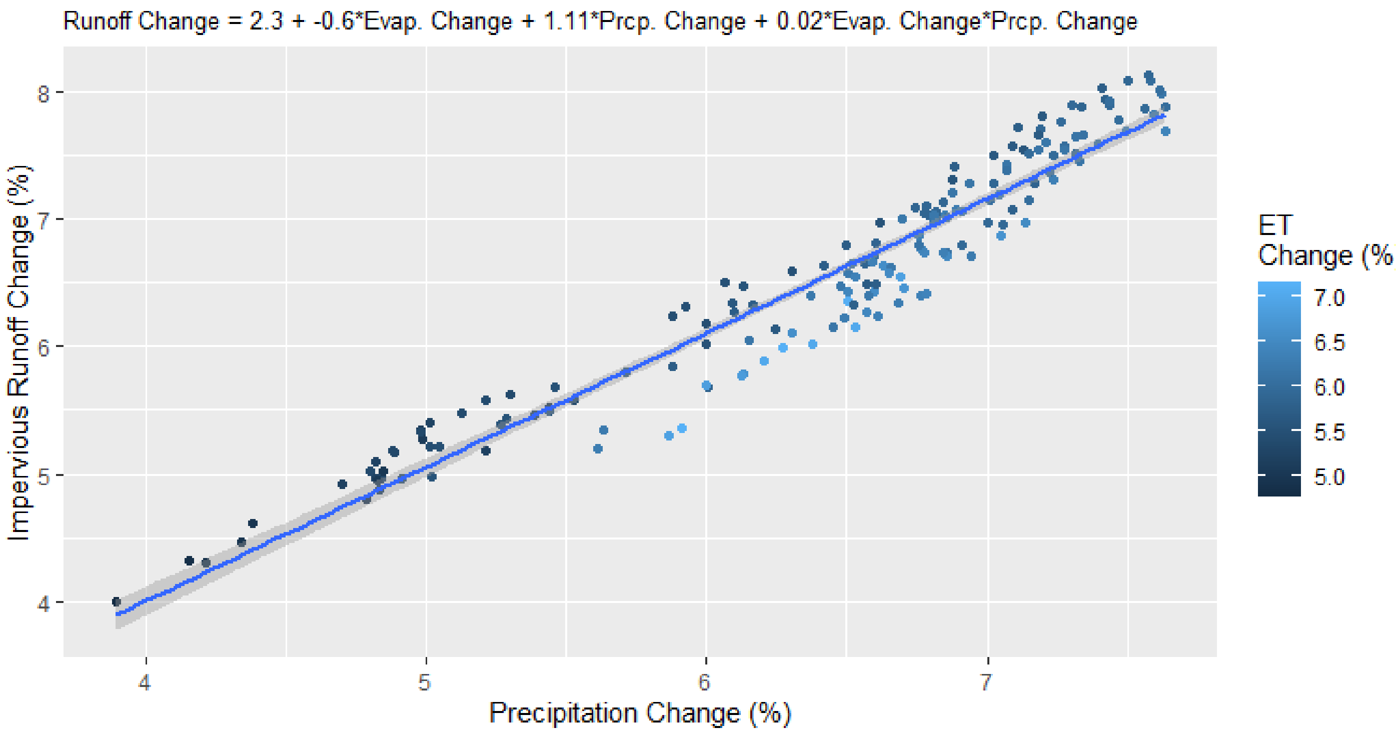

Figure 5.39: Relationship between Evapotranspiration, Precipitation, and Runoff from Impervious Surfaces in the ccP50T50 Scenario (R^2 = 0.971)

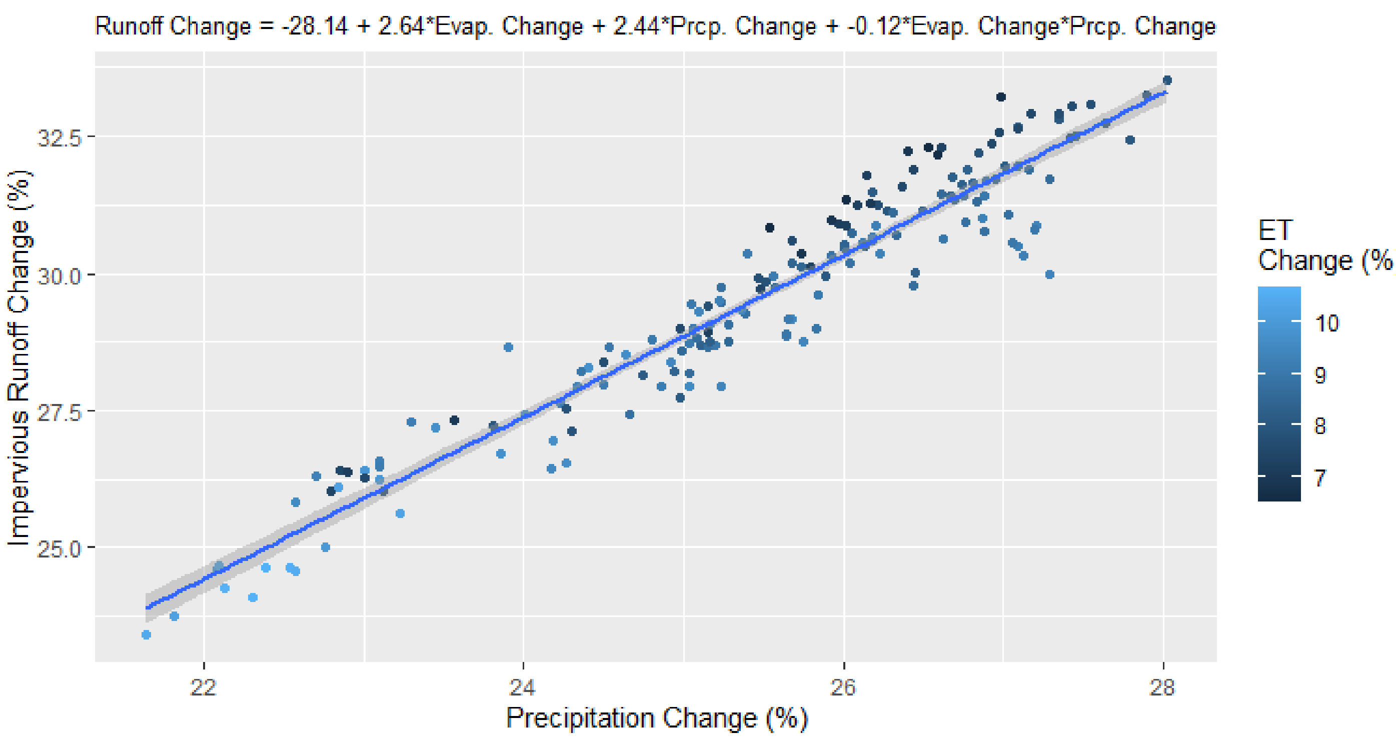

Figure 5.40: Relationship between Evapotranspiration, Precipitation, and Runoff from Impervious Surfaces in the ccP90T90 Scenario (R^2 = 0.954)

The strength of the relationship between potential evapotranspiration, precipitation, and runoff change was considerably less significant for each of the other land use groups. For the ccP10T10 scenario, the coefficient of determination in pervious land uses ranged from 0.25 (natural pervious) to 0.43 (turf grass). The relationship was far more significant in the ccP50T50 scenario, where the coefficient of determination ranged from 0.71 (hay and forage, commodity crops, and turf grass) to 0.76 (natural pervious). The relationship in the ccP90T90 scenario was less significant than in the ccP50T50 scenario, with the coefficient of determination ranging from a low of 0.67 (natural pervious) to a high of 0.77 (turf grass). The multiple linear regression relationship between the two predictors and runoff from natural pervious surfaces for the ccP10T10, ccP50T50, and ccP90T90 scenarios are shown in Figs. 5.41, 5.42, and 5.43, respectively. A list of the coefficients of determination between potential evapotranspiration, precipitation, and land use runoff for each land use group and each climate change scenario is found in Tab. 5.1.

Multiple linear regressions (MLRs) describing the relationship between the raw values of precipitation, PET, and runoff by land use are found in Appendix H. The trend of impervious land use groups having far higher values for the coefficient of determination is continued in these MLRs, with impervious R-squared values ranging from 0.938 (ccP10T10) to 0.960 (ccP90T90), which is far higher compared to the R-squared values seen in other land use groups such as the natural pervious land use group (ranging from a low of 0.687 in ccP90T90 to a high of 0.717 in ccP10T10).

5.5 Changes in Overall Unit Runoff

Each of the climate change scenarios tended to impact overall runoff generation in different ways, although the ways that each major basin was impacted by the scenarios tended to be

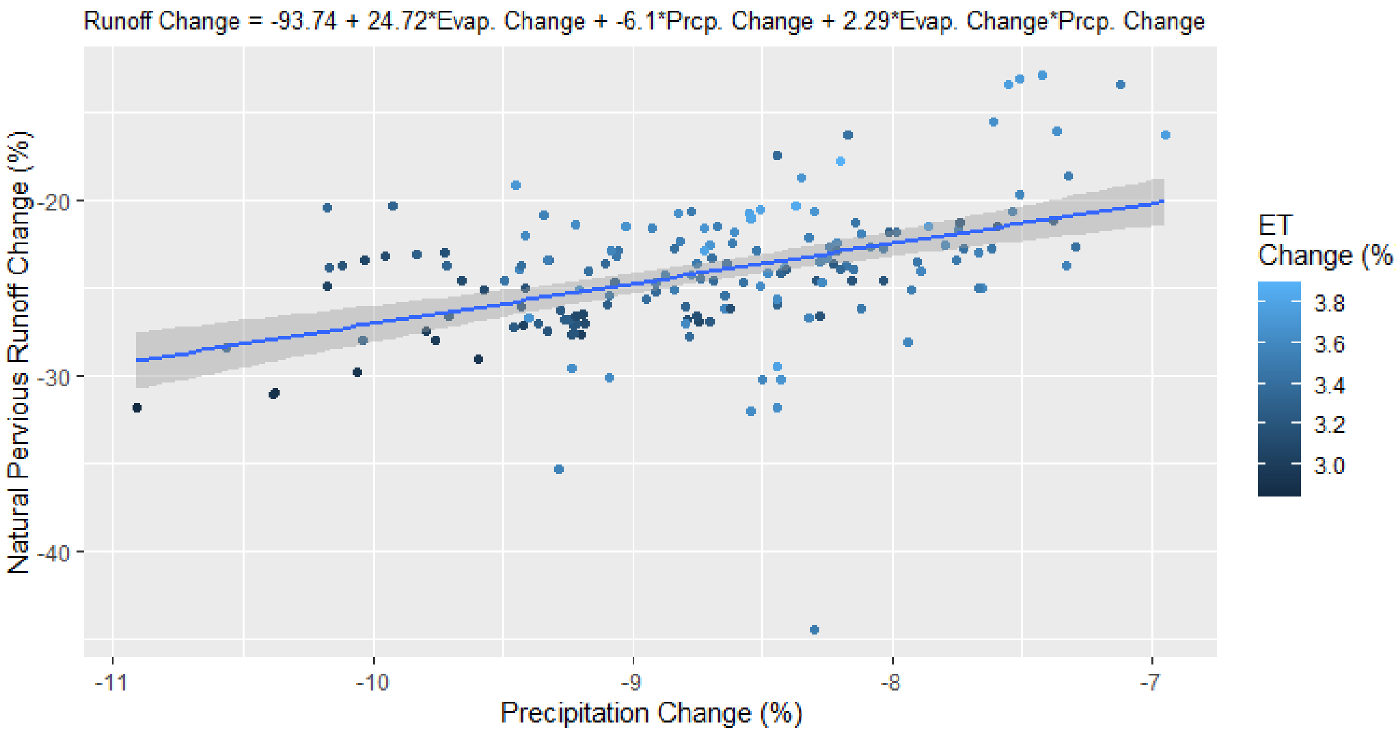

Figure 5.41: Relationship between Evapotranspiration, Precipitation, and Runoff from Natural Pervious Surfaces in the ccP10T10 Scenario ($R^2 = 0.253$)

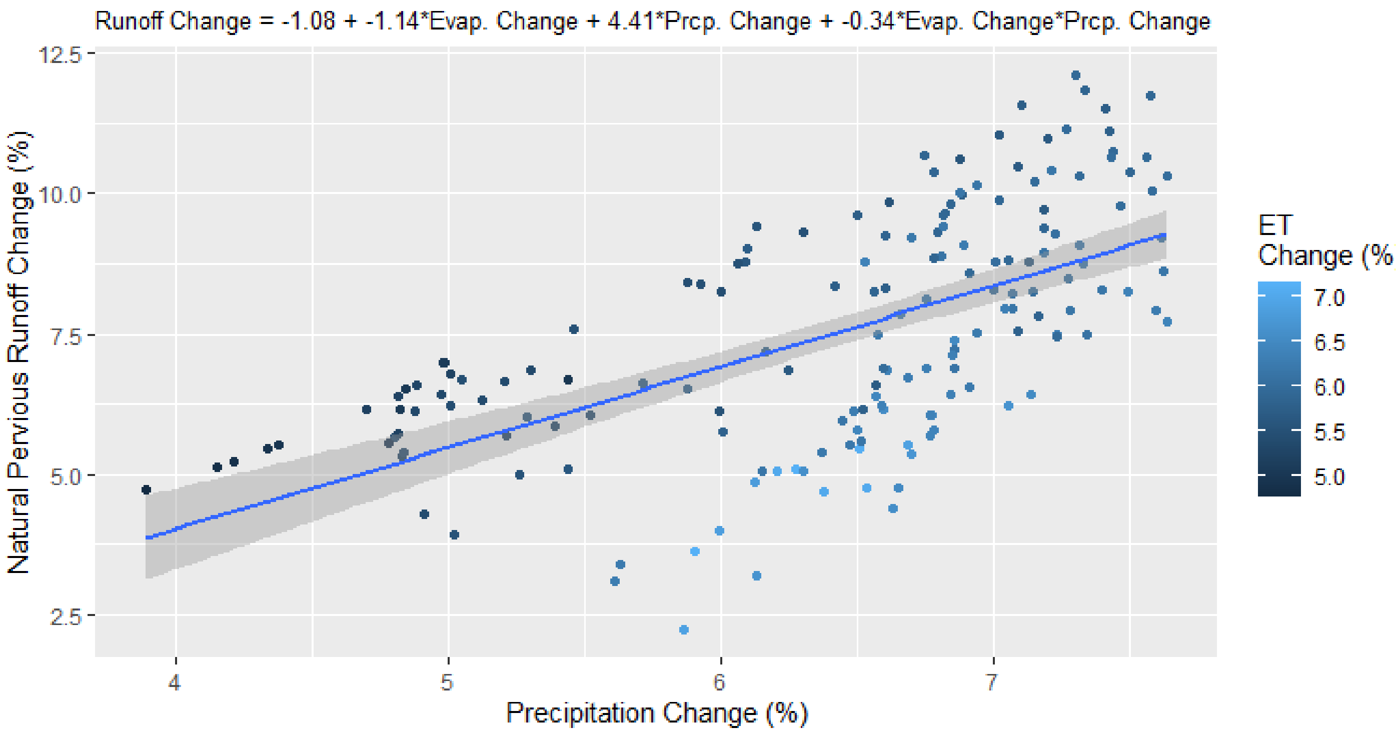

Figure 5.42: Relationship between Evapotranspiration, Precipitation, and Runoff from Natural Pervious Surfaces in the ccP50T50 Scenario ($R^2 = 0.759$)

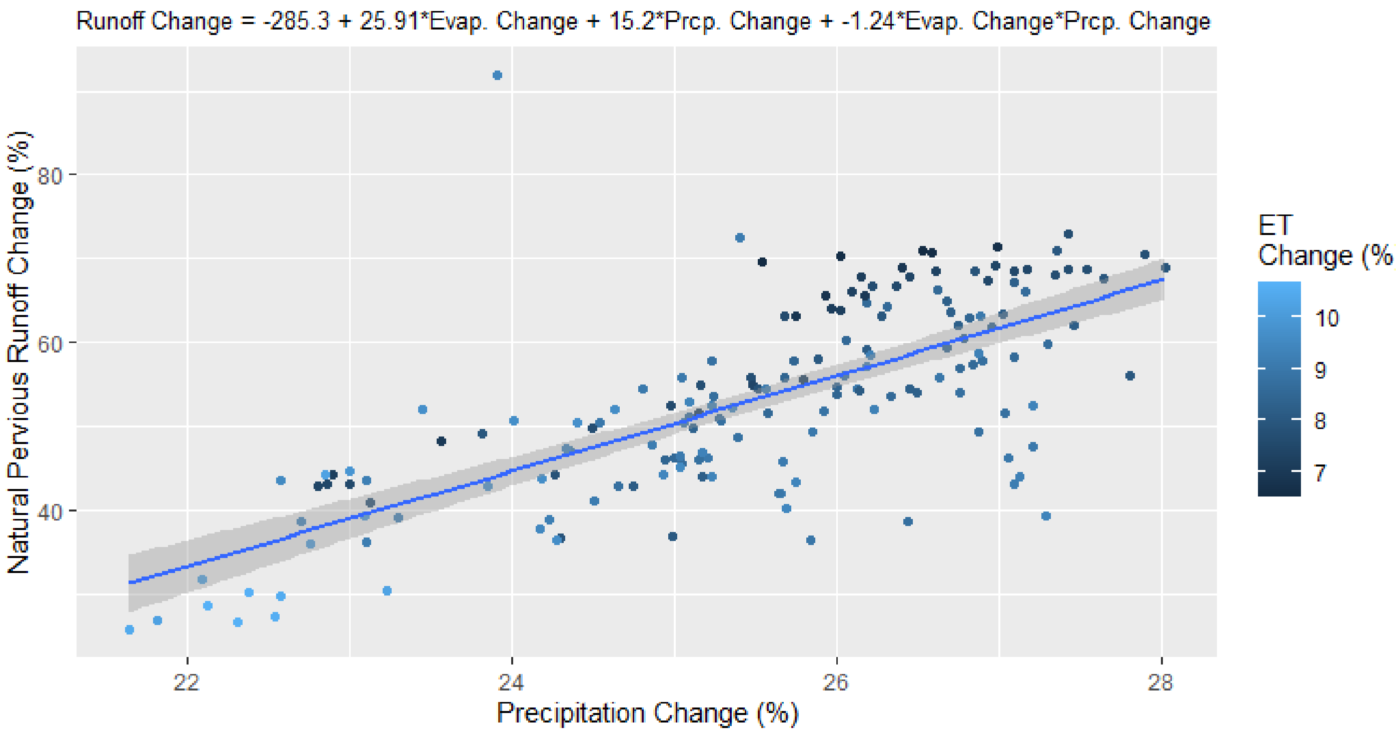

Figure 5.43: Relationship between Evapotranspiration, Precipitation, and Runoff from Natural Pervious Surfaces in the ccP90T90 Scenario ($R^2 = 0.665$)

Table 5.1: Coefficients of Determination Between Potential Evapotranspiration, Precipitation, and Land Use Runoff for Climate Change Scenarios

	ccP10T10	ccP50T50	ccP90T90
CSS True Forest	0.261	0.720	0.651
Natural Pervious	0.253	0.759	0.665
CSS Mixed Open	0.283	0.709	0.666
Natural Mixed Open	0.271	0.722	0.658
Hay and Forage	0.292	0.706	0.692
Ag Open Space	0.292	0.706	0.692
Commodity Crops	0.339	0.715	0.743
Harvested Forest	0.226	0.707	0.651
Turf Grass	0.430	0.705	0.767
Construction	0.631	0.767	0.841
Feeding Space	0.881	0.971	0.954
Impervious	0.881	0.971	0.954

quite consistent throughout the study area. The ccP10T10 scenario was often linked with the most drastic percent reductions to low-magnitude runoff quantities, such as the fifth (ranging from a -30.1% change in the median in the Pamunkey to a -39.0% change in the Upper James) and tenth (-28.8% change in the median runoff in the Middle James to -40.2% change in the Upper James) percent quantiles of runoff. Meanwhile, moderately high flows such as the seventy-fifth (-17.1% change in the median runoff in the Rappahannock to -22.2% change in the Mattaponi) and ninetieth (-17% change in the median runoff in the Rappahannock to -19.7% change in the Mattaponi) percent quantiles were less significantly impacted. The ccP50T50 scenario saw the largest percent increases to the largest flows such as the ninety-fifth percent quantile (+6.4% in the median runoff in the Upper James to +10.1% in the Appomattox). How the smallest flows, such as the fifth percent quantile, were affected in this scenario was highly variable, ranging from -2.1% in the Upper James to +11.0% in the Appomattox. However, moderate flows were more consistently altered by this scenario, such as the fiftieth percent quantile (+4.2% change in the median runoff in the Shenandoah to +7.4% in the Appomattox). Lastly, the ccP90T90 scenario saw the largest percent increases in flow in the very smallest flows, such as in the fifth percent quantile (+48.1% increase in the median runoff in the Upper James to +89.9% increase in the Appomattox), and in the very largest flows, such as in the ninety-fifth percentile (+50.3% increase in the median runoff in the Upper James to +71.7% increase in the Appomattox). Moderate flows, such as the fiftieth percentile (+31.5% in median runoff in the Upper James to +53.9% in the Appomattox) were less drastically impacted. Tables of the quantiles of raw runoff values for each river segment in each of these basins are located in Appendix C, while the percent differences in these runoff quantiles between the base and climate change scenarios are shown in Appendix D.

5.5.1 Intra-Basin Runoff Variation

Shenandoah

The Shenandoah River basin contains 23 river segments which exhibit a wide range of unit runoff responses. Many of the segments near the confluence of the Shenandoah with the Potomac (PS5_4380_4370, PS1_4830_5080, and PS1_4770_4830) or in the headwater reaches of the contributing area (PS0_6150_6160, PS0_6160_6161, and PS3_6161_6280) show median unit runoff values of approximately 0.5 cfs/mi^2 or less in the base scenario. On the other hand, a number of river segments in other headwater reaches of the basin, including PS2_6730_6660, PS2_6660_6490, and PS2_6490_6420, experience far higher median unit runoff values of 0.85 cfs/mi^2 or above in this base scenario. Although on some days of heavy rain, the maximum unit runoff can range up to 50 cfs/mi^2 or above, the maximum point excluding these outliers was less than 3.5 cfs/mi^2 in the Shenandoah and in all other basins of study for the base scenario – therefore, when visualizing unit runoff data, a scale of 0 to 3.5 cfs/mi^2 was chosen for this and all other basins, as shown in Fig. 5.44.

The daily flows of every river segment within the Shenandoah River basin were concatenated for the base, ccP10T10, ccP50T50, and ccP90T90 scenario. Then, a boxplot was created to show how unit runoff changes between these four scenarios (Fig. 5.45). Outliers were hidden in this boxplot and in the boxplots for other river basins as a result of the incredibly high number of outliers on the high side resulting from abnormally rainy or flooding days. As shown in Fig. 5.45, scenario ccP50T50 (IQR: 0.31-1.15 cfs/mi^2; median: 0.64 cfs/mi^2) had a very similar unit runoff response as the base scenario (IQR: 0.30-1.10 cfs/mi^2; median = 0.62 cfs/mi^2). On the other hand, ccP10T10 had a narrower IQR (0.21-0.90 cfs/mi^2) and lower median (0.48 cfs/mi^2) than the base scenario while ccP90T90 had a wider IQR (0.42-1.43 cfs/mi^2) and higher median (0.81 cfs/mi^2).

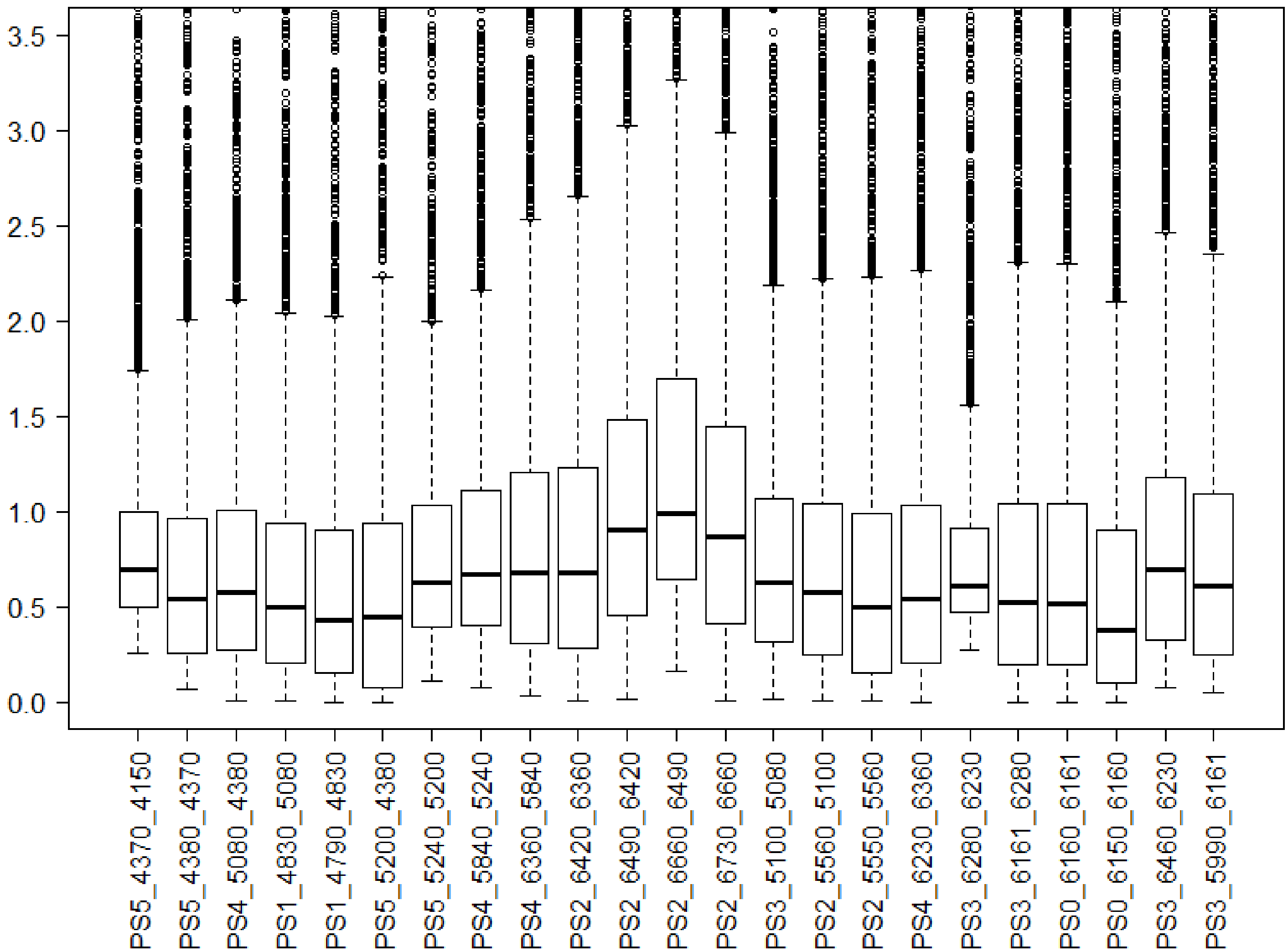

Figure 5.44: Runoff per Unit Area Land (cfs/mi^2) in the Shenandoah River Basin for the Base Scenario

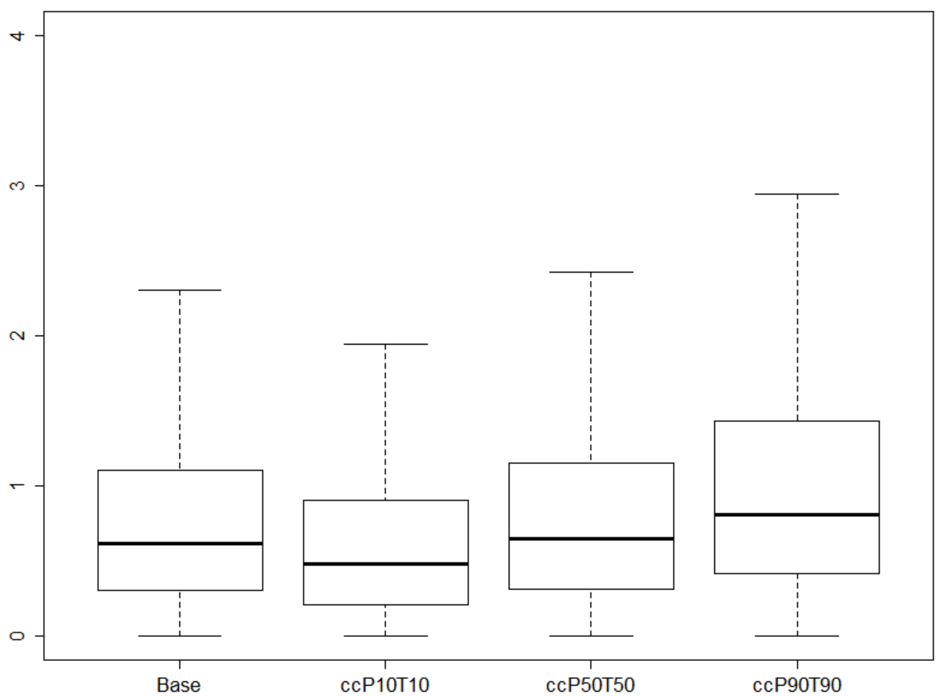

Figure 5.45: Runoff per Unit Area Land (cfs/mi^2) in the Shenandoah River Basin for the Base and Climate Change Scenarios

Mattaponi

The four river segments above the Fall Line in the Mattaponi River basin experience nearly identical runoff generation to each other in the base scenario, as shown in Fig. 5.46. However, there is a slight increasing trend in median runoff moving downstream from the headwater segment YM2_6120_6430 (median = 0.41 cfs/mi^2) to the outlet segment YM4_6620_0001 (median = 0.57 cfs/mi^2).

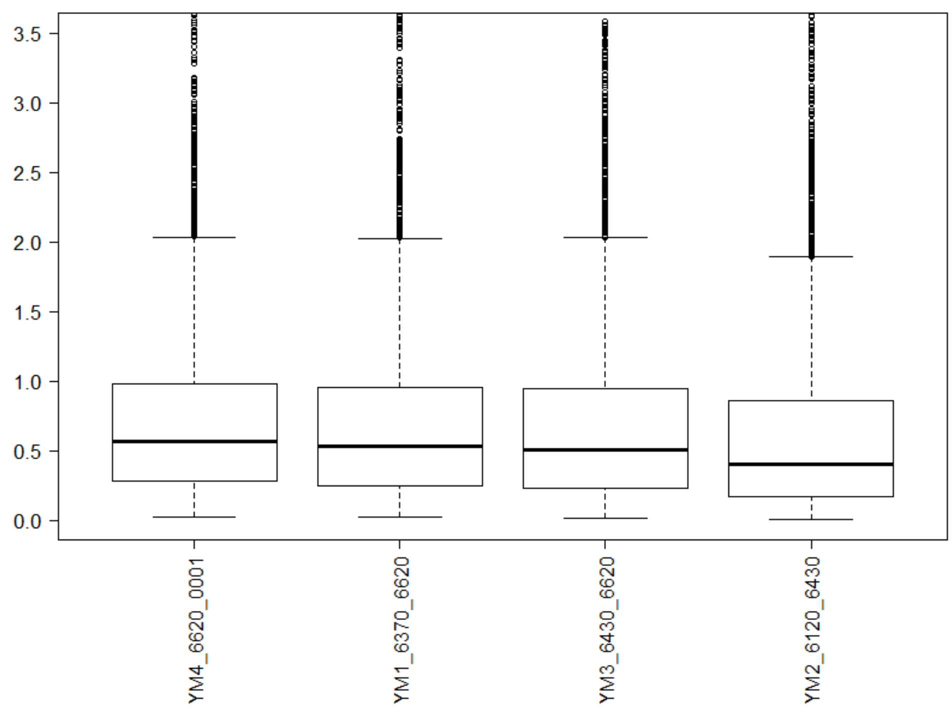

Figure 5.46: Runoff per Unit Area Land (cfs/mi^2) in the Mattaponi River Basin for the Base Scenario

As seen in the Shenandoah, the Mattaponi experiences a narrower IQR (0.16-0.73 cfs/mi^2) and lower median (0.37 cfs/mi^2) in the ccP10T10 scenario when compared with the base scenario (IQR: 0.23-0.94 cfs/mi^2; median = 0.50 cfs/mi^2). On the other hand, the ccP90T90 scenario experiences a wider IQR (0.35-1.37 cfs/mi^2) and a higher median (0.75 cfs/mi^2) compared with the base scenario. The moderate ccP50T50 scenario results in a similar

IQR (0.24-1.00 cfs/mi^2) and median (0.53 cfs/mi^2) to the base scenario. These ranges are visualized in Fig. 5.47.

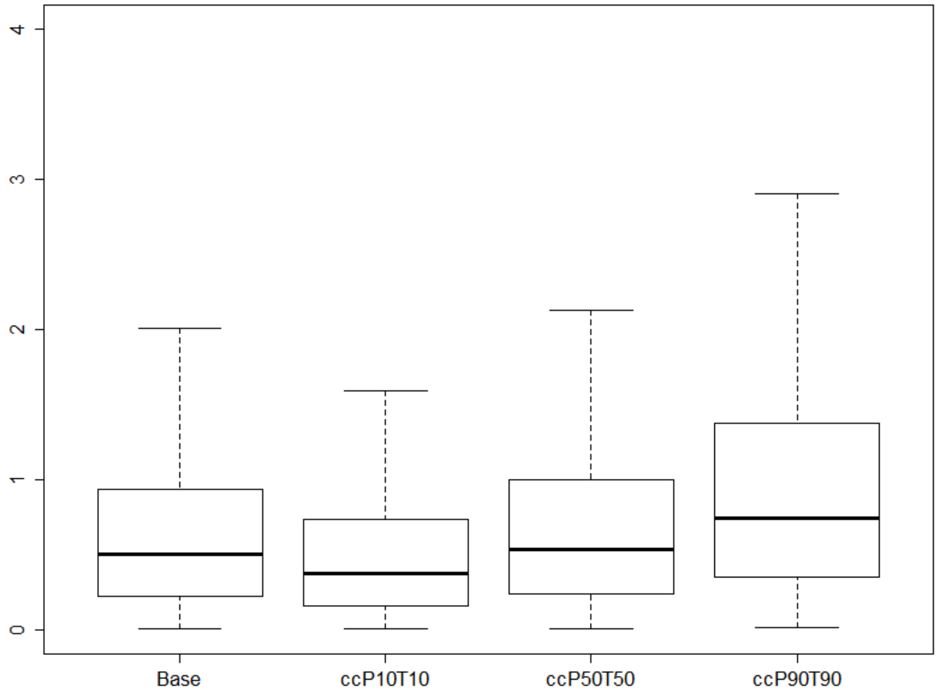

Figure 5.47: Runoff per Unit Area Land (cfs/mi^2) in the Mattaponi River Basin for the Base and Climate Change Scenarios

Pamunkey

Similar to the Mattaponi, the Pamunkey had a relatively consistent runoff response throughout the basin for the base scenario (Fig. 5.48). All of the river segments near the Pamunkey outlet into coastal areas (YP4_6750_0001, YP4_6720_6750, YP3_6670_6720, and YP1_6680_6670) had a median unit runoff of just over 0.50 cfs/mi^2 and an IQR ranging from about 0.25 to 1.00 cfs/mi^2. Further up in the basin, in many of the headwater segments (YP2_6390_6330, YP3_6470_6690, YP1_6570_6680), slightly lower unit runoffs (medians of about 0.4 cfs/mi^2 and IQRs of about 0.15-0.80 cfs/mi^2) were seen.

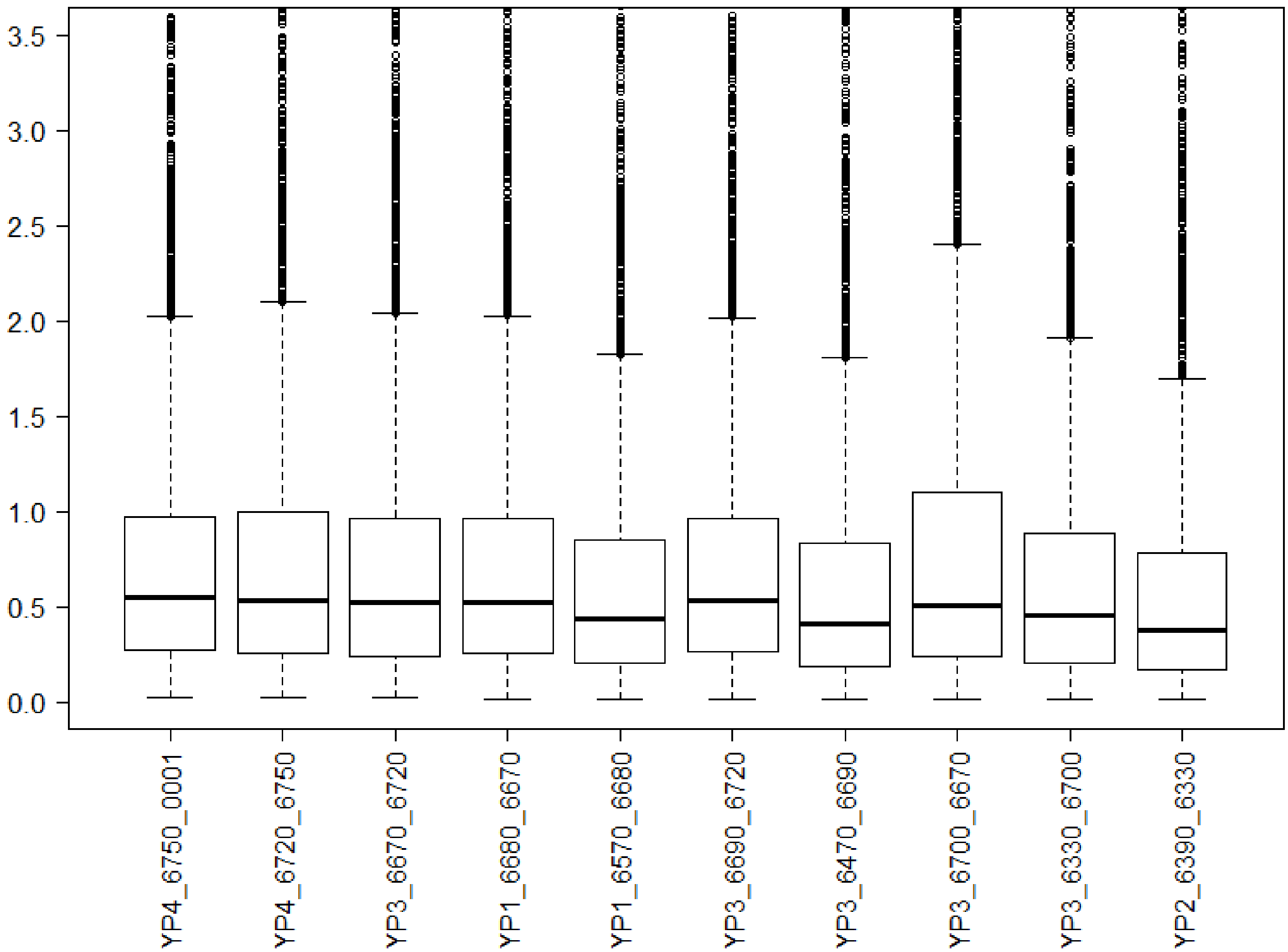

Figure 5.48: Runoff per Unit Area Land (cfs/mi^2) in the Pamunkey River Basin for the Base Scenario

Just like the previously discussed river basins, the moderate ccP50T50 scenario (IQR: 0.24-1.00 cfs/mi^2, median = 0.52 cfs/mi^2) was nearly identical to the base scenario (IQR: 0.23-0.94 cfs/mi^2) in terms of runoff response, while the ccP10T10 scenario had a narrower IQR (0.16-0.73 cfs/mi^2) and lower median (0.36 cfs/mi^2). Also, just as in other basins, the ccP90T90 scenario had a wider IQR (0.35-1.38 cfs/mi^2) and higher median (0.73 cfs/mi^2) than the base scenario, as shown in Fig. 5.49.

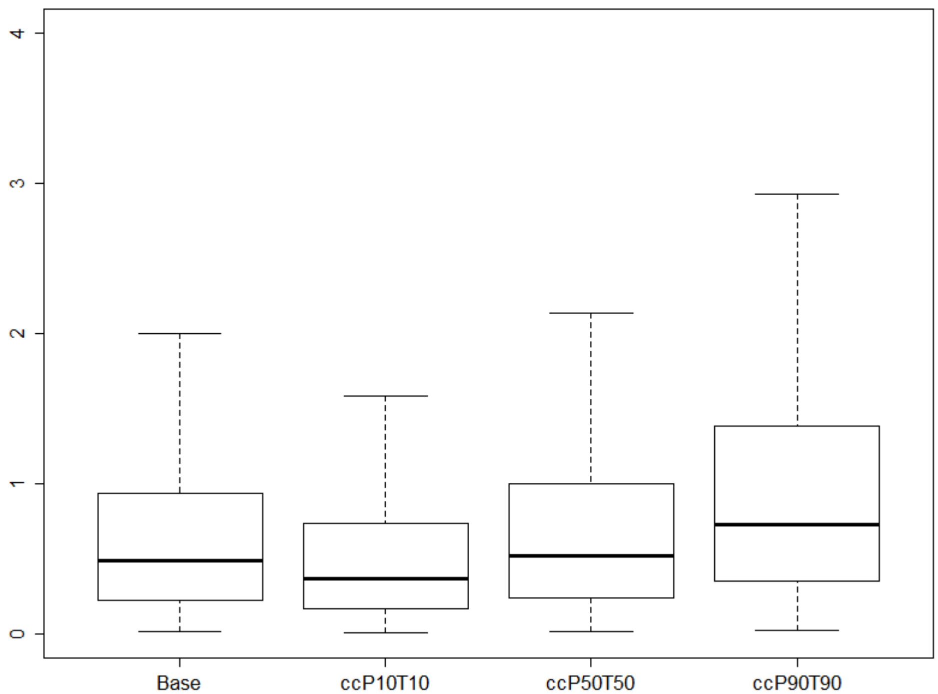

Figure 5.49: Runoff per Unit Area Land (cfs/mi^2) in the Pamunkey River Basin for the Base and Climate Change Scenarios

Rappahannock

The Rappahannock River basin experienced some of the most variability in unit runoff production among its river segments. In an opposite trend to that seen in the Pamunkey, many of the river segments near the Rappahannock's outlet to a coastal system (RU5_6030_0001, RU4_5640_6030, RU2_5220_5640, RU4_6040_6030, and RU3_6170_6040) exhibited the lowest median unit runoffs (about 0.45 cfs/mi^2) and narrowest IQRs (about 0.2 to 1.0 cfs/mi^2) in the basin in the base scenario (Fig. 5.50). On the other hand, a number of the headwater and other upstream segments (RU2_6200_6170, RU2_5940_6200, RU2_5500_5610, RU2_6090_6220, and RU2_5810_5610) were associated with far higher median unit runoffs (about 1.0 cfs/mi^2) and wider IQRs (about 0.5 to 1.5 cfs/mi^2).

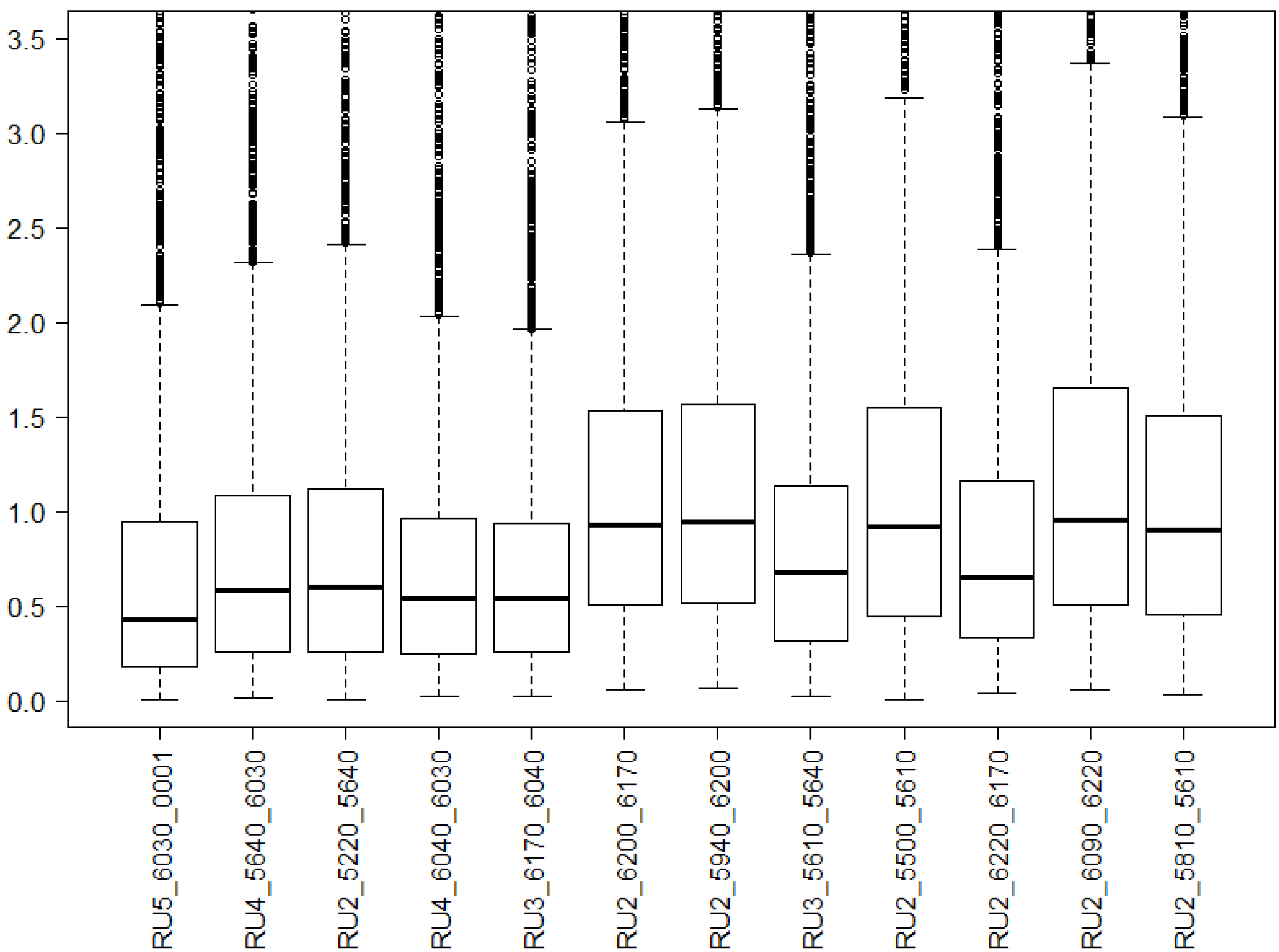

Figure 5.50: Runoff per Unit Area Land (cfs/mi^2) in the Rappahannock River Basin for the Base Scenario

Regardless of the Rappahannock bucking the trend seen in the Pamunkey basin of higher unit runoffs occurring near the outlet, the Rappahannock followed a very similar trend throughout the climate change scenarios as all the previously discussed basins (Fig. 5.51). The ccP10T10 scenario exhibited the smallest median (0.56 cfs/mi^2) and narrowest IQR (0.25-1.06 cfs/mi^2) of all the scenarios. The ccP50T50 scenario exhibited a very similar median (0.75 cfs/mi^2) and IQR (0.36-1.37 cfs/mi^2) as the base scenario (median: 0.70 cfs/mi^2; IQR: 0.34-1.28 cfs/mi^2). The ccP90T90 scenario showed both the highest median (0.94 cfs/mi^2) and widest IQR (0.47-1.68 cfs/mi^2) of any of the scenarios.

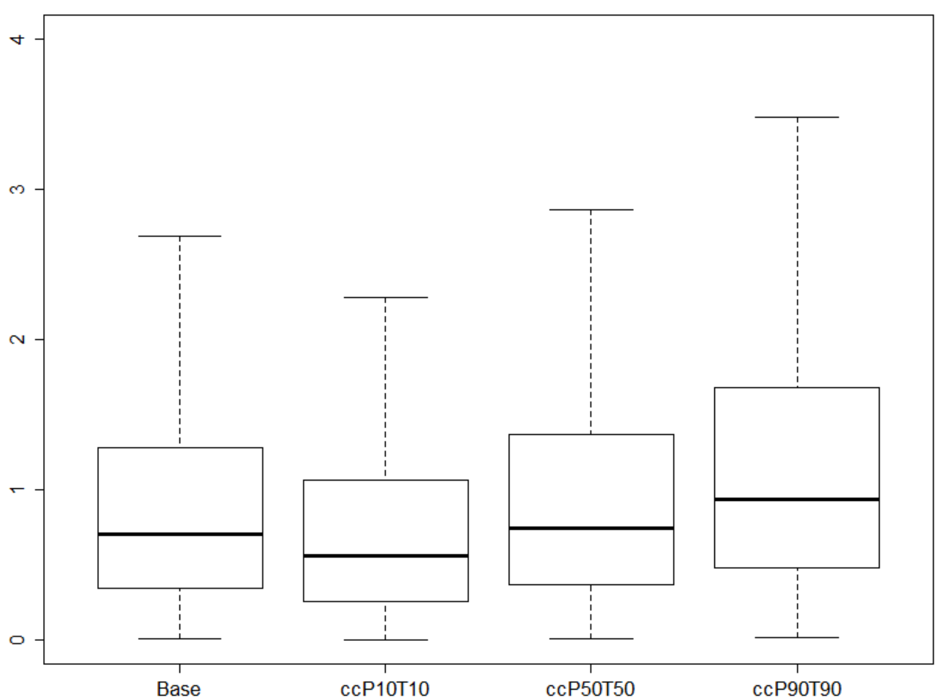

Figure 5.51: Runoff per Unit Area Land (cfs/mi^2) in the Rappahannock River Basin for the Base and Climate Change Scenarios

Upper James

The Upper James basin had considerable variability in unit runoff production within the basin in the base scenario, with geographic closeness seemingly an inadequate predictor of runoff production (Fig. 5.52). For example, the river segment JU1_6300_6650 exhibited one of the highest runoff productions in the basin (median: 0.89 cfs/mi^2; IQR: 0.47-1.57 cfs/mi^2). However, its neighboring, immediately downstream river segment JU3_6650_7300 showed one of the lowest productions in the basin (median: 0.55 cfs/mi^2; IQR: 0.20-1.07 cfs/mi^2). Elsewhere in the basin, river segment JU1_6290_6590 similarly had one of the highest runoff productions within the basin (median: 0.76 cfs/mi^2; IQR: 0.27-1.56 cfs/mi^2). However, its downstream, neighboring segment JU1_6590_6600 also had a far lower runoff production (median: 0.52 cfs/mi^2; IQR: 0.19-1.00 cfs/mi^2).

Regardless of the lack of distinct trends within the base scenario in the Upper James basin, the same trends were seen between the climate change and base scenarios as in every other basin, as shown in Fig. 5.53. The base scenario (median: 0.68 cfs/mi^2; IQR: 0.31-1.26 cfs/mi^2) was very similar to the fiftieth percentile precipitation and temperature ccP50T50 scenario (median: 0.71 cfs/mi^2, IQR: 0.31-1.33 cfs/mi^2). The ccP10T10 scenario was linked with both the smallest median (0.52 cfs/mi^2) and narrowest IQR (0.21-1.06 cfs/mi^2) of the scenarios, while the ccP90T90 scenario was linked with both the largest median (0.88 cfs/mi^2) and widest IQR (0.41-1.63 cfs/mi^2).

Middle James

Similar to the Upper James, unit runoff values were quite variable within the Middle James basin, although the regions of highest runoff generation and lowest runoff generation were often geographically distinct (Fig. 5.54). The regions near the outlet, such as

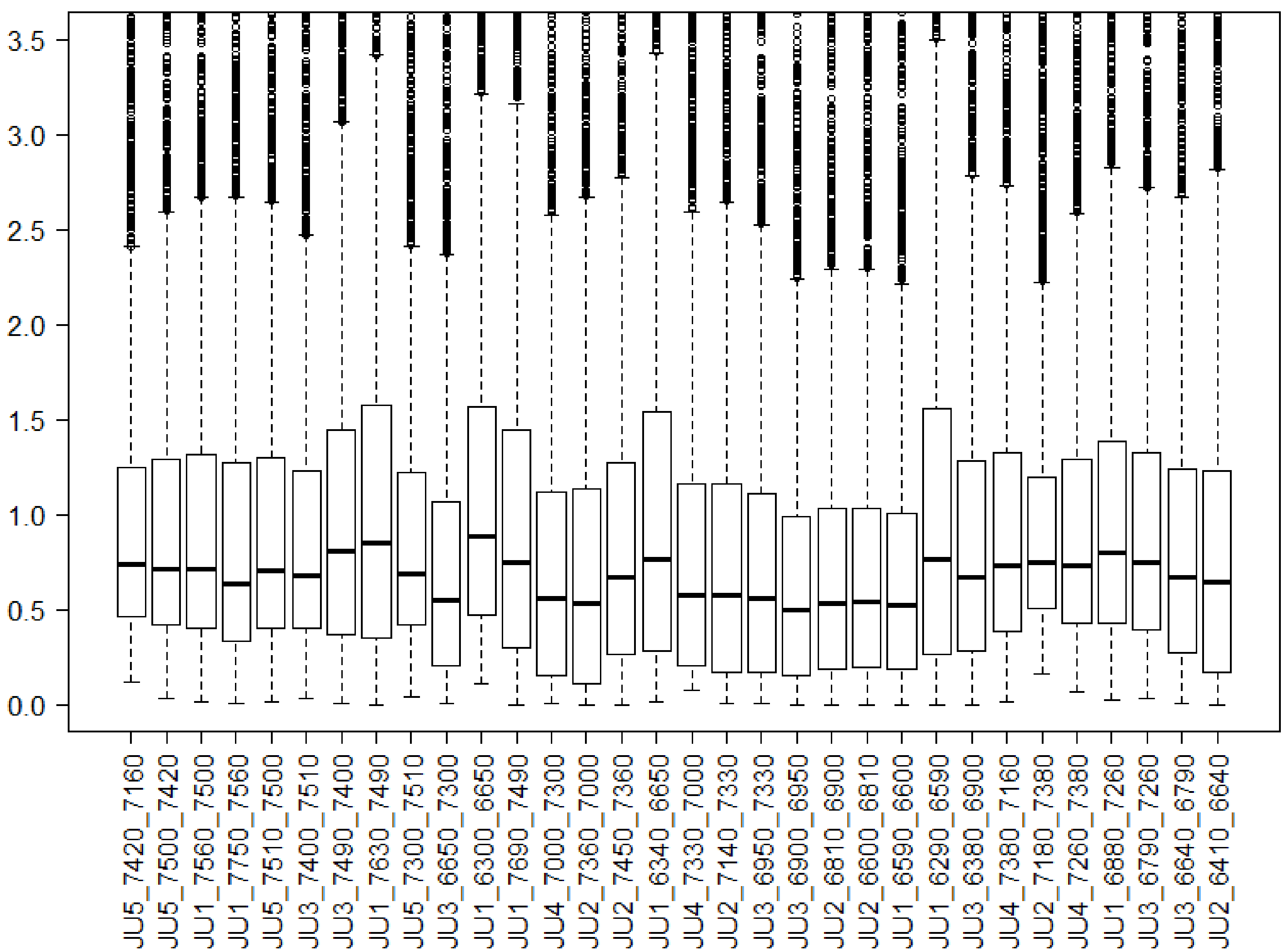

Figure 5.52: Runoff per Unit Area Land (cfs/mi^2) in the Upper James River Basin for the Base Scenario

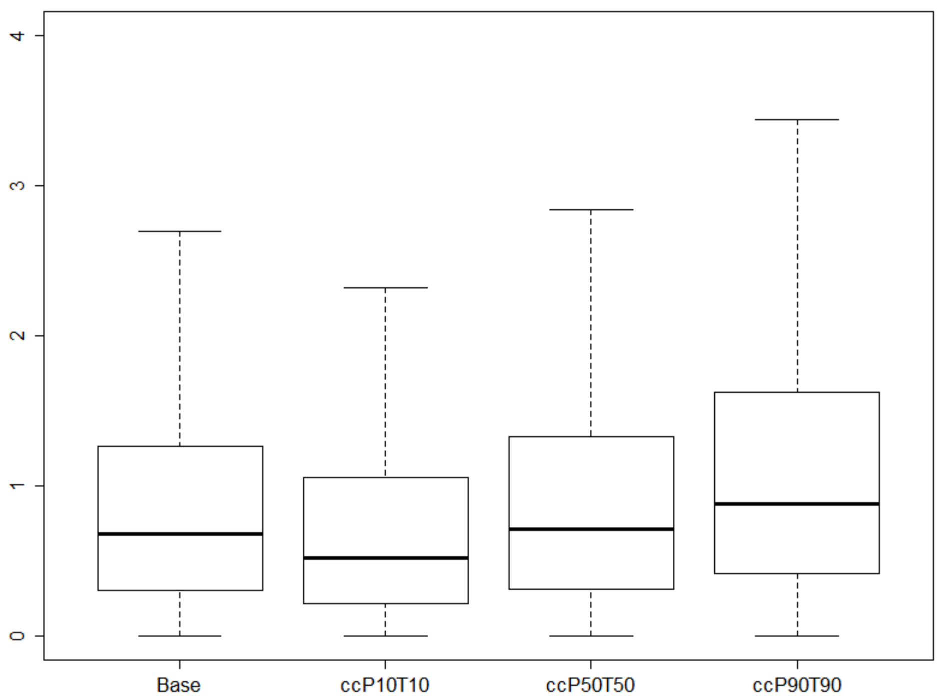

Figure 5.53: Runoff per Unit Area Land (cfs/mi^2) in the Upper James River Basin for the Base and Climate Change Scenarios

JL7_6800_7070, JL1_7170_6800, and JL7_7030_6800, often showed some of the lowest runoff generations in the basin, with medians of approximately 0.5 cfs/mi^2 and IQRs ranging from about 0.25 to 1.00 cfs/mi^2. The Rivanna River, associated with the river segment JL4_6520_6710 and its upstream segments, exhibited considerably higher flows, with a median of about 0.7 cfs/mi^2 and an IQR of about 0.35 to 1.30 cfs/mi^2. However, the Rockfish River (segments JL2_6850_6890 and JL1_6770_6850) and Buffalo and Piney Rivers (segment JL3_7090_7150 and upstream) exhibit far higher runoff generation than even the Rivanna, with medians above 1.0 cfs/mi^2 and IQRs ranging from about 0.5 to 2.0 cfs/mi^2 or higher.

Regardless of this considerable variability in inter-basin runoff generation in the base scenario, the Middle James basin is impacted identically to the other basins when run through the climate change scenarios (Fig. 5.55). The largest median (0.93 cfs/mi^2) and widest IQR (0.46-1.80 cfs/mi^2) are seen in the ccP90T90 scenario. The ccP50T50 scenario (median: 0.73 cfs/mi^2; IQR: 0.33-1.46 cfs/mi^2) has very similar unit runoff values to the base scenario (median: 0.69 cfs/mi^2; IQR: 0.31-1.38 cfs/mi^2), with values often just marginally higher in the ccP50T50 than the base scenario. The smallest median (0.54 cfs/mi^2) and narrowest IQR (0.23-1.15 cfs/mi^2) are seen in the lowest precipitation ccP10T10 scenario.

Appomattox

Although the Appomattox River is a tributary of the James River, its contributing land exhibits far more homogeneous runoff generation than either the Upper or Lower James River basins (Fig. 5.56). Throughout the entirety of the basin, median unit runoff values of approximately 0.5 cfs/mi^2 are seen, with the IQRs often ranging from about 0.2 to 0.9 cfs/mi^2.

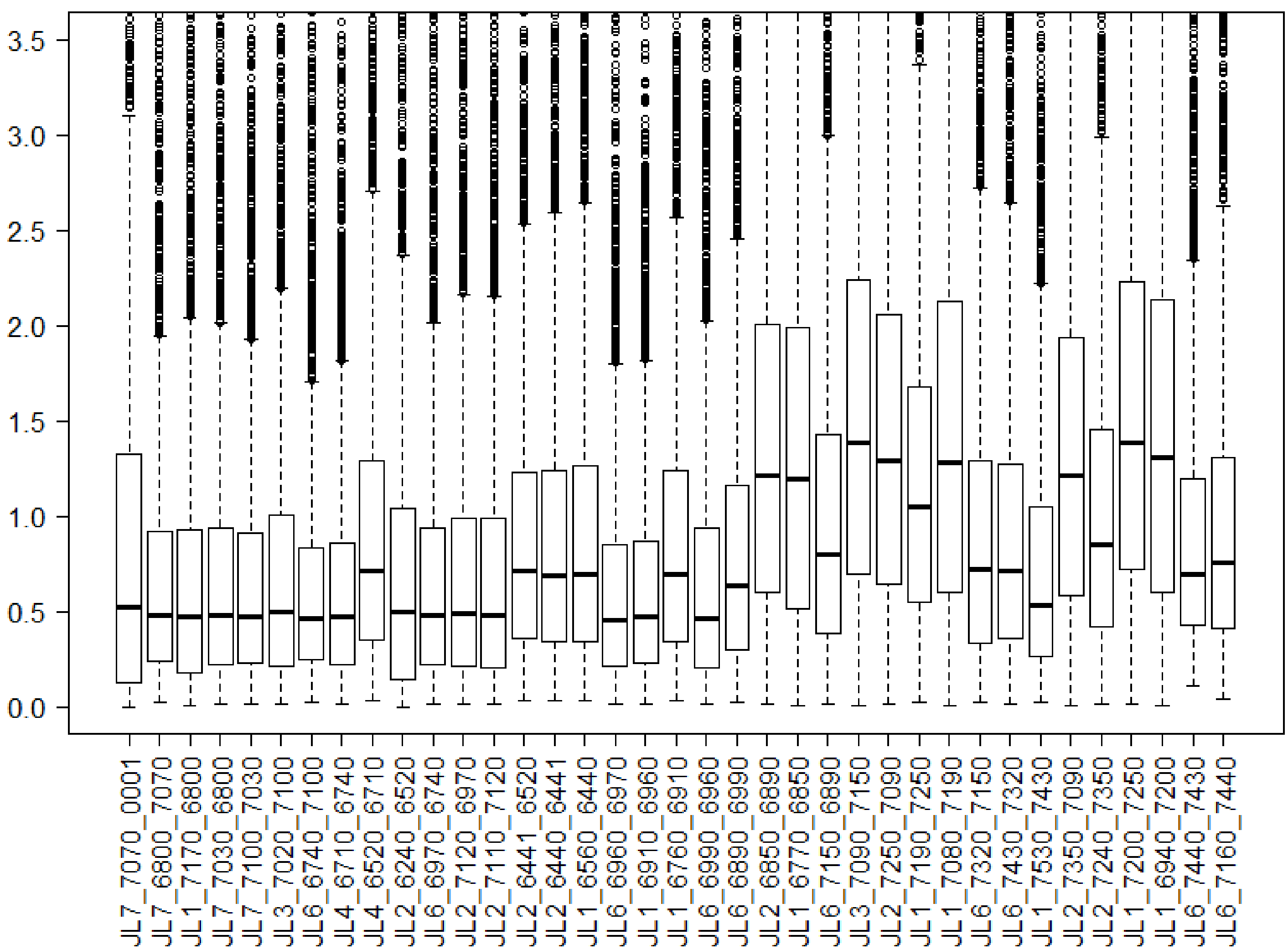

Figure 5.54: Runoff per Unit Area Land (cfs/mi^2) in the Middle James River Basin for the Base Scenario

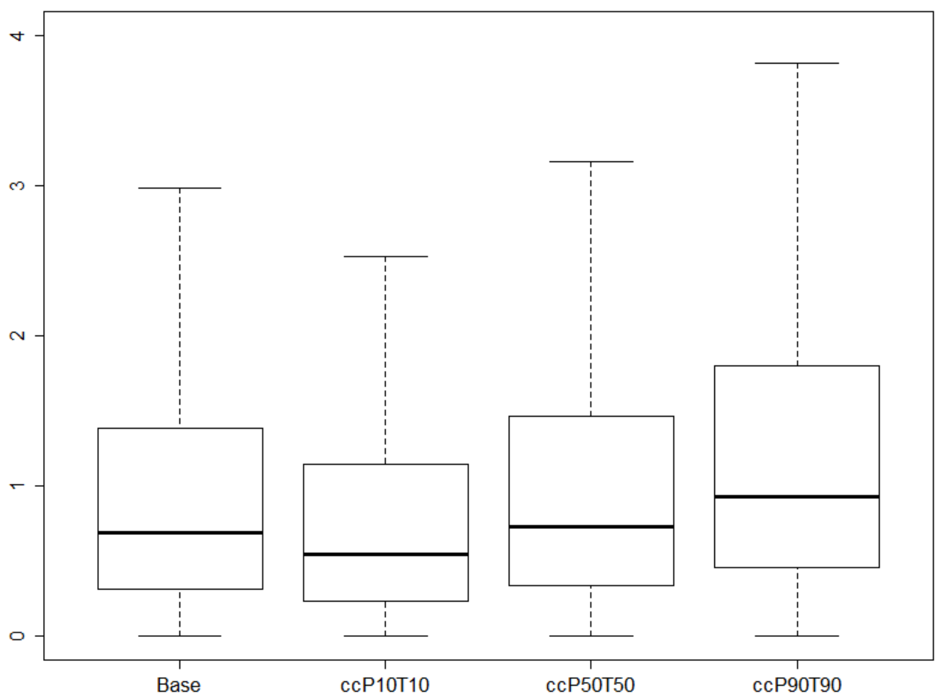

Figure 5.55: Runoff per Unit Area Land (cfs/mi^2) in the Middle James River Basin for the Base and Climate Change Scenarios

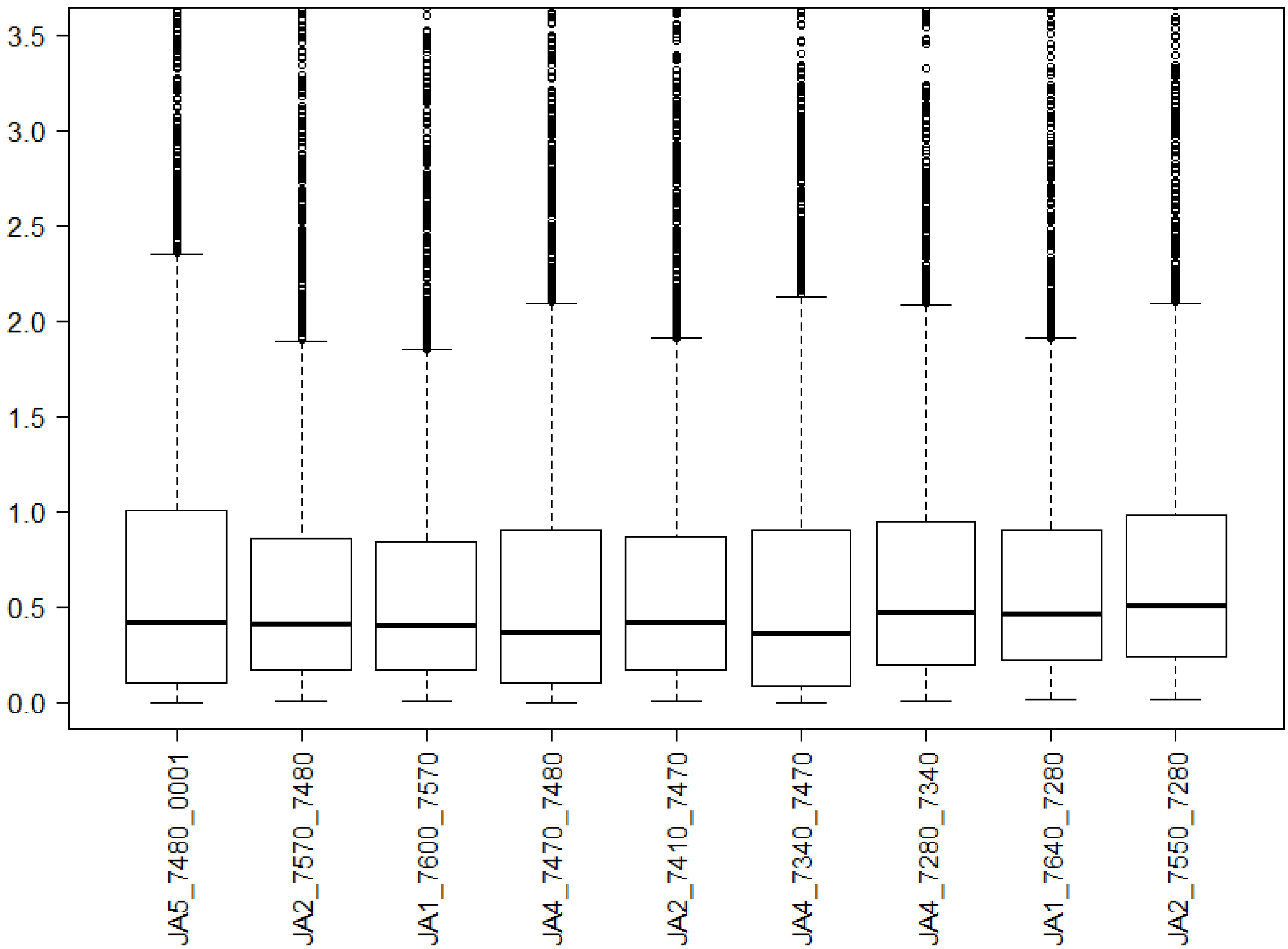

Figure 5.56: Runoff per Unit Area Land (cfs/mi^2) in the Appomattox River Basin for the Base Scenario

The Appomattox River basin also experiences the same trends in changes in runoff as a result of climate change as the other scenarios (Fig. 5.57). As a result of ccP10T10, the median runoff is reduced to 0.32 cfs/mi^2, with the IQR stretching from 0.12 to 0.73 cfs/mi^2. The ccP50T50 scenario results in a slightly higher median (0.46 cfs/mi^2) and a similar IQR (0.17-0.98 cfs/mi^2) compared with the base scenario (median: 0.43 cfs/mi^2; IQR: 0.16-0.92 cfs/mi^2). The ccP90T90 scenario results in an increase in median runoff to 0.66 cfs/mi^2 and a widening of the IQR to a range of 0.26 to 1.32 cfs/mi^2.

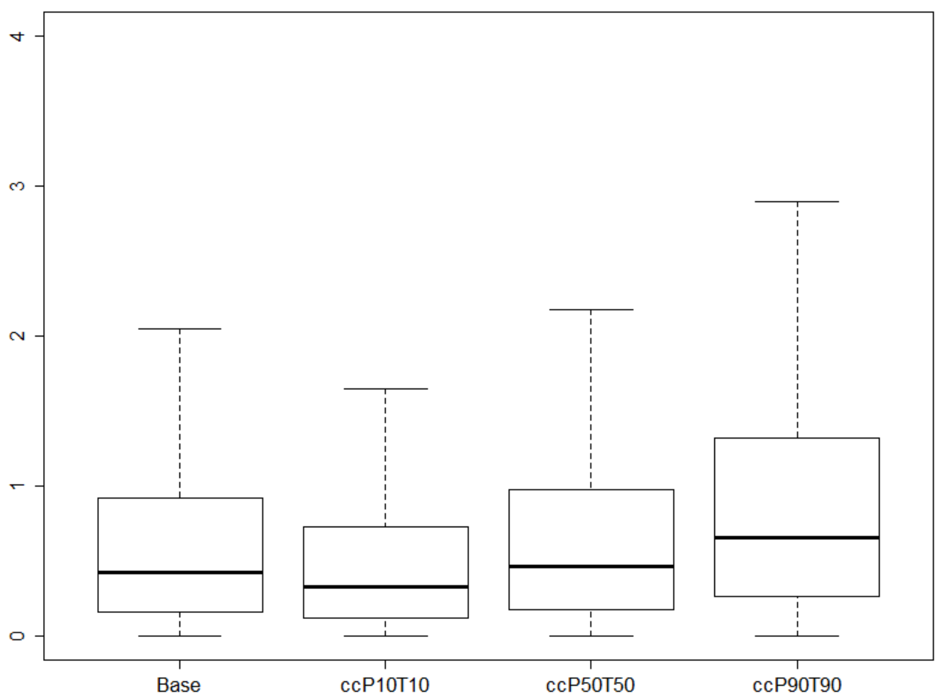

Figure 5.57: Runoff per Unit Area Land (cfs/mi^2) in the Appomattox River Basin for the Base and Climate Change Scenarios

5.5.2 Inter-Basin Runoff Variation

Even in the base scenario, unit runoff generated from the different investigated river basins in Virginia within the Chesapeake Bay watershed is quite variable. As shown in Fig. 5.58, the

Mattaponi (median = 0.50 cfs/mi^2, mean = 0.88 cfs/mi^2), Pamunkey (median = 0.49 cfs/mi^2, mean = 0.89 cfs/mi^2), and Appomattox (median = 0.43 cfs/mi^2, mean = 0.88 cfs/mi^2) exhibit some of the lowest unit runoff values. The Shenandoah basin shows slightly higher (median = 0.62 cfs/mi^2, mean = 1.07 cfs/mi^2) unit runoff values. Finally, the Rappahannock (median = 0.70 cfs/mi^2, mean = 1.23 cfs/mi^2), Upper James (median = 0.68 cfs/mi^2, mean = 1.17 cfs/mi^2), and Lower James (median = 0.69 cfs/mi^2, mean = 1.17 cfs/mi^2) are linked with the highest runoff production per unit area.

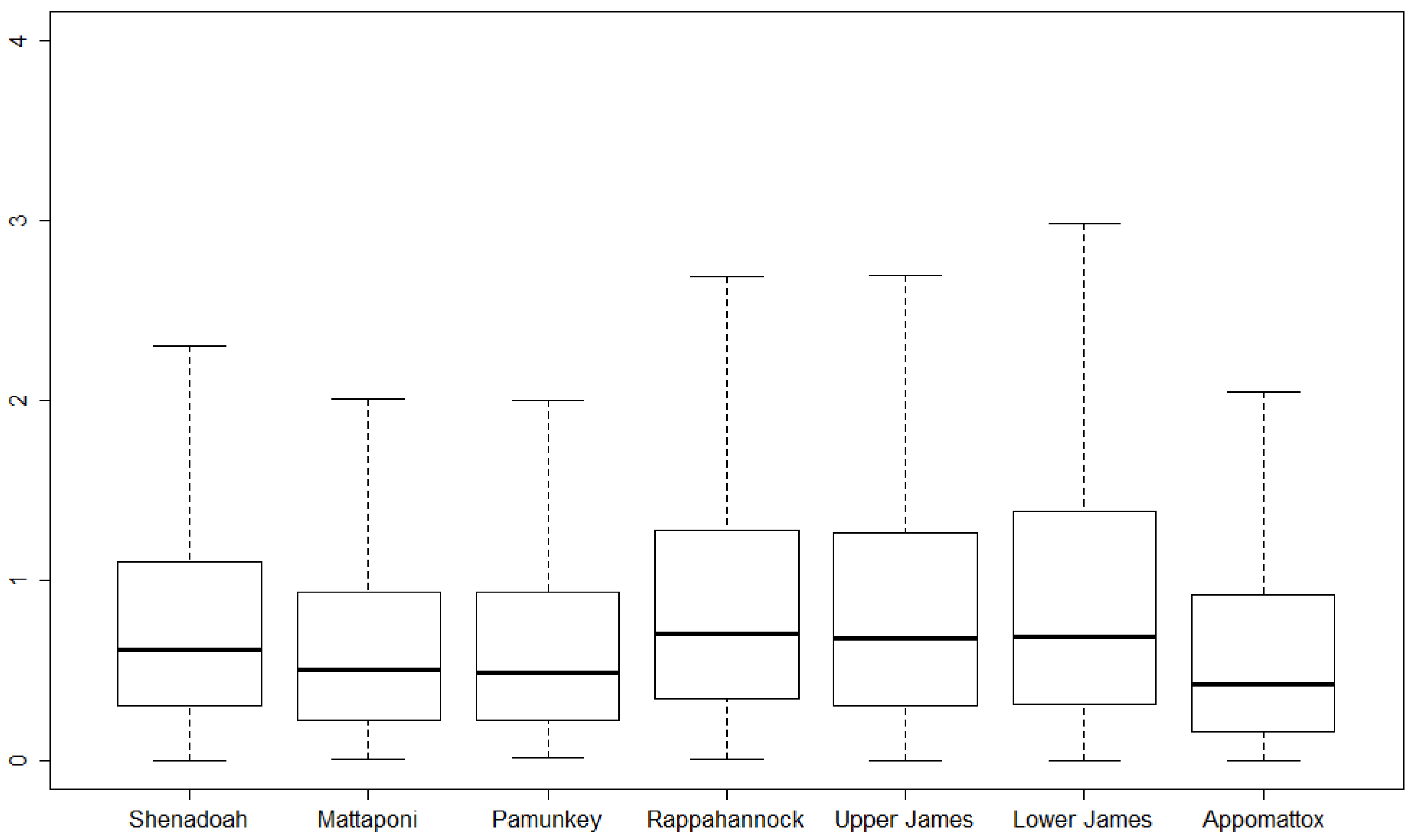

Figure 5.58: Runoff per Unit Area (cfs/mi^2) in Virginia River Basins in the Base Scenario

Although unit runoff is quite variable throughout the different basins, it has a quite uniform response to the climate change scenarios. In the ccP10T10 scenario shown in Fig. 5.59, median runoff was reduced by a low of 20.4% in the Rappahannock basin (median = 0.56

cfs/mi^2) to a high of 25.9% in the Mattaponi basin (median = 0.37 cfs/mi^2). Similarly, mean runoff was reduced by a low of 20.4% in the Middle James basin (mean = 0.97 cfs/mi^2) to a high of 22.2% in the Pamunkey basin (mean = 0.69 cfs/mi^2).

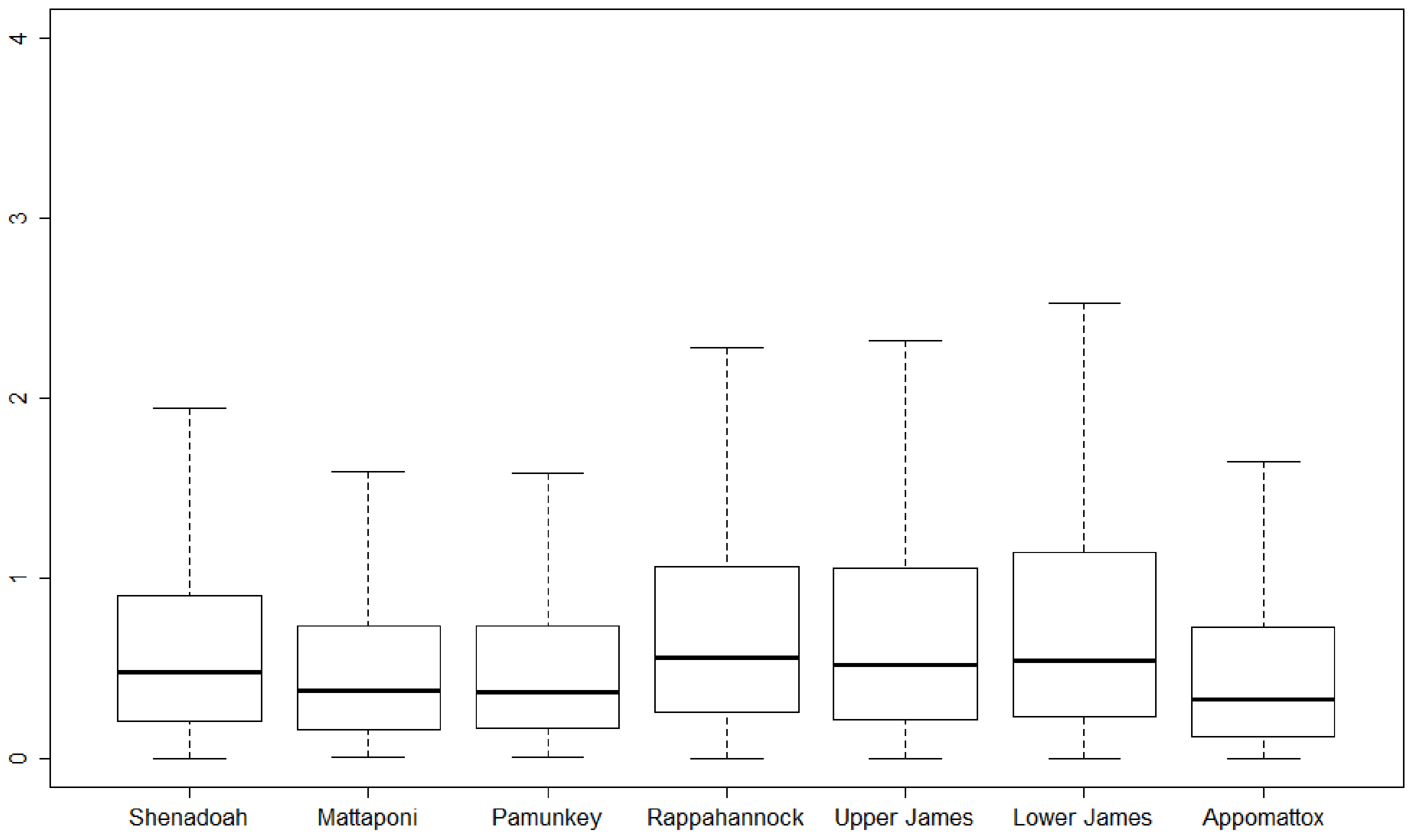

Figure 5.59: Runoff per Unit Area Land (cfs/mi^2) in Virginia River Basins in the ccP10T10 Scenario

In the ccP50T50 scenario, a slight increase from the base scenario in median and mean runoff was seen. Unit runoff values for each basin from the ccP50T50 scenario are shown in Fig. 5.60. Median runoff was increased by a low of 4.1% in the Shenandoah basin (median = 0.64 cfs/mi^2) to a high of 8.2% in the Appomattox basin (median = 0.46 cfs/mi^2). In the same vein, mean runoff increased by a low of 7.8% in the Shenandoah basin (mean = 1.16 cfs/mi^2) to a high of 9.9% in the Appomattox basin (mean = 0.96 cfs/mi^2). The higher percent increases in mean than median were indicative that the magnitude of high runoff values were more dramatically increased in the ccP50T50 scenario than the magnitude of smaller runoff values.

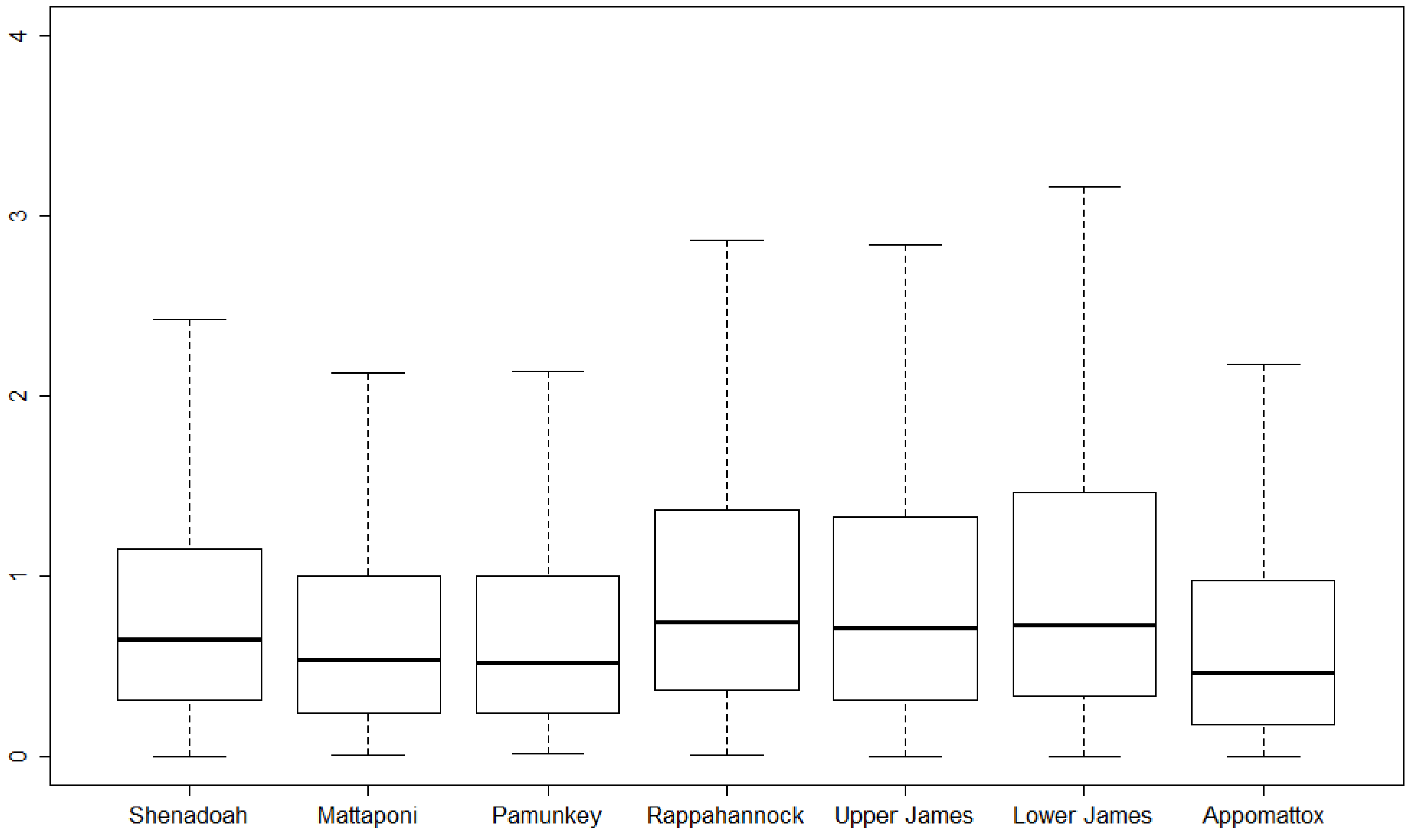

Figure 5.60: Runoff per Unit Area (cfs/mi^2) in Virginia River Basins in the ccP50T50 Scenario

Just as in the individual basins, the scenario ccP90T90 experienced the largest and most variable increases in unit runoff of any of the scenarios across the basins. The unit runoff changes seen within this scenario are shown in Fig. 5.61. Median unit runoff flows increased by a low of 30.4% in the Upper James basin (median = 0.88 cfs/mi^2) to a high of 53.7% in the Appomattox basin (median = 0.66 cfs/mi^2). Similarly, mean unit runoff flows increased by a low of 42.5% in the Upper James basin (mean = 1.67 cfs/mi^2) to a high of 64.5% in the Appomattox basin (mean = 1.44 cfs/mi^2). All three of the basins associated with the lowest unit runoffs in the base scenario (Pamunkey, Mattaponi, and Appomattox) experienced high percent changes in both median (50.4%, 48.0%, and 53.7%, respectively) and mean (58.0%, 58.2%, and 64.5%). On the other hand, the basins associated with the highest unit runoffs in the base scenario (Rappahannock, Upper James, and Middle James) experienced both the lowest percent increases in median (33.9%, 30.4%, and 35.4%) and mean (49.6%, 42.5%, and 50.3%) unit runoff.

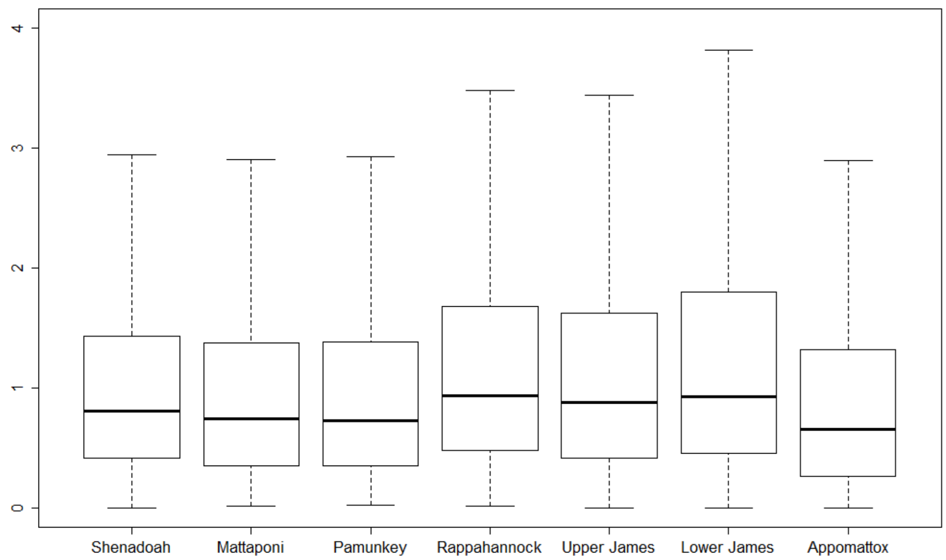

Figure 5.61: Runoff per Unit Area (cfs/mi^2) in Virginia River Basins in the ccP90T90 Scenario

5.6 Changes in Streamflow

5.6.1 Intra-Basin Flow Changes

In each of the river basins, the ccP10T10 scenario resulted in a reduction of flows while the ccP90T90 scenario resulted in an increase in flows throughout the flow regime when compared with the base scenario. The ccP50T50 scenario resulted in slightly increased flows for the vast majority of the flow regime, but occasionally resulted in a very slight decrease in some of the smallest observed flows. However, the percent difference between each of the climate change scenarios and the base scenario is one aspect which varies between the basins.

Shenandoah

The Shenandoah basin is one of the river basins which experiences minor decreases in flow in the ccP50T50 scenario in the lowest flows, associated with percent exceedances of approximately 90% and above (Fig. 5.62). However, this decrease was not enough to significantly decrease any of the corresponding low-flow metrics – l30, l90, and S10% remained the same between the base and ccP50T50 scenario (0.07, 0.13, and 0.10 cfs/mi^2) while OMF and ALF increased slightly (OMF: 1.08 to 1.16 cfs/mi^2; ALF: 0.48 to 0.49 cfs/mi^2). Decreases of between -16.7% (ALF) and -28.6% (l30) were seen in the low flow metrics between the low-precipitation ccP10T10 scenario and the base scenario, while the OMF decreased by -25%. Conversely, low flows in the high-precipitation ccP90T90 scenario exhibited increases between 18.8% (ALF) and 42.9% (l30), while the OMF increased by 45.4%. The averaged area-weighted flow values for each scenario in the Shenandoah basin are shown in Tab. 5.2.

Table 5.2: Flow Metrics (cfs/sq mi) in Shenandoah River Basin

Scenario	Overall Mean (cfs/sq mi)	30-Day Low Flow (cfs/sq mi)	90-Day Low Flow (cfs/sq mi)	August Low Flow (cfs/sq mi)	September 10% Flow (cfs/sq mi)
Base	1.08	0.07	0.13	0.48	0.10
ccP10T10	0.81	0.05	0.09	0.40	0.07
ccP50T50	1.16	0.07	0.13	0.49	0.10
ccP90T90	1.57	0.10	0.18	0.57	0.14

Mattaponi

The Mattaponi experienced relatively uniform change in each scenario throughout the flow regime, as shown in Fig. 5.63. The ccP10T10 scenario exhibited a significant decrease in OMF of 22.6%, while the ccP50T50 scenario exhibited a moderate increase of +8.6% and the ccP90T90 scenario exhibited a significant increase of +58.1%. Each of the flow metrics except

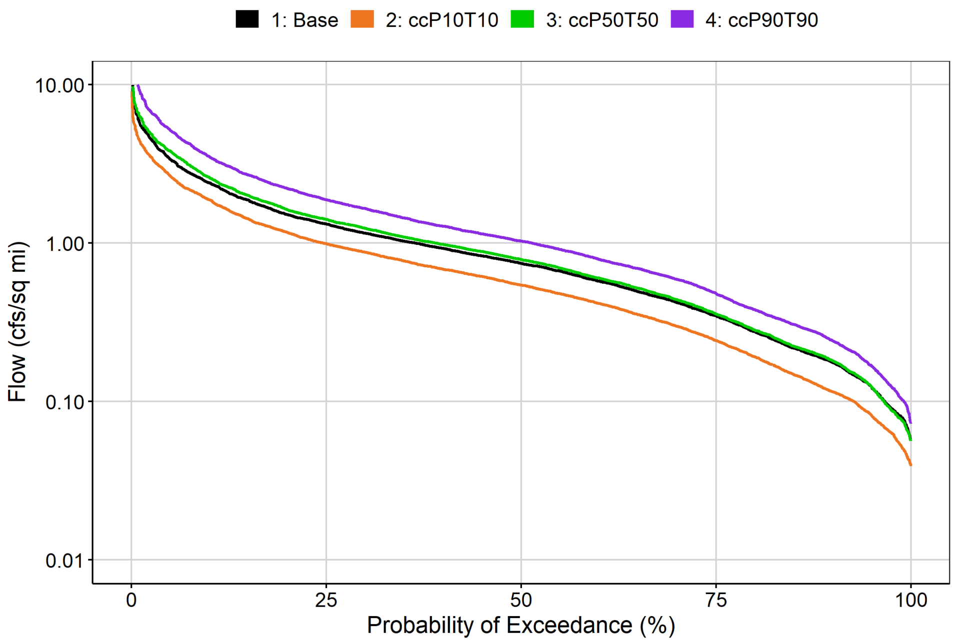

Figure 5.62: Percent Exceedance of Streamflow per Unit Area in the Shenandoah River Basin

the ALF experienced a similar percent change to the OMF. The ALF experienced smaller percent changes of -8.3% in the ccP10T10 scenario, +2.8% in the ccP50T50 scenario, and +22.2% in the ccP90T90 scenario. Area-weighted values of these metrics for the Mattaponi basin are shown in Tab. 5.3.

Table 5.3: Flow Metrics (cfs/sq mi) in Mattaponi River Basin

Scenario	Overall Mean (cfs/sq mi)	30-Day Low Flow (cfs/sq mi)	90-Day Low Flow (cfs/sq mi)	August Low Flow (cfs/sq mi)	September 10% Flow (cfs/sq mi)
Base	0.93	0.05	0.09	0.36	0.06
ccP10T10	0.72	0.04	0.07	0.33	0.04
ccP50T50	1.01	0.05	0.10	0.37	0.07
ccP90T90	1.47	0.08	0.16	0.44	0.10

Pamunkey

The Pamunkey basin had the largest change between the base and climate change scenarios in the moderate flows, shown between percent exceedances 25 and 60% on Fig. 5.64. As a result of the scenarios' convergence in lower flows, many of the low-flow metrics were

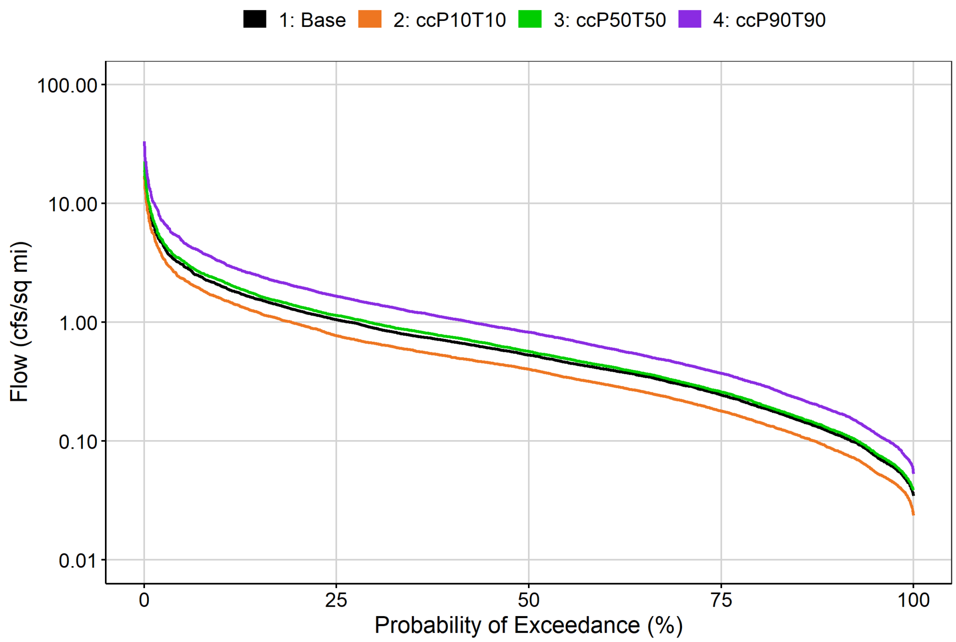

Figure 5.63: Percent Exceedance of Streamflow per Unit Area in the Mattaponi River Basin

held quite constant throughout the scenarios. Although OMF changed more significantly in the Pamunkey than in either of the two previous basins (-25.9% in ccP10T10, +9.9% in ccP50T50, and +64.2% in ccP90T90), both the ccP10T10 and ccP90T90 scenarios exhibited low-flows that were only slightly changed from the base scenario (Tab. 5.4). However, the ccP90T90 low-flow metrics were often increased by about 50%.

Table 5.4: Flow Metrics (cfs/sq mi) in Pamunkey River Basin

Scenario	Overall Mean (cfs/sq mi)	30-Day Low Flow (cfs/sq mi)	90-Day Low Flow (cfs/sq mi)	August Low Flow (cfs/sq mi)	September 10% Flow (cfs/sq mi)
Base	0.81	0.04	0.08	0.25	0.06
ccP10T10	0.60	0.04	0.06	0.23	0.04
ccP50T50	0.89	0.05	0.09	0.26	0.06
ccP90T90	1.33	0.06	0.12	0.33	0.09

Rappahannock

The Rappahannock basin was another basin that experienced quite uniform change in unit flow throughout the flow regime (Fig. 5.65). However, the change in the associated low-flow

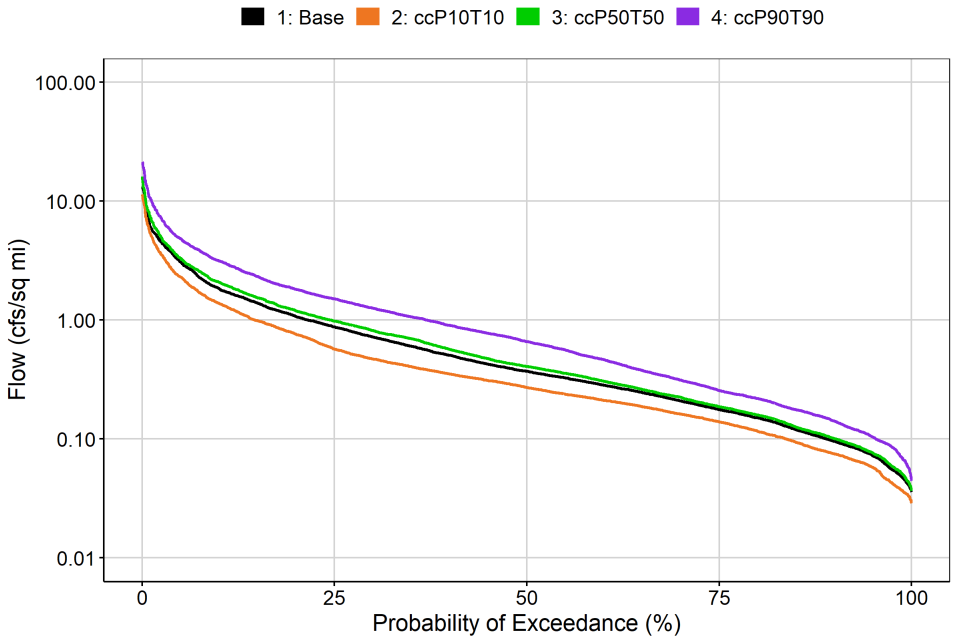

Figure 5.64: Percent Exceedance of Streamflow per Unit Area in the Pamunkey River Basin

metrics for each scenario was quite variable. In the ccP10T10 scenario, although OMF decreased by 20.6%, low-flow metrics changed from a low of -8.3% to a high of about 33.3%. In the ccP50T50 scenario, OMF increased by 9.6% while low-flow metrics stayed approximately the same (l30, S10%) or slightly increased (l90, ALF). The ccP90T90 scenario showed increases across the board, with OMF increasing 47.8% and low-flow metrics increasing between 23.0 (ALF) and 64.3% (l90). All Rappahannock metrics calculated from unit flows are shown in Tab. 5.5.

Table 5.5: Flow Metrics (cfs/sq mi) in Rappohannock River Basin

Scenario	Overall Mean (cfs/sq mi)	30-Day Low Flow (cfs/sq mi)	90-Day Low Flow (cfs/sq mi)	August Low Flow (cfs/sq mi)	September 10% Flow (cfs/sq mi)
Base	1.36	0.09	0.14	0.48	0.13
ccP10T10	1.08	0.06	0.10	0.44	0.09
ccP50T50	1.49	0.09	0.15	0.51	0.13
ccP90T90	2.01	0.14	0.23	0.59	0.18

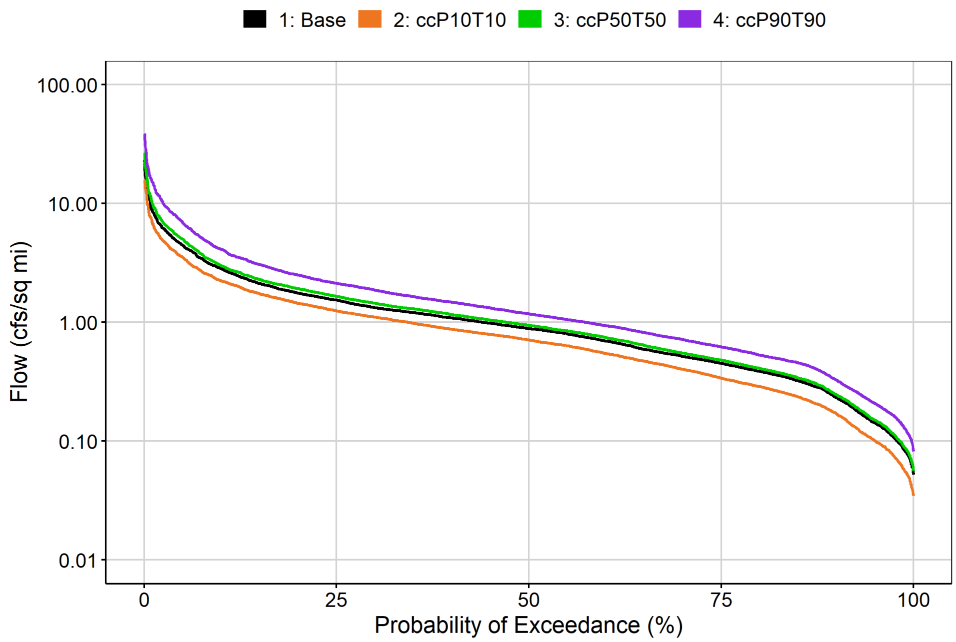

Figure 5.65: Percent Exceedance of Streamflow per Unit Area in the Rappahannock River Basin

Upper James

The Upper James basin experienced small changes in its very large (percent exceedance < 5%) and very small (percent exceedance > 95%) unit flows. However, throughout the rest of the flow regime, changes were quite consistent (Fig. 5.66). This narrowness in low-flow response to the climate change scenarios resulted in some of the smallest percent changes in low-flow metrics of any basin – while OMF change was moderate (-21.7% in ccP10T10, +5.83% in ccP50T50, and +40.0% in ccP90T90), many of the low-flow metrics (l30, ALF, S10%) varied to a lesser percent. Only the l90 flow varied significantly, reduced by 0.03 cfs/mi^2 in the ccP10T10 scenario and raised by 0.03 cfs/mi^2 in the ccP90T90 scenario. The changes in unit runoff for all of the scenarios are shown in Tab. 5.6.

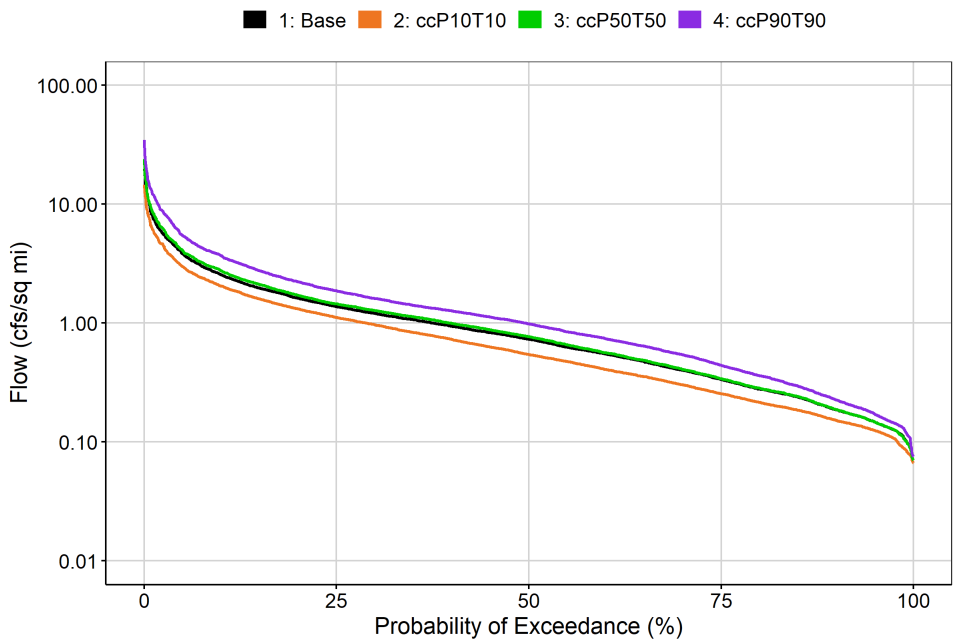

Figure 5.66: Percent Exceedance of Streamflow per Unit Area in the Upper James River Basin

Table 5.6: Flow Metrics (cfs/sq mi) in Upper James River Basin

Scenario	Overall Mean (cfs/sq mi)	30-Day Low Flow (cfs/sq mi)	90-Day Low Flow (cfs/sq mi)	August Low Flow (cfs/sq mi)	September 10% Flow (cfs/sq mi)
Base	1.20	0.07	0.14	0.47	0.12
ccP10T10	0.94	0.06	0.10	0.41	0.11
ccP50T50	1.27	0.07	0.14	0.48	0.12
ccP90T90	1.68	0.08	0.18	0.54	0.13

Middle James

For the most part, the Middle James basin had very similar responses in unit flow to the climate change scenarios as the Rappahannock. Just like the Rappahannock, changes in flow were quite uniform throughout the flow regime (Fig. 5.67). The Middle James also experienced similar changes in OMF (ccP10T10: -19.5%, ccP50T50: +8.1%, ccP90T90: +45.5%) and each of the low-flow metrics. Just like the Rappahannock, the Middle James experienced the most significant percent decrease in the l30 metric (-28.6%) as a result of the ccP10T10 scenario, but experienced the greatest percent increase in the l90 metric (+53.9%) in the ccP90T90 scenario (Tab. 5.7).

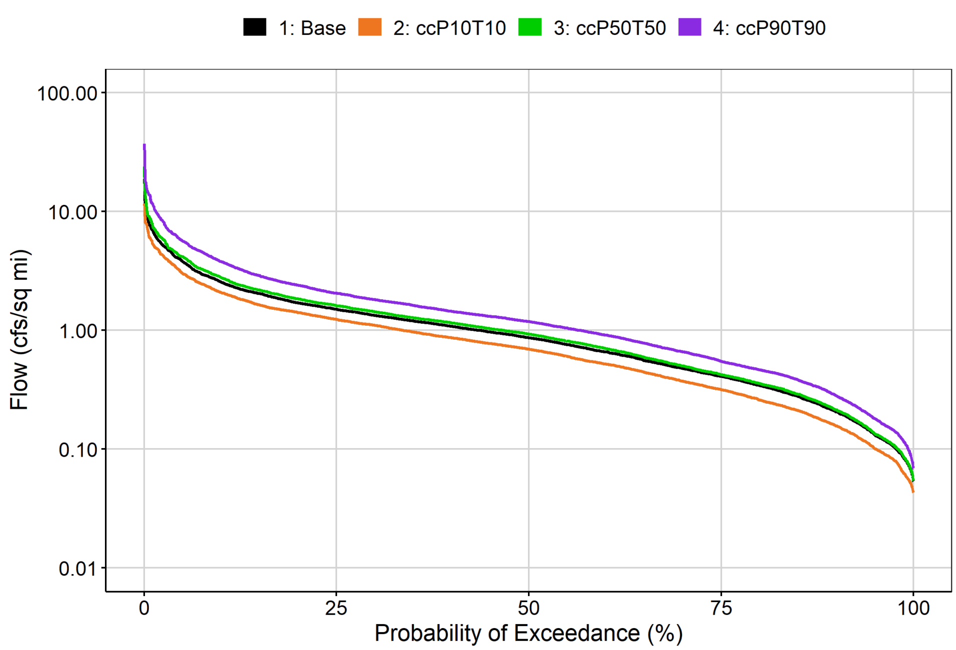

Figure 5.67: Percent Exceedance of Streamflow per Unit Area in the Middle James River Basin

Table 5.7: Flow Metrics (cfs/sq mi) in Middle James River Basin

Scenario	Overall Mean (cfs/sq mi)	30-Day Low Flow (cfs/sq mi)	90-Day Low Flow (cfs/sq mi)	August Low Flow (cfs/sq mi)	September 10% Flow (cfs/sq mi)
Base	1.23	0.07	0.13	0.54	0.11
ccP10T10	0.99	0.05	0.10	0.49	0.08
ccP50T50	1.33	0.07	0.14	0.56	0.11
ccP90T90	1.79	0.09	0.20	0.63	0.15

Appomattox

In the Appomattox basin, percent changes in flows were also quite uniform throughout the basin – however, the ccP90T90 scenario tended to result in noticeably higher increases in flow than the ccP10T10 scenario resulted in reductions (Fig. 5.68). This is exhibited in the far higher magnitude of percent increase in OMF (+65%) in the ccP90T90 scenario than of the percent decrease in the ccP10T10 scenario (-21.4%). Additionally, while the ccP10T10 scenario resulted in moderate decreases in each of the drought metrics (up to a 0.03 cfs/mi^2 decrease in ALF), the ccP90T90 scenario resulted in high increases in the same metrics (up to a 0.07 cfs/mi^2 increase in ALF). All of these metric values for the Appomattox are shown in Tab. 5.8.

Table 5.8: Flow Metrics (cfs/sq mi) in Appomattox River Basin

Scenario	Overall Mean (cfs/sq mi)	30-Day Low Flow (cfs/sq mi)	90-Day Low Flow (cfs/sq mi)	August Low Flow (cfs/sq mi)	September 10% Flow (cfs/sq mi)
Base	0.89	0.03	0.08	0.33	0.07
ccP10T10	0.70	0.02	0.06	0.30	0.05
ccP50T50	0.98	0.03	0.09	0.34	0.07
ccP90T90	1.47	0.05	0.13	0.40	0.10

5.6.2 Investigation into River Segments Associated with Extreme Land Use Runoff

In the unit runoff by land use investigation earlier in this report, several localities were identified as areas of especially low or high runoff change for each of the climate change scenarios. For the ccP10T10 scenario, Amherst was identified as a region of particularly minor runoff decrease, while Harrisonburg was identified as a city with especially drastic

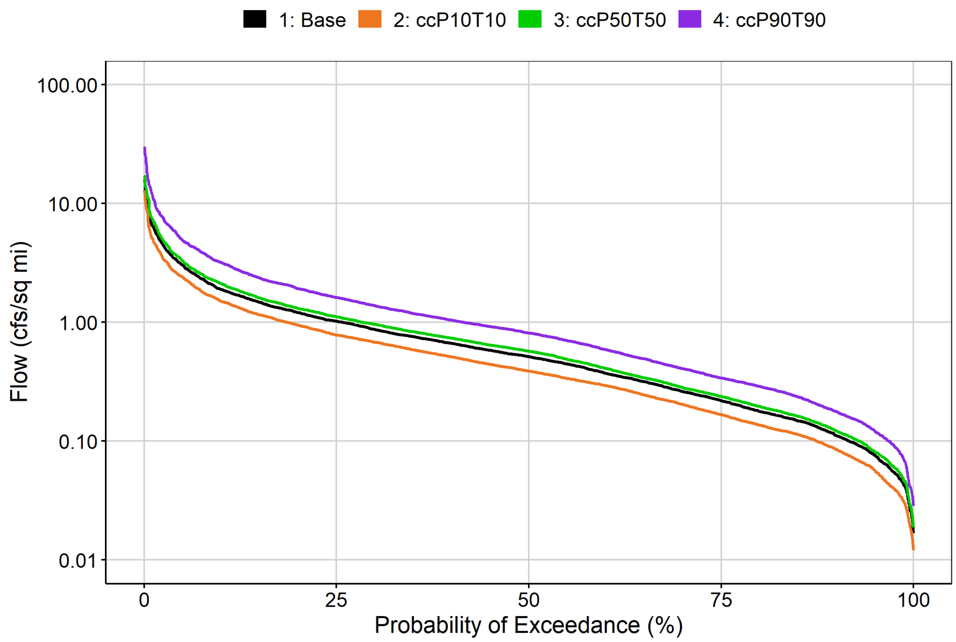

Figure 5.68: Percent Exceedance of Streamflow per Unit Area in the Appomattox River Basin

runoff decrease. In the ccP50T50 scenario, Giles was identified as a region of low runoff increase, while Culpeper was associated with especially high runoff increase. In the ccP90T90 scenario, Highland commonly had one of the smallest runoff increases, while Nottoway had one of the largest.

River segments that each of these jurisdictions were associated with were selected for further analysis. In all the jurisdictions except for Culpeper, headwater segments were found. In Culpeper, a river segment with two contributing headwater segments (Hazel River headwater and Thornton River headwater) located in neighboring Rappahannock County was identified. Headwater segments, or river segments as close as possible to the headwaters, were ideal for this analysis due to less confounding impacts by flows from upstream contributing drainage areas. Flow exceedance plots and metric tables were created for each of these jurisdictions to illustrate the impact that particularly high or low land use runoff changes have on the streamflow of the climate change scenarios. These flow exceedance plots are shown in Fig. 5.69.

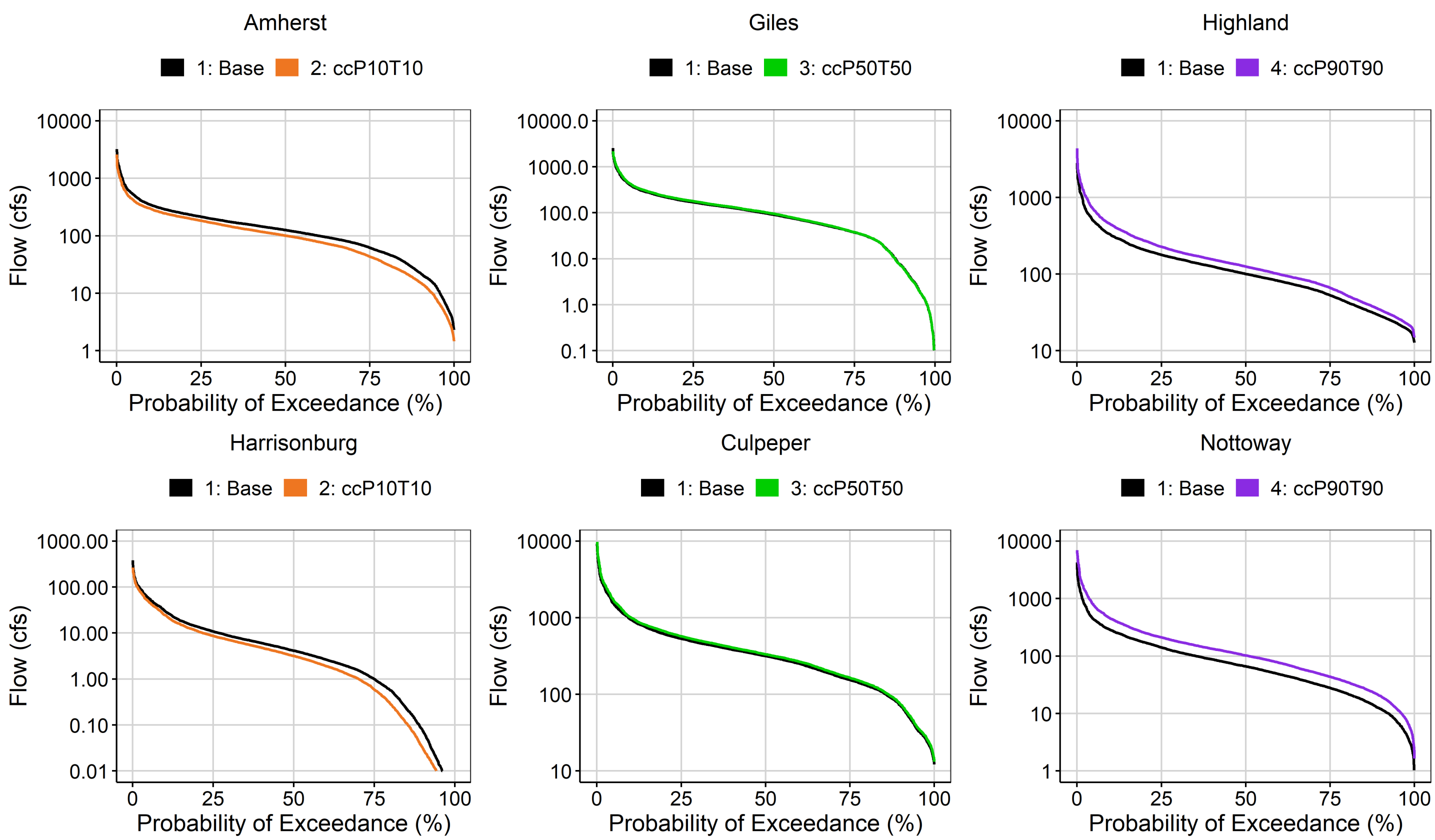

Figure 5.69: Percent Exceedance of Streamflow in Low- and High-Change Jurisdictions of Virginia

Although Amherst experienced a far less severe reduction in land use unit runoff than Harrisonburg in the ccP10T10 scenario, its associated river segment (Buffalo River) experienced a more intense reduction in overall mean flow (-19.6%) than did Harrisonburg's associated river segment (Blacks Run, -17.6%). This may be a result of the actual land use areas in each of these regions – Amherst is a rural county, with forestry and agriculture two of the largest industries. As a result, much of Amherst's land is covered by forest and cropland – two of the land use groups which tended to respond with a significant decrease in the ccP10T10 scenario. On the other hand, Harrisonburg is a city located directly on a major interstate which contains one of Virginia's major universities, James Madison University. This has resulted in significant urbanization in the city of Harrisonburg, linked with an increase in the land covered by impervious surfaces (such as roads and buildings) which had a less drastic response to the reduced precipitation seen in the ccP10T10 scenario. However, Blacks Run in Harrisonburg experienced a more drastic reduction in each of the investigated low flow metrics (l30: -42.1%, l90: -45.4%, ALF: -33.2%, S10%: -55.6%) than Amherst's Buffalo River (l30: -30.6%, l90: -24.6%, ALF: -8.3%, S10%: -40.9%). Although Blacks Run's larger percent decrease in these low-flow metrics may be a result of Harrisonburg's more drastically reduced runoff per unit area for many of the pervious land uses, it also may result from the small flow magnitudes seen in Blacks Run's headwaters. For example, a 33.2% reduction in ALF from 0.31 to 0.21 cfs (Blacks Run) may be less significant than an 8.3% reduction in ALF from 115 to 105 cfs (Buffalo River) as a result of the model's limited capability to estimate the extraordinarily low flows seen in tiny segments such as Blacks Run. All of the metrics describing flows in Amherst's Buffalo River are shown in Tab. 5.9, while the metrics describing flows in Harrisonburg's Blacks Run are shown in Tab. 5.10.

Table 5.9: Flow Metrics (cfs) in Buffalo River Basin (Amherst)

Scenario	Overall Mean (cfs)	30-Day Low Flow (cfs)	90-Day Low Flow (cfs)	August Low Flow (cfs)	September 10% Flow (cfs)
Base	181.285	4.010	13.658	114.880	9.035
ccP10T10	145.833	2.784	10.292	105.324	5.342
ccP50T50	199.311	4.130	15.694	117.103	9.069
ccP90T90	270.062	8.960	22.830	129.052	20.556

Table 5.10: Flow Metrics (cfs) in Blacks Run Basin (Harrisonburg)

Scenario	Overall Mean (cfs)	30-Day Low Flow (cfs)	90-Day Low Flow (cfs)	August Low Flow (cfs)	September 10% Flow (cfs)
Base	12.355	0.019	1.076	0.310	0.009
ccP10T10	10.178	0.011	0.586	0.207	0.004
ccP50T50	13.254	0.022	1.230	0.365	0.010
ccP90T90	17.109	0.043	2.159	0.851	0.017

The ccP50T50 scenario exhibited quite uniform responses in land use unit flow throughout the state, with unit runoff changes for each of the land uses mostly staying between about +3 and +15%. These minor changes in runoff also resulted in minor changes in flow – for both the lowest change county (Giles) and highest change county (Culpeper), only tiny percent changes in overall mean flow (+5.5% and +9.2%) were observed. In Giles' Johns Creek, slight reductions in some of the low-flow metrics (l30: -5.8%, S10%: -0.6%) were observed, while slight increases in other low-flow metrics (l90: +1.0%, ALF: +1.08%) were observed. Higher percent increases were seen in Culpeper's Hazel River (l30: +7.5%, l90: +8.4%, ALF: +4.1%, S10%: +3.7%) for each of the metrics. Due to the small percent changes seen in each of these metrics, it is difficult to draw meaningful conclusions about how low flows will be impacted by the ccP50T50 scenario. Although a slight increase is suggested in much of the state, many of the percent changes fall well within the margin of error often associated with streamflow modeling. Raw values for each of these streamflow metrics are shown for Giles' Johns Creek Basin in Tab. 5.11 and for Culpeper's Hazel River in Tab. 5.12.

Table 5.11: Flow Metrics (cfs) in Johns Creek Basin (Giles)

Scenario	Overall Mean (cfs)	30-Day Low Flow (cfs)	90-Day Low Flow (cfs)	August Low Flow (cfs)	September 10% Flow (cfs)
Base	138.295	0.172	9.703	61.515	1.064
ccP10T10	110.544	0.064	5.606	51.314	0.676
ccP50T50	145.832	0.162	9.804	62.180	1.058
ccP90T90	194.300	0.318	14.607	70.840	1.735

Table 5.12: Flow Metrics (cfs) in Hazel River Basin (Culpeper)

Scenario	Overall Mean (cfs)	30-Day Low Flow (cfs)	90-Day Low Flow (cfs)	August Low Flow (cfs)	September 10% Flow (cfs)
Base	488.011	25.211	43.683	202.074	28.529
ccP10T10	389.336	15.347	28.896	183.934	19.125
ccP50T50	532.870	27.103	47.337	210.344	29.586
ccP90T90	716.160	40.668	78.329	243.848	44.921

The ccP90T90 scenario was associated with both large percent change and large variation in percent change in unit runoff for most land uses. The southern region of Highland County, much of which drains to the Bullpasture River, often experienced some of the lower increases in unit runoff (about +30%). On the other hand, Nottoway County, containing West Creek (a tributary of Deep Creek, which in turn flows into the Appomattox River) exhibited some of the highest percent changes in unit runoff (often up to about +70%). These significant differences are reflected in the observed changes in the overall mean flow (+32.0% in Bullpasture River, +66.3% in West Creek) and in many of the low-flow metrics. In Bullpasture River, each of the low-flow metrics changed by a smaller percentage than the mean (l30: +20.8%, l90: +27.7%, ALF: +16.4%, S10%: 16.9%), implying that the majority of the flow increases were seen in the moderate and high flows which don't impact the calculation of these metrics. This larger change in moderate and high flows is also visually depicted in Fig. 5.69 in the "Highland" plot. Similarly, in West Creek, each of the percent increases seen in low flows (l30: +62.9%, l90: +52.8%, ALF: +18.6%, S10%: +61.8%) were smaller than the percent increase in the OMF, although most of them were quite similar. The ALF, which only increased by 18.6%, tended to be more resistant to change in each of the climate change scenarios in the majority of the observed locations, with Harrisonburg's tiny Blacks Run an outlier in the ccP50T50 and ccP90T90 scenarios due to its incredibly small flow magnitudes. Each of these metrics are shown in tables for the Bullpasture (Tab. 5.13) and West Creek (Tab. 5.14) river segments.

Table 5.13: Flow Metrics (cfs) in Bullpasture River Basin (Highland)

Scenario	Overall Mean (cfs)	30-Day Low Flow (cfs)	90-Day Low Flow (cfs)	August Low Flow (cfs)	September 10% Flow (cfs)
Base	160.345	18.624	24.421	59.889	22.513
ccP10T10	128.862	15.374	19.572	52.666	19.440
ccP50T50	167.663	18.850	24.608	61.373	22.865
ccP90T90	211.724	22.493	31.193	69.701	26.314

Table 5.14: Flow Metrics (cfs) in West Creek Basin (Nottoway)

Scenario	Overall Mean (cfs)	30-Day Low Flow (cfs)	90-Day Low Flow (cfs)	August Low Flow (cfs)	September 10% Flow (cfs)
Base	134.190	3.923	9.711	39.391	6.753
ccP10T10	104.633	1.473	4.635	40.852	3.206
ccP50T50	145.646	4.306	10.462	41.276	7.136
ccP90T90	223.158	6.392	14.837	46.731	10.923

Chapter 6

Discussion

6.1 Trends in Virginian Precipitation, Temperature, and Evapotranspiration Change

Moderately strong correlations between temperature and latitude existed in the study area, with the coefficient of determination equal to or exceeding 0.53 in each of the climate change scenarios. This trend was stronger in the ccP10T10 and ccP90T90 scenarios, likely as a result of their being composed of fewer GCMs (four and three, respectively) than the ccP50T50 scenario (nine). This reduced number of models in the two extreme climate change scenarios allow for some of the spatial trends visible within each individual GCM to be exhibited in the eclectic climate change scenarios ccP10T10 and ccP90T90. These trends were less evident in the ccP50T50 scenario, as it was composed of temperature and precipitation changes from too many GCMs for any of their spatial trends to peek through. However, it can be overall concluded that the northern areas of Virginia will experience more extreme temperature change than will the south (especially the southeast).

Temporal trends existed in the months of the year which exhibited especially small and large temperature changes, although the time of minimum increase changed between the different climate change scenarios. In the tenth percentile scenario, the smallest temperature increases were seen in the winter (means: Dec. = +0.82°C; Jan. = +0.74°C; Feb. = +0.77°C) while the largest temperature increases were seen in the late summer (means: Jul. = +1.36°C; Aug. = +1.30°C; Sep. = +1.60°C). In the fiftieth percentile scenario, the smallest temperature increases were seen in the late fall (Nov. mean = +1.73°C) and early spring (Mar. mean = +1.74) while the largest temperature increases were once again seen in the late summer (means: Jul. = +2.16°C; Aug. = +2.21°C; Sep. = 2.22°C). In the ninetieth percentile scenario, smallest temperature changes were seen in early summer (means: May = +2.60°C, Jun. = +2.67°C) while the largest temperature changes were again seen in late summer (means: Jul. = +3.28°C, Aug. = +3.23°C; Sep. = +3.51°C). These large temperature increases in already warm months will likely lead to reduced flows during these already low-flow periods.

Modeled potential evapotranspiration change showed similar trends to temperature change, likely as a result of the major role that temperature plays in potential evapotranspiration. However, a less direct correlation with latitude existed. Instead, for each of the climate change scenarios, the lowest changes were seen in the Virginia Beach area with modeled potential evapotranspiration change increasing northwest across the state to a high in Highland County.

Differences in precipitation between the scenarios were far higher than observed differences in potential evapotranspiration – this is seen both in the higher percent changes between the base and climate change scenarios and the magnitude of this difference in the mean values. In the ccP10T10 scenario, PET is increased by an average of 0.38 inches/year, while precipitation is reduced by an average of 4.05 inches/year. In the ccP50T50 scenario, PET is increased by an average of 1.11 inches/year, but precipitation is increased by an average of 2.46 inches/year. In the ccP90T90 scenario, PET is increased by only 1.87 inches/year, while precipitation is increased by an average of a whopping 10.67 inches/year. This extreme change in the magnitude of precipitation change compared to PET change in the ccP10T10 and ccP90T90 scenarios is the primary driver in the high changes in runoff and streamflow seen in these two scenarios. This large difference between potential evapotranspiration and precipitation change may largely be a result of the smaller role that temperature change often plays in hydrologic models than precipitation. Although temperature directly affects PET, large temperature changes in winter months with low ET may result in only a minor change to ET, while that same temperature change applied during summer months with high ET may result in drastic changes to ET. As a result, depending on the temporal application of temperature change, hydrology might be either weakly or strongly affected.

Precipitation had the most diverse responses to climate change throughout the state. The ccP10T10 scenario resulted in two high-percent reduction hotspots in regions near Virginia Beach and Page County, with precipitation decrease becoming less severe away from these areas. The moderate ccP50T50 scenario saw the largest percent increases in precipitation along the entire ridgeline of the Appalachians, with percent increase reducing when moving away from this area. The ccP90T90 scenario saw the largest percent increases in precipitation in the southernmost reaches of the study area, such as Nottoway, with the lowest percent increases seen in the furthest away counties in both directions (Highland and Accomack). As a result of the lack of spatial consistency in precipitation change across these scenarios, it is difficult to draw meaningful conclusions about how precipitation in the study area will truly be spatially altered as a result of climate change.

Precipitation also exhibited months of especially high and low change, although these months varied between scenarios and were rarely consistent seasonally. In the tenth percentile scenario, precipitation decreased most severely in some summer and autumn months (means: Jun. = -12.4%; Aug. = -12.5%; Oct. = -14.7%) while it decreased less severely in some winter and spring months (means: Feb. = -1.8%; Apr. = -3.7%). In the fiftieth percentile scenario, precipitation increased most severely in certain winter months (means: Dec. =

+10.8%; Feb. = +10.0%) and increased the least in the mid-summer months (means: Jun. +2.3%; Jul. +3.8%). In the ninetieth percentile scenario, precipitation increased the least in May (mean: +21.2%) and September (mean: +22.3%) while it increased the most in February (mean: +30.8%) and April (mean: +28.2%). This lack of consistency in the spatial and temporal response of precipitation to climate change is one of the biggest shortcomings of this study's results, especially considering the high spatial linkage between hotspots of precipitation and runoff generation from each land use.

6.2 Runoff Changes by Land Use in Virginia Jurisdictions

Unit runoff varied greatly throughout the different climate change scenarios. Highly permeable and vegetated land, such as forest and pastureland, saw the largest percent changes and largest ranges in response. On the other end of the spectrum, impervious surfaces, such as roads and buildings, saw the smallest percent changes and most consistent responses. This difference in the degree to which runoff from each land use will be altered as a result of climate change is one of the most important takeaways from this study, and it is shown in Fig. 5.24. For example, when managing to ensure adequate water supply quantities throughout the state, it may be noted that the ccP10T10 scenario exhibits larger percent decreases in runoff generation from many of the pervious land use groups (such as natural pervious) than from the impervious land use groups (Fig. 5.25). If a locality is experiencing inadequate water supplies under ccP10T10 conditions and has a lot of pervious land (forest, pasture, mixed open, etc.) in its contributing drainage area, converting some of that land to impervious surfaces may be one potential way of increasing water supplies, although this may have a number of unintended consequences for groundwater supplies and water quality. Conversely, if a town urbanizes rapidly and requires a drastic, 50% increase in water supply while experiencing conditions reflecting the ccP90T90 scenario, the opposite transformation of land use may be required. As shown in Fig. 5.27, impervious land uses experience an increase of only about 30% in runoff, while land use groups such as hay and forage and agricultural open space experience increases far closer to 50%. Therefore, it may be necessary to convert some of the impervious, urban land to agricultural land or pastureland to facilitate an increase in runoff and thus an increase in water supply. At the very least, the observation that pervious land use groups may experience the highest and least consistent changes in runoff as a result of climate change leads to the conclusion that areas with large concentrations of these land uses (such as forested national parks or rural agricultural regions) may require special planning to maintain adequate water supply as the climate continues to change. Regardless of the extent of the percent change between the base and climate change scenarios, the spatial trends in percent changes in each land use's unit runoff were quite consistent in all but the most impervious land uses. However, these trends differed considerably across the different climate change scenarios.

In the ccP10T10 scenario, high percent changes were concentrated in regions near Harrisonburg and Virginia Beach, while low percent changes occurred near Amherst County. In the ccP50T50 scenario, low percent changes were observed in the easternmost (Virginia Beach and Accomack) and westernmost (Highland) counties, with the highest percent changes observed in north-central Virginia (Culpeper) and down the Appalachian ridgeline. In the ccP90T90 scenario, lowest changes were once again seen in the westernmost (Giles to Highland) and easternmost (Eastern Shore) areas. The highest changes were concentrated in the south-central jurisdictions in the study area (near Nottoway and Virginia Beach). Although this lack of consistency in runoff generation once again made it impossible to predict exactly where runoff change will be most drastically impacted by climate change throughout the study area, a high correlation between the location of high-change runoff hotspots and high-change precipitation and potential evapotranspiration hotspots was found. This correlation suggests that precipitation and potential evapotranspiration change play a major role in the production of runoff, especially from impervious surfaces where the coefficient of determination in the relationship between the predictors potential evapotranspiration and precipitation and the response variable of runoff from impervious land was found to rise as high as 0.97 in the ccP50T50 scenario (Fig. 5.39).

The shape of the runoff exceedance curve was changed in different ways in the different scenarios, implying a difference in how those scenarios affected the runoff regime. The ccP10T10 scenario often resulted in the largest impact on the moderate to small runoff values, which underwent a high percent decrease. This was largely a result of the reduced precipitation leading in an increase in the number of near-zero runoff days. Although the ccP50T50 scenario resulted in a largely unchanged runoff regime, the ccP90T90 scenario resulted in large changes, often in the moderately high runoff values exceeded only about five to ten percent of the time. These high percent changes to high flows were a result of runoff response to antecedent moisture conditions during increasingly severe storms, with high magnitudes of precipitation rapidly being turned to runoff when soils are unable to infiltrate water.

6.3 Runoff Changes in Virginia Basins

After these inputs were run through the VA Hydro hydrologic model, it became evident that the climate change scenarios had quite similar impacts in each of the basins on different percentiles of runoff throughout the runoff regime. In the ccP10T10 scenario, runoff quantities linked with small (fifth, tenth) percentiles were decreased by the largest percent, while moderately high flows such as those occurring at the seventy-fifth and ninetieth percentiles were decreased by the smallest percent. This drastic reduction in small runoff values is especially concerning, since reduced runoff can lead to reduced flow, and significant reductions in flow during these already-low flow periods could lead to water supply shortages during drought. In the ccP50T50 scenario, the highest quantities (ninety-fifth percentile) were increased by the largest percent, while moderate quantities (fiftieth) were increased by a far smaller percent. How small runoffs responded to this scenario was highly variable. The ccP90T90 scenario resulted in drastic changes in both the smallest (fifth) and largest (ninety-fifth) percentile runoffs, with the moderate (fiftieth) percentiles of runoffs less dramatically affected.

Segments associated with localities identified as areas of the most moderate change in unit runoff per land use were not necessarily associated with the lowest unit runoff quantities reaching the stream. For example, Amherst, associated with the headwater segment of the Buffalo River (JL2_7240_7350) experienced an abnormally low change in unit runoff for most land uses in the ccP10T10 scenario but was associated with percent changes in low percentiles of overall runoff (Q5: -36.4%; Q10: -32.1%; Q25: -28.7%) which were far more dramatic than the median responses in the Middle James basin (Q5: -31.6%; Q10: -28.8%; Q25: -24.4%). However, in other cases, such as with the Bullpasture River headwaters associated with Highland County, the low percent changes in land use unit runoff in scenario ccP90T90 did translate to lower-than-median percent changes in unit runoff in all percentiles throughout the runoff regime.

Similarly, extraordinarily high percent changes in land use unit runoff did not necessarily translate to abnormally high percent changes in runoff entering the channel. In Blacks Run in Harrisonburg, the ccP10T10 changes in low percentiles were dramatic (Q5: -97.1%; Q10: -64.7%) but changes in higher percentiles were of a lesser percent than the median changes in the Shenandoah basin. Similarly, in the West Creek headwater of Nottoway, lower-than-median percent changes were associated with the river segment in all but the highest quantile (Q95: +75.5%) flows in the ccP90T90 scenario. However, this is not necessarily always the case, either – the high-change ccP50T50 segment, associated with the Hazel River in Culpeper, experienced higher changes in percentile runoffs (Q5: +11.7%; Q10: +10.5%; Q25: +8.3%; Q50: +7.5%; Q75: +7.3%; Q90: +7.7%) than the median (Q5: +6.6%; Q10: +5.5%; Q25: +6.5%; Q50: +5.7%; Q75: +6.9%; Q90: +6.2%) in all but the ninety-fifth percentile flow. This inconsistent linkage between the magnitudes of change in unit runoff from individual land uses and change in the overall runoff also carried over to inconsistent linkages between unit runoff from individual land uses and streamflow.

6.4 Flow Changes in Virginia Basins

Streamflow was similarly affected quite inconsistently throughout the climate change scenarios. The ccP10T10 scenario regularly resulted in a drastic reduction in the magnitude of flows throughout the flow regime, while the ccP50T50 scenario had a minimal impact on most flows and the ccP90T90 scenario resulted in a dramatic increase in flows throughout the flow regime. To nail down exactly which combination of precipitation and temperature change would serve as a turning point between flow increases and decreases being seen throughout the state, more scenarios representing different combinations of these precipitation and temperature GCM percentiles would be required. However, based on the starring role that potential evapotranspiration and precipitation play in streamflow change, a combination of GCMs which result in changes to precipitation and PET which balance each other out would likely serve as a scenario in which streamflow would be largely unaffected. The ccP50T50 scenario comes close to achieving this, with an average annual PET increase of 1.11 inches but an average annual precipitation increase of 2.46 inches. Perhaps a combination of the fiftieth percentile of temperature and fortieth percentile of precipitation, a so-called ”ccP40T50” scenario, might come even closer to representing this tipping point.

Streamflow did vary considerably on a basin-to-basin basis, with flow change ranging from a median of -19.8% in the Middle James to -27.1% in the Shenandoah in the ccP10T10 scenario. Flows were also spatially variable in the ccP50T50 scenario, with median flows changing between +5.4% in the Upper James and +11.0% in the Appomattox, and in the ccP90T90 scenario, with median flows increasing between +33.0% in the Rappahannock and +77.8% in the Pamunkey. However, this lack of spatial consistency in the basin of highest and lowest change leads to difficulties pinpointing the regions of Virginia which will be most severely impacted by climate change.

Similarly to unit runoff, the regions in each basin where lowest/highest percent change in streamflow occurred were not necessarily the same regions where highest percent changes in precipitation, temperature, and unit runoff occurred. Amherst, identified as one of the areas with lowest percent temperature, precipitation, and unit runoff change in the ccP10T10 scenario, was found to have higher percent decreases in certain low-flow streamflow metrics (l30: -30.6%, S10%: -40.9%) than the median of these changes in the Middle James basin (l30: -25.7%, S10%: -24.0%). Conversely, Harrisonburg was identified as an area with especially severe land use unit flow reductions, partially resulting from its high precipitation decrease and moderate temperature increase. However, the associated Blacks Run segment was associated with smaller mean flow reductions (OMF: -17.6%) than the Shenandoah median OMF (-22.7%). The Blacks Run segment was, however, associated with higher-than-median reductions in all drought flow metrics (l30: -42.1%; l90: -45.5%; ALF: -33.2%, S10%: -55.6%) than the Shenandoah median (l30: -33.0%; l90: -29.4%; ALF: -13.7%, S10%: -33.2%).

However, streamflow change bucking the trend of temperature, precipitation, and land use runoff changes is not always the case. Giles County, associated with the Johns Creek headwaters in the Upper James basin, experienced some of the most moderate meteorological changes and land use unit runoff changes in the ccP50T50 scenario and also had nearly negligible differences in drought metrics (l30: -5.8%, l90: +1.0%, ALF: +1.1%, S10%: -0.6%). Similarly, the Highland river segment, associated with some of the smallest percent increases in precipitation and land use unit runoff, was found to have smaller percent changes in OMF, l30, l90, and S10% (+32.0%, +20.8%, +27.8%, and 16.9%, respectively) than the median in the Upper James (OMF: +41.1%, l30: +36.0%, l90: +37.8%, S10%: +28.8%). The ccP90T90 high-change segment, associated with West Creek in Nottoway, was also linked with one of the highest percent changes in its basin (+66.3%).

The changes in flow associated with each of these scenarios, especially the ccP10T10 and ccP90T90 scenarios, do have important implications on both the availability of water and the life which inhabits in-stream ecosystems, even if it is difficult to determine which basins will be most severely affected. The dramatic decreases in both mean- and low-flow metrics in the ccP10T10 scenario imply the worsening of late-summer droughts, while the increases in all flows, especially high flows, in the ccP90T90 scenario imply the intensification and increased frequency of floods and a reduction in the severity of late-summer droughts. However, the validity of these streamflow changes in these climate change scenarios can be questioned as a result of these scenarios' sole reflection of changes in the magnitude of precipitation and PET as opposed to changes in timing, the number of storm events, or the relative intensity of these storm events.

6.5 Implications for Water Quality and Stream Biodiversity

Low flows are often some of the most important flows to consider when investigating the impacts that a change will have on the health and biota of a stream. However, habitat features cannot be maintained solely through these periods of low flow. Instead, higher flows are needed for the import of organic matter from the floodplain, to scour and revitalize gravel beds, and to link channels to nearby riparian wetlands (Poff et al., 1997). The archaic slogan ”dilution is the solution to pollution” is still heavily representative of how some localities deal with the disposal of their waste, with point-source polluters such as wastewater treatment plants and industrial facilities often relying on the sheer magnitude of streamflow to prevent their waste from being concentrated enough to have harmful effects on stream quality. A number of the previously discussed low-flow metrics, including ALF, S10%, and the l30 and l90 drought flows, are key to evaluating the impacts that a change will have on a riparian ecosystem during its most vulnerable times. In the low-precipitation ccP10T10 scenario, drastic decreases in these drought flow metrics of 20 to 40% were not at all uncommon. These changes could have a crippling impact on the concentration of pollution within the waterbodies, on the organisms which inhabit these ecosystems, and on the downstream users who depend on withdrawals for irrigation, industry, or consumption. These impacts can have especially devastating effects if the transition to low flows occurs especially quickly, which could result in the separation of habitats and the stranding of creatures away from their food sources (Poff et al., 1997).

Conversely, the ccP50T50 scenario exhibited very small changes to these low-flow metrics, implying that it might have minimal impacts on the diversity and abundance of riparian biota or on the supply of available water. The ccP90T90 scenario was linked with high-percent increases, often on the magnitude of +20 to +50%. Although these increases may be beneficial in terms of mitigating water supply withdrawal issues during times of drought, they can also have dramatic effects on the stream ecosystem. Different habitat features can be created and modified by different magnitudes of flows, so conditions resulting in the reduced magnitude and frequency of low flows can result in drastically altered ecosystem conditions (Poff et al., 1997). Oftentimes, riparian creatures require a variety of habitats at different points throughout their life cycles, and alterations to the timing and magnitude of the flows which create and maintain these habitats can result in the reduced ability of those organisms to complete their life cycle (Poff et al., 1997). Numerous additional components of the flow regime besides flow magnitude are also critical to the formation and maintenance of these stream ecosystems. These components include the frequency, duration, and timing of flows as well as the rate of change of in-stream conditions (Poff et al., 1997). However, as a result of the method used to model altered precipitation for the CBP climate change scenarios, which resulted in the increase or decrease in severity of recorded storms rather than altered timing, frequency, duration, or relative frequency of large- and small-magnitude storms, changes in these components of the flow regime are not fully reflected in the investigated climate change scenarios.

6.6 Shortcomings and Areas for Future Research

As mentioned previously, one of the greatest shortcomings in this research results from difficulties creating synthetic time series of precipitation to reflect possible avenues of climate change. In this study, climate change time series were created reflecting altered intensities of precipitation in the observed storms recorded in the baseline scenario. Although this scaling can effectively modify precipitation quantities to reflect those feasibly resulting from climate change, a number of different aspects of the precipitation regime (duration of storm events, number of storm events, relative frequency of different size storm events) which will realistically be altered as a result of climate change are not altered in these time series. Precipitation time series' change in magnitude are shown in Fig. 5.20, while the effect that these magnitude-only changes to precipitation may have on streamflow is shown in many of the flow exceedance plots, such as Fig. 5.65, which exhibits nearly uniform decreases in streamflow in the ccP10T10 scenario and nearly uniform increases in streamflow in the ccP50T50 and ccP90T90 scenarios throughout the flow regime reflecting the uniform scaling of precipitation increase in the corresponding precipitation scenarios. The characteristics of precipitation that are not taken into consideration in this study may in turn alter runoff generation and streamflow to abnormally high degrees during some of the most critical water supply periods, such as during late-summer droughts or during periods of flooding caused by intensified storms. However, further research is needed to confirm or reject this hypothesis – specifically, when improved time series more accurately reflecting changes to many characteristics of the precipitation regime can be analyzed.

This question of how uncertain climate change precipitation time series impact streamflow within these climate change scenarios goes hand-in-hand with the question of whether changes in streamflow resulting from these climate change scenarios are feasible changes resulting from the RCP4.5 emissions pathway of climate change or if these streamflow changes are a relic of the process by which these scenarios were generated. Precipitation and PET time series, created from different GCMs in different regions of the state, with solely changes in precipitation and PET magnitudes compared to the original baseline climatic time series, may be inadequate to use to investigate resultant changes to the timing or magnitudes of extreme streamflow events.

Similarly, future research can dig more deeply into the links between changes to the PET time series for each scenario and the changes to the daily values of ET which truly occur, as well as how this link may impact streamflow during times of the year associated with particularly high or low PET. Only cursory research was conducted into how PET changes throughout the year, but times of particularly high PET (such as summer, when temperature tends to be hottest) are hypothesized to occasionally be linked with low changes to actual ET resulting from low baseflow and dry antecedent moisture conditions, leading to small quantities of additional water available to be evaporated or transpired. The importance of PET increases during this late summer time period resulting from increased temperature could be an important and interesting area of research. Research into this topic could be compounded to describe how runoff and streamflow may change through different periods of the year and how this seasonality reflects the seasonality of PET and ET – something which this research barely touched upon. Example summary tables of PET and precipitation mean, median, and variance for the four scenarios are shown in Appendix I, with tables for each land segment in the area of study available in the repository located at `https://github.com/HARPgroup/cbp6/tree/master/daniel's%20thesis%20scripts/Monthly%20Climate%20Data`. From a cursory investigation, precipitation tends to have a higher variance than PET, and the variance in both precipitation and PET tends to be highest in the summer and early autumn seasons.

Although GCMs were often found to be assigned to each climate change scenario in large, regionally-consistent swaths of land segments (as shown in Figs. 5.8, 5.9, and 5.10), none of these scenarios reflect single-GCM changes across the entire state. Another possible avenue of future research would involved the creation of single-GCM climate change scenarios to investigate how spatial trends differ between single-GCM and multi-GCM climate change scenarios. A downside of this possible research involves the high error associated with individual GCMs – which is why these multi-GCM compilation climate change scenarios were created and investigated in this research in the first place.

Chapter 7

Conclusions

A wide variety of climatic futures are possible in the coming decades resulting from uncertain changes in human behavior (affecting greenhouse gas concentrations) and uncertain amounts of radiative forcing (affecting how these greenhouse gases absorb and retain energy from the sun). Even when these uncertain factors are assumed to be certain, and the RCP 4.5 climate change scenario is analyzed, further uncertainty arises from the use of many GCMs which predict widely varying temperature and precipitation change throughout the state. Even within this one, moderate climate change scenario, Virginia temperature change ranges from an average increase of 1.12°C in the tenth percentile temperature scenario to an average increase of 2.76°C in the ninetieth percentile temperature scenario. Similarly, potential evapotranspiration change ranges from an average increase of 3.36% in scenario ccP10T10 to an average increase of 8.32% in scenario ccP90T90, while precipitation change ranges from an average decrease of 8.73% in scenario ccP10T10 to an average increase of 26.03% in scenario ccP90T90. This massive difference in precipitation and PET change in the ccP10T10 (PET = +0.38 inches/year; precipitation = -4.05 inches/year) and ccP90T90 (PET = +1.88 inches/year; precipitation = +10.67 inches/year) scenarios is the primary driver in runoff and flow changes seen between these and the base scenarios.

This uncertainty is compounded further when these meteorological inputs are used to predict runoff generation for a variety of land uses and future streamflow produced by this runoff. In the ccP10T10 and ccP90T90 scenarios, the most extreme changes in unit flows were observed in the CSS True Forest (mean change = -24.1% in ccP10T10, +53.0% in ccP90T90) and Natural Pervious (mean change = -24.1% in ccP10T10, +52.9% in ccP90T90) land use groups. However, in the ccP50T50 scenario, the most extreme changes in unit flows were seen in the Ag Open Space (+8.8%) and Hay and Forage (+8.8%) land use groups. In all three scenarios, the least drastic changes were seen in the Impervious (mean change = -11.4% in ccP10T10, +6.5% in ccP50T50, +29.5% in ccP90T90) and Feeding Space (mean change = -11.4% in ccP10T10, +6.5% in ccP50T50, +29.5% in ccP90T90) land use groups. Spatial changes were found to be quite uniform amongst the land use groups, with the change far more dependent on the scenario than on the land use group.

Drastic changes in the overall unit runoff were also seen in a number of river basins in the ccP10T10 and ccP90T90 scenarios. In the ccP10T10 scenario, median unit runoff decreased between 20.4% (Rappahannock) and 25.9% (Mattaponi), while mean unit runoff decreased between 20.4% (Upper James) and 22.2% (Pamunkey). In the ccP90T90 scenario, median unit runoff increased between +30.4% (Upper James) and +53.7% (Appomattox), while mean unit runoff increased between +42.5% (Upper James) and +64.5% (Appomattox). Streamflow exhibited similar percent changes as unit runoff in the climate change scenarios. In the ccP10T10 scenario, median streamflow decreased between 19.8% (Middle James) and 27.1% (Shenandoah) while mean streamflow decreased between 19.5% (Middle James) and 25.4% (Pamunkey). In the ccP90T90 scenario, median streamflow increased between 35.0% (Upper James) and 78% (Pamunkey) while mean streamflow increased between 40.6% (Upper James) and 64.8% (Pamunkey). Only moderate increases in streamflow were seen in the ccP50T50 scenario, with median flow increasing between 5.4% (Upper James) and 11.0% (Appomattox) and mean flow increasing between 5.9% (Upper James) and 10.8% (Pamunkey).

To reiterate, there are a number of shortcomings in these climate change scenarios which warrant further iterations of the climate change scenarios and further analysis of these scenarios. Precipitation and PET change time series for the climate change scenarios are simply the baseline precipitation and PET time series with magnitudes scaled to reflect increases or decreases in these processes. Refined synthetic time series of these processes may reflect further likely changes to climate, such as increased storm frequency and duration. These improved time series of precipitation and PET will allow for improved modeling of runoff and streamflow, allowing for more meaningful analysis of low- and high-flow timing and of how climate change may differently affect the magnitudes of low- and high-flows in the regime. Similarly, the creation of single-GCM climate change scenarios may be useful when delving deeper into the analysis of spatial trends of precipitation, PET, runoff, and streamflow throughout the state.

Bibliography

Ahiablame, L., Sheshukov, A. Y., Rahmani, V., and Moriasi, D. (2017). Annual baseflow variations as influenced by climate variability and agricultural land use change in the Missouri River basin. *Journal of Hydrology*, 551:188–202. http://dx.doi.org/10.1016/j.jhydrol.2017.05.055.

Andrews, E. (2008). Chesapeake Bay Watershed Model: Phase 5 modeling segments [map]. https://www.chesapeakebay.net/what/maps/chesapeake_bay_watershed_model_phase_5_modeling_segments.

Astuti, I. S., Sahoo, K., Milewski, A., and Mishra, D. R. (2019). Impact of land use land cover (LULC) change on surface runoff in an increasingly urbanized tropical watershed. *Water Resources Management*, 33:4087–4103. http://dx.doi.org/10.1007/s11269-019-02320-w.

Bhaduri, B., Harbor, J., Engel, B., and Grove, M. (2000). Assessing watershed-scale, long-term hydrologic impacts of land-use change using a GIS-NPS model. *Environmental Management*, 26(6):643–658. http://dx.doi.org/10.1007/s002670010122.

Brogan, C. (2018). A dam conundrum: The role of impoundments in stream flow alteration. Master's thesis, Virginia Polytechnic Institute and State University.

Burcher, C. L., Valett, H. M., and Benfield, E. F. (2007). The land-cover cascade: Relationships coupling land and water. *Ecology*, 88(1):228–242. http://dx.doi.org/10.1890/0012-9658(2007)88[228:TLCRCL]2.0.CO;2.

Calijuri, M. L., de Siqueira Castro, J., Costa, L. S., Assemany, P. P., and Alves, H. E. M.

(2015). Impact of land use/land cover changes on water quality and hydrological behavior of an agricultural subwatershed. *Environmental Earth Sciences*, 74:5373–5382. http://dx.doi.org/10.1007/s12665-015-4550-0.

CBP (2016). 2013 phase 6 mapped land uses. https://chesapeake.usgs.gov/phase6/map/metadata/P6%20Land%20Use%20Classification%2011-01-16.pdf.

CBP (2017a). Chesapeake Bay Program phase 6 watershed model – section 5 – land use. ftp://ftp.chesapeakebay.net/Modeling/Phase6/Draft_Phase_6/Documentation.

CBP (2017b). Phase 6 modeling tools [Fact sheet]. https://www.chesapeakebay.net/documents/Phase_6_Modeling_Tools_1-page_factsheet_12-18-17.pdf.

Clarke, L., Edmonds, J., Jacoby, H., Pitcher, H., Reilly, J., and Richels, R. (2007). Scenarios of greenhouse gas emissions and atmospheric concentrations. Technical report, U.S. Department of Energy. https://digitalcommons.unl.edu/usdoepub/6.

De Cicco, L. A., Lorenz, D., Hirsch, R. M., and Watkins, W. (2018). *dataRetrieval: R packages for discovering and retrieving water data available from U.S. federal hydrologic web services*. Reston, VA.

Donigian, Jr., A., Imhoff, J., Bicknell, B., and Kittle, Jr., J. (1984). Application guide for Hydrological Simulation Program - FORTRAN (HSPF). Technical Report EPA/600/3-84/065, U.S. Environmental Protection Agency.

Dow, C. L. (2007). Assessing regional land-use/cover influences on New Jersey pinelands streamflow through hydrograph analysis. *Hydrological Processes*, 21:185–197. http://dx.doi.org/10.1002/hyp.6232".

Esri (2014). USA rivers and streams [shapefile]. https://hub.arcgis.com/datasets/esri::usa-rivers-and-streams.

Fujino, J., Nair, R., Kainuma, M., Masui, T., and Matsuoka, Y. (2006). Multi-gas mitigation analysis on stabilization scenarios using aim global model. *The Energy Journal*, Special Issue 3:343–354. http://dx.doi.org/10.2307/23297089.

Garg, V., Aggarwal, S. P., Gupta, P. K., Nikam, B. R., Thakur, P. K., Srivastav, S. K., and Kumar, A. S. (2017). Assessment of land use land cover change impact on hydrological regime of a basin. *Environmental Earth Sciences*, 76:635. http://dx.doi.org/10.1007/s12665-017-6976-z.

Goetz, S. J., Jantz, C. A., Prince, S. D., Smith, A. J., Varlyguin, D., and Wright, R. K. (2004). Integrated analysis of ecosystem interactions with land use change: The Chesapeake Bay watershed. *Geophysical Monograph Series*, 153:263–275. http://dx.doi.org/10.1029/153GM20.

Guzha, A. C., Rufino, M. C., Okoth, S., Jacobs, S., and Nobrega, R. L. B. (2018). Impacts of land use and land cover change on surface runoff, discharge and low flows: Evidence from East Africa. *Journal of Hydrology: Regional Studies*, 15:49–67. http://dx.doi.org/10.1016/j.ejrh.2017.11.005.

Hijioka, Y., Matsuoka, Y., Nishimoto, H., Masui, M., and Kainuma, M. (2008). Global GHG emissions scenarios under GHG concentration stabilization targets. *Journal of Global Environmental Engineering*, 13:97–108.

Hurkmans, R. T. W. L., Terink, W., Uijlenhoet, R., Moors, E. J., Troch, P. A., and Verburg, P. H. (2008). Effects of land use changes on streamflow generation in the Rhine basin. *Water Resources Research*, 45(6). http://dx.doi.org/10.1029/2008WR007574.

Julian, J. P. and Gardner, R. H. (2012). Land cover effects on runoff patterns in eastern Piedmont (USA) watersheds. *Hydrological Processes*, 28:1525–1538. http://dx.doi.org/10.1002/hyp.9692.

Kandissounon, G. A., Kalra, A., and Ahmad, S. (2018). Integrating system dynamics and remote sensing to estimate future water usage and average surface runoff in Lagos, Nigeria. *Civil Engineering Journal*, 4(2):378–393. http://dx.doi.org/10.28991/cej-030998.

Krstolic, J. L., Martucci, S. K., Hopkins, K. J., and Raffensperger, J. P. (2005). SIR2005-5073_CBRWM_watersheds [shapefile]. https://water.usgs.gov/lookup/getspatial?sir2005-5073_CBRWM_watersheds.

Kuroda, K., Hayashi, T., Do, A. T., Canh, V. D., Nga, T. T. V., Funabiki, A., and Takizawa, S. (2017). Groundwater recharge in suburban areas of Hanoi, Vietnam: Effect of decreasing surface-water bodies and land-use change. *Journal of Hydrology*, 25:727–742. http://dx.doi.org/10.1007/s10040-016-1528-2.

Law, J. (2013). *IHA: This package implements The Nature Conservancy's Indicators of Hydrologic Alteration software in R.* R package version 0.2-41/r41.

Leong, D. N. S. and Donner, S. D. (2014). Climate change impacts on streamflow availability for the Athabasca oil sands. *Climatic Change*, 133:651–663. http://dx.doi.org/10.1007/s10584-015-1479-y.

Linker, L. C., Batiuk, R. A., Shenk, G. W., and Cerco, C. F. (2013). Development of the Chesapeake Bay watershed Total Maximum Daily Load allocation. *Journal of the American Water Resources Association*, 49(5):1–21. http://dx.doi.org/10.1111/jawr.12105.

Liu, M., Tian, H., Chen, G., Ren, W., Zhang, C., and Liu, J. (2008). Effects of land-use and land-cover change on evapotranspiration and water yield in China during 1900-2000. *Journal of the American Water Resources Association*, 44(5):1193–1207. http://dx.doi.org/10.1111/j.1752-1688.2008.00243.x.

Lu, J., Sun, G., McNulty, S. G., and Amatya, D. M. (2005). A comparison of six potential evapotranspiration methods for regional use in the southeastern United States. *Journal of the American Water Resources Association*, 41(3):621–633. https://www.srs.fs.usda.gov/pubs/ja/ja_lu004.pdf.

Martucci, S. K., Krstolic, J. L., Raffensperger, J. P., and Hopkins, K. J. (2005). Development of land segmentation, stream-reach network, and watersheds in support of Hydrological Simulation Program-Fortran (HSPF) modeling, Chesapeake Bay watershed, and adjacent parts of Maryland, Delaware, and Virginia. Technical Report SIR 2005-5073, U.S. Geological Survey. http://dx.doi.org/10.3133/sir20055073.

Mauricio Zambrano-Bigiarini (2020). *hydroGOF: Goodness-of-fit functions for comparison of simulated and observed hydrological time series*. R package version 0.4-0.

Meinshausen, M., Smith, S. J., Calvin, K., Daniel, J. S., Kainuma, M. L. T., Lamarque, J.-F., Matsumoto, K., Montzka, S. A., Raper, S. C. B., Riahi, K., Thomson, A., Velders, G. J. M., and van Vuuren, D. P. P. (2011). The RCP greenhouse gas concentrations and their extensions from 1765 to 2300. *Climate Change*, 109:213. http://dx.doi.org/10.1007/s10584-011-0156-z.

Moss, R. H., Edmonds, J. A., Hibbard, K. A., Manning, M. R., Rose, S. K., van Vuuren, D. P., Carter, T. R., Emori, S., Kainuma, M., Kram, T., Meehl, G. A., Mitchell, J. F. B., Nakicenovic, N., Riahi, K., Smith, S. J., Stouffer, R. J., Thomson, A. M., Weyant, J. P., and Wilbanks, T. J. (2010). The next generation of scenarios for climate change research and assessment. *Nature*, 463(11):747–756. http://dx.doi.org/10.1038/nature08823.

Mukundan, R., Acharya, N., Gelda, R. K., Frei, A., and Owens, E. M. (2019). Modeling streamflow sensitivity to climate change in New York City water supply streams using a stochastic weather generator. *Journal of Hydrology: Regional Studies*, 21:147–158. http://dx.doi.org/10.1016/j.ejrh.2019.01.001.

Mukundan, R., Hoang, L., Gelda, R. K., Yeo, M.-H., and Owens, E. M. (2020). Climate change impact on nutrient loading in a water supply watershed. *Journal of Hydrology*, 586:124868. http://dx.doi.org/10.1016/j.jhydrol.2020.124868.

Nash, J. E. and Sutcliffe, J. V. (1970). River flow forecasting through conceptual models part I – a discussion of principles. *Journal of Hydrology*, 10(3):282–290. http://dx.doi.org/10.1016/0022-1694(70)90255-6.

Paolisso, M., Trombley, J., Hood, R. R., and Sellner, K. G. (2015). Environmental models and public stakeholders in the Chesapeake Bay watershed. *Estuaries and Coasts*, 38 (Suppl 1):S97–S113. http://dx.doi.org/10.1007/s12237-013-9650-z.

Poff, N. L., Allan, J. D., Bain, M. B., Karr, J. R., Prestegaard, K. L., Richter, B. D., Sparks, R. E., and Stromberg, J. C. (1997). The natural flow regime. *BioScience*, 47(11):769–784. http://dx.doi.org/10.2307/1313099.

Pumo, D., Caracciolo, D., Viola, F., and Noto, L. V. (2015). Climate change effects on the hydrological regime of small non-perennial river basins. *Science of the Total Environment*, 542:76–92. http://dx.doi.org/10.1016/j.scitotenv.2015.10.109.

R Core Team (2019). *R: A Language and Environment for Statistical Computing*. R Foundation for Statistical Computing, Vienna, Austria.

Riahi, K., Gruebler, A., and Nakicenovic, N. (2007). Scenarios of long-term socio-economic and environmental development under climate stabilization. *Technological Forecasting and Social Change*, 74(7):887–935. http://dx.doi/10.1016/j.techfore.2006.05.026.

Rice, K. C., Moyer, D. L., and Mills, A. L. (2017). Riverine discharges to Chesapeake Bay: Analysis of long-term (1927-2014) records and implications for future flows in the Chesapeake Bay basin. *Journal of Environmental Management*, 204:246–254. http://dx.doi.org/10.1016/j.jenvman.2017.08.057.

Richter, B. D., Baumgartner, J. V., Powell, J., and Braun, D. P. (1996). A method for assessing hydrologic alteration within ecosystems. *Conservation Biology*, 10(4):1163–1174. http://dx.doi.org/10.1046/j.1523-1739.1996.10041163.x.

Rodrigues, A. L. M., Reis, G. B., dos Santos, M. T., da Silva, D. D., dos Santos, V. J., de Siqueira Castro, J., and Calijuri, M. L. (2019). Influence of land use and land cover's change on the hydrological regime at a Brazilian southeast urbanized watershed. *Environmental Earth Sciences*, 78:595. http://dx.doi.org/10.1007/s12665-019-8601-9.

Sajikumar, N. and Remya, R. S. (2015). Impact of land cover and land use change on runoff characteristics. *Journal of Environmental Management*, 161:460–468. http://dx.doi.org/10.1016/j.jenvman.2014.12.041.

Schottler, S. P., Ulrich, J., Belmont, P., Moore, R., Lauer, J. W., Engstrom, D. R., and Almendinger, J. E. (2013). Twentieth century agricultural drainage creates more erosive rivers. *Hydrological Processes*, 28:1951–1961. http://dx.doi.org/10.1002/hyp.9738.

Shenk, G. W. and Linker, L. C. (2013). Development and application of the 2010 Chesapeake Bay watershed Total Maximum Daily Load model. *Journal of the American Water Resources Association*, 49(5):1042–1056. http://dx.doi.org/10.1111/jawr.12109.

Shenk, G. W., Wu, J., and Linker, L. C. (2012). Enhanced HSPF model structure for Chesapeake Bay watershed simulation. http://dx.doi.org/:10.1061/(ASCE)EE.1943-7870.0000555.

Smith, S. J. and Wigley, T. M. L. (2006). Multi-gas forcing stabilization with MiniCAM. *The Energy Journal*, 27:373–391. http://dx.doi.org/10.5547/ISSN0195-6574-EJ-VolSI2006-NoSI3-19.

Teng, J., Vaze, J., Chiew, F. H. S., Wang, B., and Perraud, J.-M. (2011). Estimating the relative uncertainties sourced from GCMs and hydrological models in modeling climate change impact on runoff. *Journal of Hydrometeorology*, 13:122–139. http://dx.doi.org/10.1016/10.1175/JHM-D-11-058.1.

USEPA (2010). Chesapeake Bay phase 5.3 community watershed model. Technical Report EPA 903S10002 - CBP/TRS-303-10, U.S. Environmental Protection Agency.

VADEQ (2018). Status of Virginia's water resources. Technical report, Virginia Department of Environmental Quality. https://www.deq.virginia.gov/Portals/0/DEQ/Water/WaterSupplyPlanning/AWRR_2018-09-30.pdf.

van Vuuren, D. P., den Elzen, M. G. J., Lucas, P. L., Eickhout, B., Strengers, B. J., Wonink, S., and van Houdt, R. (2007). Stabilizing greenhouse gas concentrations at low levels: an assessment of reduction strategies and costs. *Climatic Change*, 81:119–159. http://dx.doi.org/10.1007/s10584-006-9172-9.

Wagner, P. D., Kumar, S., and Schneider, K. (2013). An assessment of land use change impacts on the water resources of the Mula and Mutha rivers catchment upstream of Pune, India. *Hydrology and Earth System Sciences*, 17:2233–2246. http://dx.doi.org/10.5194/hess-17-2233-2013.

Wise, M., Calvin, K., Thomson, A., Clarke, L., Bond-Lamberty, B., Sands, R., Smith, S. J., Janetos, A., and Edmonds, J. (2009). Implications of limiting CO2 concentrations for land use and energy. *Science*, 324:1183–1186. http://dx.doi.org/10.1126/science.1168475.

Zhang, Q., Brady, D. C., and Ball, W. P. (2013). Long-term seasonal trends of nitrogen, phosphorus, and suspended sediment load from the non-tidal Susquehanna River basin to Chesapeake Bay. *Science of the Total Environment*, 452-453:208–221. http://dx.doi.org/10.1016/j.scitotenv.2013.02.012.

Zhang, Y., Guan, D., Jin, C., Wang, A., Wu, J., and Yuan, F. (2012). Impacts of climate change and land use change on runoff of forest catchment in northeast China. *Hydrological Processes*, 28:186–196. http://dx.doi.org/10.1002/hyp.9564.

Zhang, Y.-K. and Schilling, K. E. (2006). Increasing streamflow and baseflow in Mississippi River since the 1940's: Effect of land use change. *Journal of Hydrology*, 324:412–422. http://dx.doi.org/10.1016/j.jhydrol.2005.09.033.

Appendices

Appendix A

R Script Names, Github Locations, and Descriptions

Table A.1: R Script Names, Locations, and Descriptions

Script Name	Script URL	Script Description
batch.land.use.summarize.R	https://github.com/HARPgroup/cbp6/blob/master/daniel's%20thesis%20scripts/batch.land.use.summarize.R	If given the location of a directory containing SURO, AGWO, and IFWO combined land use files, this function will combine the different files and land uses to create one file with all land use data. This function should be run on the deq2 server.
batch_Qout_summarize.R	https://github.com/HARPgroup/cbp6/blob/master/daniel's%20thesis%20scripts/batch_Qout_summarize.R	If given the location of a directory containing surface runoff flow files (0111), this function will create a file containing the mean flows of all the river segments in this directory. This function should be run on the deq2 server.
Download_Runit_and_Qout_Data.R	https://github.com/HARPgroup/cbp6/blob/master/daniel's%20thesis%20scripts/Download_Runit_and_Qout_Data.R	Downloads Runit and Qout data from VA Hydro for each of the river segments investigated in this thesis.
flow_exceedance_comparison.R	https://github.com/HARPgroup/cbp6/blob/master/daniel's%20thesis%20scripts/flow_exceedance_comparison.R	This is an example script to exhibit how to download data for the same river segment for a number of different VA Hydro scenarios, and to then create flow exceedance plots comparing these different scenarios.
gage_comparison_thesis.R	https://github.com/HARPgroup/cbp6/blob/master/daniel's%20thesis%20scripts/gage_comparison_thesis.R	For the river segments analyzed in this thesis, this script will link river segments to their associated USGS gages, download data, and compare model fits. Kable tables, compatible with Overleaf, will also be created.
land.use.time series.R	https://github.com/HARPgroup/cbp6/blob/master/daniel's%20thesis%20scripts/land.use.time series.R	For the land uses cursorily investigated in this thesis research, this function will sum SURO, AGWO, and IFWO flows for each land use and create time series of these summed data. This function should be run on the deq2 server.
land_use_radar_charts.R	https://github.com/HARPgroup/cbp6/blob/master/daniel's%20thesis%20scripts/land_use_radar_charts.R	Following the creation of the pct.changes scenario data frames, this script will create radar charts showing the land use unit flows for each land use group.
mods.R	https://github.com/HARPgroup/cbp6/blob/master/daniel's%20thesis%20scripts/mods.R	Using the GCM data now stored in GCM Precipitation Data and GCM Temperature Data directories, this script will determine which model is associated with the tenth, fiftieth, and ninetieth percentiles of precipitation and temperature for each land segment in the area of study.
prcp.evap.landuse.table.R	https://github.com/HARPgroup/cbp6/blob/master/daniel's%20thesis%20scripts/prcp.evap.landuse.table.R	Creates pct.changes scenario dataframes. Also, creates plots of evaporation against precipitation, precipitation/evaporation against land use, maps of evaporation/precipitation/land use/temperature change, and longitude/latitude against these changes.
precip_and_temp_latitude_by_model.R	https://github.com/HARPgroup/cbp6/blob/master/daniel's%20thesis%20scripts/precip_and_temp_latitude_by_model.R	Creates plots of temperature/precipitation against latitude/longitude, with the used GCMs designated by color and described in the legends of the generated images.
precip_and_temp_mapper.R	https://github.com/HARPgroup/cbp6/blob/master/daniel's%20thesis%20scripts/precip_and_temp_mapper.R	Creates monthly maps of temperature and precipitation.
precip_and_temp_mapper_vahydro.R	https://github.com/HARPgroup/cbp6/blob/master/daniel's%20thesis%20scripts/precip_and_temp_mapper_vahydro.R	Creates many versions of temperature and precipitation maps, some of which have a more presentable layout for use in reports and presentations.
precip_and_temp_model_frequency.R	https://github.com/HARPgroup/cbp6/blob/master/daniel's%20thesis%20scripts/precip_and_temp_model_frequency.R	Calculates the frequency of GCMs appearing in the tenth, fiftieth, and ninetieth percentile of each model scenario, by land segment.
precip_and_temp_scenario_analysis.R	https://github.com/HARPgroup/cbp6/blob/master/daniel's%20thesis%20scripts/precip_and_temp_scenario_analysis.R	Determines how GCMs are assigned to the climate change scenarios (conclusion: by land segment).
precip_and_temp_vs_Qout_plots_and_regressions.R	https://github.com/HARPgroup/cbp6/blob/master/daniel's%20thesis%20scripts/precip_and_temp_vs_Qout_plots_and_regressions.R	Creates plots of changes between GCM temperature and precipitation inputs and resultant VA Hydro model precipitation, evapotranspiration, and surface runoff (Qout) flows.
precip_and_temp_vs_Qout_tables.R	https://github.com/HARPgroup/cbp6/blob/master/daniel's%20thesis%20scripts/precip_and_temp_vs_Qout_tables.R	Creates output .csv files describing GCM precipitation and temperature as well as climate change scenario precipitation, evapotranspiration, and flow quantity/change from baseline scenario.
precip_evap_landuse_PCA.R	https://github.com/HARPgroup/cbp6/blob/master/daniel's%20thesis%20scripts/precip_evap_landuse_PCA.R	Creates principal component analysis plots describing correlations between precipitation/temperature and land use unit runoff values.
qunit_boxplot.R	https://github.com/HARPgroup/cbp6/blob/master/daniel's%20thesis%20scripts/qunit_boxplot.R	Creates boxplots and kable tables (for Overleaf) describing flow per unit area for each of the river segments and major basins described within this thesis. Additionally, creates flow exceedance plots describing these climate change scenarios. Also, calculates flow metrics of choice and outputs kable tables of raw values and percent changes from baseline scenario.
rcp_plotter.R	https://github.com/HARPgroup/cbp6/blob/master/daniel's%20thesis%20scripts/rcp_plotter.R	Using the RCP data stored in the Relative Concentration Pathway Data repository, a line graph of this data over time is created.
runit_all_scens.R	https://github.com/HARPgroup/cbp6/blob/master/daniel's%20thesis%20scripts/runit_all_scens.R	Creates maps of unit runoff (Runit) flows and creates kable tables (for Overleaf) describing these raw runoff values and percent differences from the baseline scenario.
runoff_boxplots.R	https://github.com/HARPgroup/cbp6/blob/master/daniel's%20thesis%20scripts/runoff_boxplots.R	Creates boxplots of unit runoff (Runit) values, previously downloaded using the "Download_Runit_and_Qout_Data" script. Additionally, calculates median and mean percent changes and calculates quantiles of percent runoff changes.
runoff_regime.R	https://github.com/HARPgroup/cbp6/blob/master/daniel's%20thesis%20scripts/runoff_regime.R	Downloads land use data from the deq2 server. Creates percent exceedance plots for some select land use runoff time series.

Appendix B

USGS Gage and VA Hydro Base Scenario Streamflow Metrics

Table B.1: Streamflow Metrics of USGS Gage Data (cfs)

River Segment	USGS Gage	Overall Mean Flow	30-Day Low Flow	90-Day Low Flow	August Low Flow	September 10% Flow
PS5_4380_4370	01636500	3309.0	365.4	446.9	1655.0	631.7
PS1_4790_4830	01634500	115.9	5.1	7.5	32.5	7.8
PS5_5240_5200	01631000	1854.3	281.1	330.5	918.5	422.8
PS4_5840_5240	01629500	1628.6	235.3	268.8	737.0	367.8
PS4_6360_5840	01628500	1201.0	166.8	191.0	533.5	270.8
PS2_6490_6420	01627500	285.0	50.1	56.5	126.0	65.0
PS2_6660_6490	01626850	241.8	55.0	61.6	117.5	56.0
PS2_6730_6660	01626000	172.9	25.4	29.5	63.5	34.0
PS3_5100_5080	01634000	722.2	55.1	72.9	309.0	108.0
PS2_5560_5100	01633000	476.9	6.1	19.6	178.0	41.0
PS2_5550_5560	01632000	224.8	0.6	4.0	34.5	1.7
PS3_6161_6280	01622000	456.0	39.4	50.2	197.0	75.0
PS3_6460_6230	01625000	364.7	54.1	62.7	182.0	89.0
YM1_6370_6620	01674500	532.2	8.2	25.4	185.0	14.9
YM2_6120_6430	01674000	234.9	0.9	4.0	51.0	1.7
YP4_6720_6750	01673000	1063.8	60.2	86.7	311.5	61.0
YP1_6570_6680	01671100	96.7	0.7	2.0	33.0	1.1
YP3_6470_6690	01672500	376.0	18.7	35.8	123.0	16.8
YP3_6330_6700	01671020	408.5	42.7	50.5	80.0	43.0
YP2_6390_6330	01670400	299.4	41.8	46.5	47.0	42.0
RU5_6030_0001	01668000	1874.8	35.2	106.1	668.0	108.7
RU2_5220_5640	01664000	798.2	15.1	33.0	319.0	21.0
RU3_6170_6040	01667500	629.4	19.1	46.9	229.0	52.9
RU2_5940_6200	01666500	255.2	9.7	21.8	101.5	25.0
RU2_6090_6220	01665500	167.1	6.6	15.1	65.0	14.9
JA5_7480_0001	02041650	1231.6	56.7	100.9	406.5	71.9
JA1_7600_7570	02041000	137.3	1.8	7.0	38.0	2.3
JA4_7280_7340	02040000	727.0	62.9	92.8	289.0	89.9
JA2_7550_7280	02039500	324.8	36.2	56.5	157.0	62.0
JU5_7500_7420	02019500	2570.8	442.7	505.1	1135.0	565.9
JU1_7750_7560	02018500	34.6	1.3	2.0	12.5	3.5
JU3_7490_7400	02018000	401.6	40.0	48.8	147.5	39.0
JU1_7630_7490	02017500	137.1	9.5	14.1	52.0	9.5
JU3_6650_7300	02016500	1677.7	355.5	398.7	773.0	418.0
JU1_6300_6650	02015700	158.8	25.8	31.1	79.5	32.0
JU4_7000_7300	02016000	562.7	72.0	86.8	229.0	77.0
JU2_7450_7360	02014000	172.4	20.8	25.1	79.0	21.0
JU2_7140_7330	02013000	176.5	12.6	15.4	68.0	15.0
JU3_6950_7330	02013100	711.1	180.7	197.6	349.0	272.0
JU3_6900_6950	02011800	445.1	114.7	114.9	258.0	252.0
JU2_6600_6810	02011500	182.8	9.7	14.1	48.5	18.0
JU1_6590_6600	02011470	118.7	2.5	5.6	20.5	13.0
JU1_6290_6590	02011460	95.6	1.8	4.6	26.5	2.8
JU3_6380_6900	02011400	167.9	17.4	21.8	82.0	19.0
JU1_6880_7260	02024000	741.2	87.3	97.7	277.0	96.0
JU3_6640_6790	02021500	412.4	18.2	23.8	102.0	21.0
JU2_6410_6640	02020500	175.9	2.5	5.4	40.0	5.6
JL7_7070_0001	02037500	7535.0	651.9	948.6	4055.0	1149.0
JL7_6800_7070	02037000	136.2	5.0	6.2	50.0	63.0
JL7_7100_7030	02035000	7530.5	983.9	1251.4	3945.0	1249.0
JL4_6520_6710	02034000	759.9	46.0	64.5	292.0	72.0
JL2_6240_6520	02032680	185.8	16.6	72.6	93.5	12.0
JL2_7110_7120	02030500	219.3	35.0	45.5	96.0	29.9
JL2_6441_6520	02032515	337.7	28.1	43.3	104.0	15.0
JL1_6560_6440	02031000	114.9	4.8	9.5	55.0	16.0
JL1_6760_6910	02030000	133.8	4.2	11.3	65.0	18.0
JL6_6890_6990	02029000	5520.7	777.8	955.6	3075.0	1070.0
JL1_6770_6850	02028500	154.3	3.0	6.3	64.5	9.3
JL1_7080_7190	02027500	100.6	3.7	7.9	41.0	4.2
JL6_7430_7320	02026000	4264.0	715.3	860.0	2455.0	914.9
JL2_7240_7350	02027800	171.5	20.7	44.3	101.0	20.9
JL1_6940_7200	02027000	173.8	6.7	12.8	69.5	12.0
JL6_7160_7440	02025500	3677.8	668.7	750.1	1680.0	761.9

Table B.2: Streamflow Metrics of VA Hydro River Segment Data (cfs)

River Segment	USGS Gage	Overall Mean Flow	30-Day Low Flow	90-Day Low Flow	August Low Flow	September 10% Flow
PS5_4380_4370	01636500	3187.7	296.0	458.4	2028.8	504.1
PS1_4790_4830	01634500	85.7	0.4	2.0	31.5	1.2
PS5_5240_5200	01631000	1805.6	220.7	334.7	1135.9	339.5
PS4_5840_5240	01629500	1532.4	165.3	249.8	851.5	232.2
PS4_6360_5840	01628500	1215.7	124.3	181.3	593.7	149.4
PS2_6490_6420	01627500	292.3	28.7	46.7	157.9	40.1
PS2_6660_6490	01626850	210.6	15.6	28.6	127.4	24.3
PS2_6730_6660	01626000	162.0	6.4	15.9	78.2	11.2
PS3_5100_5080	01634000	780.1	19.8	55.3	347.8	48.0
PS2_5560_5100	01633000	498.0	6.4	30.2	164.6	13.2
PS2_5550_5560	01632000	192.8	2.5	7.1	47.2	4.0
PS3_6161_6280	01622000	385.6	23.7	39.0	130.7	29.4
PS3_6460_6230	01625000	412.5	41.2	62.6	190.1	48.1
YM1_6370_6620	01674500	120.4	6.3	14.8	56.7	8.1
YM2_6120_6430	01674000	253.0	13.1	17.7	73.1	14.7
YP4_6720_6750	01673000	886.2	50.7	94.0	300.5	63.1
YP1_6570_6680	01671100	92.0	3.1	9.4	30.5	4.7
YP3_6470_6690	01672500	365.2	29.0	45.0	119.2	25.7
YP3_6330_6700	01671020	345.9	24.9	32.2	80.8	29.8
YP2_6390_6330	01670400	243.6	20.0	20.0	40.0	20.0
RU5_6030_0001	01668000	2007.6	143.7	202.6	819.9	195.7
RU2_5220_5640	01664000	296.1	11.5	21.6	92.2	11.3
RU3_6170_6040	01667500	637.4	50.6	78.5	224.0	82.6
RU2_5940_6200	01666500	255.5	21.3	34.4	85.3	35.8
RU2_6090_6220	01665500	153.3	13.6	21.4	44.8	20.9
JA5_7480_0001	02041650	1157.5	41.6	80.9	385.1	77.8
JA1_7600_7570	02041000	134.2	3.9	9.7	39.4	6.8
JA4_7280_7340	02040000	680.9	26.2	65.9	273.0	60.7
JA2_7550_7280	02039500	282.8	10.3	27.9	110.8	25.6
JU5_7500_7420	02019500	2391.9	234.3	393.8	1083.5	353.0
JU1_7750_7560	02018500	39.5	0.8	5.3	12.7	3.1
JU3_7490_7400	02018000	420.5	2.9	35.3	202.8	9.7
JU1_7630_7490	02017500	138.1	0.2	9.7	61.4	1.1
JU3_6650_7300	02016500	550.0	28.6	52.2	243.9	34.4
JU1_6300_6650	02015700	159.8	18.6	24.3	59.7	22.4
JU4_7000_7300	02016000	132.2	22.6	27.8	50.2	32.1
JU2_7450_7360	02014000	170.8	1.7	17.3	77.0	6.7
JU2_7140_7330	02013000	168.4	1.7	12.5	52.8	4.9
JU3_6950_7330	02013100	431.0	53.6	90.4	133.0	131.6
JU3_6900_6950	02011800	392.8	79.8	84.3	151.3	182.0
JU2_6600_6810	02011500	159.5	10.1	15.5	54.3	15.2
JU1_6590_6600	02011470	97.9	7.3	9.6	20.4	12.1
JU1_6290_6590	02011460	90.2	0.3	3.5	14.8	0.4
JU3_6380_6900	02011400	187.1	2.1	8.8	62.9	1.7
JU1_6880_7260	02024000	155.1	7.0	13.4	78.7	10.9
JU3_6640_6790	02021500	366.4	4.3	19.8	147.2	6.7
JU2_6410_6640	02020500	140.5	1.4	4.8	51.6	1.8
JL7_7070_0001	02037500	7806.4	754.2	1019.6	3951.1	1058.7
JL7_6800_7070	02037000	77.4	7.7	10.4	39.4	11.0
JL7_7100_7030	02035000	7424.5	771.3	1047.0	3681.2	1043.2
JL4_6520_6710	02034000	717.0	43.8	71.5	213.6	60.4
JL2_6240_6520	02032680	135.5	2.4	38.7	37.6	0.1
JL2_7110_7120	02030500	238.9	21.5	37.5	56.7	17.4
JL2_6441_6520	02032515	254.5	15.7	34.7	81.6	19.3
JL1_6560_6440	02031000	105.8	6.3	13.6	33.1	10.7
JL1_6760_6910	02030000	124.7	7.9	14.2	37.9	14.0
JL6_6890_6990	02029000	5679.7	476.3	816.5	3056.0	769.1
JL1_6770_6850	02028500	155.1	4.7	13.8	58.7	6.3
JL1_7080_7190	02027500	82.4	1.9	8.7	33.9	2.1
JL6_7430_7320	02026000	4283.2	396.8	625.0	2322.1	644.6
JL2_7240_7350	02027800	185.7	4.1	33.6	117.6	13.9
JL1_6940_7200	02027000	162.6	4.1	13.1	66.3	4.9
JL6_7160_7440	02025500	3776.2	308.1	512.8	1895.5	496.3

Table B.3: Percent Difference in Streamflow Metrics Between USGS Gage and VA Hydro River Segment Data (%)

River Segment	USGS Gage	Overall Mean Flow	30-Day Low Flow	90-Day Low Flow	August Low Flow	September 10% Flow
PS5_4380_4370	01636500	-3.67	-19.00	2.57	22.58	-20.20
PS1_4790_4830	01634500	-26.12	-91.26	-73.17	-3.09	-84.38
PS5_5240_5200	01631000	-2.63	-21.49	1.26	23.67	-19.71
PS4_5840_5240	01629500	-5.91	-29.77	-7.05	15.54	-36.86
PS4_6360_5840	01628500	1.22	-25.46	-5.09	11.29	-44.81
PS2_6490_6420	01627500	2.57	-42.78	-17.38	25.28	-38.24
PS2_6660_6490	01626850	-12.90	-71.58	-53.53	8.45	-56.58
PS2_6730_6660	01626000	-6.29	-74.88	-46.21	23.10	-67.07
PS3_5100_5080	01634000	8.01	-64.13	-24.08	12.56	-55.53
PS2_5560_5100	01633000	4.42	5.00	54.62	-7.52	-67.85
PS2_5550_5560	01632000	-14.23	325.45	78.52	37.03	138.02
PS3_6161_6280	01622000	-15.44	-39.89	-22.25	-33.68	-60.83
PS3_6460_6230	01625000	13.12	-23.96	-0.05	4.47	-45.94
YM1_6370_6620	01674500	-77.38	-23.53	-41.78	-69.33	-45.72
YM2_6120_6430	01674000	7.70	1332.37	337.03	43.28	771.17
YP4_6720_6750	01673000	-16.69	-15.72	8.33	-3.52	3.50
YP1_6570_6680	01671100	-4.84	317.03	363.23	-7.51	328.65
YP3_6470_6690	01672500	-2.89	54.72	25.89	-3.08	52.89
YP3_6330_6700	01671020	-15.32	-41.67	-36.15	0.94	-30.64
YP2_6390_6330	01670400	-18.61	-52.18	-56.98	-14.88	-52.37
RU5_6030_0001	01668000	7.08	308.00	90.91	22.74	79.99
RU2_5220_5640	01664000	-62.90	-24.29	-34.70	-71.08	-46.08
RU3_6170_6040	01667500	1.28	164.59	67.28	-2.16	56.11
RU2_5940_6200	01666500	0.14	119.81	57.66	-15.99	43.23
RU2_6090_6220	01665500	-8.27	105.00	41.86	-31.02	40.01
JA5_7480_0001	02041650	-6.01	-26.61	-19.83	-5.27	8.24
JA1_7600_7570	02041000	-2.26	116.39	39.51	3.70	194.99
JA4_7280_7340	02040000	-6.33	-58.33	-28.92	-5.53	-32.49
JA2_7550_7280	02039500	-12.93	-71.69	-50.58	-29.45	-58.68
JU5_7500_7420	02019500	-6.96	-47.08	-22.04	-4.54	-37.63
JU1_7750_7560	02018500	14.13	-40.10	169.72	1.92	-11.12
JU3_7490_7400	02018000	4.70	-92.85	-27.70	37.49	-75.06
JU1_7630_7490	02017500	0.75	-98.20	-31.35	18.13	-88.80
JU3_6650_7300	02016500	-67.22	-91.95	-86.90	-68.45	-91.76
JU1_6300_6650	02015700	0.64	-28.08	-21.73	-24.94	-29.90
JU4_7000_7300	02016000	-76.51	-68.66	-67.99	-78.08	-58.27
JU2_7450_7360	02014000	-0.89	-91.64	-31.01	-2.56	-67.94
JU2_7140_7330	02013000	-4.59	-86.58	-18.87	-22.35	-67.59
JU3_6950_7330	02013100	-39.38	-70.32	-54.24	-61.88	-51.63
JU3_6900_6950	02011800	-11.75	-30.45	-26.67	-41.36	-27.76
JU2_6600_6810	02011500	-12.77	3.93	9.67	11.97	-15.60
JU1_6590_6600	02011470	-17.51	193.78	69.96	-0.66	-6.59
JU1_6290_6590	02011460	-5.67	-82.19	-23.26	-44.27	-84.23
JU3_6380_6900	02011400	11.42	-88.23	-59.82	-23.30	-91.14
JU1_6880_7260	02024000	-79.08	-91.94	-86.27	-71.59	-88.66
JU3_6640_6790	02021500	-11.15	-76.08	-16.73	44.27	-68.17
JU2_6410_6640	02020500	-20.15	-45.99	-10.19	28.90	-66.91
JL7_7070_0001	02037500	3.60	15.69	7.48	-2.56	-7.86
JL7_6800_7070	02037000	-43.16	55.05	67.57	-21.17	-82.54
JL7_7100_7030	02035000	-1.41	-21.61	-16.34	-6.69	-16.48
JL4_6520_6710	02034000	-5.64	-4.83	10.81	-26.84	-16.09
JL2_6240_6520	02032680	-27.08	-85.34	-46.73	-59.81	-99.54
JL2_7110_7120	02030500	8.94	-38.54	-17.50	-40.91	-41.74
JL2_6441_6520	02032515	-24.63	-44.11	-20.00	-21.54	28.90
JL1_6560_6440	02031000	-7.93	30.83	42.32	-39.85	-33.05
JL1_6760_6910	02030000	-6.80	88.68	25.79	-41.73	-22.16
JL6_6890_6990	02029000	2.88	-38.76	-14.55	-0.62	-28.12
JL1_6770_6850	02028500	0.51	53.68	119.60	-8.94	-32.01
JL1_7080_7190	02027500	-18.11	-47.95	9.95	-17.37	-50.05
JL6_7430_7320	02026000	0.45	-44.54	-27.33	-5.41	-29.54
JL2_7240_7350	02027800	8.29	-80.41	-24.22	16.46	-33.50
JL1_6940_7200	02027000	-6.44	-39.17	2.66	-4.58	-59.10
JL6_7160_7440	02025500	2.67	-53.92	-31.63	12.83	-34.86

Appendix C

Runoff Quantiles

Table C.1: Runoff Quantiles in Shenandoah River Segments (Base Scenario)

River Segment	Q5 (cfs/sq mi)	Q10 (cfs/sq mi)	Q25 (cfs/sq mi)	Q50 (cfs/sq mi)	Q75 (cfs/sq mi)	Q90 (cfs/sq mi)	Q95 (cfs/sq mi)
PS5_4370_4150	0.35	0.39	0.50	0.69	1.00	1.74	2.65
PS5_4380_4370	0.12	0.15	0.26	0.54	0.96	1.80	2.99
PS4_5080_4380	0.05	0.12	0.28	0.58	1.01	1.89	2.95
PS1_4830_5080	0.04	0.09	0.21	0.49	0.94	1.85	3.29
PS1_4790_4830	0.01	0.05	0.15	0.43	0.90	1.68	2.77
PS5_5200_4380	0.00	0.01	0.08	0.45	0.94	1.90	3.41
PS5_5240_5200	0.22	0.27	0.40	0.63	1.04	1.68	2.66
PS4_5840_5240	0.20	0.26	0.40	0.67	1.11	1.98	3.17
PS4_6360_5840	0.10	0.16	0.31	0.68	1.20	2.19	3.45
PS2_6420_6360	0.05	0.10	0.28	0.68	1.23	2.38	3.68
PS2_6490_6420	0.10	0.20	0.45	0.90	1.48	2.55	3.73
PS2_6660_6490	0.28	0.38	0.64	0.99	1.69	3.18	5.10
PS2_6730_6660	0.08	0.16	0.41	0.87	1.45	2.52	3.62
PS3_5100_5080	0.05	0.14	0.32	0.63	1.07	2.02	3.25
PS2_5560_5100	0.04	0.09	0.25	0.58	1.04	2.06	3.37
PS2_5550_5560	0.02	0.04	0.15	0.50	0.99	1.93	3.15
PS4_6230_6360	0.00	0.05	0.21	0.54	1.03	2.17	3.69
PS3_6280_6230	0.37	0.40	0.48	0.61	0.91	1.46	2.34
PS3_6161_6280	0.01	0.04	0.20	0.53	1.04	2.25	3.97
PS0_6160_6161	0.01	0.04	0.20	0.51	1.04	2.42	4.33
PS0_6150_6160	0.00	0.01	0.10	0.38	0.90	2.15	5.05
PS3_6460_6230	0.13	0.16	0.33	0.70	1.18	2.14	3.39
PS3_5990_6161	0.09	0.11	0.25	0.61	1.09	2.01	3.12

Table C.2: Runoff Quantiles in Shenandoah River Segments (ccP10T10 Scenario)

River Segment	Q5 (cfs/sq mi)	Q10 (cfs/sq mi)	Q25 (cfs/sq mi)	Q50 (cfs/sq mi)	Q75 (cfs/sq mi)	Q90 (cfs/sq mi)	Q95 (cfs/sq mi)
PS5_4370_4150	0.28	0.31	0.40	0.59	0.84	1.47	2.21
PS5_4380_4370	0.10	0.12	0.20	0.43	0.81	1.53	2.35
PS4_5080_4380	0.03	0.05	0.16	0.42	0.82	1.55	2.25
PS1_4830_5080	0.02	0.05	0.14	0.38	0.77	1.56	2.47
PS1_4790_4830	0.00	0.02	0.09	0.30	0.69	1.36	2.17
PS5_5200_4380	0.00	0.00	0.04	0.33	0.78	1.62	2.70
PS5_5240_5200	0.15	0.18	0.28	0.48	0.87	1.38	2.02
PS4_5840_5240	0.14	0.17	0.29	0.50	0.90	1.58	2.36
PS4_6360_5840	0.08	0.12	0.23	0.51	0.94	1.78	2.59
PS2_6420_6360	0.03	0.06	0.19	0.52	1.01	1.90	2.91
PS2_6490_6420	0.05	0.12	0.33	0.71	1.24	2.11	2.99
PS2_6660_6490	0.20	0.29	0.52	0.81	1.42	2.74	4.28
PS2_6730_6660	0.03	0.10	0.29	0.67	1.21	2.09	2.96
PS3_5100_5080	0.04	0.08	0.21	0.48	0.88	1.68	2.50
PS2_5560_5100	0.02	0.05	0.16	0.43	0.85	1.68	2.60
PS2_5550_5560	0.01	0.02	0.07	0.32	0.73	1.52	2.29
PS4_6230_6360	0.00	0.01	0.13	0.41	0.84	1.74	2.78
PS3_6280_6230	0.29	0.32	0.38	0.50	0.76	1.19	1.82
PS3_6161_6280	0.00	0.02	0.13	0.40	0.85	1.84	3.07
PS0_6160_6161	0.00	0.02	0.14	0.40	0.86	1.93	3.47
PS0_6150_6160	0.00	0.00	0.06	0.30	0.73	1.75	4.13
PS3_6460_6230	0.10	0.12	0.24	0.53	0.98	1.75	2.61
PS3_5990_6161	0.07	0.08	0.16	0.43	0.85	1.62	2.40

Table C.3: Runoff Quantiles in Shenandoah River Segments (ccP50T50 Scenario)

River Segment	Q5 (cfs/sq mi)	Q10 (cfs/sq mi)	Q25 (cfs/sq mi)	Q50 (cfs/sq mi)	Q75 (cfs/sq mi)	Q90 (cfs/sq mi)	Q95 (cfs/sq mi)
PS5_4370_4150	0.36	0.41	0.52	0.72	1.04	1.91	3.01
PS5_4380_4370	0.12	0.16	0.28	0.57	1.02	1.96	3.27
PS4_5080_4380	0.04	0.11	0.28	0.60	1.05	2.01	3.25
PS1_4830_5080	0.04	0.09	0.21	0.52	0.99	2.00	3.41
PS1_4790_4830	0.01	0.05	0.15	0.45	0.94	1.85	3.00
PS5_5200_4380	0.00	0.01	0.08	0.47	0.98	2.08	3.75
PS5_5240_5200	0.23	0.28	0.41	0.66	1.07	1.79	3.00
PS4_5840_5240	0.20	0.26	0.42	0.69	1.16	2.08	3.49
PS4_6360_5840	0.11	0.16	0.32	0.71	1.26	2.34	3.76
PS2_6420_6360	0.05	0.10	0.28	0.71	1.29	2.54	4.09
PS2_6490_6420	0.10	0.20	0.47	0.95	1.56	2.74	4.14
PS2_6660_6490	0.28	0.38	0.66	1.02	1.75	3.46	5.57
PS2_6730_6660	0.08	0.16	0.42	0.91	1.53	2.70	4.04
PS3_5100_5080	0.05	0.14	0.33	0.65	1.11	2.12	3.53
PS2_5560_5100	0.04	0.09	0.26	0.60	1.10	2.23	3.56
PS2_5550_5560	0.02	0.04	0.15	0.52	1.04	2.06	3.41
PS4_6230_6360	0.00	0.05	0.21	0.55	1.09	2.30	3.88
PS3_6280_6230	0.39	0.42	0.51	0.65	0.96	1.61	2.53
PS3_6161_6280	0.01	0.04	0.20	0.54	1.09	2.40	4.21
PS0_6160_6161	0.01	0.05	0.20	0.53	1.09	2.49	4.56
PS0_6150_6160	0.00	0.01	0.11	0.40	0.93	2.26	5.35
PS3_6460_6230	0.14	0.17	0.33	0.73	1.24	2.30	3.74
PS3_5990_6161	0.09	0.12	0.25	0.64	1.16	2.11	3.40

Table C.4: Runoff Quantiles in Shenandoah River Segments (ccP90T90 Scenario)

River Segment	Q5 (cfs/sq mi)	Q10 (cfs/sq mi)	Q25 (cfs/sq mi)	Q50 (cfs/sq mi)	Q75 (cfs/sq mi)	Q90 (cfs/sq mi)	Q95 (cfs/sq mi)
PS5_4370_4150	0.45	0.51	0.64	0.87	1.27	2.51	4.20
PS5_4380_4370	0.15	0.21	0.38	0.72	1.25	2.63	4.48
PS4_5080_4380	0.08	0.20	0.42	0.79	1.31	2.61	4.94
PS1_4830_5080	0.06	0.13	0.30	0.66	1.21	2.60	4.89
PS1_4790_4830	0.03	0.09	0.24	0.63	1.20	2.46	4.57
PS5_5200_4380	0.00	0.02	0.15	0.61	1.20	2.69	5.22
PS5_5240_5200	0.29	0.39	0.57	0.84	1.33	2.44	4.60
PS4_5840_5240	0.25	0.35	0.55	0.90	1.45	2.82	5.06
PS4_6360_5840	0.14	0.21	0.42	0.90	1.59	3.13	5.37
PS2_6420_6360	0.07	0.14	0.38	0.87	1.59	3.34	5.70
PS2_6490_6420	0.16	0.28	0.61	1.15	1.89	3.52	5.87
PS2_6660_6490	0.35	0.48	0.79	1.22	2.12	4.31	7.08
PS2_6730_6660	0.13	0.24	0.56	1.11	1.86	3.41	5.83
PS3_5100_5080	0.09	0.22	0.45	0.81	1.37	2.77	5.32
PS2_5560_5100	0.07	0.14	0.35	0.76	1.38	2.92	5.21
PS2_5550_5560	0.03	0.06	0.25	0.71	1.35	2.75	4.80
PS4_6230_6360	0.02	0.08	0.29	0.70	1.36	3.00	5.34
PS3_6280_6230	0.49	0.54	0.64	0.82	1.21	2.10	3.65
PS3_6161_6280	0.02	0.07	0.28	0.67	1.36	3.13	5.75
PS0_6160_6161	0.02	0.08	0.27	0.66	1.36	3.21	6.24
PS0_6150_6160	0.00	0.02	0.17	0.54	1.18	2.96	6.63
PS3_6460_6230	0.17	0.23	0.45	0.89	1.51	3.00	5.33
PS3_5990_6161	0.12	0.15	0.36	0.82	1.46	2.83	4.91

Table C.5: Runoff Quantiles in Mattaponi River Segments (Base Scenario)

River Segment	Q5 (cfs/sq mi)	Q10 (cfs/sq mi)	Q25 (cfs/sq mi)	Q50 (cfs/sq mi)	Q75 (cfs/sq mi)	Q90 (cfs/sq mi)	Q95 (cfs/sq mi)
YM4_6620_0001	0.08	0.12	0.28	0.57	0.98	1.74	2.48
YM1_6370_6620	0.07	0.10	0.24	0.53	0.96	1.79	2.64
YM3_6430_6620	0.06	0.10	0.23	0.51	0.95	1.80	2.74
YM2_6120_6430	0.04	0.06	0.17	0.41	0.86	1.78	2.95

Table C.6: Runoff Quantiles in Mattaponi River Segments (ccP10T10 Scenario)

River Segment	Q5 (cfs/sq mi)	Q10 (cfs/sq mi)	Q25 (cfs/sq mi)	Q50 (cfs/sq mi)	Q75 (cfs/sq mi)	Q90 (cfs/sq mi)	Q95 (cfs/sq mi)
YM4_6620_0001	0.05	0.08	0.20	0.42	0.76	1.37	1.96
YM1_6370_6620	0.04	0.07	0.17	0.39	0.75	1.45	2.17
YM3_6430_6620	0.04	0.07	0.16	0.38	0.74	1.48	2.24
YM2_6120_6430	0.02	0.04	0.12	0.30	0.68	1.42	2.30

Table C.7: Runoff Quantiles in Mattaponi River Segments (ccP50T50 Scenario)

River Segment	Q5 (cfs/sq mi)	Q10 (cfs/sq mi)	Q25 (cfs/sq mi)	Q50 (cfs/sq mi)	Q75 (cfs/sq mi)	Q90 (cfs/sq mi)	Q95 (cfs/sq mi)
YM4_6620_0001	0.08	0.13	0.30	0.60	1.04	1.89	2.67
YM1_6370_6620	0.07	0.11	0.26	0.56	1.02	1.93	2.84
YM3_6430_6620	0.06	0.10	0.24	0.54	1.01	1.96	2.97
YM2_6120_6430	0.04	0.07	0.18	0.43	0.91	1.89	3.35

Table C.8: Runoff Quantiles in Mattaponi River Segments (ccP90T90 Scenario)

River Segment	Q5 (cfs/sq mi)	Q10 (cfs/sq mi)	Q25 (cfs/sq mi)	Q50 (cfs/sq mi)	Q75 (cfs/sq mi)	Q90 (cfs/sq mi)	Q95 (cfs/sq mi)
YM4_6620_0001	0.14	0.20	0.43	0.85	1.47	2.64	3.85
YM1_6370_6620	0.11	0.17	0.38	0.79	1.42	2.68	4.24
YM3_6430_6620	0.10	0.15	0.36	0.75	1.38	2.70	4.42
YM2_6120_6430	0.06	0.10	0.26	0.61	1.19	2.61	4.94

Table C.9: Runoff Quantiles in Pamunkey River Segments (Base Scenario)

River Segment	Q5 (cfs/sq mi)	Q10 (cfs/sq mi)	Q25 (cfs/sq mi)	Q50 (cfs/sq mi)	Q75 (cfs/sq mi)	Q90 (cfs/sq mi)	Q95 (cfs/sq mi)
YP4_6750_0001	0.08	0.13	0.27	0.55	0.97	1.80	2.58
YP4_6720_6750	0.07	0.12	0.26	0.54	0.99	1.87	2.70
YP3_6670_6720	0.06	0.10	0.24	0.52	0.96	1.81	2.69
YP1_6680_6670	0.07	0.11	0.25	0.52	0.96	1.77	2.53
YP1_6570_6680	0.06	0.09	0.20	0.44	0.85	1.72	2.70
YP3_6690_6720	0.07	0.12	0.26	0.54	0.97	1.77	2.51
YP3_6470_6690	0.06	0.09	0.19	0.41	0.84	1.71	2.95
YP3_6700_6670	0.06	0.11	0.24	0.51	1.10	2.41	3.95
YP3_6330_6700	0.05	0.08	0.20	0.46	0.89	1.75	2.67
YP2_6390_6330	0.05	0.08	0.17	0.38	0.78	1.61	2.93

Table C.10: Runoff Quantiles in Pamunkey River Segments (ccP10T10 Scenario)

River Segment	Q5 (cfs/sq mi)	Q10 (cfs/sq mi)	Q25 (cfs/sq mi)	Q50 (cfs/sq mi)	Q75 (cfs/sq mi)	Q90 (cfs/sq mi)	Q95 (cfs/sq mi)
YP4_6750_0001	0.06	0.09	0.20	0.42	0.78	1.45	2.10
YP4_6720_6750	0.05	0.08	0.19	0.41	0.79	1.52	2.27
YP3_6670_6720	0.04	0.07	0.18	0.39	0.75	1.50	2.22
YP1_6680_6670	0.05	0.08	0.18	0.39	0.76	1.43	2.07
YP1_6570_6680	0.04	0.06	0.15	0.33	0.66	1.34	2.08
YP3_6690_6720	0.05	0.09	0.20	0.41	0.76	1.43	2.08
YP3_6470_6690	0.04	0.06	0.14	0.31	0.65	1.36	2.20
YP3_6700_6670	0.05	0.08	0.18	0.39	0.88	2.09	3.33
YP3_6330_6700	0.03	0.06	0.14	0.34	0.69	1.40	2.15
YP2_6390_6330	0.03	0.06	0.12	0.29	0.61	1.30	2.17

Table C.11: Runoff Quantiles in Pamunkey River Segments (ccP50T50 Scenario)

River Segment	Q5 (cfs/sq mi)	Q10 (cfs/sq mi)	Q25 (cfs/sq mi)	Q50 (cfs/sq mi)	Q75 (cfs/sq mi)	Q90 (cfs/sq mi)	Q95 (cfs/sq mi)
YP4_6750_0001	0.09	0.14	0.29	0.59	1.03	1.92	2.84
YP4_6720_6750	0.08	0.13	0.28	0.57	1.07	2.00	2.92
YP3_6670_6720	0.07	0.11	0.26	0.56	1.03	1.97	2.93
YP1_6680_6670	0.07	0.12	0.27	0.57	1.04	1.89	2.72
YP1_6570_6680	0.06	0.10	0.22	0.47	0.92	1.85	3.00
YP3_6690_6720	0.08	0.13	0.28	0.58	1.05	1.90	2.73
YP3_6470_6690	0.06	0.09	0.20	0.44	0.89	1.87	3.35
YP3_6700_6670	0.07	0.12	0.26	0.54	1.17	2.59	4.21
YP3_6330_6700	0.05	0.09	0.22	0.49	0.94	1.86	2.99
YP2_6390_6330	0.05	0.08	0.18	0.41	0.83	1.75	3.17

Table C.12: Runoff Quantiles in Pamunkey River Segments (ccP90T90 Scenario)

River Segment	Q5 (cfs/sq mi)	Q10 (cfs/sq mi)	Q25 (cfs/sq mi)	Q50 (cfs/sq mi)	Q75 (cfs/sq mi)	Q90 (cfs/sq mi)	Q95 (cfs/sq mi)
YP4_6750_0001	0.13	0.20	0.42	0.82	1.45	2.67	4.07
YP4_6720_6750	0.12	0.19	0.40	0.81	1.48	2.76	4.19
YP3_6670_6720	0.11	0.17	0.38	0.77	1.41	2.69	4.31
YP1_6680_6670	0.12	0.19	0.41	0.83	1.47	2.64	3.92
YP1_6570_6680	0.09	0.15	0.31	0.67	1.29	2.59	4.66
YP3_6690_6720	0.13	0.20	0.42	0.83	1.46	2.65	3.99
YP3_6470_6690	0.09	0.13	0.28	0.61	1.20	2.60	4.94
YP3_6700_6670	0.10	0.17	0.37	0.78	1.59	3.47	5.73
YP3_6330_6700	0.09	0.14	0.32	0.69	1.30	2.61	4.56
YP2_6390_6330	0.08	0.11	0.25	0.55	1.08	2.50	4.87

Table C.13: Runoff Quantiles in Rappahannock River Segments (Base Scenario)

River Segment	Q5 (cfs/sq mi)	Q10 (cfs/sq mi)	Q25 (cfs/sq mi)	Q50 (cfs/sq mi)	Q75 (cfs/sq mi)	Q90 (cfs/sq mi)	Q95 (cfs/sq mi)
RU5_6030_0001	0.04	0.07	0.18	0.43	0.95	2.03	3.59
RU4_5640_6030	0.07	0.11	0.26	0.58	1.08	2.07	3.36
RU2_5220_5640	0.05	0.10	0.26	0.60	1.12	2.23	3.66
RU4_6040_6030	0.07	0.11	0.25	0.54	0.96	1.84	2.93
RU3_6170_6040	0.07	0.12	0.25	0.54	0.94	1.75	2.78
RU2_6200_6170	0.19	0.30	0.51	0.93	1.53	2.59	3.78
RU2_5940_6200	0.19	0.30	0.52	0.95	1.56	2.65	3.95
RU3_5610_5640	0.08	0.14	0.32	0.68	1.13	1.99	3.03
RU2_5500_5610	0.06	0.17	0.44	0.92	1.55	2.77	4.46
RU2_6220_6170	0.11	0.18	0.34	0.66	1.16	2.11	3.44
RU2_6090_6220	0.17	0.27	0.50	0.95	1.65	2.96	4.68
RU2_5810_5610	0.12	0.22	0.46	0.90	1.51	2.64	4.15

Table C.14: Runoff Quantiles in Rappahannock River Segments (ccP10T10 Scenario)

River Segment	Q5 (cfs/sq mi)	Q10 (cfs/sq mi)	Q25 (cfs/sq mi)	Q50 (cfs/sq mi)	Q75 (cfs/sq mi)	Q90 (cfs/sq mi)	Q95 (cfs/sq mi)
RU5_6030_0001	0.03	0.05	0.13	0.33	0.76	1.64	2.97
RU4_5640_6030	0.05	0.08	0.19	0.46	0.90	1.70	2.72
RU2_5220_5640	0.03	0.06	0.19	0.48	0.94	1.84	2.88
RU4_6040_6030	0.05	0.08	0.18	0.41	0.78	1.50	2.31
RU3_6170_6040	0.05	0.08	0.19	0.42	0.76	1.47	2.14
RU2_6200_6170	0.13	0.21	0.39	0.75	1.27	2.17	3.07
RU2_5940_6200	0.13	0.22	0.40	0.76	1.30	2.23	3.12
RU3_5610_5640	0.05	0.10	0.23	0.53	0.94	1.70	2.43
RU2_5500_5610	0.03	0.09	0.32	0.77	1.33	2.36	3.61
RU2_6220_6170	0.08	0.13	0.25	0.52	0.94	1.74	2.59
RU2_6090_6220	0.13	0.21	0.40	0.78	1.37	2.42	3.59
RU2_5810_5610	0.08	0.15	0.34	0.73	1.27	2.21	3.31

Table C.15: Runoff Quantiles in Rappahannock River Segments (ccP50T50 Scenario)

River Segment	Q5 (cfs/sq mi)	Q10 (cfs/sq mi)	Q25 (cfs/sq mi)	Q50 (cfs/sq mi)	Q75 (cfs/sq mi)	Q90 (cfs/sq mi)	Q95 (cfs/sq mi)
RU5_6030_0001	0.04	0.07	0.19	0.45	0.97	2.16	3.93
RU4_5640_6030	0.07	0.12	0.27	0.62	1.15	2.20	3.72
RU2_5220_5640	0.05	0.10	0.27	0.64	1.20	2.41	4.02
RU4_6040_6030	0.08	0.12	0.27	0.58	1.03	1.94	3.23
RU3_6170_6040	0.08	0.13	0.27	0.58	1.01	1.89	3.11
RU2_6200_6170	0.20	0.32	0.54	0.99	1.63	2.73	4.09
RU2_5940_6200	0.20	0.31	0.55	1.00	1.67	2.81	4.24
RU3_5610_5640	0.09	0.16	0.34	0.73	1.22	2.14	3.31
RU2_5500_5610	0.06	0.17	0.47	0.96	1.66	2.94	5.00
RU2_6220_6170	0.12	0.19	0.36	0.70	1.24	2.28	3.71
RU2_6090_6220	0.18	0.28	0.54	1.00	1.74	3.11	5.03
RU2_5810_5610	0.13	0.23	0.48	0.95	1.62	2.81	4.55

Table C.16: Runoff Quantiles in Rappahannock River Segments (ccP90T90 Scenario)

River Segment	Q5 (cfs/sq mi)	Q10 (cfs/sq mi)	Q25 (cfs/sq mi)	Q50 (cfs/sq mi)	Q75 (cfs/sq mi)	Q90 (cfs/sq mi)	Q95 (cfs/sq mi)
RU5_6030_0001	0.06	0.10	0.26	0.61	1.25	2.97	5.62
RU4_5640_6030	0.11	0.17	0.38	0.79	1.44	3.07	5.30
RU2_5220_5640	0.08	0.15	0.37	0.81	1.53	3.24	5.63
RU4_6040_6030	0.11	0.18	0.37	0.75	1.31	2.63	4.69
RU3_6170_6040	0.12	0.19	0.37	0.75	1.28	2.53	4.55
RU2_6200_6170	0.27	0.40	0.70	1.19	1.98	3.50	5.88
RU2_5940_6200	0.27	0.40	0.71	1.21	2.05	3.57	5.93
RU3_5610_5640	0.14	0.23	0.46	0.92	1.52	2.79	4.69
RU2_5500_5610	0.12	0.27	0.62	1.17	1.99	3.83	7.00
RU2_6220_6170	0.17	0.26	0.47	0.88	1.55	3.08	5.31
RU2_6090_6220	0.23	0.35	0.67	1.20	2.09	4.10	7.29
RU2_5810_5610	0.18	0.32	0.63	1.15	1.97	3.63	6.33

Table C.17: Runoff Quantiles in Upper James River Segments (Base Scenario)

River Segment	Q5 (cfs/sq mi)	Q10 (cfs/sq mi)	Q25 (cfs/sq mi)	Q50 (cfs/sq mi)	Q75 (cfs/sq mi)	Q90 (cfs/sq mi)	Q95 (cfs/sq mi)
JU5_7420_7160	0.22	0.29	0.47	0.74	1.25	2.18	3.47
JU5_7500_7420	0.18	0.25	0.42	0.71	1.29	2.26	3.50
JU1_7560_7500	0.16	0.23	0.41	0.71	1.31	2.28	3.57
JU1_7750_7560	0.11	0.19	0.33	0.63	1.27	2.32	3.48
JU5_7510_7500	0.16	0.23	0.40	0.70	1.30	2.28	3.52
JU3_7400_7510	0.17	0.23	0.40	0.68	1.23	2.15	3.20
JU3_7490_7400	0.07	0.13	0.37	0.81	1.45	2.58	3.85
JU1_7630_7490	0.01	0.04	0.35	0.85	1.58	2.71	3.94
JU5_7300_7510	0.18	0.25	0.42	0.69	1.22	2.11	3.21
JU3_6650_7300	0.01	0.05	0.20	0.55	1.07	1.95	3.25
JU1_6300_6650	0.20	0.25	0.47	0.89	1.57	2.94	4.44
JU1_7690_7490	0.02	0.05	0.30	0.75	1.45	2.55	3.81
JU4_7000_7300	0.01	0.03	0.15	0.56	1.12	2.17	3.58
JU2_7360_7000	0.00	0.01	0.11	0.53	1.13	2.16	3.59
JU2_7450_7360	0.06	0.10	0.27	0.67	1.28	2.24	3.51
JU1_6340_6650	0.03	0.04	0.28	0.77	1.54	3.28	5.15
JU4_7330_7000	0.09	0.11	0.20	0.58	1.16	2.56	4.02
JU2_7140_7330	0.04	0.06	0.17	0.58	1.16	2.13	3.42
JU3_6950_7330	0.01	0.04	0.17	0.56	1.11	2.13	3.53
JU3_6900_6950	0.00	0.03	0.16	0.50	0.99	1.80	3.04
JU2_6810_6900	0.00	0.04	0.19	0.53	1.03	1.84	3.14
JU2_6600_6810	0.01	0.04	0.20	0.54	1.03	1.86	3.19
JU1_6590_6600	0.01	0.04	0.19	0.52	1.01	1.80	3.11
JU1_6290_6590	0.00	0.02	0.27	0.76	1.56	3.34	5.30
JU3_6380_6900	0.02	0.07	0.28	0.67	1.28	2.58	4.06
JU4_7380_7160	0.06	0.12	0.38	0.73	1.32	2.58	4.23
JU2_7180_7380	0.25	0.31	0.51	0.75	1.19	2.15	3.44
JU4_7260_7380	0.12	0.18	0.43	0.73	1.29	2.50	4.02
JU1_6880_7260	0.10	0.16	0.43	0.80	1.39	2.57	4.06
JU3_6790_7260	0.09	0.15	0.39	0.75	1.32	2.57	4.13
JU3_6640_6790	0.03	0.08	0.28	0.67	1.24	2.28	3.73
JU2_6410_6640	0.01	0.03	0.17	0.64	1.23	2.19	3.55

Table C.18: Runoff Quantiles in Upper James River Segments (ccP10T10 Scenario)

River Segment	Q5 (cfs/sq mi)	Q10 (cfs/sq mi)	Q25 (cfs/sq mi)	Q50 (cfs/sq mi)	Q75 (cfs/sq mi)	Q90 (cfs/sq mi)	Q95 (cfs/sq mi)
JU5_7420_7160	0.17	0.22	0.35	0.58	1.04	1.76	2.61
JU5_7500_7420	0.14	0.19	0.34	0.57	1.09	1.84	2.67
JU1_7560_7500	0.12	0.18	0.33	0.57	1.10	1.86	2.72
JU1_7750_7560	0.08	0.14	0.26	0.50	1.06	1.90	2.71
JU5_7510_7500	0.12	0.18	0.32	0.56	1.09	1.86	2.72
JU3_7400_7510	0.12	0.17	0.31	0.53	1.03	1.74	2.52
JU3_7490_7400	0.05	0.09	0.26	0.63	1.25	2.12	3.00
JU1_7630_7490	0.00	0.02	0.23	0.66	1.35	2.28	3.10
JU5_7300_7510	0.13	0.18	0.33	0.54	1.02	1.71	2.51
JU3_6650_7300	0.01	0.02	0.11	0.39	0.87	1.60	2.49
JU1_6300_6650	0.17	0.20	0.36	0.73	1.32	2.37	3.58
JU1_7690_7490	0.01	0.03	0.19	0.57	1.25	2.15	2.98
JU4_7000_7300	0.01	0.01	0.09	0.40	0.93	1.72	2.73
JU2_7360_7000	0.00	0.00	0.05	0.38	0.93	1.75	2.73
JU2_7450_7360	0.03	0.07	0.18	0.50	1.08	1.83	2.67
JU1_6340_6650	0.02	0.03	0.18	0.62	1.32	2.66	4.15
JU4_7330_7000	0.08	0.09	0.14	0.45	1.00	2.09	3.32
JU2_7140_7330	0.02	0.04	0.11	0.42	0.96	1.72	2.64
JU3_6950_7330	0.01	0.01	0.10	0.40	0.93	1.70	2.68
JU3_6900_6950	0.00	0.00	0.08	0.33	0.80	1.48	2.34
JU2_6810_6900	0.00	0.00	0.09	0.38	0.84	1.54	2.36
JU2_6600_6810	0.00	0.01	0.09	0.39	0.84	1.55	2.37
JU1_6590_6600	0.00	0.01	0.09	0.37	0.81	1.50	2.31
JU1_6290_6590	0.00	0.01	0.17	0.62	1.33	2.72	4.18
JU3_6380_6900	0.01	0.03	0.18	0.52	1.06	2.05	3.29
JU4_7380_7160	0.03	0.06	0.27	0.58	1.10	2.03	3.14
JU2_7180_7380	0.20	0.24	0.38	0.60	1.00	1.71	2.54
JU4_7260_7380	0.09	0.12	0.31	0.58	1.08	2.02	3.09
JU1_6880_7260	0.05	0.09	0.32	0.63	1.16	2.04	3.05
JU3_6790_7260	0.06	0.09	0.29	0.59	1.11	2.02	3.10
JU3_6640_6790	0.01	0.04	0.19	0.48	1.02	1.84	2.76
JU2_6410_6640	0.00	0.01	0.08	0.44	0.98	1.78	2.61

Table C.19: Runoff Quantiles in Upper James River Segments (ccP50T50 Scenario)

River Segment	Q5 (cfs/sq mi)	Q10 (cfs/sq mi)	Q25 (cfs/sq mi)	Q50 (cfs/sq mi)	Q75 (cfs/sq mi)	Q90 (cfs/sq mi)	Q95 (cfs/sq mi)
JU5_7420_7160	0.22	0.30	0.49	0.78	1.32	2.35	3.78
JU5_7500_7420	0.18	0.26	0.44	0.76	1.37	2.47	3.77
JU1_7560_7500	0.16	0.24	0.43	0.76	1.39	2.48	3.79
JU1_7750_7560	0.12	0.20	0.35	0.68	1.35	2.45	3.68
JU5_7510_7500	0.16	0.24	0.43	0.76	1.38	2.47	3.78
JU3_7400_7510	0.17	0.24	0.42	0.73	1.32	2.27	3.50
JU3_7490_7400	0.07	0.13	0.38	0.86	1.53	2.72	4.06
JU1_7630_7490	0.01	0.04	0.35	0.89	1.65	2.85	4.10
JU5_7300_7510	0.18	0.25	0.45	0.73	1.31	2.24	3.49
JU3_6650_7300	0.01	0.04	0.20	0.57	1.12	2.08	3.44
JU1_6300_6650	0.20	0.26	0.48	0.93	1.64	3.10	4.69
JU1_7690_7490	0.02	0.05	0.30	0.78	1.52	2.70	4.03
JU4_7000_7300	0.01	0.02	0.14	0.57	1.17	2.30	3.77
JU2_7360_7000	0.00	0.00	0.10	0.55	1.17	2.25	3.83
JU2_7450_7360	0.06	0.10	0.27	0.70	1.32	2.35	3.72
JU1_6340_6650	0.03	0.04	0.28	0.80	1.63	3.42	5.41
JU4_7330_7000	0.09	0.11	0.20	0.60	1.20	2.73	4.27
JU2_7140_7330	0.04	0.06	0.16	0.60	1.20	2.24	3.64
JU3_6950_7330	0.01	0.03	0.17	0.58	1.16	2.31	3.66
JU3_6900_6950	0.00	0.02	0.16	0.52	1.03	1.95	3.18
JU2_6810_6900	0.00	0.03	0.19	0.56	1.09	2.00	3.42
JU2_6600_6810	0.01	0.03	0.20	0.56	1.09	1.99	3.43
JU1_6590_6600	0.00	0.03	0.19	0.55	1.06	1.93	3.32
JU1_6290_6590	0.00	0.02	0.27	0.80	1.65	3.48	5.65
JU3_6380_6900	0.02	0.07	0.28	0.69	1.34	2.73	4.35
JU4_7380_7160	0.06	0.12	0.39	0.77	1.39	2.76	4.49
JU2_7180_7380	0.25	0.32	0.53	0.79	1.28	2.36	3.72
JU4_7260_7380	0.12	0.18	0.43	0.76	1.36	2.69	4.43
JU1_6880_7260	0.10	0.16	0.44	0.85	1.46	2.78	4.35
JU3_6790_7260	0.09	0.15	0.40	0.78	1.40	2.73	4.45
JU3_6640_6790	0.03	0.08	0.28	0.70	1.30	2.52	3.93
JU2_6410_6640	0.01	0.03	0.16	0.68	1.31	2.34	3.78

Table C.20: Runoff Quantiles in Upper James River Segments (ccP90T90 Scenario)

River Segment	Q5 (cfs/sq mi)	Q10 (cfs/sq mi)	Q25 (cfs/sq mi)	Q50 (cfs/sq mi)	Q75 (cfs/sq mi)	Q90 (cfs/sq mi)	Q95 (cfs/sq mi)
JU5_7420_7160	0.28	0.37	0.61	0.96	1.64	3.24	5.43
JU5_7500_7420	0.22	0.32	0.54	0.95	1.67	3.32	5.29
JU1_7560_7500	0.20	0.30	0.53	0.95	1.69	3.34	5.36
JU1_7750_7560	0.15	0.25	0.45	0.89	1.68	3.26	5.24
JU5_7510_7500	0.20	0.30	0.52	0.95	1.68	3.32	5.35
JU3_7400_7510	0.21	0.30	0.52	0.92	1.64	3.10	5.01
JU3_7490_7400	0.10	0.18	0.51	1.06	1.88	3.56	5.81
JU1_7630_7490	0.02	0.10	0.49	1.11	1.98	3.71	5.73
JU5_7300_7510	0.23	0.32	0.55	0.92	1.61	3.09	5.07
JU3_6650_7300	0.02	0.08	0.29	0.73	1.36	2.78	4.96
JU1_6300_6650	0.23	0.30	0.59	1.10	1.96	3.98	6.31
JU1_7690_7490	0.03	0.09	0.42	1.01	1.83	3.57	5.67
JU4_7000_7300	0.01	0.05	0.23	0.72	1.44	3.10	5.30
JU2_7360_7000	0.00	0.01	0.17	0.70	1.45	3.13	5.35
JU2_7450_7360	0.08	0.13	0.37	0.89	1.62	3.10	5.20
JU1_6340_6650	0.03	0.06	0.37	0.94	1.97	4.41	7.21
JU4_7330_7000	0.10	0.12	0.28	0.72	1.46	3.56	6.02
JU2_7140_7330	0.05	0.08	0.25	0.76	1.49	3.06	5.26
JU3_6950_7330	0.02	0.06	0.25	0.73	1.43	3.05	5.14
JU3_6900_6950	0.01	0.06	0.24	0.67	1.27	2.64	4.62
JU2_6810_6900	0.01	0.07	0.29	0.72	1.33	2.67	4.89
JU2_6600_6810	0.02	0.08	0.30	0.72	1.33	2.67	4.90
JU1_6590_6600	0.01	0.07	0.30	0.70	1.28	2.59	4.76
JU1_6290_6590	0.01	0.03	0.35	0.93	1.98	4.51	7.37
JU3_6380_6900	0.05	0.11	0.37	0.84	1.62	3.65	5.79
JU4_7380_7160	0.10	0.20	0.50	0.94	1.70	3.68	6.25
JU2_7180_7380	0.32	0.41	0.65	0.95	1.55	3.15	5.34
JU4_7260_7380	0.17	0.26	0.54	0.92	1.66	3.67	6.01
JU1_6880_7260	0.15	0.24	0.56	1.03	1.81	3.66	6.06
JU3_6790_7260	0.13	0.22	0.50	0.95	1.70	3.67	6.06
JU3_6640_6790	0.06	0.13	0.38	0.89	1.60	3.39	5.60
JU2_6410_6640	0.02	0.05	0.27	0.87	1.59	3.14	5.38

Table C.21: Runoff Quantiles in Middle James River Segments (Base Scenario)

River Segment	Q5 (cfs/sq mi)	Q10 (cfs/sq mi)	Q25 (cfs/sq mi)	Q50 (cfs/sq mi)	Q75 (cfs/sq mi)	Q90 (cfs/sq mi)	Q95 (cfs/sq mi)
JL7_7070_0001	0.00	0.01	0.13	0.52	1.32	3.08	5.73
JL7_6800_7070	0.09	0.12	0.24	0.48	0.92	1.78	2.96
JL1_7170_6800	0.04	0.07	0.18	0.48	0.93	1.84	3.21
JL7_7030_6800	0.08	0.11	0.22	0.48	0.94	1.89	3.43
JL7_7100_7030	0.09	0.12	0.23	0.47	0.91	1.97	3.68
JL3_7020_7100	0.07	0.11	0.21	0.50	1.01	2.15	3.80
JL6_6740_7100	0.10	0.13	0.25	0.46	0.83	1.56	2.42
JL4_6710_6740	0.07	0.11	0.22	0.47	0.86	1.61	2.42
JL4_6520_6710	0.12	0.18	0.35	0.71	1.29	2.28	3.36
JL2_6240_6520	0.01	0.03	0.15	0.50	1.04	2.06	3.57
JL6_6970_6740	0.08	0.12	0.22	0.48	0.94	1.85	3.01
JL2_7120_6970	0.07	0.11	0.21	0.49	0.99	2.13	3.55
JL2_7110_7120	0.07	0.11	0.21	0.48	0.99	2.05	3.35
JL2_6441_6520	0.12	0.18	0.36	0.71	1.23	2.11	3.08
JL2_6440_6441	0.11	0.17	0.34	0.68	1.24	2.18	3.25
JL1_6560_6440	0.11	0.17	0.34	0.70	1.27	2.33	3.40
JL6_6960_6970	0.07	0.11	0.22	0.46	0.85	1.59	2.37
JL1_6910_6960	0.08	0.11	0.23	0.48	0.86	1.61	2.44
JL1_6760_6910	0.12	0.17	0.35	0.69	1.24	2.14	3.16
JL6_6990_6960	0.07	0.11	0.21	0.47	0.94	1.88	3.07
JL6_6890_6990	0.10	0.16	0.30	0.63	1.17	2.11	3.25
JL2_6850_6890	0.09	0.23	0.60	1.22	2.00	3.30	4.85
JL1_6770_6850	0.07	0.19	0.51	1.19	1.99	3.20	4.70
JL6_7150_6890	0.09	0.16	0.38	0.80	1.43	2.60	3.95
JL3_7090_7150	0.09	0.27	0.69	1.38	2.24	3.60	5.35
JL2_7250_7090	0.13	0.28	0.65	1.29	2.05	3.31	4.96
JL1_7190_7250	0.13	0.24	0.55	1.05	1.68	2.71	3.99
JL1_7080_7190	0.08	0.23	0.60	1.28	2.12	3.41	4.93
JL6_7320_7150	0.09	0.15	0.34	0.72	1.29	2.31	3.48
JL6_7430_7320	0.10	0.17	0.36	0.71	1.28	2.14	3.20
JL1_7530_7430	0.09	0.14	0.26	0.53	1.05	1.90	2.95
JL2_7350_7090	0.10	0.23	0.58	1.21	1.94	3.12	4.64
JL2_7240_7350	0.08	0.15	0.42	0.85	1.45	2.36	3.39
JL1_7200_7250	0.13	0.31	0.73	1.39	2.23	3.54	5.28
JL1_6940_7200	0.08	0.22	0.60	1.30	2.14	3.42	4.90
JL6_7440_7430	0.20	0.26	0.43	0.70	1.20	2.20	3.40
JL6_7160_7440	0.11	0.17	0.41	0.76	1.31	2.10	3.05

Table C.22: Runoff Quantiles in Middle James River Segments (ccP10T10 Scenario)

River Segment	Q5 (cfs/sq mi)	Q10 (cfs/sq mi)	Q25 (cfs/sq mi)	Q50 (cfs/sq mi)	Q75 (cfs/sq mi)	Q90 (cfs/sq mi)	Q95 (cfs/sq mi)
JL7_7070_0001	0.00	0.00	0.08	0.41	1.12	2.74	4.94
JL7_6800_7070	0.07	0.09	0.18	0.37	0.75	1.46	2.31
JL1_7170_6800	0.02	0.05	0.13	0.36	0.75	1.47	2.38
JL7_7030_6800	0.06	0.08	0.17	0.37	0.76	1.51	2.49
JL7_7100_7030	0.07	0.10	0.18	0.38	0.74	1.53	2.72
JL3_7020_7100	0.05	0.08	0.16	0.38	0.81	1.65	2.78
JL6_6740_7100	0.07	0.10	0.19	0.35	0.66	1.25	1.86
JL4_6710_6740	0.05	0.08	0.17	0.36	0.69	1.29	1.94
JL4_6520_6710	0.08	0.12	0.26	0.55	1.02	1.85	2.64
JL2_6240_6520	0.00	0.01	0.08	0.37	0.83	1.63	2.64
JL6_6970_6740	0.05	0.08	0.17	0.37	0.76	1.46	2.28
JL2_7120_6970	0.05	0.08	0.16	0.37	0.79	1.61	2.60
JL2_7110_7120	0.05	0.08	0.16	0.36	0.79	1.54	2.49
JL2_6441_6520	0.08	0.13	0.27	0.55	0.99	1.72	2.42
JL2_6440_6441	0.07	0.12	0.25	0.51	0.96	1.76	2.52
JL1_6560_6440	0.08	0.12	0.26	0.53	1.01	1.89	2.77
JL6_6960_6970	0.05	0.08	0.16	0.35	0.68	1.27	1.89
JL1_6910_6960	0.06	0.08	0.17	0.36	0.70	1.30	1.96
JL1_6760_6910	0.08	0.12	0.26	0.53	0.97	1.73	2.47
JL6_6990_6960	0.05	0.08	0.16	0.35	0.75	1.47	2.32
JL6_6890_6990	0.07	0.11	0.23	0.48	0.91	1.68	2.41
JL2_6850_6890	0.05	0.14	0.46	1.04	1.73	2.74	3.82
JL1_6770_6850	0.04	0.12	0.39	1.00	1.70	2.72	3.74
JL6_7150_6890	0.06	0.11	0.29	0.67	1.19	2.05	3.02
JL3_7090_7150	0.05	0.16	0.54	1.21	1.97	3.02	4.24
JL2_7250_7090	0.08	0.18	0.51	1.11	1.79	2.81	3.87
JL1_7190_7250	0.08	0.17	0.42	0.88	1.45	2.31	3.17
JL1_7080_7190	0.05	0.15	0.47	1.10	1.84	2.83	3.96
JL6_7320_7150	0.06	0.11	0.26	0.58	1.06	1.82	2.70
JL6_7430_7320	0.07	0.12	0.27	0.57	1.05	1.78	2.52
JL1_7530_7430	0.07	0.11	0.21	0.42	0.86	1.53	2.28
JL2_7350_7090	0.05	0.14	0.44	1.02	1.69	2.65	3.62
JL2_7240_7350	0.05	0.10	0.30	0.69	1.24	2.01	2.80
JL1_7200_7250	0.09	0.20	0.58	1.23	1.96	3.01	4.21
JL1_6940_7200	0.05	0.14	0.46	1.12	1.85	2.86	3.92
JL6_7440_7430	0.17	0.21	0.33	0.57	1.03	1.84	2.78
JL6_7160_7440	0.08	0.12	0.29	0.61	1.11	1.78	2.44

Table C.23: Runoff Quantiles in Middle James River Segments (ccP50T50 Scenario)

River Segment	Q5 (cfs/sq mi)	Q10 (cfs/sq mi)	Q25 (cfs/sq mi)	Q50 (cfs/sq mi)	Q75 (cfs/sq mi)	Q90 (cfs/sq mi)	Q95 (cfs/sq mi)
JL7_7070_0001	0.00	0.01	0.13	0.55	1.39	3.32	6.29
JL7_6800_7070	0.10	0.13	0.26	0.51	0.97	1.91	3.27
JL1_7170_6800	0.04	0.08	0.20	0.51	0.99	1.99	3.42
JL7_7030_6800	0.08	0.12	0.24	0.51	0.99	2.04	3.78
JL7_7100_7030	0.09	0.13	0.24	0.50	0.97	2.13	4.01
JL3_7020_7100	0.07	0.11	0.22	0.52	1.06	2.30	4.10
JL6_6740_7100	0.11	0.14	0.27	0.50	0.90	1.67	2.71
JL4_6710_6740	0.08	0.12	0.24	0.51	0.93	1.72	2.60
JL4_6520_6710	0.12	0.18	0.37	0.76	1.38	2.42	3.71
JL2_6240_6520	0.01	0.03	0.16	0.54	1.10	2.21	4.00
JL6_6970_6740	0.08	0.12	0.23	0.52	1.02	1.97	3.37
JL2_7120_6970	0.07	0.11	0.22	0.52	1.05	2.24	3.91
JL2_7110_7120	0.07	0.11	0.22	0.52	1.05	2.16	3.71
JL2_6441_6520	0.13	0.19	0.38	0.77	1.33	2.25	3.38
JL2_6440_6441	0.12	0.18	0.36	0.74	1.32	2.29	3.42
JL1_6560_6440	0.12	0.18	0.37	0.74	1.35	2.47	3.73
JL6_6960_6970	0.08	0.12	0.23	0.50	0.93	1.72	2.57
JL1_6910_6960	0.09	0.13	0.25	0.52	0.94	1.74	2.63
JL1_6760_6910	0.12	0.18	0.37	0.75	1.33	2.29	3.42
JL6_6990_6960	0.08	0.12	0.22	0.50	1.01	1.99	3.45
JL6_6890_6990	0.11	0.17	0.32	0.68	1.25	2.25	3.50
JL2_6850_6890	0.09	0.24	0.63	1.28	2.09	3.47	5.30
JL1_6770_6850	0.08	0.20	0.54	1.26	2.07	3.42	5.06
JL6_7150_6890	0.09	0.16	0.40	0.86	1.51	2.76	4.29
JL3_7090_7150	0.09	0.27	0.73	1.45	2.33	3.84	5.73
JL2_7250_7090	0.13	0.28	0.68	1.36	2.14	3.52	5.33
JL1_7190_7250	0.13	0.26	0.57	1.12	1.78	2.91	4.46
JL1_7080_7190	0.09	0.23	0.63	1.36	2.22	3.60	5.35
JL6_7320_7150	0.10	0.16	0.35	0.77	1.38	2.49	3.79
JL6_7430_7320	0.10	0.18	0.38	0.76	1.36	2.36	3.53
JL1_7530_7430	0.10	0.15	0.28	0.58	1.12	2.06	3.29
JL2_7350_7090	0.10	0.23	0.61	1.28	2.03	3.33	5.01
JL2_7240_7350	0.08	0.16	0.45	0.92	1.54	2.51	3.81
JL1_7200_7250	0.14	0.32	0.75	1.46	2.32	3.80	5.70
JL1_6940_7200	0.08	0.23	0.63	1.38	2.21	3.61	5.39
JL6_7440_7430	0.21	0.28	0.46	0.75	1.28	2.40	3.99
JL6_7160_7440	0.11	0.18	0.44	0.82	1.40	2.26	3.32

Table C.24: Runoff Quantiles in Middle James River Segments (ccP90T90 Scenario)

River Segment	Q5 (cfs/sq mi)	Q10 (cfs/sq mi)	Q25 (cfs/sq mi)	Q50 (cfs/sq mi)	Q75 (cfs/sq mi)	Q90 (cfs/sq mi)	Q95 (cfs/sq mi)
JL7_7070_0001	0.00	0.02	0.21	0.72	1.70	4.12	8.19
JL7_6800_7070	0.14	0.20	0.36	0.69	1.30	2.67	4.93
JL1_7170_6800	0.07	0.13	0.29	0.68	1.33	2.79	5.19
JL7_7030_6800	0.12	0.17	0.32	0.66	1.30	3.00	5.74
JL7_7100_7030	0.12	0.17	0.32	0.63	1.23	3.14	6.03
JL3_7020_7100	0.10	0.15	0.30	0.68	1.35	3.38	6.35
JL6_6740_7100	0.16	0.21	0.38	0.69	1.22	2.34	4.20
JL4_6710_6740	0.13	0.19	0.35	0.71	1.26	2.35	3.85
JL4_6520_6710	0.17	0.25	0.49	0.97	1.71	3.28	5.43
JL2_6240_6520	0.02	0.05	0.25	0.70	1.38	2.98	5.89
JL6_6970_6740	0.12	0.18	0.33	0.69	1.33	2.86	5.01
JL2_7120_6970	0.11	0.16	0.30	0.68	1.33	3.22	5.93
JL2_7110_7120	0.11	0.16	0.30	0.68	1.32	3.12	5.63
JL2_6441_6520	0.18	0.26	0.51	0.97	1.67	3.09	5.01
JL2_6440_6441	0.17	0.24	0.49	0.96	1.71	3.13	5.13
JL1_6560_6440	0.16	0.24	0.49	0.95	1.73	3.32	5.51
JL6_6960_6970	0.13	0.18	0.34	0.70	1.25	2.35	3.94
JL1_6910_6960	0.13	0.19	0.36	0.71	1.26	2.38	3.96
JL1_6760_6910	0.18	0.25	0.50	0.96	1.68	3.14	5.12
JL6_6990_6960	0.11	0.16	0.31	0.67	1.29	2.90	5.05
JL6_6890_6990	0.16	0.22	0.43	0.87	1.57	3.07	5.31
JL2_6850_6890	0.16	0.33	0.79	1.49	2.47	4.54	7.53
JL1_6770_6850	0.13	0.28	0.71	1.49	2.45	4.45	7.13
JL6_7150_6890	0.13	0.23	0.52	1.04	1.84	3.73	6.39
JL3_7090_7150	0.17	0.39	0.89	1.67	2.71	4.95	8.13
JL2_7250_7090	0.20	0.40	0.85	1.58	2.52	4.63	7.57
JL1_7190_7250	0.21	0.36	0.74	1.35	2.12	3.85	6.49
JL1_7080_7190	0.14	0.33	0.79	1.59	2.65	4.64	7.35
JL6_7320_7150	0.14	0.22	0.47	0.95	1.71	3.41	5.91
JL6_7430_7320	0.15	0.25	0.50	0.97	1.70	3.12	5.28
JL1_7530_7430	0.14	0.21	0.39	0.77	1.42	2.79	4.91
JL2_7350_7090	0.16	0.35	0.78	1.50	2.39	4.41	7.31
JL2_7240_7350	0.15	0.24	0.62	1.15	1.86	3.21	5.79
JL1_7200_7250	0.22	0.43	0.92	1.67	2.70	4.94	8.06
JL1_6940_7200	0.14	0.33	0.80	1.61	2.59	4.64	7.58
JL6_7440_7430	0.27	0.37	0.60	0.93	1.54	3.15	5.62
JL6_7160_7440	0.18	0.27	0.61	1.05	1.71	2.95	5.20

Table C.25: Runoff Quantiles in Appomattox River Segments (Base Scenario)

River Segment	Q5 (cfs/sq mi)	Q10 (cfs/sq mi)	Q25 (cfs/sq mi)	Q50 (cfs/sq mi)	Q75 (cfs/sq mi)	Q90 (cfs/sq mi)	Q95 (cfs/sq mi)
JA5_7480_0001	0.01	0.03	0.10	0.42	1.00	1.97	2.79
JA2_7570_7480	0.03	0.07	0.17	0.41	0.86	1.77	2.83
JA1_7600_7570	0.04	0.07	0.17	0.40	0.84	1.75	2.80
JA4_7470_7480	0.02	0.04	0.10	0.37	0.90	1.86	2.94
JA2_7410_7470	0.03	0.07	0.17	0.42	0.87	1.78	2.88
JA4_7340_7470	0.01	0.03	0.09	0.36	0.90	1.87	2.92
JA4_7280_7340	0.05	0.09	0.19	0.47	0.95	1.91	3.23
JA1_7640_7280	0.07	0.11	0.22	0.46	0.90	1.67	2.66
JA2_7550_7280	0.08	0.12	0.24	0.50	0.98	1.86	2.98

Table C.26: Runoff Quantiles in Appomattox River Segments (ccP10T10 Scenario)

River Segment	Q5 (cfs/sq mi)	Q10 (cfs/sq mi)	Q25 (cfs/sq mi)	Q50 (cfs/sq mi)	Q75 (cfs/sq mi)	Q90 (cfs/sq mi)	Q95 (cfs/sq mi)
JA5_7480_0001	0.01	0.02	0.07	0.30	0.78	1.58	2.26
JA2_7570_7480	0.02	0.05	0.13	0.32	0.68	1.43	2.21
JA1_7600_7570	0.02	0.05	0.13	0.32	0.69	1.44	2.21
JA4_7470_7480	0.01	0.03	0.07	0.26	0.70	1.51	2.29
JA2_7410_7470	0.02	0.05	0.13	0.32	0.69	1.44	2.24
JA4_7340_7470	0.01	0.02	0.06	0.25	0.71	1.54	2.33
JA4_7280_7340	0.04	0.07	0.16	0.38	0.78	1.59	2.71
JA1_7640_7280	0.05	0.08	0.17	0.35	0.72	1.36	2.03
JA2_7550_7280	0.06	0.09	0.19	0.38	0.79	1.48	2.24

Table C.27: Runoff Quantiles in Appomattox River Segments (ccP50T50 Scenario)

River Segment	Q5 (cfs/sq mi)	Q10 (cfs/sq mi)	Q25 (cfs/sq mi)	Q50 (cfs/sq mi)	Q75 (cfs/sq mi)	Q90 (cfs/sq mi)	Q95 (cfs/sq mi)
JA5_7480_0001	0.02	0.03	0.11	0.45	1.06	2.12	3.09
JA2_7570_7480	0.04	0.07	0.18	0.44	0.91	1.88	3.13
JA1_7600_7570	0.04	0.08	0.18	0.43	0.89	1.87	3.08
JA4_7470_7480	0.02	0.04	0.11	0.40	0.95	1.98	3.18
JA2_7410_7470	0.04	0.08	0.18	0.45	0.92	1.89	3.19
JA4_7340_7470	0.01	0.03	0.09	0.39	0.97	1.99	3.21
JA4_7280_7340	0.06	0.10	0.22	0.52	1.03	2.15	3.94
JA1_7640_7280	0.08	0.12	0.24	0.51	0.95	1.77	2.89
JA2_7550_7280	0.09	0.13	0.26	0.55	1.04	1.97	3.26

Table C.28: Runoff Quantiles in Appomattox River Segments (ccP90T90 Scenario)

River Segment	Q5 (cfs/sq mi)	Q10 (cfs/sq mi)	Q25 (cfs/sq mi)	Q50 (cfs/sq mi)	Q75 (cfs/sq mi)	Q90 (cfs/sq mi)	Q95 (cfs/sq mi)
JA5_7480_0001	0.03	0.06	0.19	0.70	1.49	2.94	4.61
JA2_7570_7480	0.06	0.12	0.27	0.63	1.25	2.71	4.95
JA1_7600_7570	0.07	0.12	0.26	0.62	1.25	2.67	4.91
JA4_7470_7480	0.03	0.07	0.17	0.59	1.30	2.81	5.01
JA2_7410_7470	0.06	0.12	0.27	0.64	1.26	2.72	4.96
JA4_7340_7470	0.03	0.06	0.15	0.58	1.31	2.85	5.02
JA4_7280_7340	0.09	0.15	0.31	0.67	1.36	3.09	5.82
JA1_7640_7280	0.12	0.17	0.35	0.71	1.27	2.52	4.27
JA2_7550_7280	0.13	0.19	0.37	0.75	1.37	2.78	4.82

Appendix D

Percent Differences between Base and Climate Change Runoff Quantiles

Table D.1: Percent Changes in Runoff Quantiles in Shenandoah River Segments (ccP10T10 Scenario)

River Segment	Q5 (%)	Q10 (%)	Q25 (%)	Q50 (%)	Q75 (%)	Q90 (%)	Q95 (%)
PS5_4370_4150	-20.43	-20.85	-19.02	-14.34	-15.64	-15.70	-16.83
PS5_4380_4370	-20.26	-23.62	-24.78	-20.84	-15.74	-15.06	-21.41
PS4_5080_4380	-41.23	-54.89	-40.76	-27.45	-18.84	-17.99	-23.59
PS1_4830_5080	-35.69	-41.09	-33.22	-22.90	-18.27	-15.50	-24.93
PS1_4790_4830	-61.13	-59.43	-43.35	-28.77	-23.50	-18.87	-21.59
PS5_5200_4380	-72.34	-68.21	-48.02	-26.36	-16.65	-14.73	-20.74
PS5_5240_5200	-33.40	-34.07	-28.80	-24.54	-16.07	-18.20	-24.02
PS4_5840_5240	-33.35	-31.95	-29.20	-24.67	-18.48	-20.14	-25.70
PS4_6360_5840	-26.19	-23.06	-25.89	-25.78	-21.51	-18.57	-25.04
PS2_6420_6360	-30.78	-35.50	-32.90	-24.00	-17.87	-20.11	-20.97
PS2_6490_6420	-49.95	-39.35	-26.93	-22.03	-16.38	-17.24	-19.96
PS2_6660_6490	-27.17	-23.72	-19.27	-17.83	-15.95	-13.89	-16.05
PS2_6730_6660	-56.36	-41.09	-28.61	-23.30	-16.53	-17.11	-18.09
PS3_5100_5080	-32.81	-46.02	-34.34	-23.23	-17.53	-17.06	-23.03
PS2_5560_5100	-40.75	-41.59	-33.61	-25.58	-17.91	-18.50	-22.65
PS2_5550_5560	-32.12	-38.24	-51.33	-34.62	-26.04	-21.25	-27.22
PS4_6230_6360	-99.70	-71.08	-35.57	-24.00	-18.66	-19.64	-24.88
PS3_6280_6230	-20.96	-19.52	-20.73	-18.67	-16.98	-18.10	-22.35
PS3_6161_6280	-99.70	-64.19	-35.91	-24.18	-18.70	-17.88	-22.60
PS0_6160_6161	-97.07	-64.65	-31.02	-21.86	-17.74	-20.15	-19.84
PS0_6150_6160	-66.77	-58.25	-40.60	-22.31	-19.56	-18.52	-18.25
PS3_6460_6230	-22.13	-28.48	-27.46	-23.38	-16.93	-18.56	-22.92
PS3_5990_6161	-20.78	-25.23	-35.33	-29.15	-21.75	-19.38	-23.34

Table D.2: Percent Changes in Runoff Quantiles in Shenandoah River Segments (ccP50T50 Scenario)

River Segment	Q5 (%)	Q10 (%)	Q25 (%)	Q50 (%)	Q75 (%)	Q90 (%)	Q95 (%)
PS5_4370_4150	2.69	3.53	3.35	3.93	4.19	9.89	13.54
PS5_4380_4370	1.94	2.56	6.25	5.19	5.84	9.13	9.33
PS4_5080_4380	-6.78	-4.30	2.28	4.22	3.75	6.32	10.33
PS1_4830_5080	2.08	-0.97	3.25	4.63	4.90	8.19	3.61
PS1_4790_4830	-12.79	-2.14	1.31	5.48	4.71	10.18	8.41
PS5_5200_4380	-12.96	-10.67	-2.73	4.11	4.05	9.93	10.04
PS5_5240_5200	1.43	1.97	4.74	4.09	3.42	6.09	12.47
PS4_5840_5240	-3.05	0.77	3.17	3.70	4.23	5.36	9.92
PS4_6360_5840	1.76	2.19	1.90	3.86	4.74	6.79	8.88
PS2_6420_6360	0.85	2.65	0.22	4.02	4.91	6.62	11.06
PS2_6490_6420	-0.58	0.65	2.45	4.59	5.43	7.33	11.01
PS2_6660_6490	-0.10	-0.48	2.16	3.08	3.57	8.76	9.14
PS2_6730_6660	-3.45	1.28	2.16	4.40	5.48	7.01	11.76
PS3_5100_5080	1.70	-2.06	2.78	3.66	3.68	5.08	8.35
PS2_5560_5100	0.54	1.90	2.77	4.16	5.44	8.25	5.63
PS2_5550_5560	0.28	-1.10	0.20	5.00	5.54	6.71	8.12
PS4_6230_6360	-8.79	-0.27	2.56	2.96	5.14	5.96	5.07
PS3_6280_6230	6.52	6.66	6.53	6.55	5.58	10.45	8.10
PS3_6161_6280	-9.63	0.60	0.07	2.40	4.88	6.77	6.19
PS0_6160_6161	-8.75	2.30	1.69	2.94	4.56	2.76	5.46
PS0_6150_6160	2.58	9.24	10.89	6.01	3.27	5.17	5.91
PS3_6460_6230	4.21	3.36	2.84	4.45	5.32	7.42	10.43
PS3_5990_6161	4.60	4.06	1.77	4.62	5.96	4.88	8.87

Table D.3: Percent Changes in Runoff Quantiles in Shenandoah River Segments (ccP90T90 Scenario)

River Segment	Q5 (%)	Q10 (%)	Q25 (%)	Q50 (%)	Q75 (%)	Q90 (%)	Q95 (%)
PS5_4370_4150	26.04	30.00	27.40	25.83	27.24	44.70	58.32
PS5_4380_4370	28.06	34.05	44.42	33.29	29.48	45.95	49.88
PS4_5080_4380	67.16	67.66	51.81	37.03	29.45	37.93	67.42
PS1_4830_5080	71.99	50.10	47.22	34.11	28.92	40.70	48.55
PS1_4790_4830	159.31	84.98	57.68	46.91	32.97	46.26	64.99
PS5_5200_4380	129.93	110.92	87.36	36.32	26.92	41.83	53.31
PS5_5240_5200	30.69	42.35	45.09	33.66	28.55	44.67	72.81
PS4_5840_5240	24.76	35.89	36.86	34.12	30.54	42.58	59.57
PS4_6360_5840	31.25	28.08	36.47	31.81	32.30	43.05	55.61
PS2_6420_6360	42.27	41.10	37.22	28.22	29.27	40.18	54.81
PS2_6490_6420	58.39	41.33	33.91	26.97	27.57	37.70	57.26
PS2_6660_6490	28.30	24.46	22.22	23.93	25.04	35.67	38.82
PS2_6730_6660	62.59	46.13	35.15	27.64	28.33	35.22	61.17
PS3_5100_5080	68.83	56.32	40.99	30.26	28.19	36.96	63.40
PS2_5560_5100	66.60	55.21	41.34	31.82	32.59	41.87	54.79
PS2_5550_5560	44.58	49.18	64.33	43.24	36.93	42.42	52.42
PS4_6230_6360	378.05	74.97	39.75	29.37	31.23	38.31	44.42
PS3_6280_6230	31.82	35.55	34.90	34.17	32.32	44.26	56.13
PS3_6161_6280	261.04	69.73	40.15	27.73	30.28	39.41	45.03
PS0_6160_6161	228.02	72.51	39.23	28.74	29.70	32.36	44.12
PS0_6150_6160	129.47	118.07	75.80	41.70	30.55	37.58	31.18
PS3_6460_6230	30.27	39.13	37.92	28.18	27.45	40.16	57.17
PS3_5990_6161	31.59	37.29	44.35	34.85	33.25	40.74	57.10

Table D.4: Percent Changes in Runoff Quantiles in Mattaponi River Segments (ccP10T10 Scenario)

River Segment	Q5 (%)	Q10 (%)	Q25 (%)	Q50 (%)	Q75 (%)	Q90 (%)	Q95 (%)
YM4_6620_0001	-35.69	-31.21	-28.37	-26.34	-22.64	-21.14	-20.95
YM1_6370_6620	-33.40	-32.44	-29.34	-26.24	-21.99	-19.39	-17.51
YM3_6430_6620	-31.84	-30.28	-28.67	-25.70	-22.34	-17.85	-18.23
YM2_6120_6430	-36.12	-32.54	-29.24	-25.51	-21.11	-20.00	-22.02

Table D.5: Percent Changes in Runoff Quantiles in Mattaponi River Segments (ccP50T50 Scenario)

River Segment	Q5 (%)	Q10 (%)	Q25 (%)	Q50 (%)	Q75 (%)	Q90 (%)	Q95 (%)
YM4_6620_0001	7.24	5.19	6.20	5.45	6.09	8.64	7.44
YM1_6370_6620	5.94	6.89	6.32	6.44	6.41	7.38	7.77
YM3_6430_6620	7.70	6.79	5.63	6.66	6.75	9.12	8.11
YM2_6120_6430	5.58	4.41	4.61	6.63	5.28	6.13	13.68

Table D.6: Percent Changes in Runoff Quantiles in Mattaponi River Segments (ccP90T90 Scenario)

River Segment	Q5 (%)	Q10 (%)	Q25 (%)	Q50 (%)	Q75 (%)	Q90 (%)	Q95 (%)
YM4_6620_0001	73.97	65.25	53.32	49.87	49.73	51.89	55.19
YM1_6370_6620	69.35	63.83	55.28	49.19	48.86	49.35	60.76
YM3_6430_6620	70.62	60.25	55.61	47.92	45.73	50.24	61.11
YM2_6120_6430	74.03	61.48	53.65	49.29	38.11	46.89	67.61

Table D.7: Percent Changes in Runoff Quantiles in Pamunkey River Segments (ccP10T10 Scenario)

River Segment	Q5 (%)	Q10 (%)	Q25 (%)	Q50 (%)	Q75 (%)	Q90 (%)	Q95 (%)
YP4_6750_0001	-29.84	-27.75	-25.85	-23.92	-20.34	-19.38	-18.86
YP4_6720_6750	-28.92	-29.27	-25.72	-24.26	-20.81	-18.62	-16.03
YP3_6670_6720	-31.71	-29.52	-27.90	-25.02	-21.51	-17.08	-17.59
YP1_6680_6670	-31.33	-31.51	-28.22	-25.57	-21.55	-19.19	-18.25
YP1_6570_6680	-30.37	-30.01	-27.35	-25.27	-22.72	-22.19	-22.90
YP3_6690_6720	-29.80	-28.43	-26.16	-24.33	-20.86	-18.99	-16.92
YP3_6470_6690	-28.70	-27.18	-26.81	-24.90	-22.44	-20.81	-25.26
YP3_6700_6670	-28.12	-28.68	-26.27	-23.76	-20.42	-13.30	-15.52
YP3_6330_6700	-34.96	-31.33	-29.35	-25.89	-21.86	-19.94	-19.67
YP2_6390_6330	-31.75	-27.86	-27.12	-24.66	-21.22	-19.65	-26.04

Table D.8: Percent Changes in Runoff Quantiles in Pamunkey River Segments (ccP50T50 Scenario)

River Segment	Q5 (%)	Q10 (%)	Q25 (%)	Q50 (%)	Q75 (%)	Q90 (%)	Q95 (%)
YP4_6750_0001	6.49	7.76	6.32	7.16	6.23	6.64	10.06
YP4_6720_6750	8.71	8.73	7.01	7.24	7.29	7.40	8.09
YP3_6670_6720	7.04	7.38	6.02	6.73	7.18	8.44	8.75
YP1_6680_6670	8.84	8.21	7.32	8.17	7.63	6.99	7.44
YP1_6570_6680	7.07	7.43	6.86	7.98	7.70	7.80	10.89
YP3_6690_6720	8.81	9.07	7.42	8.09	8.30	7.58	8.99
YP3_6470_6690	6.94	5.87	6.01	6.89	6.47	9.06	13.72
YP3_6700_6670	6.82	6.70	7.39	7.15	6.08	7.35	6.67
YP3_6330_6700	6.46	6.46	5.56	6.94	6.57	6.05	11.92
YP2_6390_6330	8.19	5.49	6.22	7.01	6.70	8.30	8.22

Table D.9: Percent Changes in Runoff Quantiles in Pamunkey River Segments (ccP90T90 Scenario)

River Segment	Q5 (%)	Q10 (%)	Q25 (%)	Q50 (%)	Q75 (%)	Q90 (%)	Q95 (%)
YP4_6750_0001	65.31	58.39	52.60	49.93	49.20	48.20	57.53
YP4_6720_6750	68.20	64.31	54.12	51.88	48.36	47.80	55.18
YP3_6670_6720	66.22	61.67	54.66	48.67	47.13	48.48	60.04
YP1_6680_6670	76.44	69.91	60.46	58.23	53.02	49.46	54.90
YP1_6570_6680	66.93	61.81	55.94	54.54	51.88	50.90	72.28
YP3_6690_6720	72.21	64.68	57.36	55.02	51.24	49.70	59.38
YP3_6470_6690	59.13	54.74	50.20	48.32	43.72	51.88	67.58
YP3_6700_6670	63.82	58.61	55.03	53.06	44.21	43.93	45.20
YP3_6330_6700	71.85	64.03	55.84	51.82	46.46	49.03	70.59
YP2_6390_6330	61.10	49.34	48.72	43.91	38.60	54.60	66.14

Table D.10: Percent Changes in Runoff Quantiles in Rappahannock River Segments (ccP10T10 Scenario)

River Segment	Q5 (%)	Q10 (%)	Q25 (%)	Q50 (%)	Q75 (%)	Q90 (%)	Q95 (%)
RU5_6030_0001	-33.47	-29.56	-28.58	-24.41	-19.24	-19.20	-17.44
RU4_5640_6030	-30.77	-28.28	-25.65	-20.40	-16.80	-17.89	-19.14
RU2_5220_5640	-36.55	-36.33	-27.28	-20.32	-16.17	-17.63	-21.50
RU4_6040_6030	-33.06	-29.68	-27.27	-23.19	-19.07	-18.44	-21.08
RU3_6170_6040	-30.47	-27.93	-25.50	-22.34	-18.75	-16.44	-23.04
RU2_6200_6170	-31.43	-27.65	-22.87	-19.80	-16.85	-16.18	-18.83
RU2_5940_6200	-31.20	-26.24	-23.50	-19.94	-17.08	-15.98	-21.11
RU3_5610_5640	-34.79	-30.87	-26.44	-21.54	-17.16	-14.37	-19.82
RU2_5500_5610	-48.39	-44.92	-27.70	-16.61	-14.19	-14.75	-19.01
RU2_6220_6170	-30.16	-28.32	-24.25	-20.23	-18.79	-17.56	-24.55
RU2_6090_6220	-25.84	-23.06	-20.93	-17.52	-17.11	-18.30	-23.21
RU2_5810_5610	-32.92	-30.66	-25.80	-18.75	-15.80	-16.36	-20.31

Table D.11: Percent Changes in Runoff Quantiles in Rappahannock River Segments (ccP50T50 Scenario)

River Segment	Q5 (%)	Q10 (%)	Q25 (%)	Q50 (%)	Q75 (%)	Q90 (%)	Q95 (%)
RU5_6030_0001	3.57	3.25	3.97	5.16	3.10	6.47	9.26
RU4_5640_6030	9.87	6.86	7.17	6.65	6.70	6.17	10.62
RU2_5220_5640	9.10	3.18	5.86	5.39	6.58	8.15	9.68
RU4_6040_6030	9.59	9.41	7.31	8.13	7.23	5.21	10.37
RU3_6170_6040	12.13	9.78	6.84	7.71	7.88	7.44	11.92
RU2_6200_6170	6.44	6.56	6.47	5.78	6.78	5.49	8.21
RU2_5940_6200	5.40	5.24	6.53	5.58	7.11	6.01	7.39
RU3_5610_5640	11.69	10.46	8.29	7.47	7.27	7.71	9.27
RU2_5500_5610	5.40	0.93	4.89	4.75	7.32	6.23	12.21
RU2_6220_6170	6.76	5.85	6.80	7.25	6.29	7.68	8.05
RU2_6090_6220	4.89	4.66	6.20	5.45	5.23	5.07	7.42
RU2_5810_5610	5.56	3.70	6.06	5.17	7.48	6.13	9.58

Table D.12: Percent Changes in Runoff Quantiles in Rappahannock River Segments (ccP90T90 Scenario)

River Segment	Q5 (%)	Q10 (%)	Q25 (%)	Q50 (%)	Q75 (%)	Q90 (%)	Q95 (%)
RU5_6030_0001	58.50	49.90	47.65	41.62	32.70	46.59	56.53
RU4_5640_6030	63.74	50.56	47.19	34.83	33.35	48.44	57.60
RU2_5220_5640	75.03	56.51	43.34	33.24	36.08	45.34	53.63
RU4_6040_6030	63.42	58.10	47.49	39.44	35.98	43.10	60.23
RU3_6170_6040	63.34	59.35	46.63	39.43	36.20	44.10	63.89
RU2_6200_6170	43.35	34.71	37.15	27.08	29.65	35.15	55.57
RU2_5940_6200	40.79	33.93	36.70	27.54	31.03	34.67	50.03
RU3_5610_5640	67.54	61.51	46.06	35.46	34.28	40.14	55.09
RU2_5500_5610	98.88	61.54	40.03	27.23	28.25	38.36	56.89
RU2_6220_6170	47.57	39.62	38.95	33.33	33.66	45.60	54.45
RU2_6090_6220	35.39	29.36	32.34	25.68	26.04	38.76	55.71
RU2_5810_5610	52.87	45.31	37.65	27.14	30.41	37.35	52.30

Table D.13: Percent Changes in Runoff Quantiles in Upper James River Segments (ccP10T10 Scenario)

River Segment	Q5 (%)	Q10 (%)	Q25 (%)	Q50 (%)	Q75 (%)	Q90 (%)	Q95 (%)
JU5_7420_7160	-22.01	-23.44	-24.87	-20.96	-16.86	-19.28	-24.79
JU5_7500_7420	-21.70	-21.91	-19.95	-20.02	-15.66	-18.63	-23.80
JU1_7560_7500	-23.53	-22.37	-19.51	-20.31	-16.15	-18.37	-23.71
JU1_7750_7560	-26.67	-23.40	-21.02	-21.71	-16.89	-18.06	-21.98
JU5_7510_7500	-23.88	-23.67	-20.72	-20.25	-15.99	-18.45	-22.67
JU3_7400_7510	-26.11	-24.89	-22.39	-21.81	-15.99	-18.90	-21.33
JU3_7490_7400	-29.58	-28.30	-29.03	-22.15	-13.70	-17.96	-22.04
JU1_7630_7490	-59.40	-56.92	-33.38	-22.14	-14.25	-15.77	-21.22
JU5_7300_7510	-26.74	-25.46	-23.17	-20.76	-16.14	-19.00	-22.02
JU3_6650_7300	-41.49	-68.27	-47.94	-28.56	-19.13	-17.81	-23.51
JU1_6300_6650	-16.35	-19.78	-23.13	-18.03	-15.52	-19.16	-19.42
JU1_7690_7490	-55.18	-46.10	-35.68	-24.55	-13.86	-15.72	-21.76
JU4_7000_7300	-20.02	-61.33	-43.16	-28.17	-16.79	-20.47	-23.66
JU2_7360_7000	-99.86	-72.81	-58.16	-28.56	-17.51	-19.14	-23.89
JU2_7450_7360	-48.07	-33.70	-32.20	-25.17	-15.46	-18.18	-23.96
JU1_6340_6650	-20.65	-34.42	-35.30	-19.15	-14.50	-18.67	-19.40
JU4_7330_7000	-10.60	-11.93	-31.67	-21.64	-14.49	-18.35	-17.54
JU2_7140_7330	-40.90	-34.22	-35.40	-27.73	-17.21	-19.25	-22.92
JU3_6950_7330	-31.39	-60.83	-39.39	-28.46	-16.46	-19.96	-24.04
JU3_6900_6950	-64.59	-88.83	-47.94	-33.12	-19.08	-17.76	-23.20
JU2_6810_6900	-60.12	-91.80	-55.12	-29.19	-18.56	-16.66	-24.75
JU2_6600_6810	-49.34	-81.19	-53.40	-28.22	-18.55	-16.54	-25.56
JU1_6590_6600	-55.76	-86.37	-53.07	-28.35	-18.96	-16.37	-25.64
JU1_6290_6590	-92.23	-58.42	-36.50	-18.95	-14.71	-18.54	-21.10
JU3_6380_6900	-65.44	-64.79	-34.27	-22.26	-17.11	-20.52	-18.91
JU4_7380_7160	-51.06	-47.41	-28.10	-21.46	-16.78	-21.08	-25.84
JU2_7180_7380	-20.51	-22.70	-25.56	-20.32	-15.86	-20.37	-25.98
JU4_7260_7380	-28.69	-36.54	-27.62	-20.80	-16.11	-19.46	-23.18
JU1_6880_7260	-47.38	-42.44	-25.97	-21.57	-16.16	-20.75	-24.93
JU3_6790_7260	-37.16	-37.91	-25.12	-21.25	-15.70	-21.17	-24.92
JU3_6640_6790	-64.63	-54.29	-32.32	-28.10	-17.84	-19.62	-25.87
JU2_6410_6640	-60.88	-57.30	-53.88	-31.33	-20.03	-19.02	-26.55

Table D.14: Percent Changes in Runoff Quantiles in Upper James River Segments (ccP50T50 Scenario)

River Segment	Q5 (%)	Q10 (%)	Q25 (%)	Q50 (%)	Q75 (%)	Q90 (%)	Q95 (%)
JU5_7420_7160	1.28	3.32	5.01	5.36	6.09	7.67	9.10
JU5_7500_7420	1.76	3.75	5.79	6.34	5.95	9.22	7.69
JU1_7560_7500	1.70	3.92	6.26	6.79	5.67	8.68	6.24
JU1_7750_7560	2.21	3.04	6.05	6.55	6.30	5.69	5.79
JU5_7510_7500	2.42	3.26	5.64	7.16	5.97	8.57	7.35
JU3_7400_7510	1.54	3.19	5.35	6.91	7.12	5.71	9.38
JU3_7490_7400	1.17	2.25	2.75	5.80	5.71	5.38	5.61
JU1_7630_7490	-1.60	-7.14	0.89	5.05	4.80	5.30	4.15
JU5_7300_7510	0.66	2.93	5.15	6.89	7.29	5.92	8.72
JU3_6650_7300	-3.73	-16.31	-1.10	3.99	4.82	6.69	6.00
JU1_6300_6650	1.99	1.09	2.04	4.36	4.37	5.50	5.61
JU1_7690_7490	-1.60	-3.14	-0.06	4.32	4.89	5.99	5.67
JU4_7000_7300	-4.47	-10.67	-3.76	2.39	3.83	6.11	5.50
JU2_7360_7000	-37.93	-8.12	-7.40	3.01	3.39	4.16	6.77
JU2_7450_7360	-2.91	-2.51	-0.36	4.20	3.46	4.67	5.93
JU1_6340_6650	0.78	-2.72	0.22	4.83	6.04	4.53	5.13
JU4_7330_7000	0.23	0.15	-2.13	2.81	3.13	6.50	6.26
JU2_7140_7330	-1.87	-1.91	-3.57	3.59	3.76	5.12	6.35
JU3_6950_7330	-4.32	-10.23	-1.10	3.02	4.40	8.35	3.53
JU3_6900_6950	-30.09	-21.50	0.14	4.01	4.19	8.32	4.46
JU2_6810_6900	-23.45	-23.69	-0.66	5.56	5.03	8.51	8.84
JU2_6600_6810	-10.05	-20.73	0.00	4.34	5.59	7.27	7.62
JU1_6590_6600	-13.76	-21.38	-0.34	4.82	5.46	7.38	6.73
JU1_6290_6590	-14.61	-11.06	-0.56	4.76	5.69	4.31	6.72
JU3_6380_6900	-15.37	-5.93	0.96	3.72	4.22	5.86	7.19
JU4_7380_7160	-6.49	-1.18	0.77	5.15	5.15	7.11	6.15
JU2_7180_7380	1.06	4.17	4.50	5.15	6.77	9.73	8.26
JU4_7260_7380	-2.47	-0.21	0.86	4.00	5.29	7.50	10.22
JU1_6880_7260	-0.33	2.62	1.88	5.78	5.31	8.36	7.29
JU3_6790_7260	-2.33	0.25	2.03	4.68	5.66	6.47	7.69
JU3_6640_6790	-12.09	-4.21	-0.19	4.96	4.81	10.16	5.57
JU2_6410_6640	-12.91	-3.14	-2.94	6.03	6.65	6.88	6.38

Table D.15: Percent Changes in Runoff Quantiles in Upper James River Segments (ccP90T90 Scenario)

River Segment	Q5 (%)	Q10 (%)	Q25 (%)	Q50 (%)	Q75 (%)	Q90 (%)	Q95 (%)
JU5_7420_7160	28.91	29.40	30.56	30.48	31.85	48.56	56.59
JU5_7500_7420	25.50	27.74	28.96	33.50	29.49	47.11	51.11
JU1_7560_7500	25.88	28.05	29.32	34.23	28.69	46.36	50.22
JU1_7750_7560	33.66	30.33	33.31	39.85	32.32	40.44	50.66
JU5_7510_7500	27.62	27.94	29.89	35.28	29.52	45.87	52.00
JU3_7400_7510	27.66	30.61	30.25	34.85	33.11	44.24	56.37
JU3_7490_7400	36.46	37.56	38.28	31.39	30.11	37.99	50.93
JU1_7630_7490	95.25	150.17	40.27	30.63	25.64	37.22	45.51
JU5_7300_7510	25.84	29.67	29.75	34.51	31.52	45.90	57.67
JU3_6650_7300	62.11	75.26	43.65	33.08	27.25	42.68	52.68
JU1_6300_6650	18.33	19.34	24.38	23.54	25.10	35.62	42.29
JU1_7690_7490	69.89	91.35	43.59	33.98	26.36	40.12	48.83
JU4_7000_7300	56.16	75.17	50.11	28.74	28.45	43.16	48.09
JU2_7360_7000	921.00	91.29	57.92	31.05	27.95	45.05	48.95
JU2_7450_7360	43.65	32.70	37.06	32.28	27.08	38.18	48.12
JU1_6340_6650	24.32	33.07	32.13	22.99	28.00	34.60	40.07
JU4_7330_7000	9.85	12.88	34.36	24.96	25.75	38.83	49.62
JU2_7140_7330	37.59	31.90	44.12	31.65	28.26	43.40	53.55
JU3_6950_7330	57.07	69.49	46.03	29.44	28.68	43.15	45.56
JU3_6900_6950	327.58	104.33	50.84	34.46	27.90	46.83	51.86
JU2_6810_6900	397.96	100.62	53.75	36.23	28.28	45.04	55.69
JU2_6600_6810	109.87	87.66	53.33	34.52	28.11	44.10	53.55
JU1_6590_6600	172.42	87.10	54.36	34.13	27.84	44.43	52.88
JU1_6290_6590	99.77	62.37	31.26	22.28	26.90	35.27	39.16
JU3_6380_6900	110.58	53.20	32.73	25.96	26.32	41.23	42.50
JU4_7380_7160	64.21	59.33	30.90	27.96	28.54	42.97	47.73
JU2_7180_7380	29.02	32.12	28.88	27.37	29.49	46.76	55.42
JU4_7260_7380	40.04	39.78	26.17	25.90	28.81	46.42	49.49
JU1_6880_7260	52.48	52.38	30.12	28.83	30.21	42.46	49.28
JU3_6790_7260	42.76	46.67	28.17	26.52	28.39	42.89	46.62
JU3_6640_6790	68.89	60.80	37.49	32.29	29.73	48.53	50.30
JU2_6410_6640	59.87	62.80	58.34	35.84	29.60	43.16	51.47

Table D.16: Percent Changes in Runoff Quantiles in Middle James River Segments (ccP10T10 Scenario)

River Segment	Q5 (%)	Q10 (%)	Q25 (%)	Q50 (%)	Q75 (%)	Q90 (%)	Q95 (%)
JL7_7070_0001	-43.65	-52.34	-36.50	-21.57	-15.22	-11.01	-13.77
JL7_6800_7070	-25.92	-25.04	-24.12	-22.64	-18.37	-17.90	-21.93
JL1_7170_6800	-37.26	-31.14	-28.18	-24.10	-19.43	-19.91	-26.08
JL7_7030_6800	-26.51	-23.78	-24.38	-22.76	-19.33	-20.10	-27.58
JL7_7100_7030	-22.02	-21.61	-21.57	-20.41	-18.27	-22.40	-26.05
JL3_7020_7100	-28.30	-23.48	-23.29	-22.86	-19.79	-23.32	-26.83
JL6_6740_7100	-25.97	-26.21	-24.44	-23.49	-21.07	-19.98	-23.41
JL4_6710_6740	-28.88	-28.78	-24.95	-24.33	-19.61	-19.64	-19.93
JL4_6520_6710	-31.81	-29.25	-26.63	-22.79	-21.34	-18.50	-21.40
JL2_6240_6520	-64.22	-47.01	-43.54	-25.91	-20.22	-21.20	-25.91
JL6_6970_6740	-29.45	-26.51	-24.56	-24.29	-19.56	-21.14	-24.16
JL2_7120_6970	-31.08	-26.51	-26.07	-24.40	-19.89	-24.42	-26.77
JL2_7110_7120	-31.60	-26.92	-25.07	-24.71	-20.45	-25.24	-25.74
JL2_6441_6520	-30.15	-27.81	-24.56	-22.54	-19.71	-18.23	-21.51
JL2_6440_6441	-34.12	-28.90	-26.96	-25.82	-22.60	-19.32	-22.25
JL1_6560_6440	-31.31	-28.00	-24.97	-23.41	-19.89	-19.01	-18.57
JL6_6960_6970	-30.06	-29.19	-25.41	-24.56	-20.35	-20.04	-20.26
JL1_6910_6960	-27.85	-28.08	-24.34	-23.99	-18.92	-19.13	-19.70
JL1_6760_6910	-31.52	-28.40	-26.03	-23.78	-21.47	-19.09	-21.75
JL6_6990_6960	-30.79	-26.64	-25.11	-24.12	-19.99	-21.90	-24.26
JL6_6890_6990	-31.65	-28.79	-25.06	-24.06	-21.61	-20.38	-25.75
JL2_6850_6890	-40.72	-40.09	-23.49	-14.32	-13.82	-17.20	-21.23
JL1_6770_6850	-40.71	-36.90	-24.38	-16.18	-14.38	-14.96	-20.47
JL6_7150_6890	-34.48	-32.55	-23.40	-16.82	-16.74	-20.88	-23.71
JL3_7090_7150	-40.88	-39.65	-21.85	-12.30	-12.18	-16.02	-20.66
JL2_7250_7090	-36.49	-35.97	-21.07	-13.50	-12.67	-15.20	-22.02
JL1_7190_7250	-35.11	-29.47	-24.12	-16.26	-13.74	-14.83	-20.49
JL1_7080_7190	-39.26	-34.59	-21.19	-13.70	-13.23	-17.13	-19.60
JL6_7320_7150	-32.21	-29.76	-22.75	-19.81	-17.88	-20.96	-22.51
JL6_7430_7320	-30.24	-27.77	-24.03	-20.32	-17.44	-16.95	-21.21
JL1_7530_7430	-24.77	-22.07	-21.42	-21.38	-17.49	-19.18	-22.55
JL2_7350_7090	-45.55	-37.52	-23.94	-15.45	-13.05	-15.06	-22.02
JL2_7240_7350	-36.37	-32.11	-28.71	-19.27	-14.32	-15.00	-17.56
JL1_7200_7250	-35.61	-36.58	-19.86	-11.63	-11.88	-14.91	-20.29
JL1_6940_7200	-40.44	-38.88	-23.55	-14.14	-13.51	-16.34	-20.00
JL6_7440_7430	-15.23	-22.50	-22.78	-18.46	-14.35	-16.37	-18.28
JL6_7160_7440	-23.39	-25.01	-29.43	-20.22	-15.13	-15.46	-20.24

Table D.17: Percent Changes in Runoff Quantiles in Middle James River Segments (ccP50T50 Scenario)

River Segment	Q5 (%)	Q10 (%)	Q25 (%)	Q50 (%)	Q75 (%)	Q90 (%)	Q95 (%)
JL7_7070_0001	18.46	13.90	0.41	4.94	5.17	7.82	9.73
JL7_6800_7070	8.27	7.48	7.82	6.39	5.06	7.13	10.37
JL1_7170_6800	11.14	10.65	8.95	8.01	7.16	8.15	6.27
JL7_7030_6800	6.60	8.35	6.82	6.96	5.89	8.25	10.03
JL7_7100_7030	7.19	6.64	6.23	5.67	6.31	7.71	8.83
JL3_7020_7100	5.55	5.80	4.94	5.61	5.75	6.90	7.81
JL6_6740_7100	9.09	8.24	8.43	8.95	7.50	6.74	11.97
JL4_6710_6740	11.83	9.78	7.84	9.60	8.17	6.87	7.12
JL4_6520_6710	4.69	4.82	6.24	7.26	6.57	6.15	10.31
JL2_6240_6520	17.19	7.39	5.22	7.42	5.96	7.08	12.07
JL6_6970_6740	8.81	7.18	6.75	7.43	8.35	6.89	11.75
JL2_7120_6970	6.24	5.70	4.87	6.84	5.82	5.13	10.10
JL2_7110_7120	5.43	4.88	5.44	7.07	6.71	5.34	10.74
JL2_6441_6520	7.68	5.42	6.60	7.72	7.75	6.89	9.43
JL2_6440_6441	4.50	4.44	5.71	7.71	6.65	5.36	5.38
JL1_6560_6440	4.34	5.12	6.56	6.68	6.66	5.82	9.83
JL6_6960_6970	10.29	9.86	7.93	9.37	8.79	7.92	8.14
JL1_6910_6960	12.64	9.92	8.28	9.05	8.54	7.95	7.86
JL1_6760_6910	4.78	6.01	5.53	7.88	7.77	7.05	8.34
JL6_6990_6960	7.28	6.35	6.09	7.66	7.57	6.03	12.31
JL6_6890_6990	6.23	6.12	5.77	6.39	7.02	6.85	7.79
JL2_6850_6890	4.65	3.74	4.43	5.44	4.17	5.03	9.41
JL1_6770_6850	2.74	2.47	4.27	5.51	4.21	6.92	7.66
JL6_7150_6890	3.72	4.12	4.27	6.40	5.47	6.51	8.48
JL3_7090_7150	3.45	1.36	4.72	4.98	4.13	6.67	7.12
JL2_7250_7090	4.47	1.75	5.22	5.21	4.14	6.23	7.36
JL1_7190_7250	3.61	5.15	4.13	6.35	6.13	7.21	11.64
JL1_7080_7190	2.85	1.35	5.95	6.30	4.38	5.43	8.59
JL6_7320_7150	3.82	3.98	4.84	6.40	6.48	8.11	8.90
JL6_7430_7320	5.14	6.54	4.68	6.87	6.15	9.86	10.13
JL1_7530_7430	10.97	8.49	7.60	8.43	6.94	8.66	11.69
JL2_7350_7090	2.13	2.45	4.23	5.28	4.77	6.77	7.87
JL2_7240_7350	5.52	9.09	6.22	8.12	6.22	6.10	12.26
JL1_7200_7250	5.33	2.13	3.79	5.35	4.41	7.29	7.93
JL1_6940_7200	4.01	2.84	3.95	5.95	3.70	5.57	9.92
JL6_7440_7430	4.99	6.42	6.72	7.42	6.41	9.44	17.30
JL6_7160_7440	7.35	7.85	6.26	8.45	7.35	7.65	8.69

Table D.18: Percent Changes in Runoff Quantiles in Middle James River Segments (ccP90T90 Scenario)

River Segment	Q5 (%)	Q10 (%)	Q25 (%)	Q50 (%)	Q75 (%)	Q90 (%)	Q95 (%)
JL7_7070_0001	153.95	227.99	59.00	37.31	28.98	33.89	42.96
JL7_6800_7070	56.18	58.18	52.27	42.23	40.35	49.77	66.36
JL1_7170_6800	103.87	79.07	58.09	42.41	42.93	51.67	61.49
JL7_7030_6800	52.40	52.95	45.71	38.05	38.19	58.81	67.19
JL7_7100_7030	45.82	42.16	40.00	32.70	35.18	58.89	63.79
JL3_7020_7100	48.01	44.95	41.54	36.78	34.05	57.00	67.01
JL6_6740_7100	58.97	59.52	53.34	48.59	45.72	49.89	73.16
JL4_6710_6740	72.53	70.35	57.01	50.58	46.38	45.98	58.97
JL4_6520_6710	46.74	41.84	41.45	36.51	32.12	44.00	61.60
JL2_6240_6520	130.17	93.36	69.30	39.07	33.06	44.29	65.08
JL6_6970_6740	63.37	53.79	48.86	42.48	42.03	55.10	66.30
JL2_7120_6970	55.25	46.89	43.44	39.01	33.86	50.92	67.11
JL2_7110_7120	55.09	46.43	44.23	41.26	33.56	51.80	68.03
JL2_6441_6520	50.11	42.61	42.05	35.89	35.54	46.59	62.33
JL2_6440_6441	48.41	44.00	43.83	40.83	37.64	44.02	58.09
JL1_6560_6440	41.97	40.68	42.92	36.62	36.34	42.47	62.27
JL6_6960_6970	73.54	69.65	56.79	51.95	46.81	47.76	66.12
JL1_6910_6960	70.50	68.74	56.74	48.76	45.85	47.88	62.31
JL1_6760_6910	51.07	45.46	42.86	38.38	36.23	46.72	61.94
JL6_6990_6960	60.99	49.83	46.81	43.02	37.46	54.09	64.73
JL6_6890_6990	50.69	43.11	41.20	36.59	34.77	45.63	63.38
JL2_6850_6890	80.63	45.53	30.78	22.61	23.48	37.34	55.36
JL1_6770_6850	76.48	46.78	37.89	24.67	23.12	39.30	51.66
JL6_7150_6890	52.40	46.80	34.56	29.18	29.03	43.62	61.66
JL3_7090_7150	87.29	45.62	28.35	20.39	20.96	37.66	51.94
JL2_7250_7090	58.45	42.27	30.75	22.27	22.64	39.76	52.45
JL1_7190_7250	61.16	46.11	34.66	28.75	26.38	42.13	62.70
JL1_7080_7190	64.28	43.27	32.77	24.76	24.67	35.99	49.30
JL6_7320_7150	50.46	44.40	38.71	31.89	32.44	48.09	69.75
JL6_7430_7320	56.35	47.54	39.21	37.22	32.89	45.67	64.81
JL1_7530_7430	63.56	54.95	47.68	43.49	35.29	47.12	66.74
JL2_7350_7090	62.33	52.37	32.53	23.78	23.10	41.29	57.46
JL2_7240_7350	94.13	68.08	46.65	34.63	27.98	35.96	70.65
JL1_7200_7250	61.64	39.38	27.05	20.47	21.29	39.56	52.70
JL1_6940_7200	84.80	48.49	32.84	23.51	21.16	35.70	54.62
JL6_7440_7430	35.90	40.87	39.49	33.77	28.39	43.24	65.10
JL6_7160_7440	70.41	60.17	47.44	38.96	30.72	40.35	70.36

Table D.19: Percent Changes in Runoff Quantiles in Appomattox River Segments (ccP10T10 Scenario)

River Segment	Q5 (%)	Q10 (%)	Q25 (%)	Q50 (%)	Q75 (%)	Q90 (%)	Q95 (%)
JA5_7480_0001	-36.20	-33.09	-31.42	-30.05	-22.14	-19.52	-19.27
JA2_7570_7480	-32.45	-29.93	-23.78	-23.13	-20.91	-19.22	-21.74
JA1_7600_7570	-54.48	-35.40	-26.40	-19.56	-18.49	-17.48	-21.06
JA4_7470_7480	-35.87	-30.57	-26.70	-28.78	-21.96	-18.41	-21.96
JA2_7410_7470	-30.97	-28.24	-23.62	-23.04	-20.72	-18.94	-22.12
JA4_7340_7470	-39.82	-34.25	-29.50	-31.54	-21.98	-17.83	-20.25
JA4_7280_7340	-14.81	-16.91	-18.54	-19.74	-17.56	-16.99	-16.18
JA1_7640_7280	-25.70	-25.77	-24.38	-24.45	-19.82	-18.74	-23.74
JA2_7550_7280	-26.92	-24.46	-23.61	-24.14	-19.26	-20.38	-24.90

Table D.20: Percent Changes in Runoff Quantiles in Appomattox River Segments (ccP50T50 Scenario)

River Segment	Q5 (%)	Q10 (%)	Q25 (%)	Q50 (%)	Q75 (%)	Q90 (%)	Q95 (%)
JA5_7480_0001	10.82	7.34	7.62	6.19	5.85	7.72	10.50
JA2_7570_7480	12.08	7.25	8.42	7.39	6.42	6.38	10.85
JA1_7600_7570	8.15	7.06	6.97	7.10	6.09	6.54	10.05
JA4_7470_7480	11.50	7.17	6.97	7.67	6.14	6.75	8.40
JA2_7410_7470	12.62	8.24	8.30	6.95	6.09	6.33	10.71
JA4_7340_7470	10.97	9.40	7.33	7.03	6.97	6.54	9.76
JA4_7280_7340	28.28	18.52	13.75	10.06	8.46	12.53	21.86
JA1_7640_7280	7.48	7.61	7.39	9.84	6.10	5.41	8.48
JA2_7550_7280	7.47	7.47	7.19	8.16	5.96	5.84	9.42

Table D.21: Percent Changes in Runoff Quantiles in Appomattox River Segments (ccP90T90 Scenario)

River Segment	Q5 (%)	Q10 (%)	Q25 (%)	Q50 (%)	Q75 (%)	Q90 (%)	Q95 (%)
JA5_7480_0001	107.87	93.19	83.82	67.03	47.96	49.27	65.21
JA2_7570_7480	92.57	71.84	61.50	53.18	45.19	52.83	75.26
JA1_7600_7570	71.28	66.26	55.38	53.83	48.32	52.47	75.51
JA4_7470_7480	101.69	74.71	69.02	61.07	44.53	51.15	70.55
JA2_7410_7470	89.48	73.13	60.73	51.08	44.92	53.11	72.19
JA4_7340_7470	107.54	86.06	71.95	61.31	44.70	52.50	71.67
JA4_7280_7340	89.90	70.00	58.37	42.42	42.85	61.65	80.13
JA1_7640_7280	70.50	59.69	56.86	53.86	40.84	50.42	60.52
JA2_7550_7280	62.31	54.98	50.49	47.57	38.84	48.86	61.67

Appendix E

Streamflow Metrics

Table E.1: Flow Metrics in Shenandoah River Segments (Base Scenario)

River Segment	Overall Mean (cfs)	30-Day Low Flow (cfs)	90-Day Low Flow (cfs)	August Low Flow (cfs)	September 10% Flow (cfs)
PS5_4370_4150	3213.488	305.979	469.050	2064.614	532.932
PS5_4380_4370	3187.583	295.998	458.397	2028.716	504.054
PS4_5080_4380	1014.737	16.375	55.325	480.068	55.567
PS1_4830_5080	136.233	0.728	3.190	51.796	1.708
PS1_4790_4830	85.724	0.443	2.015	31.521	1.216
PS5_5200_4380	1850.269	228.114	348.430	1185.070	354.335
PS5_5240_5200	1809.814	221.221	335.460	1138.592	340.272
PS4_5840_5240	1536.371	165.714	250.491	853.705	232.833
PS4_6360_5840	1214.716	124.214	181.137	593.282	149.327
PS2_6420_6360	319.331	30.760	50.261	174.012	42.260
PS2_6490_6420	292.924	28.710	46.776	158.185	40.228
PS2_6660_6490	200.139	15.702	28.771	102.005	22.907
PS2_6730_6660	162.422	6.398	15.931	78.364	11.223
PS3_5100_5080	783.832	19.847	55.604	349.457	48.257
PS2_5560_5100	498.949	6.386	30.300	164.934	13.206
PS2_5550_5560	192.697	2.462	7.086	47.177	4.044
PS4_6230_6360	870.690	86.629	125.194	389.196	103.692
PS3_6280_6230	425.962	39.823	55.415	167.611	49.229
PS3_6161_6280	386.293	23.703	39.067	130.888	29.429
PS0_6160_6161	49.076	0.233	5.625	7.397	0.153
PS0_6150_6160	12.355	0.019	1.076	0.310	0.009
PS3_6460_6230	414.433	41.351	62.911	191.003	48.331
PS3_5990_6161	312.996	10.433	18.031	97.162	14.316

Table E.2: Flow Metrics in Shenandoah River Segments (ccP10T10 Scenario)

River Segment	Overall Mean (cfs)	30-Day Low Flow (cfs)	90-Day Low Flow (cfs)	August Low Flow (cfs)	September 10% Flow (cfs)
PS5_4370_4150	1696.052	145.802	259.809	1270.713	241.614
PS5_4380_4370	1673.866	136.452	249.460	1253.708	229.349
PS4_5080_4380	761.893	8.889	32.666	396.791	35.637
PS1_4830_5080	103.364	0.466	1.916	45.213	1.047
PS1_4790_4830	64.272	0.296	1.168	27.211	0.687
PS5_5200_4380	1433.030	173.102	254.680	1037.345	253.942
PS5_5240_5200	1400.075	166.378	250.410	1015.868	242.479
PS4_5840_5240	1189.944	122.710	185.355	757.355	153.390
PS4_6360_5840	946.761	91.605	134.641	516.889	99.746
PS2_6420_6360	254.863	21.764	35.482	155.037	31.296
PS2_6490_6420	234.324	20.614	33.728	140.708	29.369
PS2_6660_6490	159.152	9.036	19.242	89.942	15.679
PS2_6730_6660	127.288	2.824	9.926	68.271	6.475
PS3_5100_5080	589.797	12.403	35.969	293.718	34.825
PS2_5560_5100	370.971	3.407	21.477	139.478	8.647
PS2_5550_5560	138.050	1.650	4.702	34.102	3.041
PS4_6230_6360	673.182	64.359	92.650	338.483	63.194
PS3_6280_6230	324.627	31.500	42.535	144.135	38.602
PS3_6161_6280	293.062	18.971	29.255	109.190	22.355
PS0_6160_6161	39.477	0.085	4.162	6.311	0.070
PS0_6150_6160	10.178	0.011	0.586	0.207	0.004
PS3_6460_6230	325.891	36.506	48.725	167.129	38.146
PS3_5990_6161	231.734	7.639	12.018	78.380	10.528

Table E.3: Flow Metrics in Shenandoah River Segments (ccP50T50 Scenario)

River Segment	Overall Mean (cfs)	30-Day Low Flow (cfs)	90-Day Low Flow (cfs)	August Low Flow (cfs)	September 10% Flow (cfs)
PS5_4370_4150	3463.517	310.323	464.636	2094.878	535.645
PS5_4380_4370	3435.934	300.640	455.206	2056.619	516.148
PS4_5080_4380	1091.367	18.936	59.527	494.967	54.416
PS1_4830_5080	147.582	0.842	3.563	52.304	1.606
PS1_4790_4830	92.627	0.497	2.118	31.731	1.123
PS5_5200_4380	1993.499	227.664	346.423	1214.061	347.948
PS5_5240_5200	1949.515	220.204	342.264	1159.089	334.995
PS4_5840_5240	1652.275	163.840	260.075	872.570	222.797
PS4_6360_5840	1306.492	118.868	188.333	604.003	129.721
PS2_6420_6360	341.959	31.500	51.086	177.162	42.228
PS2_6490_6420	313.619	29.451	47.537	161.065	40.619
PS2_6660_6490	214.634	15.237	29.422	103.796	22.649
PS2_6730_6660	174.398	6.683	16.275	79.594	11.382
PS3_5100_5080	841.132	22.237	59.399	357.944	48.452
PS2_5560_5100	534.955	7.396	31.876	162.489	13.603
PS2_5550_5560	205.202	2.732	7.338	44.369	4.162
PS4_6230_6360	938.271	79.563	131.364	395.864	88.315
PS3_6280_6230	457.905	41.710	58.929	171.141	46.965
PS3_6161_6280	414.509	24.417	41.476	130.924	27.334
PS0_6160_6161	52.788	0.338	6.084	7.662	0.158
PS0_6150_6160	13.254	0.022	1.230	0.365	0.010
PS3_6460_6230	449.132	42.851	66.556	194.261	49.778
PS3_5990_6161	336.885	11.254	19.614	97.113	15.581

Table E.4: Flow Metrics in Shenandoah River Segments (ccP90T90 Scenario)

River Segment	Overall Mean (cfs)	30-Day Low Flow (cfs)	90-Day Low Flow (cfs)	August Low Flow (cfs)	September 10% Flow (cfs)
PS5_4370_4150	4734.821	414.507	604.020	2446.260	713.789
PS5_4380_4370	4700.006	403.874	594.431	2397.950	665.053
PS4_5080_4380	1523.954	34.023	91.165	599.901	92.069
PS1_4830_5080	208.519	1.645	5.964	59.625	3.839
PS1_4790_4830	131.946	0.933	3.564	36.231	2.343
PS5_5200_4380	2700.129	304.932	445.590	1425.134	457.651
PS5_5240_5200	2640.750	296.953	440.568	1365.641	448.139
PS4_5840_5240	2226.778	221.838	353.458	1008.977	305.998
PS4_6360_5840	1748.920	158.551	256.548	699.966	195.042
PS2_6420_6360	448.402	41.217	64.077	197.561	53.333
PS2_6490_6420	410.480	38.469	59.691	179.408	50.626
PS2_6660_6490	282.411	21.814	37.968	116.205	30.662
PS2_6730_6660	231.767	11.277	22.533	89.940	15.425
PS3_5100_5080	1167.269	34.567	85.708	427.701	74.391
PS2_5560_5100	745.562	12.753	47.162	193.515	21.238
PS2_5550_5560	291.290	4.148	11.095	58.523	5.477
PS4_6230_6360	1264.678	109.041	177.396	468.582	135.280
PS3_6280_6230	624.533	51.943	79.157	209.772	64.409
PS3_6161_6280	566.154	31.173	56.880	160.571	38.088
PS0_6160_6161	69.490	0.649	8.408	9.806	0.410
PS0_6150_6160	17.109	0.043	2.159	0.851	0.017
PS3_6460_6230	597.586	51.451	89.034	223.675	63.218
PS3_5990_6161	468.049	15.913	30.616	125.075	22.216

Table E.5: Flow Metrics in Mattaponi River Segments (Base Scenario)

River Segment	Overall Mean (cfs)	30-Day Low Flow (cfs)	90-Day Low Flow (cfs)	August Low Flow (cfs)	September 10% Flow (cfs)
YM4_6620_0001	644.650	37.596	76.958	279.913	46.587
YM1_6370_6620	119.221	6.220	14.667	56.204	8.010
YM3_6430_6620	433.226	25.213	37.159	159.693	28.934
YM2_6120_6430	254.411	13.154	17.791	73.472	14.803

Table E.6: Flow Metrics in Mattaponi River Segments (ccP10T10 Scenario)

River Segment	Overall Mean (cfs)	30-Day Low Flow (cfs)	90-Day Low Flow (cfs)	August Low Flow (cfs)	September 10% Flow (cfs)
YM4_6620_0001	499.511	28.667	55.271	254.286	33.299
YM1_6370_6620	92.188	4.389	10.344	52.394	5.194
YM3_6430_6620	336.937	17.956	27.272	147.093	21.495
YM2_6120_6430	197.644	9.915	14.042	66.964	11.546

Table E.7: Flow Metrics in Mattaponi River Segments (ccP50T50 Scenario)

River Segment	Overall Mean (cfs)	30-Day Low Flow (cfs)	90-Day Low Flow (cfs)	August Low Flow (cfs)	September 10% Flow (cfs)
YM4_6620_0001	700.214	40.075	82.137	294.260	50.441
YM1_6370_6620	129.199	6.703	16.386	58.194	8.530
YM3_6430_6620	472.060	26.743	39.630	166.098	30.919
YM2_6120_6430	277.884	14.018	18.795	76.330	15.434

Table E.8: Flow Metrics in Mattaponi River Segments (ccP90T90 Scenario)

River Segment	Overall Mean (cfs)	30-Day Low Flow (cfs)	90-Day Low Flow (cfs)	August Low Flow (cfs)	September 10% Flow (cfs)
YM4_6620_0001	1019.605	58.702	130.201	349.889	75.678
YM1_6370_6620	188.988	10.813	26.629	65.856	14.079
YM3_6430_6620	683.638	37.117	61.865	197.563	44.670
YM2_6120_6430	401.725	20.379	28.387	89.940	21.303

Table E.9: Flow Metrics in Pamunkey River Segments (Base Scenario)

River Segment	Overall Mean (cfs)	30-Day Low Flow (cfs)	90-Day Low Flow (cfs)	August Low Flow (cfs)	September 10% Flow (cfs)
YP4_6750_0001	966.191	57.179	104.333	351.502	71.380
YP4_6720_6750	905.625	51.819	96.018	307.105	64.514
YP3_6670_6720	459.104	25.181	40.813	127.832	32.852
YP1_6680_6670	100.372	4.439	11.479	40.071	6.533
YP1_6570_6680	90.375	3.102	9.329	33.122	4.851
YP3_6690_6720	413.006	22.060	45.371	153.953	27.215
YP3_6470_6690	352.956	18.135	33.266	120.183	22.128
YP3_6700_6670	339.854	14.991	23.431	73.261	19.063
YP3_6330_6700	347.047	25.009	32.331	81.019	29.924
YP2_6390_6330	241.447	20.000	20.000	40.000	20.000

Table E.10: Flow Metrics in Pamunkey River Segments (ccP10T10 Scenario)

River Segment	Overall Mean (cfs)	30-Day Low Flow (cfs)	90-Day Low Flow (cfs)	August Low Flow (cfs)	September 10% Flow (cfs)
YP4_6750_0001	726.756	46.377	80.807	317.380	48.672
YP4_6720_6750	679.582	42.591	70.908	272.859	44.546
YP3_6670_6720	339.184	22.116	34.181	118.053	23.585
YP1_6680_6670	75.881	3.094	8.470	35.529	4.330
YP1_6570_6680	68.048	1.993	6.647	29.134	3.067
YP3_6690_6720	314.338	14.578	32.244	136.180	19.425
YP3_6470_6690	267.568	12.222	23.631	101.846	15.713
YP3_6700_6670	247.559	11.374	20.251	67.724	13.667
YP3_6330_6700	255.526	23.634	29.343	77.065	25.385
YP2_6390_6330	173.955	20.000	20.000	40.000	20.000

Table E.11: Flow Metrics in Pamunkey River Segments (ccP50T50 Scenario)

River Segment	Overall Mean (cfs)	30-Day Low Flow (cfs)	90-Day Low Flow (cfs)	August Low Flow (cfs)	September 10% Flow (cfs)
YP4_6750_0001	1067.010	60.667	118.883	366.818	77.559
YP4_6720_6750	1001.356	54.900	104.375	323.202	70.347
YP3_6670_6720	511.469	26.134	45.292	132.875	37.061
YP1_6680_6670	110.113	4.916	13.446	42.497	7.139
YP1_6570_6680	99.261	3.516	10.955	35.409	5.355
YP3_6690_6720	453.330	24.151	49.961	162.740	29.815
YP3_6470_6690	387.779	19.582	36.710	127.193	24.017
YP3_6700_6670	381.236	15.917	25.759	75.737	21.048
YP3_6330_6700	388.084	25.442	34.441	83.182	32.537
YP2_6390_6330	272.920	20.000	20.000	40.000	20.000

Table E.12: Flow Metrics in Pamunkey River Segments (ccP90T90 Scenario)

River Segment	Overall Mean (cfs)	30-Day Low Flow (cfs)	90-Day Low Flow (cfs)	August Low Flow (cfs)	September 10% Flow (cfs)
YP4_6750_0001	1580.500	81.309	178.835	462.613	113.803
YP4_6720_6750	1484.420	73.549	159.763	401.749	104.859
YP3_6670_6720	769.356	32.477	63.706	158.245	55.284
YP1_6680_6670	162.567	7.786	19.033	54.712	10.785
YP1_6570_6680	146.780	6.057	15.688	46.621	8.754
YP3_6690_6720	661.543	34.946	74.439	210.284	43.784
YP3_6470_6690	565.513	27.462	56.917	170.004	35.523
YP3_6700_6670	579.637	18.994	34.710	88.318	38.126
YP3_6330_6700	584.724	28.327	42.790	93.766	49.470
YP2_6390_6330	416.643	20.000	20.000	40.000	40.000

Table E.13: Flow Metrics in Rappahannock River Segments (Base Scenario)

River Segment	Overall Mean (cfs)	30-Day Low Flow (cfs)	90-Day Low Flow (cfs)	August Low Flow (cfs)	September 10% Flow (cfs)
RU5_6030_0001	2010.713	143.882	202.924	821.168	195.960
RU4_5640_6030	1109.215	56.867	97.445	440.365	66.010
RU2_5220_5640	290.408	11.239	21.142	90.466	11.104
RU4_6040_6030	851.301	62.407	94.933	341.795	110.044
RU3_6170_6040	637.119	50.584	78.492	223.949	82.546
RU2_6200_6170	277.937	23.551	37.633	97.033	39.573
RU2_5940_6200	256.729	21.383	34.592	85.667	35.973
RU3_5610_5640	488.011	25.211	43.683	202.074	28.529
RU2_5500_5610	235.935	7.138	17.211	87.753	6.456
RU2_6220_6170	331.399	23.364	36.716	102.466	36.470
RU2_6090_6220	181.356	13.555	21.318	46.305	18.522
RU2_5810_5610	178.212	11.208	18.153	66.806	13.577

Table E.14: Flow Metrics in Rappahannock River Segments (ccP10T10 Scenario)

River Segment	Overall Mean (cfs)	30-Day Low Flow (cfs)	90-Day Low Flow (cfs)	August Low Flow (cfs)	September 10% Flow (cfs)
RU5_6030_0001	1604.271	101.715	144.498	752.321	142.525
RU4_5640_6030	891.850	39.119	67.189	404.094	47.260
RU2_5220_5640	232.019	7.789	14.083	83.074	7.959
RU4_6040_6030	671.367	44.247	67.373	310.907	79.139
RU3_6170_6040	503.387	35.968	55.937	203.438	57.874
RU2_6200_6170	219.850	16.521	26.925	87.977	27.201
RU2_5940_6200	202.962	14.883	24.585	77.531	23.992
RU3_5610_5640	389.336	15.347	28.896	183.934	19.125
RU2_5500_5610	188.581	4.003	10.473	79.836	3.917
RU2_6220_6170	261.387	16.354	25.539	92.751	26.318
RU2_6090_6220	143.598	9.505	14.880	41.932	13.589
RU2_5810_5610	141.841	7.269	12.315	60.648	9.539

Table E.15: Flow Metrics in Rappahannock River Segments (ccP50T50 Scenario)

River Segment	Overall Mean (cfs)	30-Day Low Flow (cfs)	90-Day Low Flow (cfs)	August Low Flow (cfs)	September 10% Flow (cfs)
RU5_6030_0001	2205.603	152.345	220.085	862.714	207.417
RU4_5640_6030	1214.784	61.825	106.693	458.331	69.668
RU2_5220_5640	319.028	12.032	23.233	93.788	11.804
RU4_6040_6030	936.842	66.409	102.329	363.633	115.358
RU3_6170_6040	698.517	53.317	83.022	238.952	87.295
RU2_6200_6170	304.390	24.794	39.761	104.164	41.575
RU2_5940_6200	281.136	22.512	36.528	92.072	37.860
RU3_5610_5640	532.870	27.103	47.337	210.344	29.586
RU2_5500_5610	256.065	7.762	18.625	90.470	6.898
RU2_6220_6170	363.297	24.671	38.870	109.239	38.441
RU2_6090_6220	197.274	14.072	22.101	49.313	19.811
RU2_5810_5610	194.492	11.873	19.401	70.033	14.257

Table E.16: Flow Metrics in Rappahannock River Segments (ccP90T90 Scenario)

River Segment	Overall Mean (cfs)	30-Day Low Flow (cfs)	90-Day Low Flow (cfs)	August Low Flow (cfs)	September 10% Flow (cfs)
RU5_6030_0001	2993.228	210.294	331.702	988.562	277.125
RU4_5640_6030	1644.111	87.768	170.967	525.943	100.348
RU2_5220_5640	438.414	17.649	38.115	110.461	17.843
RU4_6040_6030	1275.237	98.446	147.946	417.493	151.056
RU3_6170_6040	941.939	77.196	116.686	275.643	112.165
RU2_6200_6170	408.099	36.911	55.897	121.493	54.985
RU2_5940_6200	377.034	33.700	51.445	108.217	49.092
RU3_5610_5640	716.160	40.668	78.329	243.848	44.921
RU2_5500_5610	342.388	13.343	33.950	105.634	11.559
RU2_6220_6170	491.377	35.565	54.923	125.863	49.920
RU2_6090_6220	262.829	19.367	30.540	57.272	25.928
RU2_5810_5610	260.855	17.429	29.844	81.592	20.027

Table E.17: Flow Metrics in Upper James River Segments (Base Scenario)

River Segment	Overall Mean (cfs)	30-Day Low Flow (cfs)	90-Day Low Flow (cfs)	August Low Flow (cfs)	September 10% Flow (cfs)
JU5_7420_7160	2572.505	260.169	424.234	1227.506	393.489
JU5_7500_7420	2402.083	235.289	395.436	1088.093	354.468
JU1_7560_7500	136.258	3.974	19.549	55.273	14.888
JU1_7750_7560	39.464	0.760	5.343	12.737	3.110
JU5_7510_7500	2131.054	221.425	356.166	925.078	315.474
JU3_7400_7510	471.215	5.367	45.070	235.989	17.394
JU3_7490_7400	421.957	2.870	35.376	203.507	9.759
JU1_7630_7490	138.295	0.172	9.703	61.515	1.064
JU5_7300_7510	1635.134	214.705	293.820	676.042	292.284
JU3_6650_7300	551.069	28.668	52.333	244.407	34.499
JU1_6300_6650	160.345	18.624	24.421	59.889	22.513
JU1_7690_7490	139.860	0.099	9.231	60.723	0.808
JU4_7000_7300	983.059	167.841	206.621	373.293	238.983
JU2_7360_7000	194.996	1.900	18.433	83.770	7.098
JU2_7450_7360	174.174	1.772	17.680	78.487	6.865
JU1_6340_6650	111.822	1.784	5.433	20.942	2.119
JU4_7330_7000	677.956	146.109	172.720	256.700	225.613
JU2_7140_7330	175.698	1.759	13.001	55.107	5.074
JU3_6950_7330	432.262	53.778	90.692	133.413	131.937
JU3_6900_6950	393.805	80.000	84.496	151.686	182.513
JU2_6810_6900	166.860	10.204	15.925	58.718	15.230
JU2_6600_6810	159.865	10.140	15.528	54.431	15.227
JU1_6590_6600	100.402	7.500	9.822	20.880	12.450
JU1_6290_6590	89.359	0.320	3.497	14.636	0.438
JU3_6380_6900	188.940	2.073	8.847	63.520	1.700
JU4_7380_7160	1014.764	60.774	100.366	488.487	86.393
JU2_7180_7380	160.968	27.411	35.089	102.458	35.251
JU4_7260_7380	836.002	30.121	63.751	381.789	47.766
JU1_6880_7260	155.288	7.051	13.430	78.793	10.901
JU3_6790_7260	621.858	15.158	41.576	270.784	25.367
JU3_6640_6790	367.374	4.357	19.898	147.545	6.702
JU2_6410_6640	152.475	1.380	4.855	51.750	1.727

Table E.18: Flow Metrics in Upper James River Segments (ccP10T10 Scenario)

River Segment	Overall Mean (cfs)	30-Day Low Flow (cfs)	90-Day Low Flow (cfs)	August Low Flow (cfs)	September 10% Flow (cfs)
JU5_7420_7160	2016.579	237.968	336.766	1104.025	360.233
JU5_7500_7420	1883.179	216.710	313.757	977.824	328.094
JU1_7560_7500	107.049	2.533	13.533	49.290	11.778
JU1_7750_7560	31.060	0.486	3.767	10.762	2.365
JU5_7510_7500	1668.957	206.513	285.414	825.098	296.212
JU3_7400_7510	374.353	3.727	29.589	202.210	13.904
JU3_7490_7400	335.985	1.935	22.359	176.290	7.440
JU1_7630_7490	110.544	0.064	5.606	51.314	0.676
JU5_7300_7510	1275.037	201.243	249.547	599.523	278.737
JU3_6650_7300	430.347	22.222	38.309	217.562	28.400
JU1_6300_6650	128.862	15.374	19.572	52.666	19.440
JU1_7690_7490	111.016	0.026	5.550	49.288	0.395
JU4_7000_7300	765.287	159.964	189.764	316.996	236.190
JU2_7360_7000	151.881	0.721	11.955	67.340	3.947
JU2_7450_7360	135.835	0.668	11.407	63.775	3.749
JU1_6340_6650	89.111	1.476	3.588	18.306	1.729
JU4_7330_7000	528.486	147.401	169.312	222.571	232.046
JU2_7140_7330	135.587	0.966	8.998	41.376	3.121
JU3_6950_7330	325.263	62.219	73.061	124.107	141.292
JU3_6900_6950	309.891	80.000	80.282	149.349	192.773
JU2_6810_6900	130.130	9.613	11.469	52.500	10.211
JU2_6600_6810	124.863	9.604	11.366	48.048	10.017
JU1_6590_6600	79.701	7.500	8.050	18.218	7.500
JU1_6290_6590	71.346	0.205	2.113	12.787	0.290
JU3_6380_6900	147.099	1.171	5.319	55.559	1.054
JU4_7380_7160	786.204	43.031	69.529	444.568	59.728
JU2_7180_7380	126.154	21.918	28.315	92.614	27.587
JU4_7260_7380	646.132	18.367	40.269	343.002	30.435
JU1_6880_7260	121.498	3.361	7.897	72.190	6.863
JU3_6790_7260	477.280	7.737	24.775	240.545	14.815
JU3_6640_6790	277.731	1.496	10.890	126.164	3.030
JU2_6410_6640	113.907	0.712	3.291	41.213	1.033

Table E.19: Flow Metrics in Upper James River Segments (ccP50T50 Scenario)

River Segment	Overall Mean (cfs)	30-Day Low Flow (cfs)	90-Day Low Flow (cfs)	August Low Flow (cfs)	September 10% Flow (cfs)
JU5_7420_7160	2729.361	260.714	426.704	1270.939	394.840
JU5_7500_7420	2544.204	235.705	397.733	1131.248	354.556
JU1_7560_7500	147.467	3.994	20.186	57.655	15.208
JU1_7750_7560	42.556	0.775	5.444	13.356	3.255
JU5_7510_7500	2250.102	221.629	356.947	959.440	315.155
JU3_7400_7510	500.147	5.449	46.694	240.246	18.218
JU3_7490_7400	446.791	2.882	36.616	206.376	10.063
JU1_7630_7490	145.832	0.162	9.804	62.180	1.058
JU5_7300_7510	1723.133	214.876	295.374	688.579	292.102
JU3_6650_7300	579.150	28.701	52.737	250.070	34.561
JU1_6300_6650	167.663	18.850	24.608	61.373	22.865
JU1_7690_7490	147.865	0.095	9.469	61.102	0.796
JU4_7000_7300	1034.758	166.773	206.231	383.992	239.073
JU2_7360_7000	204.621	1.709	18.460	85.411	6.847
JU2_7450_7360	182.655	1.589	17.672	80.015	6.539
JU1_6340_6650	116.357	1.805	5.104	20.536	2.120
JU4_7330_7000	713.672	143.321	174.350	261.701	227.924
JU2_7140_7330	184.588	1.637	13.142	55.899	4.971
JU3_6950_7330	458.489	54.328	94.669	137.218	133.063
JU3_6900_6950	413.976	80.000	84.786	155.251	183.742
JU2_6810_6900	174.985	10.086	16.053	59.724	14.906
JU2_6600_6810	167.594	10.065	15.576	54.892	14.820
JU1_6590_6600	104.739	7.500	9.700	20.699	7.500
JU1_6290_6590	93.037	0.297	3.218	14.287	0.455
JU3_6380_6900	198.687	1.967	8.752	64.441	1.567
JU4_7380_7160	1096.315	59.117	104.255	492.606	85.111
JU2_7180_7380	174.930	28.676	36.162	103.439	35.511
JU4_7260_7380	902.147	28.738	66.864	385.109	46.692
JU1_6880_7260	167.799	6.692	13.942	79.172	11.072
JU3_6790_7260	670.225	13.585	43.317	271.911	24.480
JU3_6640_6790	394.557	3.696	20.442	146.342	6.443
JU2_6410_6640	163.635	1.408	4.929	49.859	1.696

Table E.20: Flow Metrics in Upper James River Segments (ccP90T90 Scenario)

River Segment	Overall Mean (cfs)	30-Day Low Flow (cfs)	90-Day Low Flow (cfs)	August Low Flow (cfs)	September 10% Flow (cfs)
JU5_7420_7160	3642.929	285.266	537.145	1440.959	430.090
JU5_7500_7420	3391.727	254.917	499.281	1274.714	383.597
JU1_7560_7500	200.708	5.820	27.916	65.926	18.792
JU1_7750_7560	58.476	1.149	7.582	15.710	4.191
JU5_7510_7500	2993.281	236.289	444.377	1085.010	335.149
JU3_7400_7510	671.189	7.965	65.926	267.292	23.108
JU3_7490_7400	598.559	4.295	52.350	230.911	13.421
JU1_7630_7490	194.300	0.318	14.607	70.840	1.735
JU5_7300_7510	2285.899	226.656	352.876	790.106	309.019
JU3_6650_7300	756.971	36.935	71.981	282.279	42.237
JU1_6300_6650	211.724	22.493	31.193	69.701	26.314
JU1_7690_7490	199.484	0.197	14.248	69.462	1.630
JU4_7000_7300	1381.555	170.559	230.225	439.875	242.560
JU2_7360_7000	275.048	3.357	25.361	97.770	9.663
JU2_7450_7360	245.321	3.183	24.228	91.572	9.452
JU1_6340_6650	147.330	2.294	8.207	22.742	2.530
JU4_7330_7000	949.369	155.490	181.501	294.599	218.934
JU2_7140_7330	249.324	2.758	17.943	66.133	6.827
JU3_6950_7330	625.392	60.463	92.101	166.892	119.046
JU3_6900_6950	543.948	80.592	114.766	174.635	161.820
JU2_6810_6900	228.345	10.805	18.879	67.941	15.350
JU2_6600_6810	218.346	10.683	18.219	63.149	15.328
JU1_6590_6600	133.603	7.500	10.372	23.079	13.000
JU1_6290_6590	117.680	0.526	5.673	15.905	0.770
JU3_6380_6900	259.644	3.447	14.344	73.293	2.332
JU4_7380_7160	1473.202	78.890	158.799	544.350	113.440
JU2_7180_7380	235.264	34.561	47.648	111.868	43.930
JU4_7260_7380	1212.245	42.816	108.927	424.931	65.357
JU1_6880_7260	224.142	11.354	23.525	86.414	16.082
JU3_6790_7260	903.461	22.283	72.342	302.061	36.450
JU3_6640_6790	535.715	7.582	31.857	166.241	10.495
JU2_6410_6640	223.476	2.551	7.023	58.921	2.526

Table E.21: Flow Metrics in Middle James River Segments (Base Scenario)

River Segment	Overall Mean (cfs)	30-Day Low Flow (cfs)	90-Day Low Flow (cfs)	August Low Flow (cfs)	September 10% Flow (cfs)
JL7_7070_0001	7866.459	759.977	1027.434	3981.452	1066.866
JL7_6800_7070	7867.255	786.852	1052.313	4005.790	1117.652
JL1_7170_6800	75.925	1.465	4.710	28.386	2.754
JL7_7030_6800	7507.634	782.368	1051.274	3752.009	1062.915
JL7_7100_7030	7445.625	773.477	1049.957	3691.745	1046.195
JL3_7020_7100	307.712	10.470	25.224	82.395	19.972
JL6_6740_7100	7134.205	732.602	1025.286	3617.018	1020.459
JL4_6710_6740	816.265	46.608	76.747	271.713	75.435
JL4_6520_6710	757.068	46.256	75.488	225.556	63.791
JL2_6240_6520	192.779	1.039	4.248	21.359	0.181
JL6_6970_6740	6198.807	537.309	856.387	3277.168	836.778
JL2_7120_6970	253.238	9.679	22.136	71.324	18.135
JL2_7110_7120	233.344	8.923	20.160	65.881	16.665
JL2_6441_6520	251.255	11.810	16.597	80.023	20.000
JL2_6440_6441	59.181	3.391	6.325	16.830	6.481
JL1_6560_6440	105.829	6.262	13.559	33.100	10.718
JL6_6960_6970	5891.050	502.078	836.782	3159.244	799.844
JL1_6910_6960	147.074	8.566	16.409	55.378	16.657
JL1_6760_6910	128.904	7.853	14.158	44.638	14.206
JL6_6990_6960	5720.159	480.641	818.942	3092.501	774.858
JL6_6890_6990	5698.345	477.894	819.199	3066.087	771.611
JL2_6850_6890	414.170	16.339	38.615	168.446	19.160
JL1_6770_6850	152.381	4.575	13.589	57.698	6.205
JL6_7150_6890	5180.968	446.871	746.544	2832.540	733.175
JL3_7090_7150	659.653	19.591	67.860	325.312	31.143
JL2_7250_7090	341.764	10.185	32.960	149.527	14.340
JL1_7190_7250	115.889	3.128	12.160	53.692	4.478
JL1_7080_7190	82.039	1.921	8.657	33.738	2.084
JL6_7320_7150	4426.619	416.474	649.383	2408.100	672.695
JL6_7430_7320	4335.180	401.568	632.537	2350.238	652.447
JL1_7530_7430	57.296	2.552	6.435	24.249	5.950
JL2_7350_7090	194.270	4.809	15.852	121.479	10.054
JL2_7240_7350	181.285	4.010	13.658	114.880	9.035
JL1_7200_7250	187.942	5.268	16.248	77.924	6.583
JL1_6940_7200	163.206	4.088	13.199	66.572	4.927
JL6_7440_7430	4228.431	405.344	629.790	2289.529	646.965
JL6_7160_7440	3790.428	309.276	514.751	1902.633	498.205

Table E.22: Flow Metrics in Middle James River Segments (ccP10T10 Scenario)

River Segment	Overall Mean (cfs)	30-Day Low Flow (cfs)	90-Day Low Flow (cfs)	August Low Flow (cfs)	September 10% Flow (cfs)
JL7_7070_0001	6319.185	591.643	795.722	3636.373	849.049
JL7_6800_7070	6327.899	617.554	821.431	3671.015	904.735
JL1_7170_6800	58.899	1.127	3.656	25.683	1.869
JL7_7030_6800	6082.388	638.207	852.807	3445.236	898.575
JL7_7100_7030	6034.336	635.569	852.157	3387.649	888.928
JL3_7020_7100	234.086	7.778	17.204	74.737	15.267
JL6_6740_7100	5797.318	626.173	835.396	3317.590	868.992
JL4_6710_6740	802.793	47.952	77.285	266.951	77.468
JL4_6520_6710	605.168	37.295	61.568	205.217	54.644
JL2_6240_6520	147.654	0.619	2.787	16.348	0.086
JL6_6970_6740	4895.550	443.135	663.856	2990.402	688.777
JL2_7120_6970	189.155	7.096	15.871	63.356	13.521
JL2_7110_7120	174.178	6.539	14.506	58.411	12.351
JL2_6441_6520	210.759	9.126	13.357	74.398	18.090
JL2_6440_6441	48.291	2.444	4.587	15.489	4.686
JL1_6560_6440	82.665	4.292	10.063	30.277	7.648
JL6_6960_6970	4664.725	419.012	649.780	2873.201	661.031
JL1_6910_6960	113.353	5.721	11.781	50.043	11.757
JL1_6760_6910	99.123	5.184	10.072	40.396	10.008
JL6_6990_6960	4532.908	404.443	637.334	2810.076	641.691
JL6_6890_6990	4516.206	401.721	637.528	2784.096	635.273
JL2_6850_6890	339.221	9.931	24.462	150.250	12.440
JL1_6770_6850	124.615	2.481	8.539	49.440	3.818
JL6_7150_6890	4097.904	380.999	583.602	2573.642	610.320
JL3_7090_7150	546.598	12.504	45.144	294.878	19.001
JL2_7250_7090	287.180	6.149	21.345	134.989	8.669
JL1_7190_7250	95.596	1.912	8.192	48.567	2.451
JL1_7080_7190	67.989	1.193	5.968	30.081	1.251
JL6_7320_7150	3476.306	360.084	509.264	2184.398	570.063
JL6_7430_7320	3399.998	344.446	491.450	2127.959	553.222
JL1_7530_7430	44.979	1.799	5.067	22.622	4.766
JL2_7350_7090	156.760	3.591	12.213	111.444	6.313
JL2_7240_7350	145.833	2.784	10.292	105.324	5.342
JL1_7200_7250	160.106	3.086	10.088	71.818	3.920
JL1_6940_7200	134.384	2.225	7.621	58.722	2.414
JL6_7440_7430	3320.278	351.628	493.579	2077.164	551.645
JL6_7160_7440	2946.232	256.767	381.303	1711.308	416.744

Table E.23: Flow Metrics in Middle James River Segments (ccP50T50 Scenario)

River Segment	Overall Mean (cfs)	30-Day Low Flow (cfs)	90-Day Low Flow (cfs)	August Low Flow (cfs)	September 10% Flow (cfs)
JL7_7070_0001	8414.621	751.624	1069.078	4068.047	1062.642
JL7_6800_7070	8411.792	775.224	1087.986	4041.235	1113.605
JL1_7170_6800	83.438	1.604	4.872	29.675	3.014
JL7_7030_6800	8039.478	790.618	1100.616	3799.254	1084.436
JL7_7100_7030	7971.649	786.408	1098.525	3737.359	1073.282
JL3_7020_7100	336.456	10.796	27.770	89.270	21.130
JL6_6740_7100	7631.158	744.227	1068.920	3660.451	1045.015
JL4_6710_6740	821.347	48.802	80.180	272.674	79.301
JL4_6520_6710	823.358	47.440	78.850	235.639	65.082
JL2_6240_6520	213.784	1.134	4.806	22.391	0.239
JL6_6970_6740	6680.194	545.689	894.615	3324.839	841.224
JL2_7120_6970	277.864	9.976	24.759	75.664	19.414
JL2_7110_7120	256.054	9.195	22.542	70.092	17.750
JL2_6441_6520	268.357	12.114	18.395	83.046	20.000
JL2_6440_6441	63.539	3.448	6.585	17.625	6.725
JL1_6560_6440	115.706	6.447	14.326	34.637	11.275
JL6_6960_6970	6342.233	509.213	872.336	3198.054	812.367
JL1_6910_6960	161.571	8.979	17.618	58.550	17.282
JL1_6760_6910	141.356	8.218	15.082	48.071	14.923
JL6_6990_6960	6154.228	486.274	852.925	3130.172	780.853
JL6_6890_6990	6130.269	481.844	853.192	3103.087	776.050
JL2_6850_6890	446.502	17.264	40.404	175.775	20.656
JL1_6770_6850	164.129	4.704	14.203	59.985	6.568
JL6_7150_6890	5570.617	448.426	774.573	2865.186	737.248
JL3_7090_7150	721.941	21.321	72.312	336.283	34.141
JL2_7250_7090	375.468	11.231	35.486	156.455	16.082
JL1_7190_7250	125.571	3.357	12.720	55.406	4.611
JL1_7080_7190	88.609	2.081	8.935	34.890	2.282
JL6_7320_7150	4745.954	414.864	667.113	2426.911	677.961
JL6_7430_7320	4644.328	396.793	646.799	2365.822	653.782
JL1_7530_7430	63.296	2.923	7.362	25.161	6.397
JL2_7350_7090	213.493	5.091	18.184	124.009	10.251
JL2_7240_7350	199.311	4.130	15.694	117.103	9.069
JL1_7200_7250	208.930	6.047	17.956	84.276	7.819
JL1_6940_7200	175.744	4.504	13.927	69.433	5.524
JL6_7440_7430	4528.609	402.275	644.954	2306.258	650.165
JL6_7160_7440	4039.584	296.480	511.135	1902.090	487.457

Table E.24: Flow Metrics in Middle James River Segments (ccP90T90 Scenario)

River Segment	Overall Mean (cfs)	30-Day Low Flow (cfs)	90-Day Low Flow (cfs)	August Low Flow (cfs)	September 10% Flow (cfs)
JL7_7070_0001	11226.541	920.119	1470.097	4454.015	1289.266
JL7_6800_7070	11205.956	947.506	1477.918	4432.985	1335.968
JL1_7170_6800	122.813	2.517	6.344	35.350	5.205
JL7_7030_6800	10630.159	950.878	1455.495	4167.645	1299.040
JL7_7100_7030	10532.056	945.124	1447.938	4099.651	1280.937
JL3_7020_7100	483.967	15.488	36.780	110.540	30.024
JL6_6740_7100	10042.399	899.576	1381.996	4015.109	1239.417
JL4_6710_6740	849.783	49.881	84.336	277.235	83.346
JL4_6520_6710	1121.982	59.110	107.251	271.424	82.352
JL2_6240_6520	304.827	2.061	7.909	36.144	0.560
JL6_6970_6740	9010.474	683.232	1214.671	3668.816	1037.032
JL2_7120_6970	404.815	14.643	36.320	88.232	26.920
JL2_7110_7120	373.245	13.500	33.262	81.310	24.595
JL2_6441_6520	346.853	14.871	25.296	93.170	20.000
JL2_6440_6441	84.447	4.700	9.060	20.293	8.662
JL1_6560_6440	160.477	9.039	20.498	39.894	14.815
JL6_6960_6970	8518.294	628.407	1169.590	3530.194	979.460
JL1_6910_6960	228.884	12.958	26.370	69.786	24.056
JL1_6760_6910	199.505	11.884	22.507	57.220	20.483
JL6_6990_6960	8250.792	594.683	1141.798	3455.933	939.410
JL6_6890_6990	8216.266	589.195	1141.273	3427.560	928.417
JL2_6850_6890	584.977	24.927	64.038	197.019	31.458
JL1_6770_6850	215.101	7.028	21.177	68.892	10.603
JL6_7150_6890	7470.664	541.888	1029.670	3159.096	876.383
JL3_7090_7150	947.804	34.150	115.130	372.637	62.968
JL2_7250_7090	487.935	16.874	57.769	176.124	25.275
JL1_7190_7250	163.621	5.245	20.256	62.646	8.694
JL1_7080_7190	114.450	3.066	14.139	39.848	4.124
JL6_7320_7150	6382.179	490.487	876.581	2676.427	794.640
JL6_7430_7320	6244.948	469.283	851.113	2614.282	770.771
JL1_7530_7430	90.762	4.389	10.969	29.019	8.630
JL2_7350_7090	288.438	10.168	26.097	136.609	22.317
JL2_7240_7350	270.062	8.960	22.830	129.052	20.556
JL1_7200_7250	271.223	9.118	27.411	94.437	12.462
JL1_6940_7200	228.584	6.843	21.569	78.151	9.294
JL6_7440_7430	6076.548	471.361	842.347	2550.029	763.155
JL6_7160_7440	5426.625	348.138	683.156	2143.111	562.556

Table E.25: Flow Metrics in Appomattox River Segments (Base Scenario)

River Segment	Overall Mean (cfs)	30-Day Low Flow (cfs)	90-Day Low Flow (cfs)	August Low Flow (cfs)	September 10% Flow (cfs)
JA5_7480_0001	1158.153	41.611	80.898	385.298	77.867
JA2_7570_7480	175.320	5.193	12.412	55.530	8.873
JA1_7600_7570	134.190	3.923	9.711	39.391	6.753
JA4_7470_7480	869.741	32.060	85.673	339.130	73.469
JA2_7410_7470	123.033	3.195	7.953	42.038	6.291
JA4_7340_7470	699.367	27.140	67.911	280.628	63.033
JA4_7280_7340	682.117	26.269	66.049	273.479	60.797
JA1_7640_7280	133.712	4.823	15.263	54.037	11.340
JA2_7550_7280	292.904	10.627	28.912	114.720	26.537

Table E.26: Flow Metrics in Appomattox River Segments (ccP10T10 Scenario)

River Segment	Overall Mean (cfs)	30-Day Low Flow (cfs)	90-Day Low Flow (cfs)	August Low Flow (cfs)	September 10% Flow (cfs)
JA5_7480_0001	898.880	32.340	69.283	351.432	60.987
JA2_7570_7480	136.507	2.679	6.935	56.450	4.840
JA1_7600_7570	104.633	1.473	4.635	40.852	3.206
JA4_7470_7480	686.797	25.208	65.975	310.415	60.072
JA2_7410_7470	95.528	2.535	6.345	38.404	4.777
JA4_7340_7470	554.994	21.239	51.844	256.985	51.661
JA4_7280_7340	541.759	20.474	50.306	250.485	50.008
JA1_7640_7280	103.453	3.486	11.947	49.220	9.112
JA2_7550_7280	226.184	7.384	21.651	106.133	20.571

Table E.27: Flow Metrics in Appomattox River Segments (ccP50T50 Scenario)

River Segment	Overall Mean (cfs)	30-Day Low Flow (cfs)	90-Day Low Flow (cfs)	August Low Flow (cfs)	September 10% Flow (cfs)
JA5_7480_0001	1286.898	43.942	88.498	407.055	84.470
JA2_7570_7480	190.457	5.731	13.367	57.943	9.503
JA1_7600_7570	145.646	4.306	10.462	41.276	7.136
JA4_7470_7480	970.246	35.809	104.085	356.614	79.991
JA2_7410_7470	134.080	3.574	8.585	43.938	6.798
JA4_7340_7470	784.707	30.356	83.663	295.846	67.182
JA4_7280_7340	765.939	29.455	81.392	288.489	65.531
JA1_7640_7280	146.614	5.298	17.916	56.431	12.092
JA2_7550_7280	322.013	11.565	33.752	119.891	28.436

Table E.28: Flow Metrics in Appomattox River Segments (ccP90T90 Scenario)

River Segment	Overall Mean (cfs)	30-Day Low Flow (cfs)	90-Day Low Flow (cfs)	August Low Flow (cfs)	September 10% Flow (cfs)
JA5_7480_0001	1934.301	58.564	132.180	493.882	105.773
JA2_7570_7480	291.027	8.532	19.080	65.497	14.538
JA1_7600_7570	223.158	6.392	14.837	46.731	10.923
JA4_7470_7480	1427.690	51.996	136.437	423.990	114.213
JA2_7410_7470	202.651	5.476	12.583	50.069	10.492
JA4_7340_7470	1147.368	43.968	118.901	355.334	94.545
JA4_7280_7340	1119.298	42.874	117.079	346.949	92.581
JA1_7640_7280	218.549	7.980	25.670	68.914	17.771
JA2_7550_7280	471.854	17.686	57.463	138.615	40.398

Appendix F

Percent Differences between Base and Climate Change Flow Metrics

Table F.1: Percent Differences in Flow Metrics in Shenandoah River Segments (ccP10T10 Scenario)

River Segment	Overall Mean (%)	30-Day Low Flow (%)	90-Day Low Flow (%)	August Low Flow (%)	September 10% Flow (%)
PS5_4370_4150	-47.22	-52.35	-44.61	-38.45	-54.66
PS5_4380_4370	-47.49	-53.90	-45.58	-38.20	-54.50
PS4_5080_4380	-24.92	-45.72	-40.96	-17.35	-35.87
PS1_4830_5080	-24.13	-35.99	-39.94	-12.71	-38.70
PS1_4790_4830	-25.02	-33.18	-42.03	-13.67	-43.50
PS5_5200_4380	-22.55	-24.12	-26.91	-12.47	-28.33
PS5_5240_5200	-22.64	-24.79	-25.35	-10.78	-28.74
PS4_5840_5240	-22.55	-25.95	-26.00	-11.29	-34.12
PS4_6360_5840	-22.06	-26.25	-25.67	-12.88	-33.20
PS2_6420_6360	-20.19	-29.25	-29.40	-10.90	-25.94
PS2_6490_6420	-20.01	-28.20	-27.89	-11.05	-26.99
PS2_6660_6490	-20.48	-42.45	-33.12	-11.83	-31.55
PS2_6730_6660	-21.63	-55.86	-37.69	-12.88	-42.31
PS3_5100_5080	-24.75	-37.51	-35.31	-15.95	-27.83
PS2_5560_5100	-25.65	-46.65	-29.12	-15.43	-34.52
PS2_5550_5560	-28.36	-32.98	-33.64	-27.71	-24.80
PS4_6230_6360	-22.68	-25.71	-25.99	-13.03	-39.06
PS3_6280_6230	-23.79	-20.90	-23.24	-14.01	-21.59
PS3_6161_6280	-24.13	-19.96	-25.12	-16.58	-24.04
PS0_6160_6161	-19.56	-63.52	-26.01	-14.68	-54.25
PS0_6150_6160	-17.62	-42.11	-45.54	-33.23	-55.56
PS3_6460_6230	-21.36	-11.72	-22.55	-12.50	-21.07
PS3_5990_6161	-25.96	-26.78	-33.35	-19.33	-26.46

Table F.2: Percent Differences in Flow Metrics in Shenandoah River Segments (ccP50T50 Scenario)

River Segment	Overall Mean (%)	30-Day Low Flow (%)	90-Day Low Flow (%)	August Low Flow (%)	September 10% Flow (%)
PS5_4370_4150	7.78	1.42	-0.94	1.47	0.51
PS5_4380_4370	7.79	1.57	-0.70	1.38	2.40
PS4_5080_4380	7.55	15.64	7.60	3.10	-2.07
PS1_4830_5080	8.33	15.66	11.69	0.98	-5.97
PS1_4790_4830	8.05	12.19	5.11	0.67	-7.65
PS5_5200_4380	7.74	-0.20	-0.58	2.45	-1.80
PS5_5240_5200	7.72	-0.46	2.03	1.80	-1.55
PS4_5840_5240	7.54	-1.13	3.83	2.21	-4.31
PS4_6360_5840	7.56	-4.30	3.97	1.81	-13.13
PS2_6420_6360	7.09	2.41	1.64	1.81	-0.08
PS2_6490_6420	7.06	2.58	1.63	1.82	0.97
PS2_6660_6490	7.24	-2.96	2.26	1.76	-1.13
PS2_6730_6660	7.37	4.45	2.16	1.57	1.42
PS3_5100_5080	7.31	12.04	6.83	2.43	0.40
PS2_5560_5100	7.22	15.82	5.20	-1.48	3.01
PS2_5550_5560	6.49	10.97	3.56	-5.95	2.92
PS4_6230_6360	7.76	-8.16	4.93	1.71	-14.83
PS3_6280_6230	7.50	4.74	6.34	2.11	-4.60
PS3_6161_6280	7.30	3.01	6.17	0.03	-7.12
PS0_6160_6161	7.56	45.06	8.16	3.58	3.27
PS0_6150_6160	7.28	15.79	14.31	17.74	11.11
PS3_6460_6230	8.37	3.63	5.79	1.71	2.99
PS3_5990_6161	7.63	7.87	8.78	-0.05	8.84

Table F.3: Percent Differences in Flow Metrics in Shenandoah River Segments (ccP90T90 Scenario)

River Segment	Overall Mean (%)	30-Day Low Flow (%)	90-Day Low Flow (%)	August Low Flow (%)	September 10% Flow (%)
PS5_4370_4150	47.34	35.47	28.78	18.49	33.94
PS5_4380_4370	47.45	36.44	29.68	18.20	31.94
PS4_5080_4380	50.18	107.77	64.78	24.96	65.69
PS1_4830_5080	53.06	125.96	86.96	15.12	124.77
PS1_4790_4830	53.92	110.61	76.87	14.94	92.68
PS5_5200_4380	45.93	33.68	27.89	20.26	29.16
PS5_5240_5200	45.91	34.23	31.33	19.94	31.70
PS4_5840_5240	44.94	33.87	41.11	18.19	31.42
PS4_6360_5840	43.98	27.64	41.63	17.98	30.61
PS2_6420_6360	40.42	34.00	27.49	13.53	26.20
PS2_6490_6420	40.13	33.99	27.61	13.42	25.85
PS2_6660_6490	41.11	38.92	31.97	13.92	33.85
PS2_6730_6660	42.69	76.26	41.44	14.77	37.44
PS3_5100_5080	48.92	74.17	54.14	22.39	54.16
PS2_5560_5100	49.43	99.70	55.65	17.33	60.82
PS2_5550_5560	51.16	68.48	56.58	24.05	35.44
PS4_6230_6360	45.25	25.87	41.70	20.40	30.46
PS3_6280_6230	46.62	30.43	42.84	25.15	30.84
PS3_6161_6280	46.56	31.51	45.60	22.68	29.42
PS0_6160_6161	41.60	178.54	49.48	32.57	167.97
PS0_6150_6160	38.48	126.32	100.65	174.52	88.89
PS3_6460_6230	44.19	24.43	41.52	17.11	30.80
PS3_5990_6161	49.54	52.53	69.80	28.73	55.18

Table F.4: Percent Differences in Flow Metrics in Mattaponi River Segments (ccP10T10 Scenario)

River Segment	Overall Mean (%)	30-Day Low Flow (%)	90-Day Low Flow (%)	August Low Flow (%)	September 10% Flow (%)
YM4_6620_0001	-22.51	-23.75	-28.18	-9.16	-28.52
YM1_6370_6620	-22.67	-29.44	-29.47	-6.78	-35.16
YM3_6430_6620	-22.23	-28.78	-26.61	-7.89	-25.71
YM2_6120_6430	-22.31	-24.62	-21.07	-8.86	-22.00

Table F.5: Percent Differences in Flow Metrics in Mattaponi River Segments (ccP50T50 Scenario)

River Segment	Overall Mean (%)	30-Day Low Flow (%)	90-Day Low Flow (%)	August Low Flow (%)	September 10% Flow (%)
YM4_6620_0001	8.62	6.59	6.73	5.13	8.27
YM1_6370_6620	8.37	7.77	11.72	3.54	6.49
YM3_6430_6620	8.96	6.07	6.65	4.01	6.86
YM2_6120_6430	9.23	6.57	5.64	3.89	4.26

Table F.6: Percent Differences in Flow Metrics in Mattaponi River Segments (ccP90T90 Scenario)

River Segment	Overall Mean (%)	30-Day Low Flow (%)	90-Day Low Flow (%)	August Low Flow (%)	September 10% Flow (%)
YM4_6620_0001	58.16	56.14	69.18	25.00	62.44
YM1_6370_6620	58.52	73.84	81.56	17.17	75.77
YM3_6430_6620	57.80	47.21	66.49	23.71	54.39
YM2_6120_6430	57.90	54.93	59.56	22.41	43.91

Table F.7: Percent Differences in Flow Metrics in Pamunkey River Segments (ccP10T10 Scenario)

River Segment	Overall Mean (%)	30-Day Low Flow (%)	90-Day Low Flow (%)	August Low Flow (%)	September 10% Flow (%)
YP4_6750_0001	-24.78	-18.89	-22.55	-9.71	-31.81
YP4_6720_6750	-24.96	-17.81	-26.15	-11.15	-30.95
YP3_6670_6720	-26.12	-12.17	-16.25	-7.65	-28.21
YP1_6680_6670	-24.40	-30.30	-26.21	-11.33	-33.72
YP1_6570_6680	-24.70	-35.75	-28.75	-12.04	-36.78
YP3_6690_6720	-23.89	-33.92	-28.93	-11.54	-28.62
YP3_6470_6690	-24.19	-32.61	-28.96	-15.26	-28.99
YP3_6700_6670	-27.16	-24.13	-13.57	-7.56	-28.31
YP3_6330_6700	-26.37	-5.50	-9.24	-4.88	-15.17
YP2_6390_6330	-27.95	0.00	0.00	0.00	0.00

Table F.8: Percent Differences in Flow Metrics in Pamunkey River Segments (ccP50T50 Scenario)

River Segment	Overall Mean (%)	30-Day Low Flow (%)	90-Day Low Flow (%)	August Low Flow (%)	September 10% Flow (%)
YP4_6750_0001	10.43	6.10	13.95	4.36	8.66
YP4_6720_6750	10.57	5.95	8.70	5.24	9.04
YP3_6670_6720	11.41	3.78	10.97	3.95	12.81
YP1_6680_6670	9.70	10.75	17.14	6.05	9.28
YP1_6570_6680	9.83	13.35	17.43	6.90	10.39
YP3_6690_6720	9.76	9.48	10.12	5.71	9.55
YP3_6470_6690	9.87	7.98	10.35	5.83	8.54
YP3_6700_6670	12.18	6.18	9.94	3.38	10.41
YP3_6330_6700	11.82	1.73	6.53	2.67	8.73
YP2_6390_6330	13.04	0.00	0.00	0.00	0.00

Table F.9: Percent Differences in Flow Metrics in Pamunkey River Segments (ccP90T90 Scenario)

River Segment	Overall Mean (%)	30-Day Low Flow (%)	90-Day Low Flow (%)	August Low Flow (%)	September 10% Flow (%)
YP4_6750_0001	63.58	42.20	71.41	31.61	59.43
YP4_6720_6750	63.91	41.93	66.39	30.82	62.54
YP3_6670_6720	67.58	28.97	56.09	23.79	68.28
YP1_6680_6670	61.96	75.40	65.81	36.54	65.08
YP1_6570_6680	62.41	95.26	68.16	40.76	80.46
YP3_6690_6720	60.18	58.41	64.07	36.59	60.88
YP3_6470_6690	60.22	51.43	71.10	41.45	60.53
YP3_6700_6670	70.55	26.70	48.14	20.55	100.00
YP3_6330_6700	68.49	13.27	32.35	15.73	65.32
YP2_6390_6330	72.56	0.00	0.00	0.00	100.00

Table F.10: Percent Differences in Flow Metrics in Rappahannock River Segments (ccP10T10 Scenario)

River Segment	Overall Mean (%)	30-Day Low Flow (%)	90-Day Low Flow (%)	August Low Flow (%)	September 10% Flow (%)
RU5_6030_0001	-20.21	-29.31	-28.79	-8.38	-27.27
RU4_5640_6030	-19.60	-31.21	-31.05	-8.24	-28.40
RU2_5220_5640	-20.11	-30.70	-33.39	-8.17	-28.32
RU4_6040_6030	-21.14	-29.10	-29.03	-9.04	-28.08
RU3_6170_6040	-20.99	-28.89	-28.74	-9.16	-29.89
RU2_6200_6170	-20.90	-29.85	-28.45	-9.33	-31.26
RU2_5940_6200	-20.94	-30.40	-28.93	-9.50	-33.31
RU3_5610_5640	-20.22	-39.13	-33.85	-8.98	-32.96
RU2_5500_5610	-20.07	-43.92	-39.15	-9.02	-39.33
RU2_6220_6170	-21.13	-30.00	-30.44	-9.48	-27.84
RU2_6090_6220	-20.82	-29.88	-30.20	-9.44	-26.63
RU2_5810_5610	-20.41	-35.14	-32.16	-9.22	-29.74

Table F.11: Percent Differences in Flow Metrics in Rappahannock River Segments (ccP50T50 Scenario)

River Segment	Overall Mean (%)	30-Day Low Flow (%)	90-Day Low Flow (%)	August Low Flow (%)	September 10% Flow (%)
RU5_6030_0001	9.69	5.88	8.46	5.06	5.85
RU4_5640_6030	9.52	8.72	9.49	4.08	5.54
RU2_5220_5640	9.86	7.06	9.89	3.67	6.30
RU4_6040_6030	10.05	6.41	7.79	6.39	4.83
RU3_6170_6040	9.64	5.40	5.77	6.70	5.75
RU2_6200_6170	9.52	5.28	5.65	7.35	5.06
RU2_5940_6200	9.51	5.28	5.60	7.48	5.25
RU3_5610_5640	9.19	7.50	8.36	4.09	3.71
RU2_5500_5610	8.53	8.74	8.22	3.10	6.85
RU2_6220_6170	9.63	5.59	5.87	6.61	5.40
RU2_6090_6220	8.78	3.81	3.67	6.50	6.96
RU2_5810_5610	9.14	5.93	6.87	4.83	5.01

Table F.12: Percent Differences in Flow Metrics in Rappahannock River Segments (ccP90T90 Scenario)

River Segment	Overall Mean (%)	30-Day Low Flow (%)	90-Day Low Flow (%)	August Low Flow (%)	September 10% Flow (%)
RU5_6030_0001	48.86	46.16	63.46	20.38	41.42
RU4_5640_6030	48.22	54.34	75.45	19.43	52.02
RU2_5220_5640	50.96	57.03	80.28	22.10	60.69
RU4_6040_6030	49.80	57.75	55.84	22.15	37.27
RU3_6170_6040	47.84	52.61	48.66	23.08	35.88
RU2_6200_6170	46.83	56.73	48.53	25.21	38.95
RU2_5940_6200	46.86	57.60	48.72	26.32	36.47
RU3_5610_5640	46.75	61.31	79.31	20.67	57.46
RU2_5500_5610	45.12	86.93	97.26	20.38	79.04
RU2_6220_6170	48.27	52.22	49.59	22.83	36.88
RU2_6090_6220	44.92	42.88	43.26	23.68	39.98
RU2_5810_5610	46.37	55.50	64.40	22.13	47.51

Table F.13: Percent Differences in Flow Metrics in Upper James River Segments (ccP10T10 Scenario)

River Segment	Overall Mean (%)	30-Day Low Flow (%)	90-Day Low Flow (%)	August Low Flow (%)	September 10% Flow (%)
JU5_7420_7160	-21.61	-8.53	-20.62	-10.06	-8.45
JU5_7500_7420	-21.60	-7.90	-20.66	-10.13	-7.44
JU1_7560_7500	-21.44	-36.26	-30.77	-10.82	-20.89
JU1_7750_7560	-21.30	-36.05	-29.50	-15.51	-23.95
JU5_7510_7500	-21.68	-6.73	-19.86	-10.81	-6.11
JU3_7400_7510	-20.56	-30.56	-34.35	-14.31	-20.06
JU3_7490_7400	-20.37	-32.58	-36.80	-13.37	-23.76
JU1_7630_7490	-20.07	-62.79	-42.22	-16.58	-36.47
JU5_7300_7510	-22.02	-6.27	-15.07	-11.32	-4.63
JU3_6650_7300	-21.91	-22.49	-26.80	-10.98	-17.68
JU1_6300_6650	-19.63	-17.45	-19.86	-12.06	-13.65
JU1_7690_7490	-20.62	-73.74	-39.88	-18.83	-51.11
JU4_7000_7300	-22.15	-4.69	-8.16	-15.08	-1.17
JU2_7360_7000	-22.11	-62.05	-35.14	-19.61	-44.39
JU2_7450_7360	-22.01	-62.30	-35.48	-18.74	-45.39
JU1_6340_6650	-20.31	-17.26	-33.96	-12.59	-18.40
JU4_7330_7000	-22.05	0.88	-1.97	-13.30	2.85
JU2_7140_7330	-22.83	-45.08	-30.79	-24.92	-38.49
JU3_6950_7330	-24.75	15.70	-19.44	-6.98	7.09
JU3_6900_6950	-21.31	0.00	-4.99	-1.54	5.62
JU2_6810_6900	-22.01	-5.79	-27.98	-10.59	-32.95
JU2_6600_6810	-21.89	-5.29	-26.80	-11.73	-34.22
JU1_6590_6600	-20.62	0.00	-18.04	-12.75	-39.76
JU1_6290_6590	-20.16	-35.94	-39.58	-12.63	-33.79
JU3_6380_6900	-22.15	-43.51	-39.88	-12.53	-38.00
JU4_7380_7160	-22.52	-29.20	-30.72	-8.99	-30.86
JU2_7180_7380	-21.63	-20.04	-19.31	-9.61	-21.74
JU4_7260_7380	-22.71	-39.02	-36.83	-10.16	-36.28
JU1_6880_7260	-21.76	-52.33	-41.20	-8.38	-37.04
JU3_6790_7260	-23.25	-48.96	-40.41	-11.17	-41.60
JU3_6640_6790	-24.40	-65.66	-45.27	-14.49	-54.79
JU2_6410_6640	-25.29	-48.41	-32.21	-20.36	-40.19

Table F.14: Percent Differences in Flow Metrics in Upper James River Segments (ccP50T50 Scenario)

River Segment	Overall Mean (%)	30-Day Low Flow (%)	90-Day Low Flow (%)	August Low Flow (%)	September 10% Flow (%)
JU5_7420_7160	6.10	0.21	0.58	3.54	0.34
JU5_7500_7420	5.92	0.18	0.58	3.97	0.02
JU1_7560_7500	8.23	0.50	3.26	4.31	2.15
JU1_7750_7560	7.83	1.97	1.89	4.86	4.66
JU5_7510_7500	5.59	0.09	0.22	3.71	-0.10
JU3_7400_7510	6.14	1.53	3.60	1.80	4.74
JU3_7490_7400	5.89	0.42	3.51	1.41	3.12
JU1_7630_7490	5.45	-5.81	1.04	1.08	-0.56
JU5_7300_7510	5.38	0.08	0.53	1.85	-0.06
JU3_6650_7300	5.10	0.12	0.77	2.32	0.18
JU1_6300_6650	4.56	1.21	0.77	2.48	1.56
JU1_7690_7490	5.72	-4.04	2.58	0.62	-1.49
JU4_7000_7300	5.26	-0.64	-0.19	2.87	0.04
JU2_7360_7000	4.94	-10.05	0.15	1.96	-3.54
JU2_7450_7360	4.87	-10.33	-0.05	1.95	-4.75
JU1_6340_6650	4.06	1.18	-6.06	-1.94	0.05
JU4_7330_7000	5.27	-1.91	0.94	1.95	1.02
JU2_7140_7330	5.06	-6.94	1.08	1.44	-2.03
JU3_6950_7330	6.07	1.02	4.39	2.85	0.85
JU3_6900_6950	5.12	0.00	0.34	2.35	0.67
JU2_6810_6900	4.87	-1.16	0.80	1.71	-2.13
JU2_6600_6810	4.83	-0.74	0.31	0.85	-2.67
JU1_6590_6600	4.32	0.00	-1.24	-0.87	-39.76
JU1_6290_6590	4.12	-7.19	-7.98	-2.38	3.88
JU3_6380_6900	5.16	-5.11	-1.07	1.45	-7.82
JU4_7380_7160	8.04	-2.73	3.87	0.84	-1.48
JU2_7180_7380	8.67	4.61	3.06	0.96	0.74
JU4_7260_7380	7.91	-4.59	4.88	0.87	-2.25
JU1_6880_7260	8.06	-5.09	3.81	0.48	1.57
JU3_6790_7260	7.78	-10.38	4.19	0.42	-3.50
JU3_6640_6790	7.40	-15.17	2.73	-0.82	-3.86
JU2_6410_6640	7.32	2.03	1.52	-3.65	-1.80

Table F.15: Percent Differences in Flow Metrics in Upper James River Segments (ccP90T90 Scenario)

River Segment	Overall Mean (%)	30-Day Low Flow (%)	90-Day Low Flow (%)	August Low Flow (%)	September 10% Flow (%)
JU5_7420_7160	41.61	9.65	26.62	17.39	9.30
JU5_7500_7420	41.20	8.34	26.26	17.15	8.22
JU1_7560_7500	47.30	46.45	42.80	19.27	26.22
JU1_7750_7560	48.18	51.18	41.91	23.34	34.76
JU5_7510_7500	40.46	6.71	24.77	17.29	6.24
JU3_7400_7510	42.44	48.41	46.27	13.26	32.85
JU3_7490_7400	41.85	49.65	47.98	13.47	37.52
JU1_7630_7490	40.50	84.88	50.54	15.16	63.06
JU5_7300_7510	39.80	5.57	20.10	16.87	5.73
JU3_6650_7300	37.36	28.84	37.54	15.50	22.43
JU1_6300_6650	32.04	20.77	27.73	16.38	16.88
JU1_7690_7490	42.63	98.99	54.35	14.39	101.73
JU4_7000_7300	40.54	1.62	11.42	17.84	1.50
JU2_7360_7000	41.05	76.68	37.58	16.71	36.14
JU2_7450_7360	40.85	79.63	37.04	16.67	37.68
JU1_6340_6650	31.75	28.59	51.06	8.60	19.40
JU4_7330_7000	40.03	6.42	5.08	14.76	-2.96
JU2_7140_7330	41.90	56.79	38.01	20.01	34.55
JU3_6950_7330	44.68	12.43	1.55	25.09	-9.77
JU3_6900_6950	38.13	0.74	35.82	15.13	-11.34
JU2_6810_6900	36.85	5.89	18.55	15.71	0.79
JU2_6600_6810	36.58	5.36	17.33	16.02	0.66
JU1_6590_6600	33.07	0.00	5.60	10.53	4.42
JU1_6290_6590	31.69	64.38	62.22	8.67	75.80
JU3_6380_6900	37.42	66.28	62.13	15.39	37.18
JU4_7380_7160	45.18	29.81	58.22	11.44	31.31
JU2_7180_7380	46.16	26.08	35.79	9.18	24.62
JU4_7260_7380	45.01	42.15	70.86	11.30	36.83
JU1_6880_7260	44.34	61.03	75.17	9.67	47.53
JU3_6790_7260	45.28	47.00	74.00	11.55	43.69
JU3_6640_6790	45.82	74.02	60.10	12.67	56.60
JU2_6410_6640	46.57	84.86	44.65	13.86	46.27

Table F.16: Percent Differences in Flow Metrics in Middle James River Segments (ccP10T10 Scenario)

River Segment	Overall Mean (%)	30-Day Low Flow (%)	90-Day Low Flow (%)	August Low Flow (%)	September 10% Flow (%)
JL7_7070_0001	-19.67	-22.15	-22.55	-8.67	-20.42
JL7_6800_7070	-19.57	-21.52	-21.94	-8.36	-19.05
JL1_7170_6800	-22.42	-23.07	-22.38	-9.52	-32.14
JL7_7030_6800	-18.98	-18.43	-18.88	-8.18	-15.46
JL7_7100_7030	-18.95	-17.83	-18.84	-8.24	-15.03
JL3_7020_7100	-23.93	-25.71	-31.80	-9.29	-23.56
JL6_6740_7100	-18.74	-14.53	-18.52	-8.28	-14.84
JL4_6710_6740	-1.65	2.88	0.70	-1.75	2.70
JL4_6520_6710	-20.06	-19.37	-18.44	-9.02	-14.34
JL2_6240_6520	-23.41	-40.42	-34.39	-23.46	-52.49
JL6_6970_6740	-21.02	-17.53	-22.48	-8.75	-17.69
JL2_7120_6970	-25.31	-26.69	-28.30	-11.17	-25.44
JL2_7110_7120	-25.36	-26.72	-28.05	-11.34	-25.89
JL2_6441_6520	-16.12	-22.73	-19.52	-7.03	-9.55
JL2_6440_6441	-18.40	-27.93	-27.48	-7.97	-27.70
JL1_6560_6440	-21.89	-31.46	-25.78	-8.53	-28.64
JL6_6960_6970	-20.82	-16.54	-22.35	-9.05	-17.36
JL1_6910_6960	-22.93	-33.21	-28.20	-9.63	-29.42
JL1_6760_6910	-23.10	-33.99	-28.86	-9.50	-29.55
JL6_6990_6960	-20.76	-15.85	-22.18	-9.13	-17.19
JL6_6890_6990	-20.75	-15.94	-22.18	-9.20	-17.67
JL2_6850_6890	-18.10	-39.22	-36.65	-10.80	-35.07
JL1_6770_6850	-18.22	-45.77	-37.16	-14.31	-38.47
JL6_7150_6890	-20.90	-14.74	-21.83	-9.14	-16.76
JL3_7090_7150	-17.14	-36.17	-33.47	-9.36	-38.99
JL2_7250_7090	-15.97	-39.63	-35.24	-9.72	-39.55
JL1_7190_7250	-17.51	-38.87	-32.63	-9.55	-45.27
JL1_7080_7190	-17.13	-37.90	-31.06	-10.84	-39.97
JL6_7320_7150	-21.47	-13.54	-21.58	-9.29	-15.26
JL6_7430_7320	-21.57	-14.22	-22.30	-9.46	-15.21
JL1_7530_7430	-21.50	-29.51	-21.26	-6.71	-19.90
JL2_7350_7090	-19.31	-25.33	-22.96	-8.26	-37.21
JL2_7240_7350	-19.56	-30.57	-24.64	-8.32	-40.87
JL1_7200_7250	-14.81	-41.42	-37.91	-7.84	-40.45
JL1_6940_7200	-17.66	-45.57	-42.26	-11.79	-51.00
JL6_7440_7430	-21.48	-13.25	-21.63	-9.28	-14.73
JL6_7160_7440	-22.27	-16.98	-25.92	-10.06	-16.35

Table F.17: Percent Differences in Flow Metrics in Middle James River Segments (ccP50T50 Scenario)

River Segment	Overall Mean (%)	30-Day Low Flow (%)	90-Day Low Flow (%)	August Low Flow (%)	September 10% Flow (%)
JL7_7070_0001	6.97	-1.10	4.05	2.17	-0.40
JL7_6800_7070	6.92	-1.48	3.39	0.88	-0.36
JL1_7170_6800	9.90	9.49	3.44	4.54	9.44
JL7_7030_6800	7.08	1.05	4.69	1.26	2.02
JL7_7100_7030	7.06	1.67	4.63	1.24	2.59
JL3_7020_7100	9.34	3.11	10.09	8.34	5.80
JL6_6740_7100	6.97	1.59	4.26	1.20	2.41
JL4_6710_6740	0.62	4.71	4.47	0.35	5.12
JL4_6520_6710	8.76	2.56	4.45	4.47	2.02
JL2_6240_6520	10.90	9.14	13.14	4.83	32.04
JL6_6970_6740	7.77	1.56	4.46	1.45	0.53
JL2_7120_6970	9.72	3.07	11.85	6.08	7.05
JL2_7110_7120	9.73	3.05	11.82	6.39	6.51
JL2_6441_6520	6.81	2.57	10.83	3.78	0.00
JL2_6440_6441	7.36	1.68	4.11	4.72	3.76
JL1_6560_6440	9.33	2.95	5.66	4.64	5.20
JL6_6960_6970	7.66	1.42	4.25	1.23	1.57
JL1_6910_6960	9.86	4.82	7.37	5.73	3.75
JL1_6760_6910	9.66	4.65	6.53	7.69	5.05
JL6_6990_6960	7.59	1.17	4.15	1.22	0.77
JL6_6890_6990	7.58	0.83	4.15	1.21	0.58
JL2_6850_6890	7.81	5.66	4.63	4.35	7.81
JL1_6770_6850	7.71	2.82	4.52	3.96	5.85
JL6_7150_6890	7.52	0.35	3.75	1.15	0.56
JL3_7090_7150	9.44	8.83	6.56	3.37	9.63
JL2_7250_7090	9.86	10.27	7.66	4.63	12.15
JL1_7190_7250	8.35	7.32	4.61	3.19	2.97
JL1_7080_7190	8.01	8.33	3.21	3.41	9.50
JL6_7320_7150	7.21	-0.39	2.73	0.78	0.78
JL6_7430_7320	7.13	-1.19	2.25	0.66	0.20
JL1_7530_7430	10.47	14.54	14.41	3.76	7.51
JL2_7350_7090	9.89	5.86	14.71	2.08	1.96
JL2_7240_7350	9.94	2.99	14.91	1.94	0.38
JL1_7200_7250	11.17	14.79	10.51	8.15	18.78
JL1_6940_7200	7.68	10.18	5.52	4.30	12.12
JL6_7440_7430	7.10	-0.76	2.41	0.73	0.49
JL6_7160_7440	6.57	-4.14	-0.70	-0.03	-2.16

Table F.18: Percent Differences in Flow Metrics in Middle James River Segments (ccP90T90 Scenario)

River Segment	Overall Mean (%)	30-Day Low Flow (%)	90-Day Low Flow (%)	August Low Flow (%)	September 10% Flow (%)
JL7_7070_0001	42.71	21.07	43.08	11.87	20.85
JL7_6800_7070	42.44	20.42	40.44	10.66	19.53
JL1_7170_6800	61.76	71.81	34.69	24.53	89.00
JL7_7030_6800	41.59	21.54	38.45	11.08	22.21
JL7_7100_7030	41.45	22.19	37.90	11.05	22.44
JL3_7020_7100	57.28	47.93	45.81	34.16	50.33
JL6_6740_7100	40.76	22.79	34.79	11.01	21.46
JL4_6710_6740	4.11	7.02	9.89	2.03	10.49
JL4_6520_6710	48.20	27.79	42.08	20.34	29.10
JL2_6240_6520	58.12	98.36	86.18	69.22	209.39
JL6_6970_6740	45.36	27.16	41.84	11.95	23.93
JL2_7120_6970	59.86	51.29	64.08	23.71	48.44
JL2_7110_7120	59.95	51.29	64.99	23.42	47.58
JL2_6441_6520	38.05	25.92	52.41	16.43	0.00
JL2_6440_6441	42.69	38.60	43.24	20.58	33.65
JL1_6560_6440	51.64	44.35	51.18	20.53	38.23
JL6_6960_6970	44.60	25.16	39.77	11.74	22.46
JL1_6910_6960	55.63	51.27	60.70	26.02	44.42
JL1_6760_6910	54.77	51.33	58.97	28.19	44.19
JL6_6990_6960	44.24	23.73	39.42	11.75	21.24
JL6_6890_6990	44.19	23.29	39.32	11.79	20.32
JL2_6850_6890	41.24	52.56	65.84	16.96	64.19
JL1_6770_6850	41.16	53.62	55.84	19.40	70.88
JL6_7150_6890	44.19	21.26	37.92	11.53	19.53
JL3_7090_7150	43.68	74.31	69.66	14.55	102.19
JL2_7250_7090	42.77	65.68	75.27	17.79	76.26
JL1_7190_7250	41.19	67.68	66.58	16.68	94.15
JL1_7080_7190	39.51	59.60	63.32	18.11	97.89
JL6_7320_7150	44.18	17.77	34.99	11.14	18.13
JL6_7430_7320	44.05	16.86	34.56	11.23	18.14
JL1_7530_7430	58.41	71.98	70.46	19.67	45.04
JL2_7350_7090	48.47	111.44	64.63	12.45	121.97
JL2_7240_7350	48.97	123.44	67.15	12.34	127.52
JL1_7200_7250	44.31	73.08	68.70	21.19	89.31
JL1_6940_7200	40.06	67.39	63.41	17.39	88.63
JL6_7440_7430	43.71	16.29	33.75	11.38	17.96
JL6_7160_7440	43.17	12.57	32.72	12.64	12.92

Table F.19: Percent Differences in Flow Metrics in Appomattox River Segments (ccP10T10 Scenario)

River Segment	Overall Mean (%)	30-Day Low Flow (%)	90-Day Low Flow (%)	August Low Flow (%)	September 10% Flow (%)
JA5_7480_0001	-22.39	-22.28	-14.36	-8.79	-21.68
JA2_7570_7480	-22.14	-48.41	-44.13	1.66	-45.45
JA1_7600_7570	-22.03	-62.45	-52.27	3.71	-52.52
JA4_7470_7480	-21.03	-21.37	-22.99	-8.47	-18.23
JA2_7410_7470	-22.36	-20.66	-20.22	-8.64	-24.07
JA4_7340_7470	-20.64	-21.74	-23.66	-8.43	-18.04
JA4_7280_7340	-20.58	-22.06	-23.84	-8.41	-17.75
JA1_7640_7280	-22.63	-27.72	-21.73	-8.91	-19.65
JA2_7550_7280	-22.78	-30.52	-25.11	-7.49	-22.48

Table F.20: Percent Differences in Flow Metrics in Appomattox River Segments (ccP50T50 Scenario)

River Segment	Overall Mean (%)	30-Day Low Flow (%)	90-Day Low Flow (%)	August Low Flow (%)	September 10% Flow (%)
JA5_7480_0001	11.12	5.60	9.39	5.65	8.48
JA2_7570_7480	8.63	10.36	7.69	4.35	7.10
JA1_7600_7570	8.54	9.76	7.73	4.79	5.67
JA4_7470_7480	11.56	11.69	21.49	5.16	8.88
JA2_7410_7470	8.98	11.86	7.95	4.52	8.06
JA4_7340_7470	12.20	11.85	23.20	5.42	6.58
JA4_7280_7340	12.29	12.13	23.23	5.49	7.79
JA1_7640_7280	9.65	9.85	17.38	4.43	6.63
JA2_7550_7280	9.94	8.83	16.74	4.51	7.16

Table F.21: Percent Differences in Flow Metrics in Appomattox River Segments (ccP90T90 Scenario)

River Segment	Overall Mean (%)	30-Day Low Flow (%)	90-Day Low Flow (%)	August Low Flow (%)	September 10% Flow (%)
JA5_7480_0001	67.02	40.74	63.39	28.18	35.84
JA2_7570_7480	66.00	64.30	53.72	17.95	63.85
JA1_7600_7570	66.30	62.94	52.79	18.63	61.75
JA4_7470_7480	64.15	62.18	59.25	25.02	55.46
JA2_7410_7470	64.71	71.39	58.22	19.10	66.78
JA4_7340_7470	64.06	62.00	75.08	26.62	49.99
JA4_7280_7340	64.09	63.21	77.26	26.86	52.28
JA1_7640_7280	63.45	65.46	68.18	27.53	56.71
JA2_7550_7280	61.10	66.43	98.75	20.83	52.23

Appendix G

Radar Charts Showing Minimum, Median, and Maximum Percent Change in Runoff Metrics (l30 and l90) by Land Use Group

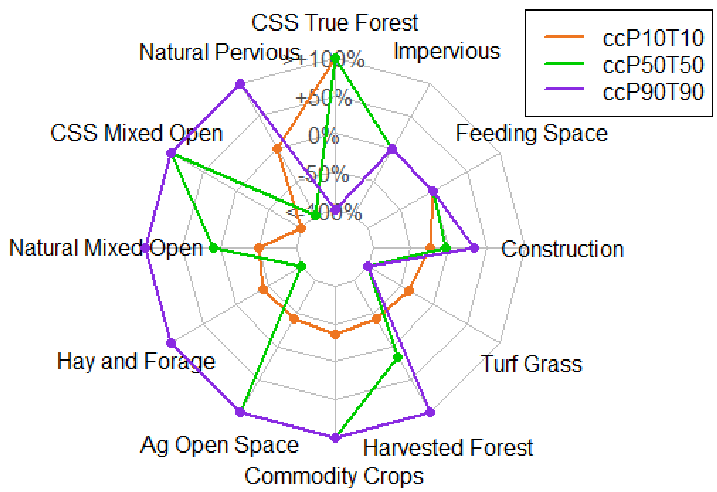

Figure G.1: Mean Percent Changes in l30 Runoff per Unit Area between the Base Scenario and Scenarios ccP10T10, ccP50T50, and ccP90T90

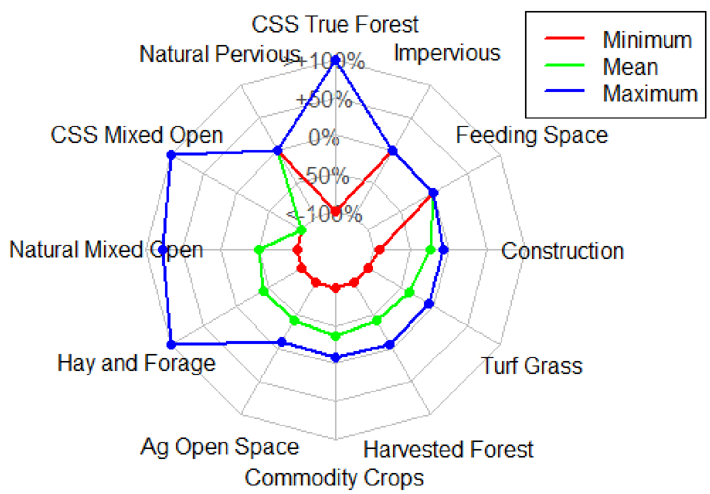

Figure G.2: Minimum, Mean, and Maximum Percent Changes in l30 Runoff per Unit Area between the Base Scenario and Scenario ccP10T10

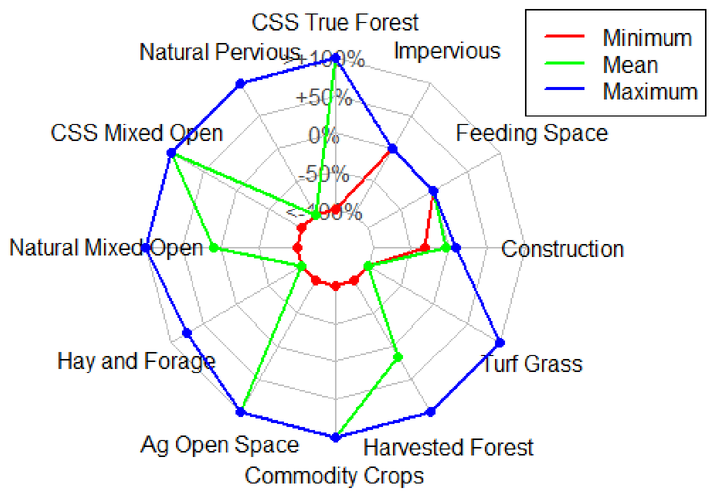

Figure G.3: Minimum, Mean, and Maximum Percent Changes in l30 Runoff per Unit Area between the Base Scenario and Scenario ccP50T50

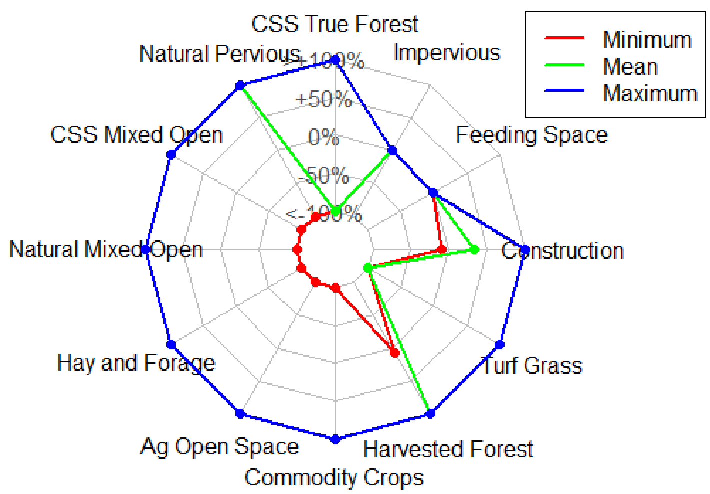

Figure G.4: Minimum, Mean, and Maximum Percent Changes in l30 Runoff per Unit Area between the Base Scenario and Scenario ccP90T90

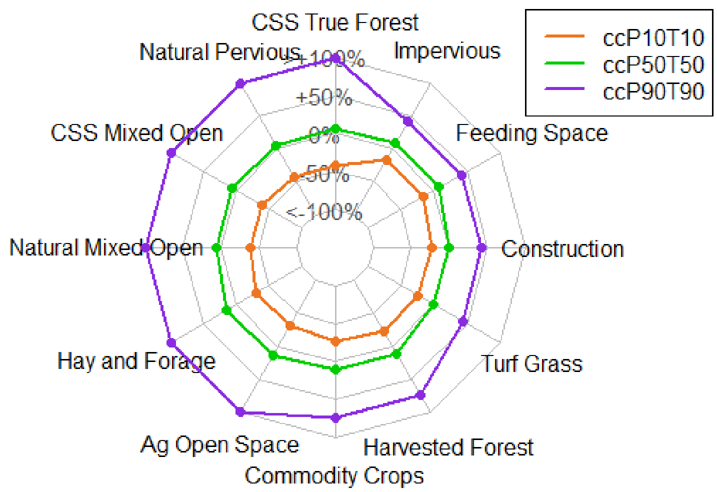

Figure G.5: Mean Percent Changes in l90 Runoff per Unit Area between the Base Scenario and Scenarios ccP10T10, ccP50T50, and ccP90T90

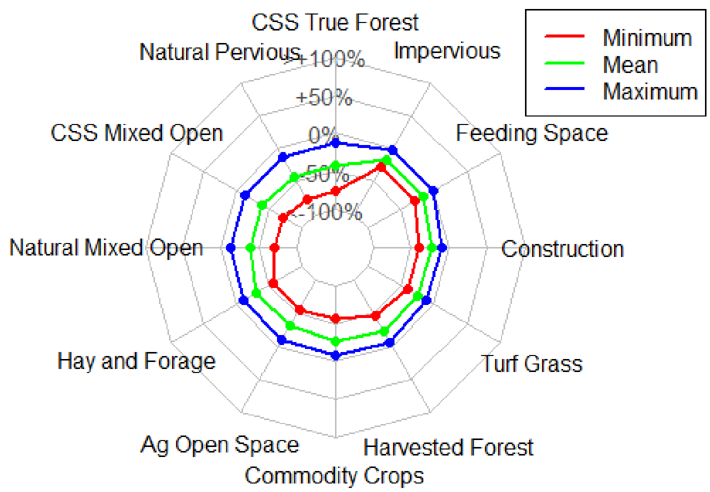

Figure G.6: Minimum, Mean, and Maximum Percent Changes in l90 Runoff per Unit Area between the Base Scenario and Scenario ccP10T10

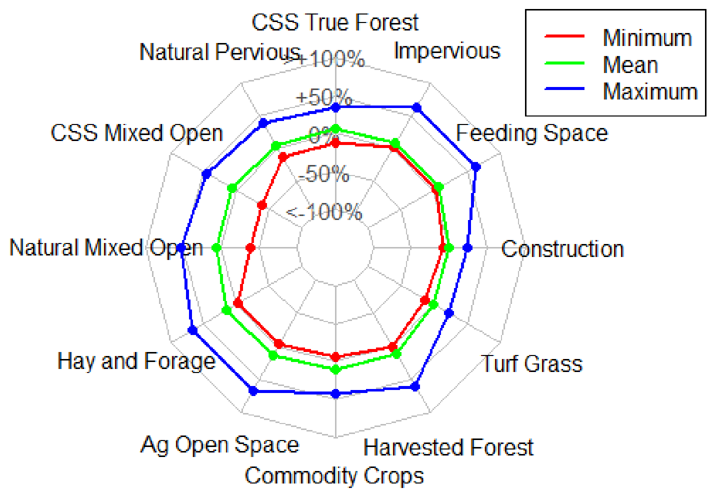

Figure G.7: Minimum, Mean, and Maximum Percent Changes in l90 Runoff per Unit Area between the Base Scenario and Scenario ccP50T50

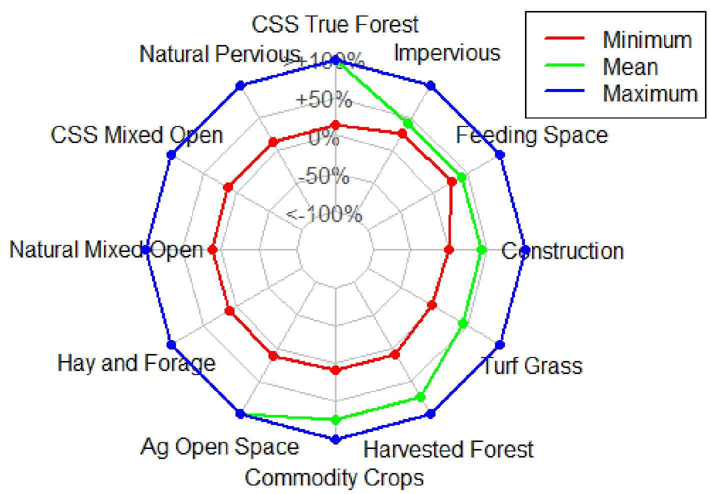

Figure G.8: Minimum, Mean, and Maximum Percent Changes in l90 Runoff per Unit Area between the Base Scenario and Scenario ccP90T90

Appendix H

Multiple Linear Regressions of Unit Flows (cfs/sq. mi.) by Land Use Against Precipitation (in/day) and PET (in/day) for Major Land Use Groups

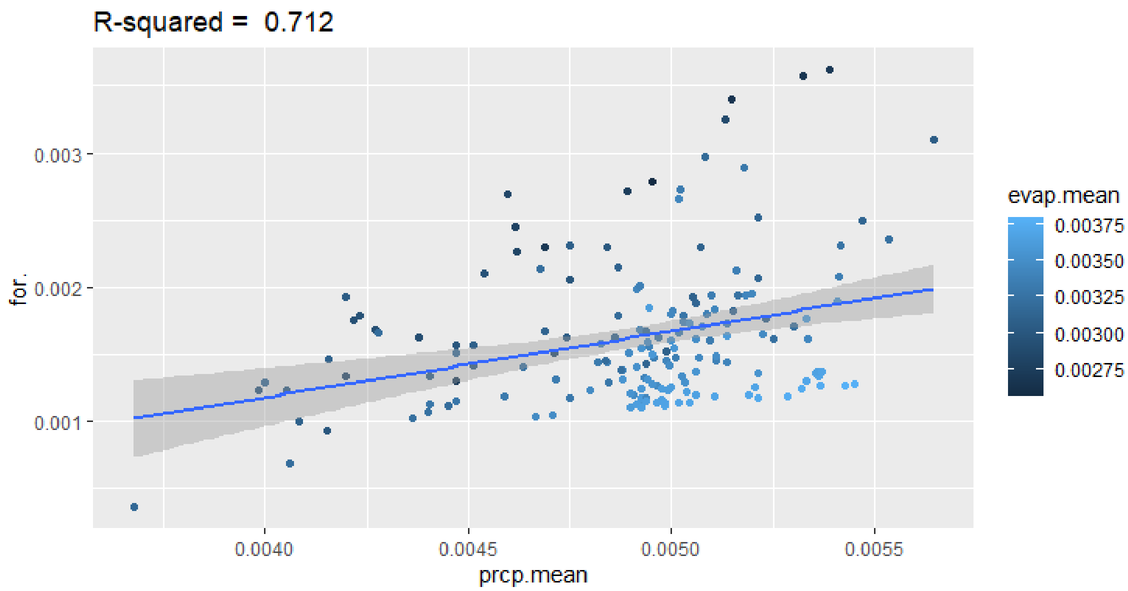

Figure H.1: MLR of Unit Runoff from Natural Pervious Land Use Group Against Precipitation and PET for Baseline Scenario

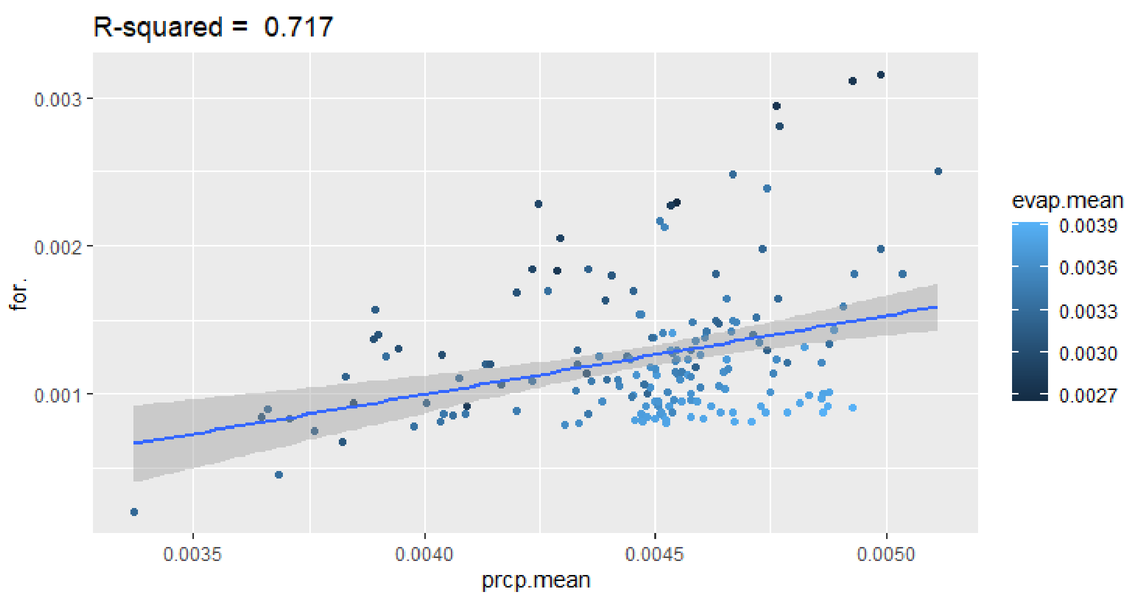

Figure H.2: MLR of Unit Runoff from Natural Pervious Land Use Group Against Precipitation and PET for ccP10T10 Scenario

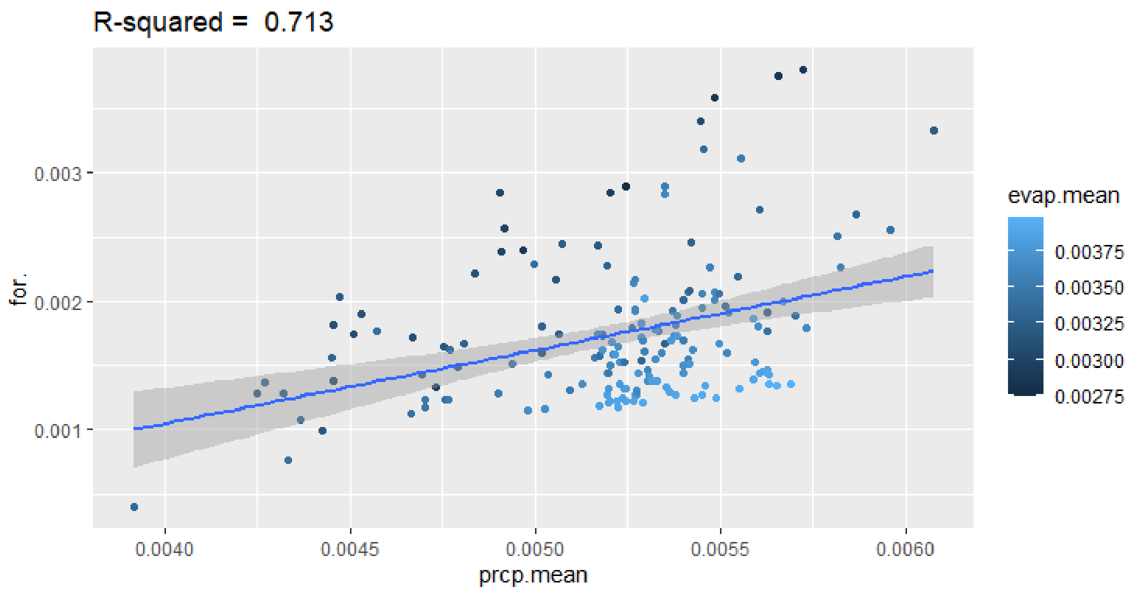

Figure H.3: MLR of Unit Runoff from Natural Pervious Land Use Group Against Precipitation and PET for ccP50T50 Scenario

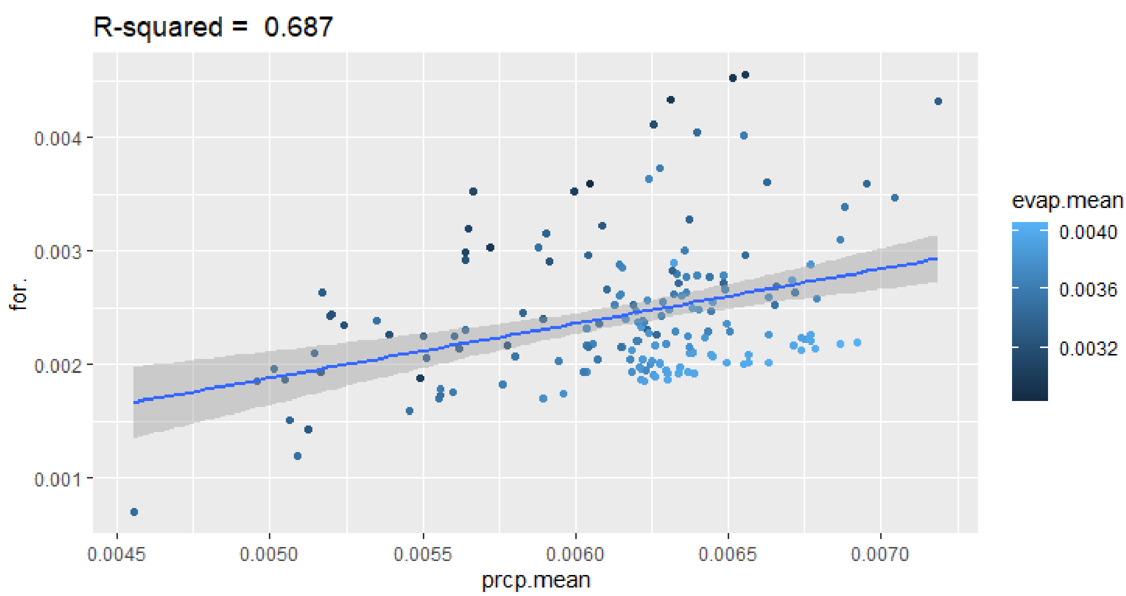

Figure H.4: MLR of Unit Runoff from Natural Pervious Land Use Group Against Precipitation and PET for ccP90T90 Scenario

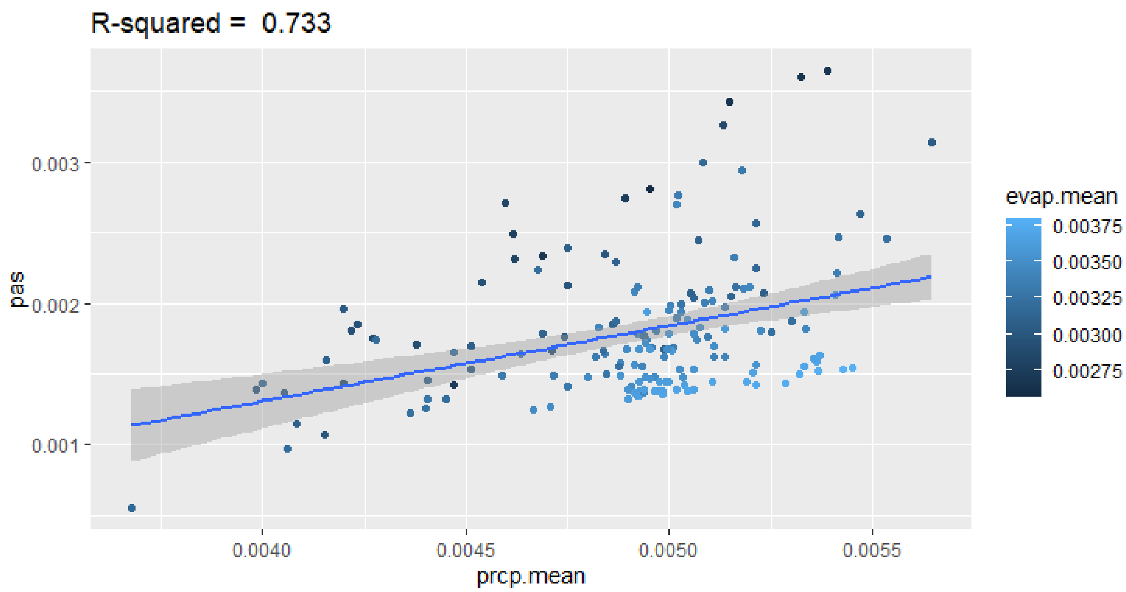

Figure H.5: MLR of Unit Runoff from Hay and Forage Land Use Group Against Precipitation and PET for Baseline Scenario

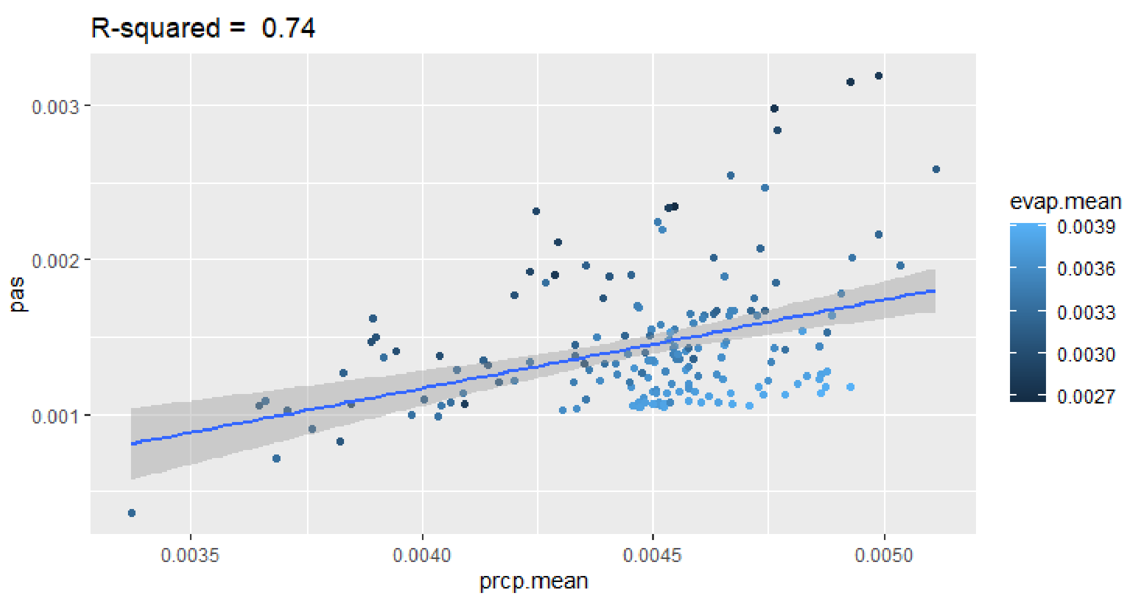

Figure H.6: MLR of Unit Runoff from Hay and Forage Land Use Group Against Precipitation and PET for ccP10T10 Scenario

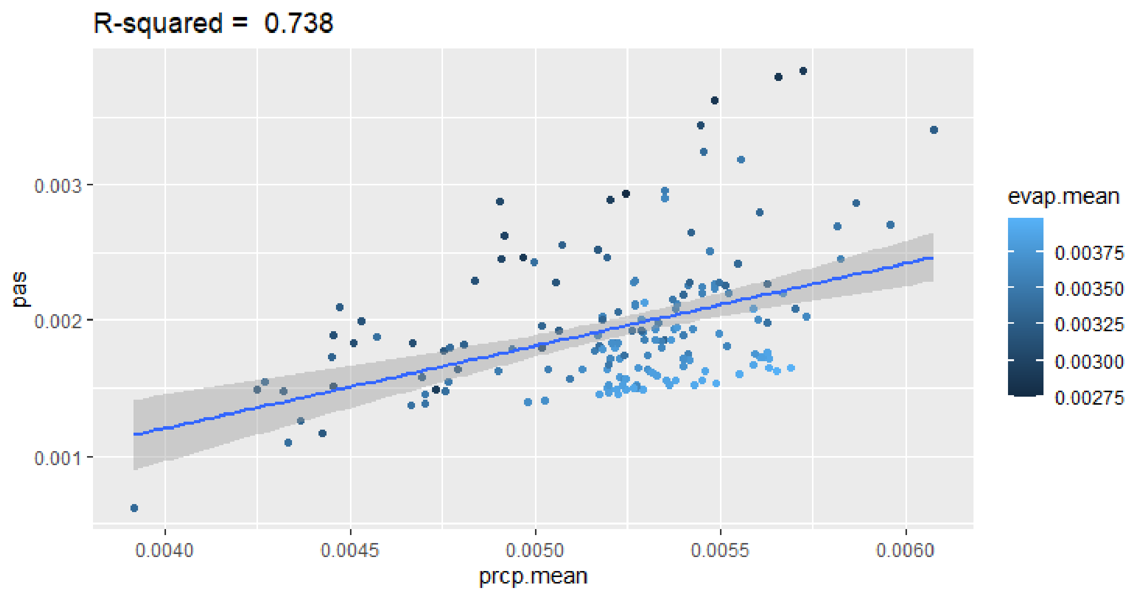

Figure H.7: MLR of Unit Runoff from Hay and Forage Land Use Group Against Precipitation and PET for ccP50T50 Scenario

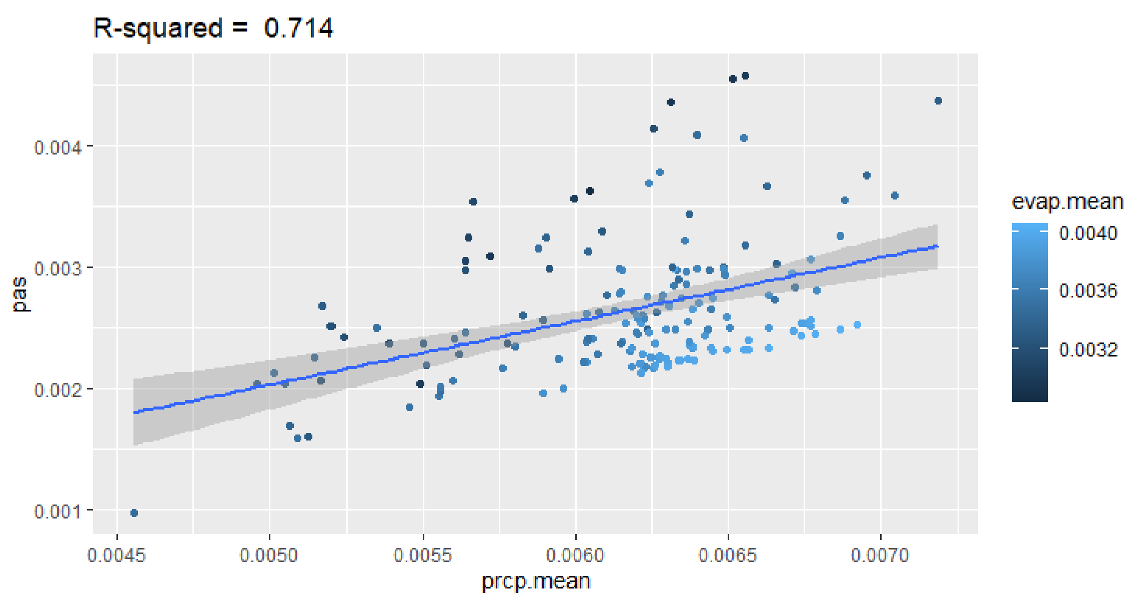

Figure H.8: MLR of Unit Runoff from Hay and Forage Land Use Group Against Precipitation and PET for ccP90T90 Scenario

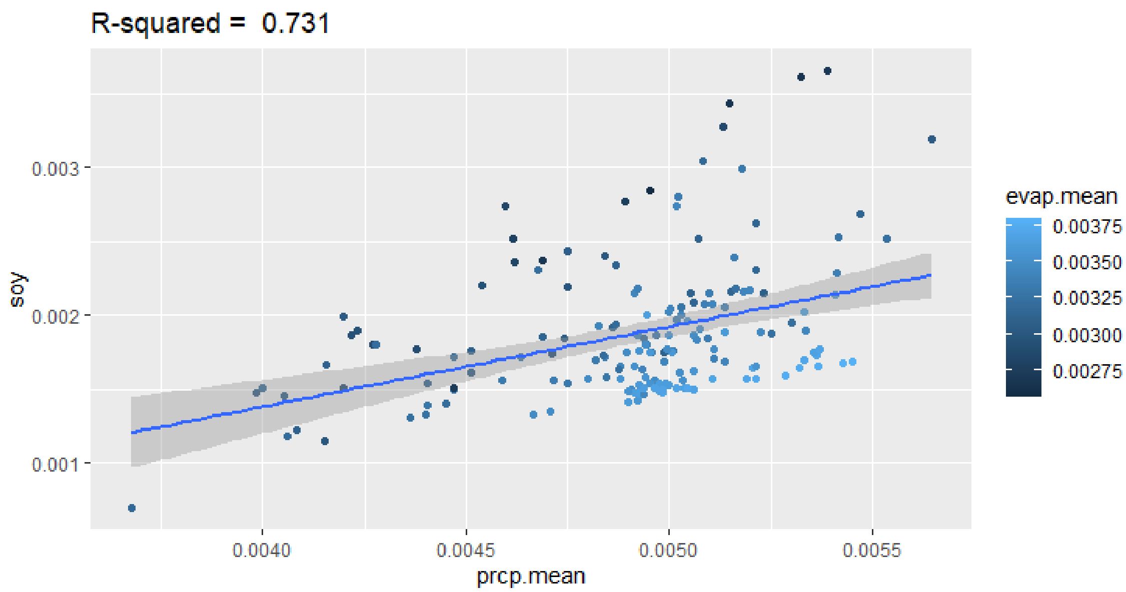

Figure H.9: MLR of Unit Runoff from Commodity Crops Land Use Group Against Precipitation and PET for Baseline Scenario

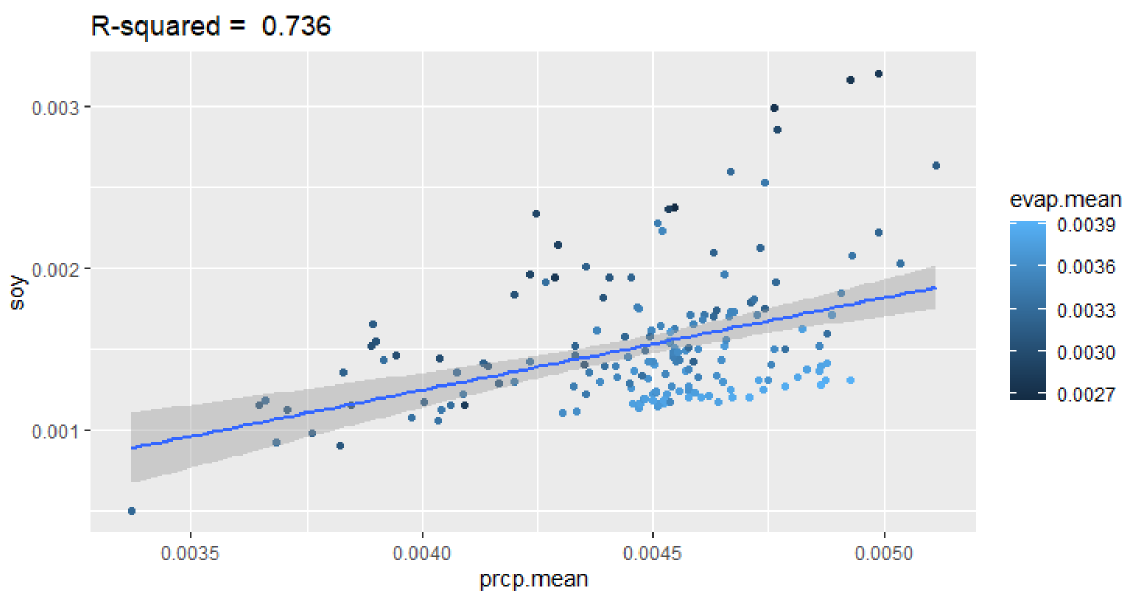

Figure H.10: MLR of Unit Runoff from Commodity Crops Land Use Group Against Precipitation and PET for ccP10T10 Scenario

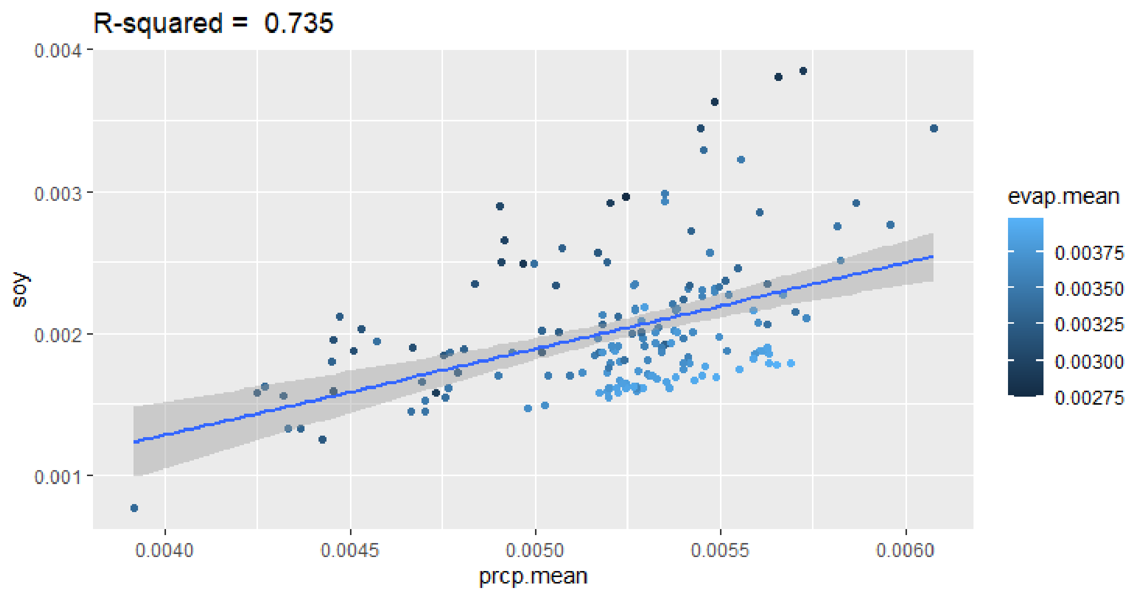

Figure H.11: MLR of Unit Runoff from Commodity Crops Land Use Group Against Precipitation and PET for ccP50T50 Scenario

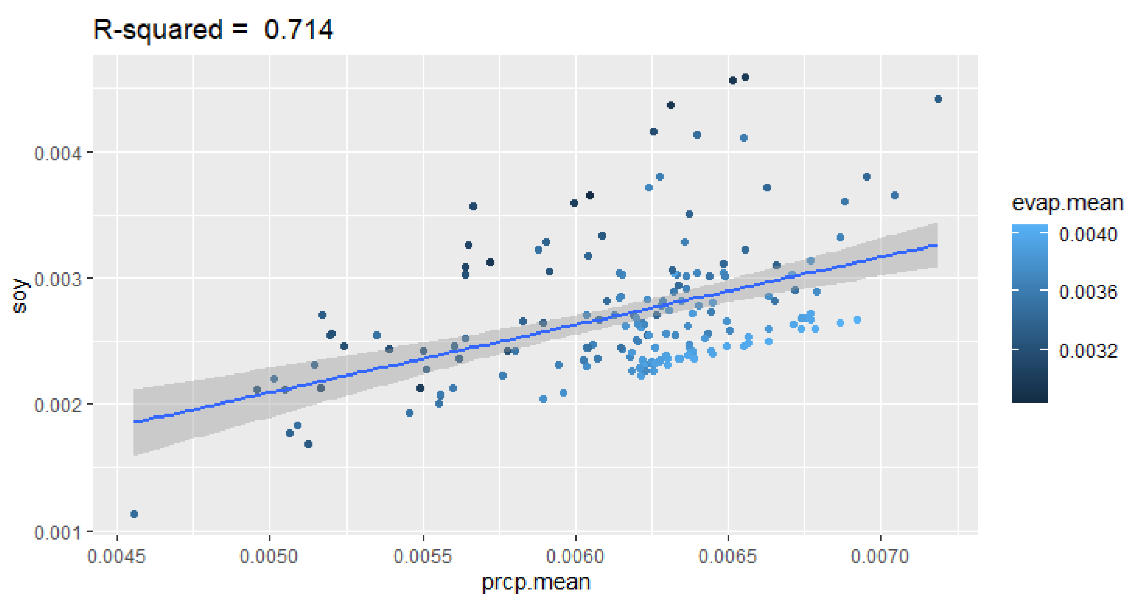

Figure H.12: MLR of Unit Runoff from Commodity Crops Land Use Group Against Precipitation and PET for ccP90T90 Scenario

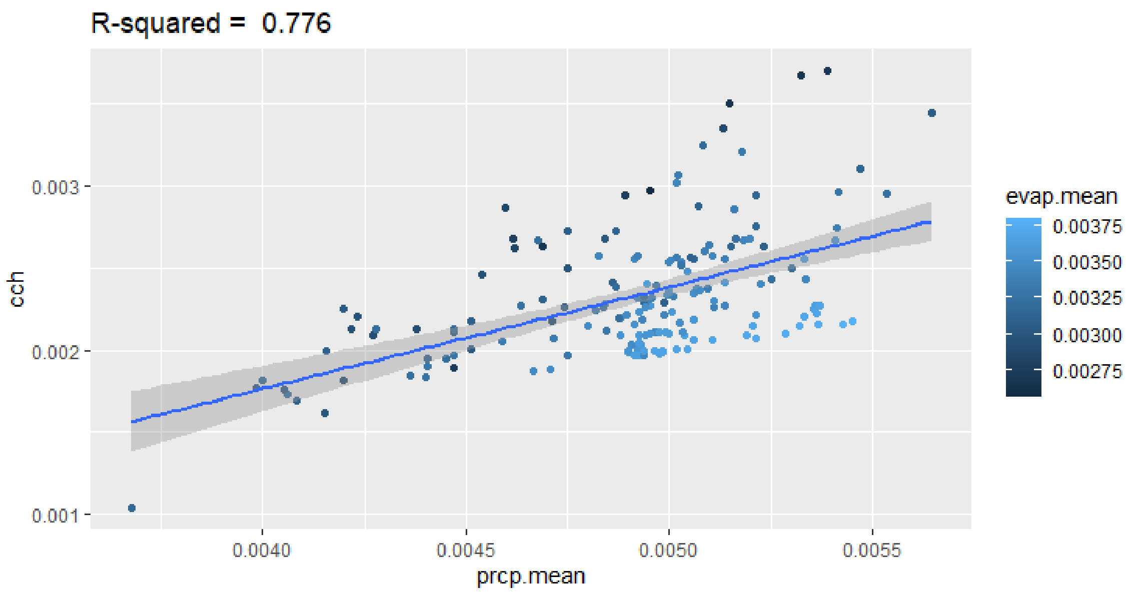

Figure H.13: MLR of Unit Runoff from Turf Grass Land Use Group Against Precipitation and PET for Baseline Scenario

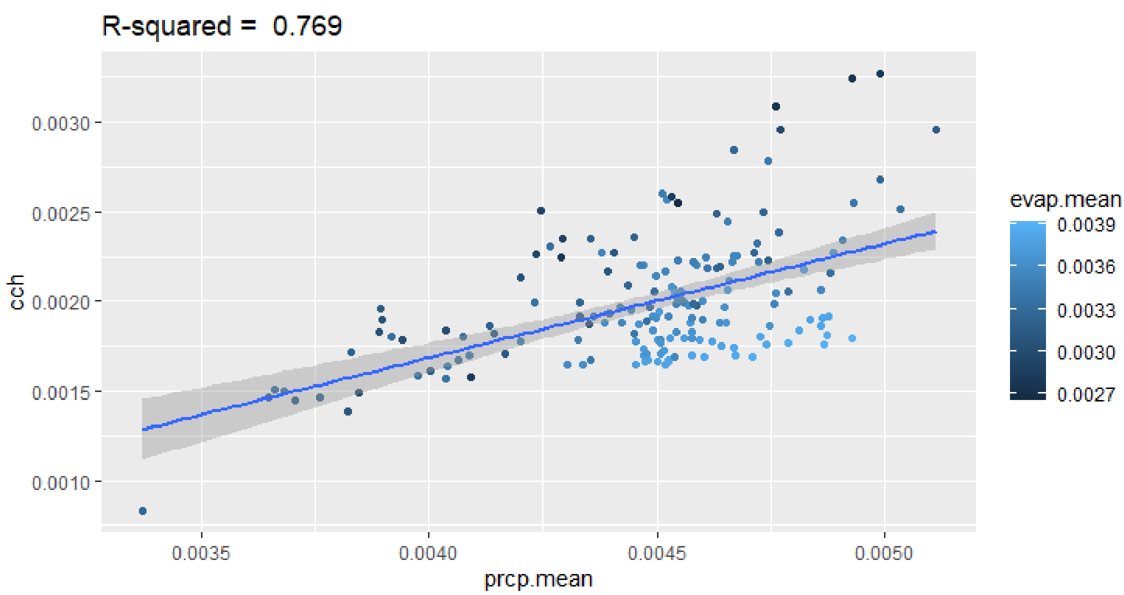

Figure H.14: MLR of Unit Runoff from Turf Grass Land Use Group Against Precipitation and PET for ccP10T10 Scenario

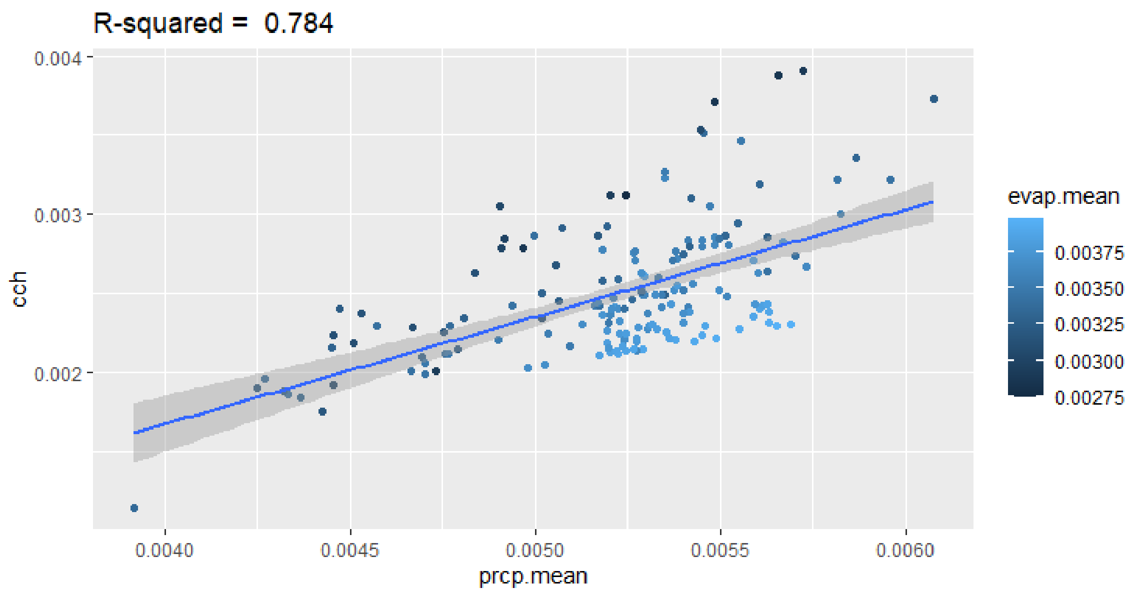

Figure H.15: MLR of Unit Runoff from Turf Grass Land Use Group Against Precipitation and PET for ccP50T50 Scenario

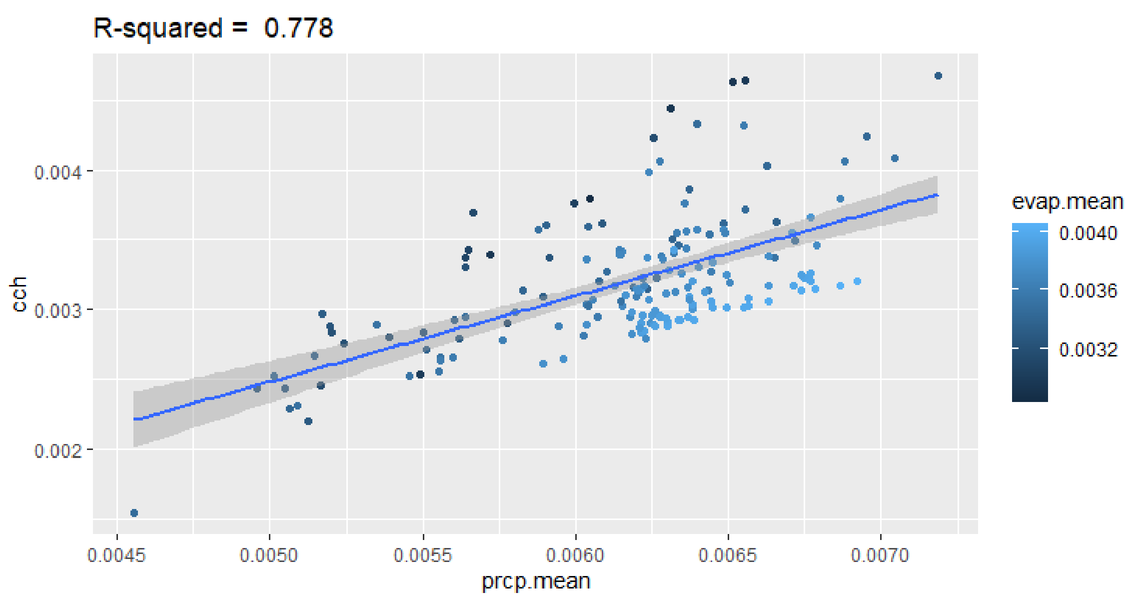

Figure H.16: MLR of Unit Runoff from Turf Grass Land Use Group Against Precipitation and PET for ccP90T90 Scenario

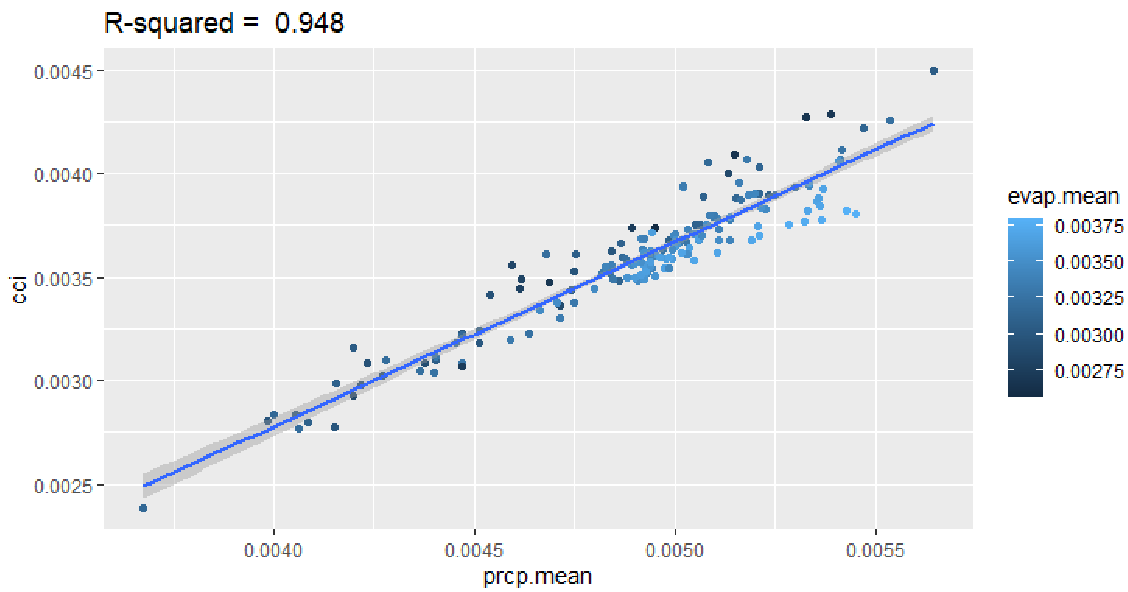

Figure H.17: MLR of Unit Runoff from Impervious Land Use Group Against Precipitation and PET for Baseline Scenario

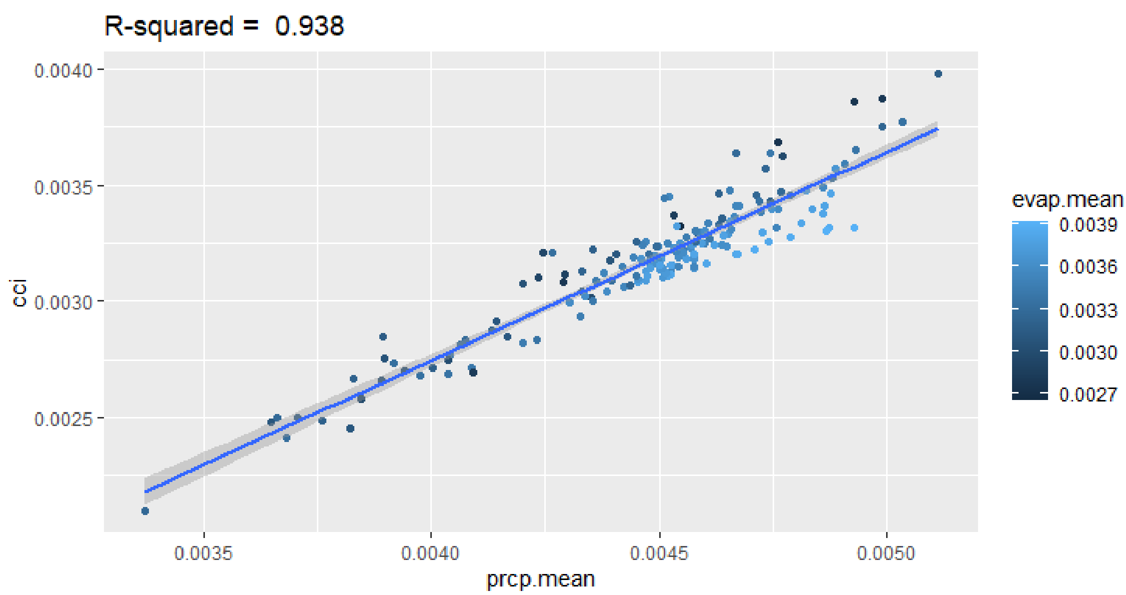

Figure H.18: MLR of Unit Runoff from Impervious Land Use Group Against Precipitation and PET for ccP10T10 Scenario

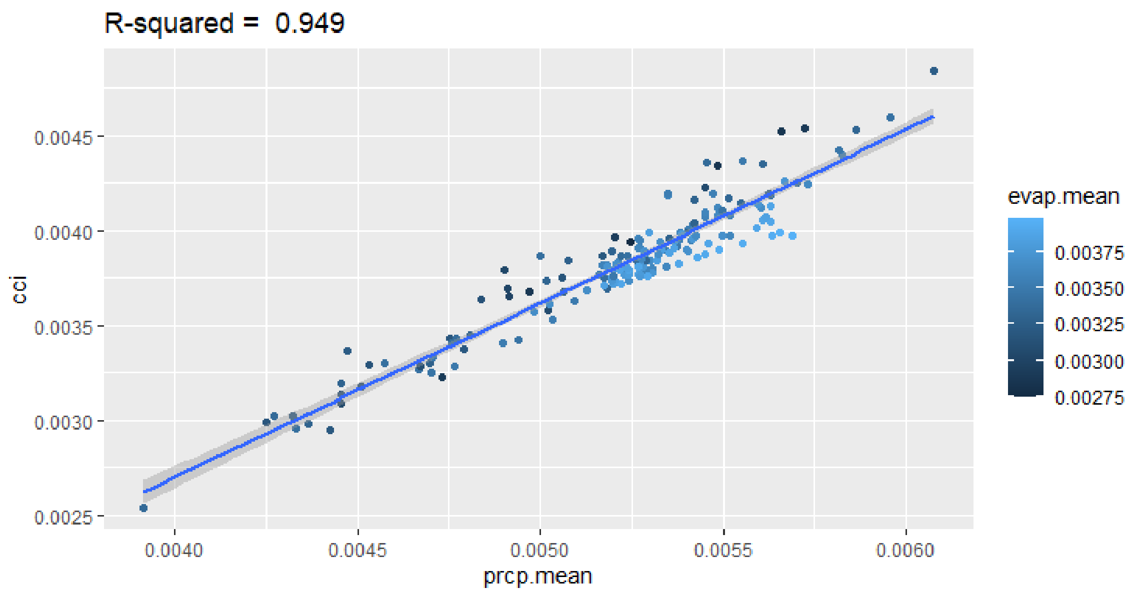

Figure H.19: MLR of Unit Runoff from Impervious Land Use Group Against Precipitation and PET for ccP50T50 Scenario

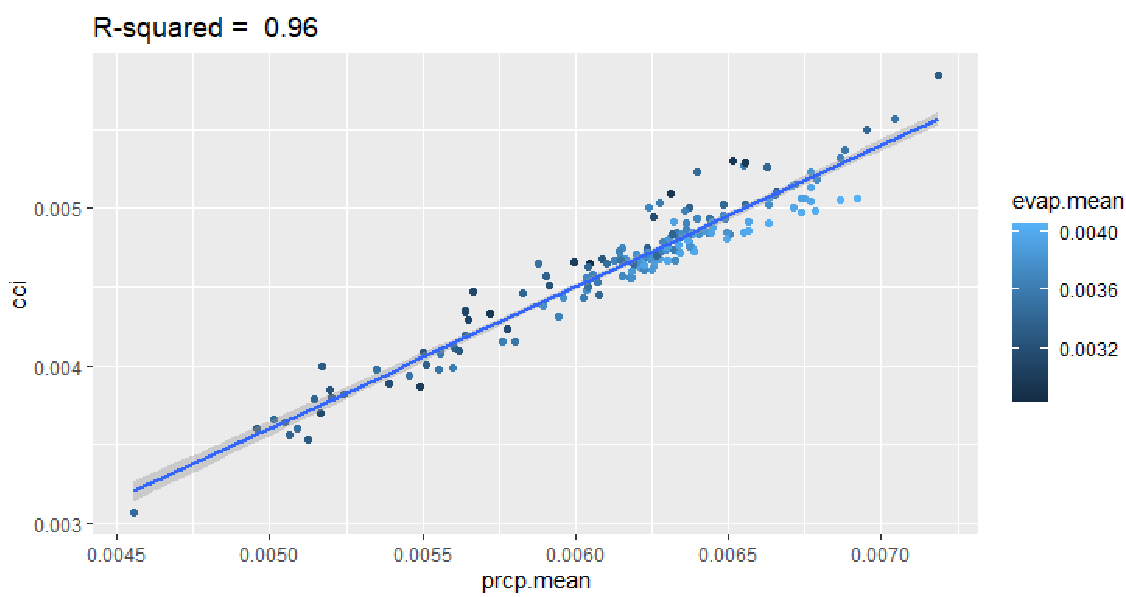

Figure H.20: MLR of Unit Runoff from Impervious Land Use Group Against Precipitation and PET for ccP90T90 Scenario

Appendix I

Example Monthly Climate Data Tables

Table I.1: Base Scenario Monthly Climate Data for Land Segment N51059 (Fairfax)

Month	PET Mean	PET Median	PET Variance	Precip. Mean	Precip. Median	Precip. Variance
Overall	0.003480	2.74e-05	3.17e-05	0.00491	0	0.000494
Jan	0.000841	0.00e+00	1.80e-06	0.00531	0	0.000463
Feb	0.001050	0.00e+00	2.50e-06	0.00415	0	0.000341
Mar	0.001750	0.00e+00	5.80e-06	0.00642	0	0.000550
Apr	0.002910	8.42e-04	1.32e-05	0.00424	0	0.000332
May	0.004870	2.27e-03	3.45e-05	0.00450	0	0.000359
Jun	0.007110	3.82e-03	6.51e-05	0.00511	0	0.000530
Jul	0.007810	3.97e-03	7.80e-05	0.00524	0	0.000544
Aug	0.006340	2.26e-03	5.53e-05	0.00462	0	0.000635
Sep	0.004450	3.47e-04	3.34e-05	0.00664	0	0.000773
Oct	0.002310	0.00e+00	1.03e-05	0.00355	0	0.000407
Nov	0.001300	0.00e+00	4.20e-06	0.00473	0	0.000613
Dec	0.000815	0.00e+00	1.80e-06	0.00434	0	0.000372

Table I.2: ccP10T10 Scenario Monthly Climate Data for Land Segment N51059 (Fairfax)

Month	PET Mean	PET Median	PET Variance	Precip. Mean	Precip. Median	Precip. Variance
Overall	0.003600	2.89e-05	3.37e-05	0.00451	0	0.000404
Jan	0.000873	0.00e+00	2.00e-06	0.00487	0	0.000374
Feb	0.001090	0.00e+00	2.70e-06	0.00414	0	0.000339
Mar	0.001830	0.00e+00	6.30e-06	0.00595	0	0.000454
Apr	0.003020	8.77e-04	1.42e-05	0.00411	0	0.000308
May	0.005010	2.34e-03	3.64e-05	0.00420	0	0.000305
Jun	0.007330	3.94e-03	6.92e-05	0.00429	0	0.000356
Jul	0.008060	4.10e-03	8.30e-05	0.00459	0	0.000400
Aug	0.006540	2.33e-03	5.89e-05	0.00403	0	0.000472
Sep	0.004640	3.63e-04	3.63e-05	0.00631	0	0.000686
Oct	0.002390	0.00e+00	1.10e-05	0.00310	0	0.000300
Nov	0.001370	0.00e+00	4.60e-06	0.00440	0	0.000521
Dec	0.000844	0.00e+00	1.90e-06	0.00409	0	0.000322

Table I.3: ccP50T50 Scenario Monthly Climate Data for Land Segment N51059 (Fairfax)

Month	PET Mean	PET Median	PET Variance	Precip. Mean	Precip. Median	Precip. Variance
Overall	0.003680	2.98e-05	3.51e-05	0.00524	0	0.000577
Jan	0.000927	0.00e+00	2.20e-06	0.00562	0	0.000532
Feb	0.001150	0.00e+00	3.00e-06	0.00458	0	0.000434
Mar	0.001870	0.00e+00	6.50e-06	0.00671	0	0.000616
Apr	0.003100	9.00e-04	1.50e-05	0.00455	0	0.000393
May	0.005150	2.42e-03	3.84e-05	0.00486	0	0.000432
Jun	0.007480	4.02e-03	7.20e-05	0.00514	0	0.000539
Jul	0.008200	4.17e-03	8.59e-05	0.00551	0	0.000611
Aug	0.006660	2.38e-03	6.11e-05	0.00500	0	0.000755
Sep	0.004700	3.68e-04	3.72e-05	0.00699	0	0.000870
Oct	0.002470	0.00e+00	1.17e-05	0.00378	0	0.000466
Nov	0.001380	0.00e+00	4.70e-06	0.00518	0	0.000750
Dec	0.000891	0.00e+00	2.10e-06	0.00495	0	0.000509

Table I.4: ccP90T90 Scenario Monthly Climate Data for Land Segment N51059 (Fairfax)

Month	PET Mean	PET Median	PET Variance	Precip. Mean	Precip. Median	Precip. Variance
Overall	0.003770	3.05e-05	3.65e-05	0.00618	0	0.000841
Jan	0.000981	0.00e+00	2.40e-06	0.00667	0	0.000803
Feb	0.001210	0.00e+00	3.30e-06	0.00557	0	0.000692
Mar	0.001960	0.00e+00	7.10e-06	0.00793	0	0.000928
Apr	0.003200	9.26e-04	1.58e-05	0.00539	0	0.000584
May	0.005230	2.46e-03	3.95e-05	0.00564	0	0.000612
Jun	0.007570	4.07e-03	7.37e-05	0.00638	0	0.000867
Jul	0.008390	4.27e-03	8.98e-05	0.00668	0	0.000948
Aug	0.006830	2.44e-03	6.41e-05	0.00569	0	0.000994
Sep	0.004860	3.80e-04	3.95e-05	0.00816	0	0.001250
Oct	0.002510	0.00e+00	1.21e-05	0.00432	0	0.000623
Nov	0.001440	0.00e+00	5.10e-06	0.00614	0	0.001090
Dec	0.000933	0.00e+00	2.30e-06	0.00563	0	0.000692